SEPT. – DEC. 1996
Volume II Number III

ISSN 0859 144X

THE ASEAN JOURNAL OF RADIOLOGY

Published by The Radiological Society and
the College of Radiologists of Thailand,
Bangkok, Thailand

Supported through an educational grant from

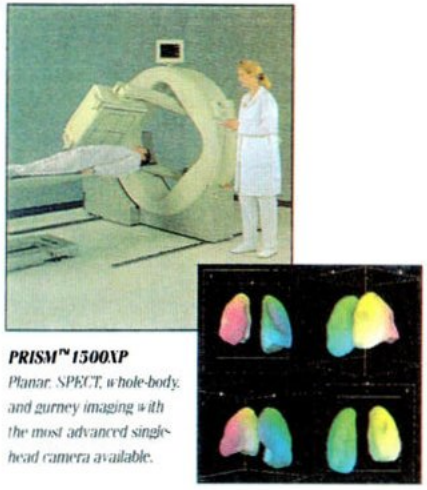

PRISM™ 1500XP
Planar, SPECT, whole-body, and gurney imaging with the most advanced single-head camera available.

3-D lung SPECT images.

PRISM™ 2000XP
Offers the broadest range of applications in nuclear medicine with throughput and image quality superior to any variable angle design.

Coincidence images using ^{18}F and Picker's revolutionary new PCD™ product.

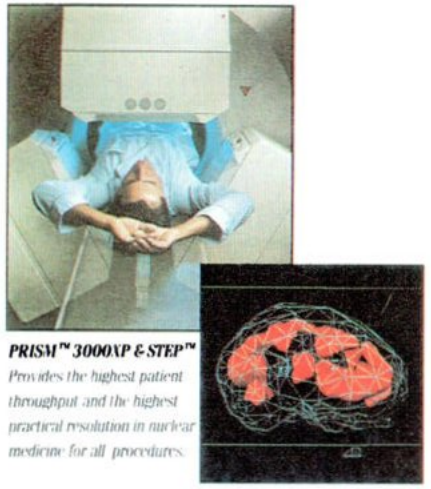

PRISM™ 3000XP & STEP™
Provides the highest patient throughput and the highest practical resolution in nuclear medicine for all procedures.

NeuroFlow™ Xenon rCBF 3-D dual-threshold brain. Red area represents blood flow in ml/min/100 grams of tissue.

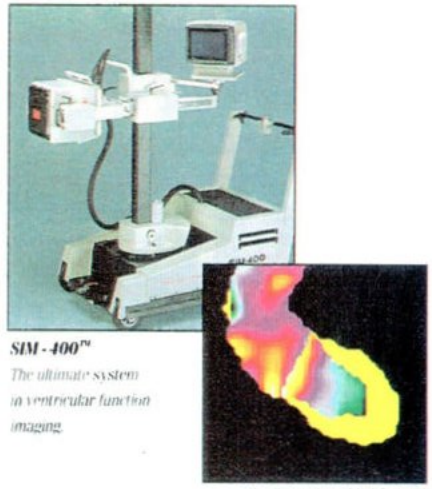

SIM-400™
The ultimate system in ventricular function imaging.

First Pass analysis of the left ventricle at rest and peak exercise.

Only one nuclear medicine company can give you an image of the *Future.*

To meet the challenges of today's changing healthcare environment, you need more than a supplier. You need a partner. A partner with innovative ideas that keep you ahead of change.

Today, Picker is leading the way in nuclear technology, developing groundbreaking new clinical applications destined to become the foundation of tomorrow's nuclear medicine. From our powerful Odyssey™ computer to our NeuroFlow™ Xenon rCBF Option and our Positron Coincidence Detection* capabilities, Picker is the industry's clinical innovator.

So if you're looking for a strategic partner to prepare you for the future, talk to Picker. Make no mistake: No one offers you more choices today, more technology for tomorrow, or better value for your nuclear department.

For more information, call Picker International at (800) 323-0550; e-mail us at @nm.picker.com; or visit us on the Web at the Nuclear Medicine Modality Home Page – http://www.picker.com/nuclear/nuclear.html.

* Pending 510(k) clearance to market.

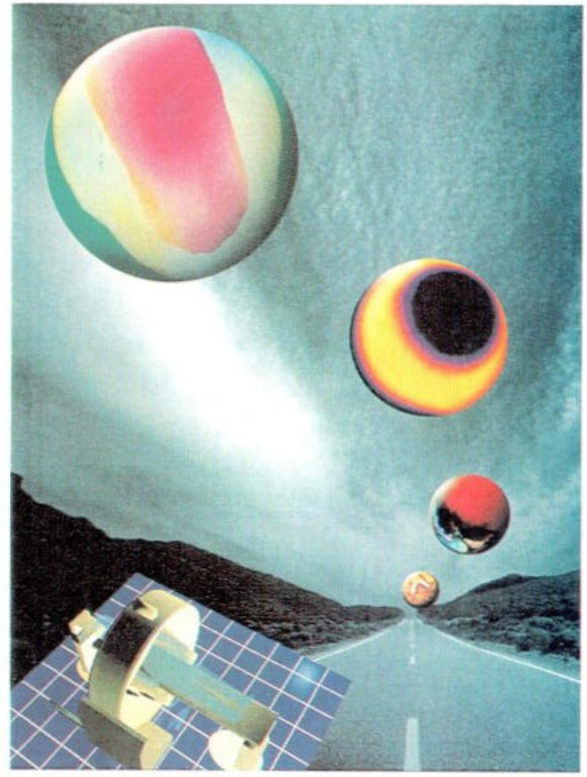

PICKER
MORE THAN IMAGES. INSIGHT.

Picker International
29/F, 2908 Suntowers Bldg.-B, 123 Vibhavadi-Rangsit Rd.
Jatujuk, Bangkok 10900 Thailand.
PO BOX 29 Suntowers Post Office
Tel. (662) 617-8212-4 Fax. (662) 617-8215

Distributor
UNITED 4 CO.,LTD.
43/1085 Raminthra 1, Raminthra Rd. Bangkhen
Bangkok 10220 Thailand.
Tel. 9707034-5, 9707037, 9707039, Fax. 5527840

SEPT. – DEC. 1996

Volume II Number III

ISSN 0859 144X

THE ASEAN JOURNAL OF RADIOLOGY

Published by The Radiological Society and
the College of Radiologists of Thailand,
Bangkok, Thailand

Supported through an educational grant from

BRACCO
INTERNATIONAL

1. The AAR Journal of Radiology publishes the papers on Radiological Sciences, such as research work, review articles, case reports, innovations in Medical Sciences related to all branches of Radiology, and letters to the editor. The aforementioned materials can be written in English only.

2. The authors have to submit 2 copies of the manuscript and a diskette: **to Prof. Dr. Kawee Tungsubutra,** 318 Kaweevej Hospital, Tarksin Road, Dhonburi, Bangkok 10600, Thailand.
or to the Associate Editors at the Radiological Society of Malaysia, Indonesia, Phillippine, Singapore and Brunei. The names and addresses of the Associate Editors in each country were published in the front page of this Journal.

3. The original copy to be submitted must be typed in a double space on one side of the page of 8″ × 11″ paper.

4. The format of the article must include:

   a. Title page and address of the author (s)

   b. Abstract

   c. Introduction (Background)

   d. Material and Method

   e. Results and discussion (Tables and Illustrations)

   f. Acknowledgement (if any)

   g. References (Follow the Vancouver style developed by ICMJE)

5. We will provide 25 copies of reprints for the author (s) who submit (s) and article for publication in the AAR Journal.

6. The illustrations and tables must be clearly prepared with legends in English as they are the art works to be reproduced.

7. The authors are responsible for the contents of the article as to its facts and findings.

8. Ethics.

Paper reporting studies which might be interpreted as human experimentation (e.g. controlled trials) should conform to the standards of the Declaration of Helsinki (see British Medical Journal 1964:2:177) and should indicate that approval that such studies may proceed has been granted by the local or hospital Ethics Committee.

When reporting experiments on animals indicate whether the institution's or the National Research Council's guide for, or any national law on, the care and use of laboratory animals was followed.

Message from

Prof. Dr. Kawee Tungsubutra

Editor-in-Chief, The Asean Journal of Radiology.

This is the third number of Volume II or the second year of the Asean Journal of Radiology. (Asean J.R.) In the previous Number, there was some haphazard of the post office in Singapore that caused the detour of the parcels for our members in Singapore and Indonesia. We tried to correct the haphazard by calling to the post office concerned and speaking, explaning to the officers concerned. Unfortunately there are too many people concerned in the transportation of the parcels, the Volume II, No. 1 have detoured twice. I am trying to solve this problem of posting and transportation and only hope that there will be no haphazard in the future, by sending the parcels to different countries on different days !!

Kawee Tungsubutra

THE ASEAN JOURNAL OF RADIOLOGY

Volume II Number III SEPT.-DEC. 1996

CONTENTS

Volume II Number III SEPT.-DEC. 1996

CONTENTS

THE CONTRALATERAL BREAST IN IPSILATERAL BREAST CARCINOMA: ROLE OF MAMMOGRAPHY

Malai MUTTARAK* M.D., Ladda CHALEOYKITTI*BSc., Nimit MARTINM.D., Hongsin TRAKOONTIVAKORN**M.D., Chanane WANAPIRAK***M.D., Benjaporn CHAIWUN****M.D., Samreung RANGDAENG****M.D.,**

This study was done to assess the value of mammography in contralateral breast of the patient with ipsilateral breast carcinoma.

MATERIALS AND METHODS:

From February 1994 through January 1996, at Maharaj Nakorn Chiang Mai Hospital, film-screen mammograms of the contralateral breast were obtained in 100 patients who had had a unilateral mastectomy to breast cancer 94 patients were asymptomatic, 4 had breast mass and 2 had axillary mass. A retrospective review was undertaken to determine the development of the second primary breast carcinoma or metastasis in the contralateral breast.

RESULTS

All symptomatic patients were abnormal on mammograms. Four patients who had breast masses had biopsy-proven second primary carcinoma. Two patients who had axillary masses had biopsy-proven metastases from breast carcinoma. Two out of 94 asymptomatic patients had abnormal mammograms, one proved to be a second primary carcinoma and the other proved to be fibroadenoma.

Patients who have had ipsilateral breast carcinoma are at increased risk for cancer in the contralateral breast. Continuing regular follow-up with careful examination and mammography of the contralateral breast are recommended for all patients having ipsilateral breast carcinoma to be detected detect early, potentially curable disease.

Key words: Bilateral breast carcinoma, mammography

INTRODUCTION

The risk of developing a second primary carcinoma in the remaining breast of a woman who has undergone unilateral mastectomy is higher with respect to the general occurrence rate of breast carcinoma.[1-6] Detection of the second primary carcinoma formerly was by physical examination, random biopsy and prophylactic contralateral mastectomy.[3,7] The advent of modern mammography has made it possible to detect contralateral breast carcinoma in its clinically occult or non-palpable stage and to make the differentiation from metastasis.[8-10]

The aim of this study was to examine the incidence of second primary breast carcinoma and assess the value of mammography in detection and differentiation of a second primary breast carcinoma from metastasis.

*Department of Radiology, **Department of Surgery, ***Department of Obstetric-Gynecology, ****Department of Pathology, Faculty of Medicine, Chiang Mai University Chiang Mai Thailand.

Supported by Faculty of Medicine Endowment Fund for Medical Research, Chiang Mai University.

MATERIALS AND METHODS

From February 1994 through January 1996, at Maharaj Nakorn Chiang Mai Hospital, film-screen mammograms of the contralateral breast were obtained in 100 patients who had had a unilateral mastectomy for breast carcinoma. Age of incidence, age at menarche and at menopause, familial history of breast cancer and pathological features (histological types and stages) were studied.

The criteria on which we base the diagnosis of a second primary carcinoma were 1). the patients did not have clinical or radiological evidence of local recurrence or distant metastasis from the first primary tumor at the time of mastectomy for the second breast carcinoma, 2). the time interval between the two independent primary carcinomas was greater than six months, and 3). histologically, the second tumor was different. There were in situ change, and different grade of differentiation.

RESULTS

Second primary breast carcinoma was diagnosed in all 4 cases who had breast masses(Fig 1,2). One of the four cases had 2 new primaries (Fig 3). Table 1. shows age at the time of diagnosis of the first primary carcinoma to be 36-61 years (mean 44.5 years) and the time interval between the two carcinoma to be 1-11 years (mean 4.8 years). Axillary lymph node involvement of the first and second primary carcinomas is shown in table 2. Tumor stage of the first and second primary is shown in table 3. All patients had infiltrating ductal carcinoma in the first and second primary. There was no evidence of local recurrence or distant metastasis at the time of mastectomy for the second primary carcinoma.

Metastatic axillary lymph node in the contralateral side was diagnosed in two cases who had axillary masses (Fig 4).Two abnormal mammograms were found in the 94 asymptomatic patients. Pathological examination showed second primary breast carcinoma in one (Fig 5) and fibroadenoma in the other (Fig 6).

Table 1.

Case	Age at first primary carcinoma (years)	Time between first and second primary carcinoma (years)
1	42	3
2	43	11
3	36	1
4	61	5
5	40	4
	mean 44.5	mean 4.8

Table 2. Involvement of axillary lymph nodes

Case	First primary	Second primary
1	Positive	Negative
2	Negative	Negative
3	Negative	Negative
4	Positive	Positive
5	Positive	Positive

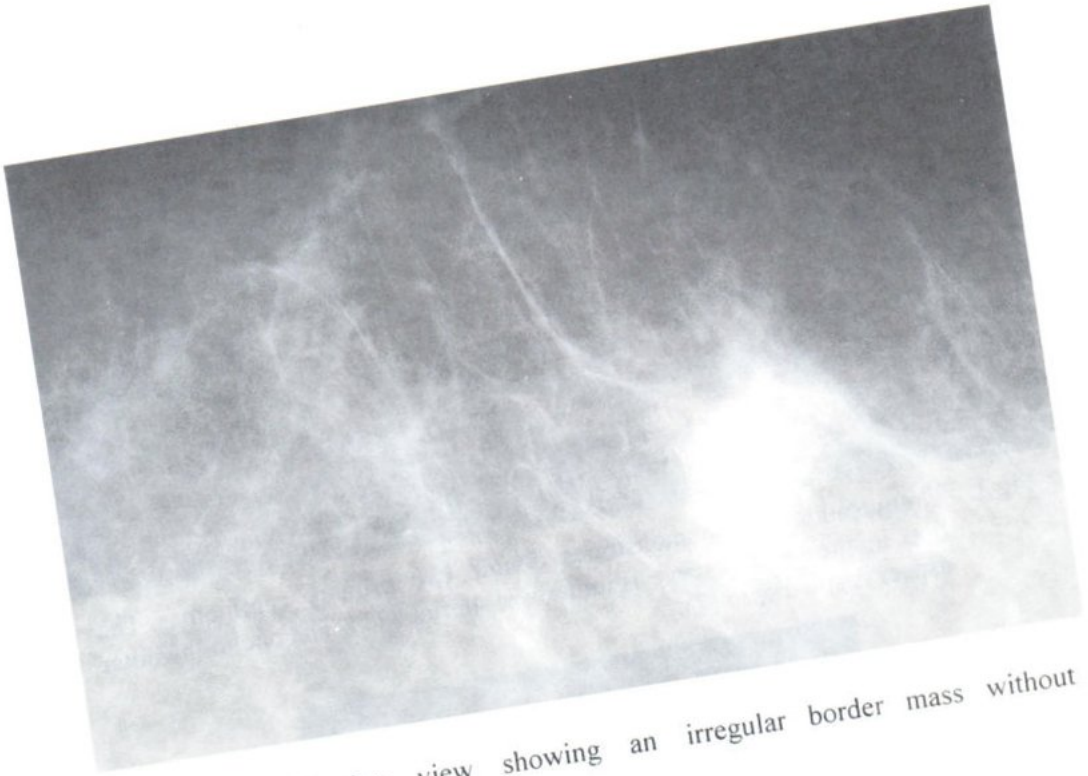

Fig 1. Magnification view showing an irregular border mass without calcification.

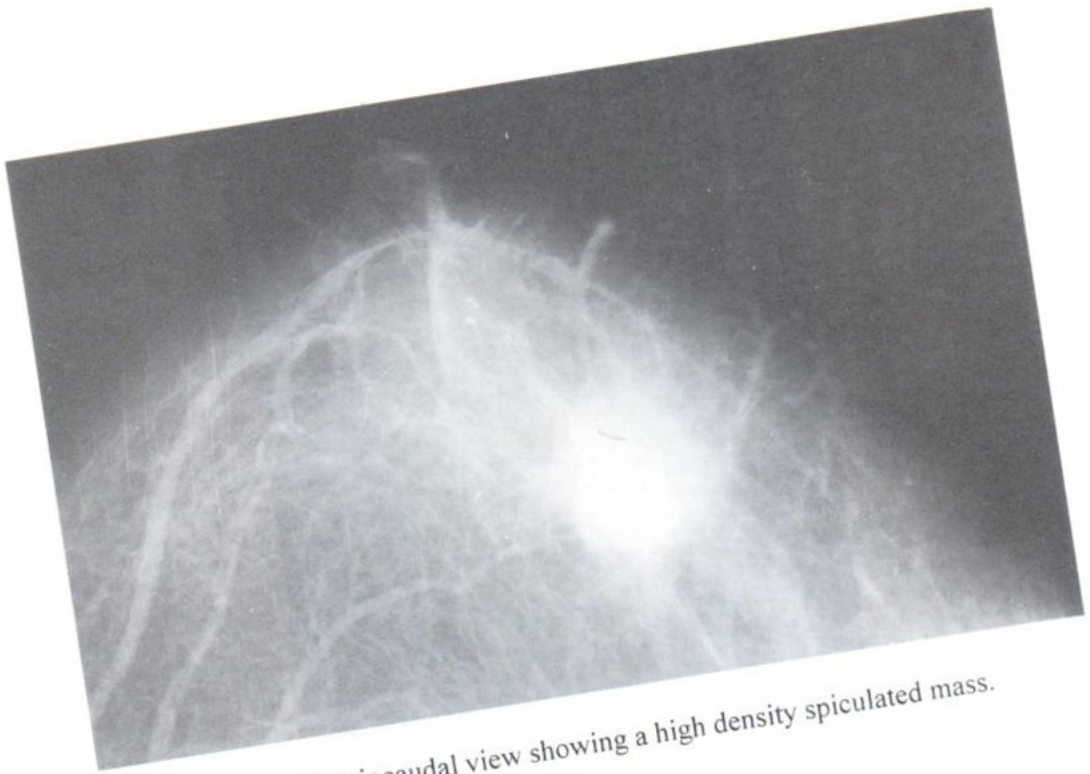

Fig 2. Craniocaudal view showing a high density spiculated mass.

Fig 3. Craniocaudal view demonstrates double two primary carcinomas. The one in the inner aspect is rather well-defined (1). The one in the outer aspect is spiculated (2).

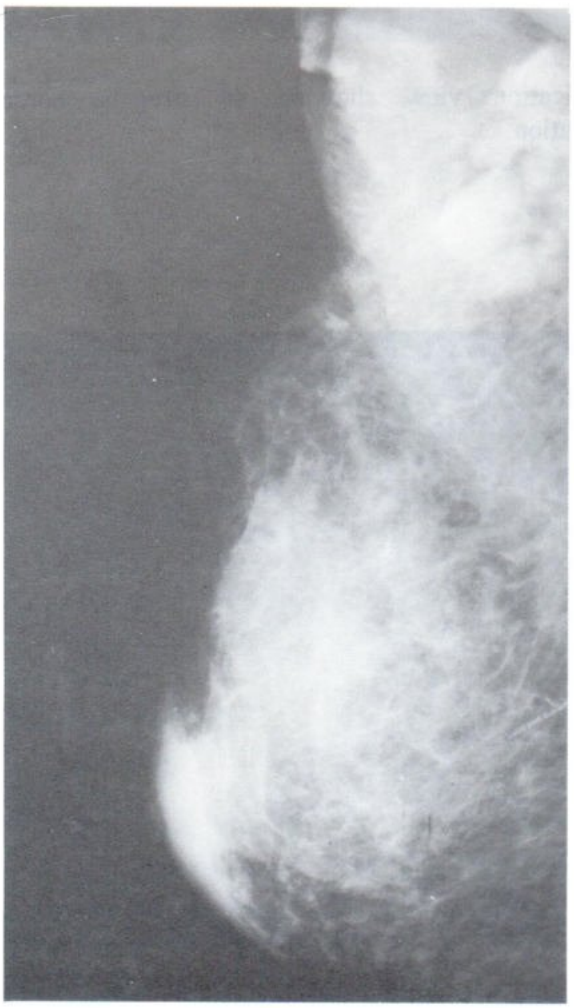

Fig 4. Mediolateral oblique view showing multiple enlarged axillary nodes, generalized increased breast density and thickening of skin.

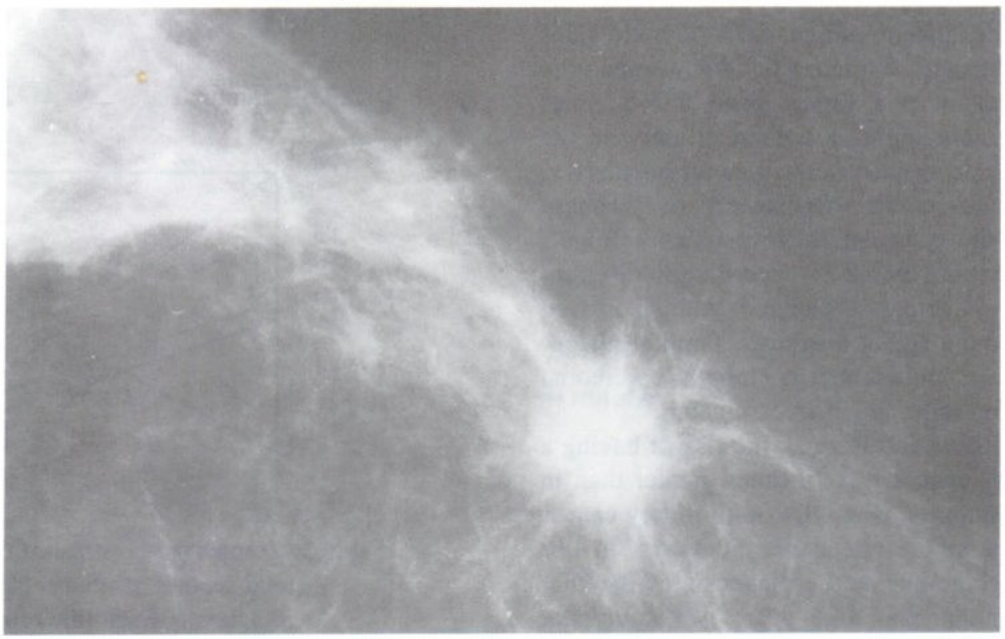

Fig 5. Magnification view demonstrates the high density, spiculated mass.

Fig 6. Craniocaudal view showing the rather well defined mass with partially obscured border.Excisional biopsy revealed fibroadenoma.

DISCUSSION

Since the breast is a paired organ, and since cancer of this region is frequently of multicentric origin, the development of simultaneous or subsequent independent malignancies on both sides is a well-established characteristic. All women who develop cancer in one breast have a 5-8 times greater risk of developing a second primary on the other side than do women in the general population.[1-6,11] The subsequent occurrence of primary carcinoma in the contralateral breast varies from a few percent to more than 20% according to different authors.[2,5,12,13] Factors associated with increased risk include young age at diagnosis, familial history of breast cancer, multicentricity, lobular carcinoma in situ and invasive lobular carcinoma.[6,10,11,14,15] According to Robin and Berg[1], the risk of having a second primary cancer was 10 times greater than in the normal population when the first primary cancer was diagnosed at the age under 50 years. In our series, the average age at the diagnosis of the first primary carcinoma was 44.5 years, We could not find any relationship between second primary carcinoma and familial history and multicentricity in our study.

The time interval between the first and second primaries was up to the sixth year in 85% of cases in Egan's series[8] and by the seventh year in Bailey's series.[16] In our study, the mean time between the two carcinomas is 4.8 years which indicates the need for careful follow-up for the first 7 years.

Mammograms of all our second primary breast carcinoma demonstrated masses with spiculated or unsharp margins while metastases to the breast are usually discrete nodules and cannot be differentiated from benign nodules such as cyst or fibroadenoma.[17]

Most of the second primary carcinomas in our study were symptomatic and positive on physical examination, even in the one asymptomatic case when retrospective physical examination was performed. Mammography is effective for detecting the second primary breast carcinoma before it becomes clinically detectable. We propose that patients who have had ipsilateral breast carcinoma should have periodic clinical examination and mammography for surveillance of the opposite breast after the treatment of primary breast carcinoma for at least 7 years after the first primary carcinoma.

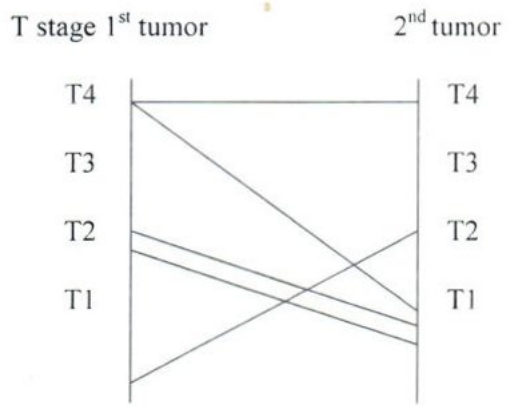

Table 3. Comparing T stage of the first and second primary tumor at diagnosis. Each line represents one patient

REFERENCES:

1. Robbins GF, Berg JW. Bilateral primary breast cancers. Cancer 1964;17:1501-27.
2. Moertel CG, Soule EH. The problem of the second breast: A study of 118 patients with bilateral carcinoma of the breast. Ann Surg 1957;146:764-71.
3. Urban J.A., Papachristoce D, Taylor J. Bilateral breast cancer: Biopsy of the opposite breast. Cancer 1977;40:1968-73.
4. Chaudary MA, Millis RR, Hoskins EO, et al. Bilateral primary breast cancer: A prospective study of disease incidence. Br J Surg 1984;71:711-4.
5. Nielsen M, Christensen L, Andersen J. Contralateral cancerous breast lesions in women with clinical invasive breast carcinoma. Cancer 1986; 57:897-903.

6. Hoffman E. The contralateral breast in ipsilateral breast carcinoma. South Med J 1990;83:1009-15.
7. Leis HP. Selective, elective , prophylactic contralateral mastectomy. Cancer 1971;28:956-61.
8. Egan RL. Bilateral breast carcinomas: Role of mammography. Cancer 1976;38:931-8.
9. Tinnemans GM, Wobbes T, Hendriks JHCL, et al. The role of mammography in the detection of bilateral primary breast cancer. World J Surg 1988;12:382-8.
10. Donovan AJ. Bilateral breast cancer. Surg Clin North Am 1990;70:1141-9.
11. Lesser ML, Rosen PP, Kinne DW. Multicentricity and bilaterality in invasive breast carcinoma. Surgery 1982;91:234-40.
12. Watanatittan S, Ram MD. Non-simultaneous bilateral breast carcinoma. Surgery 1974;75:740-5.
13. Gulay H, Hamaloglu E, Bulut O, et al. Bilateral breast carcinoma:28 years' experience. World J Surg 1990;14:529-34.
14. Tulusan AH, Ronay G, Egger H, et al. A contribution to the natural history of breast cancer. Arch Gynecol 1985;237:85-91.
15. Pomerantz RA, Murad T, Hines JR. Bilateral breast cancer. Am Surg 1989;55:441-4.
16. Bailey MJ, Royce C, Sloane JP, et al. Bilateral carcinoma of the breast. Br J Surg 1980;67:514-6.
17. Feig SA.Breast masses: Mammographic and sonographic evaluation. Radiol Clin North Am 1992;30:67-92.

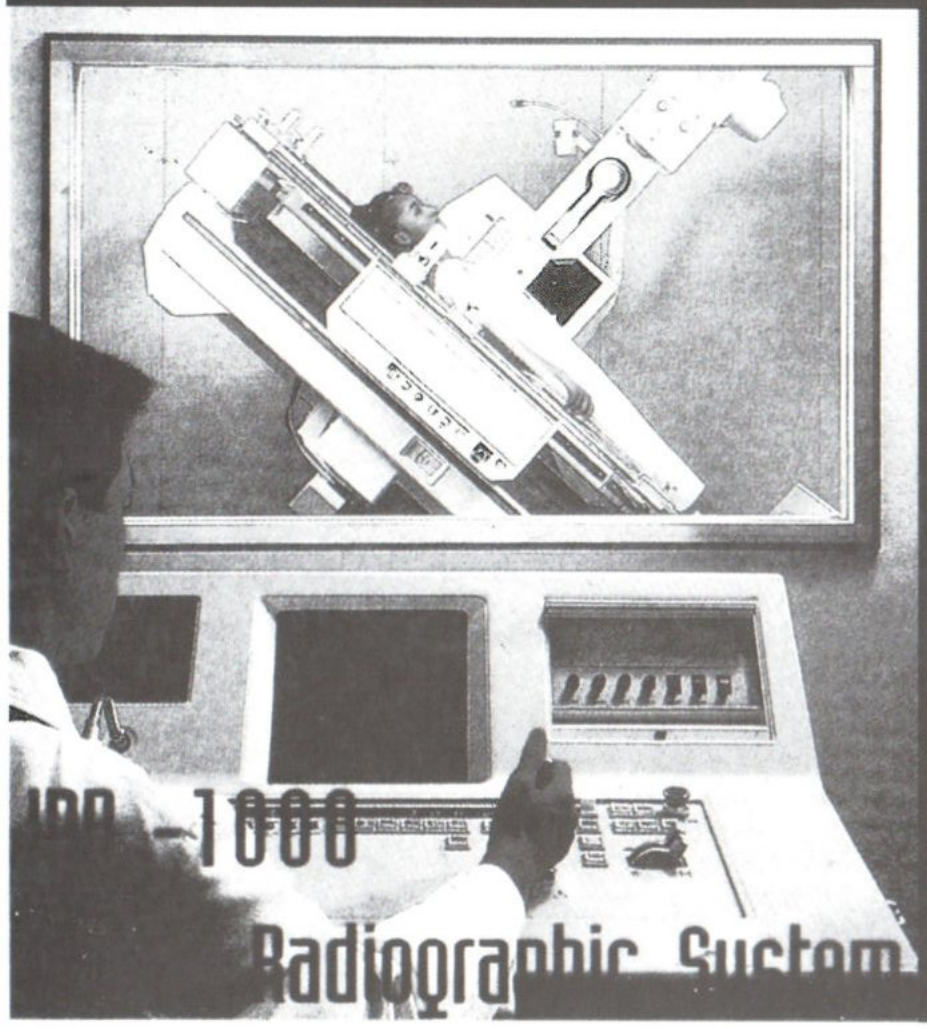

SHIMADZU

INVERTERTYPE Mobile X-ray system

SCT-4800T WHOLE BODY CT SCANNER

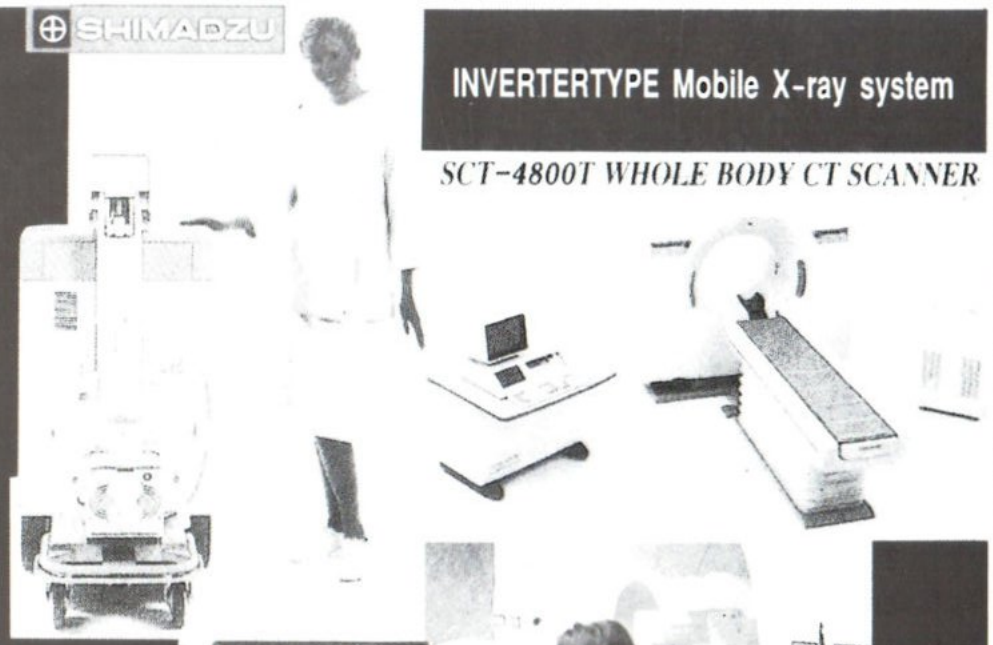

MAGNETIC
RESONANCE
IMAGING

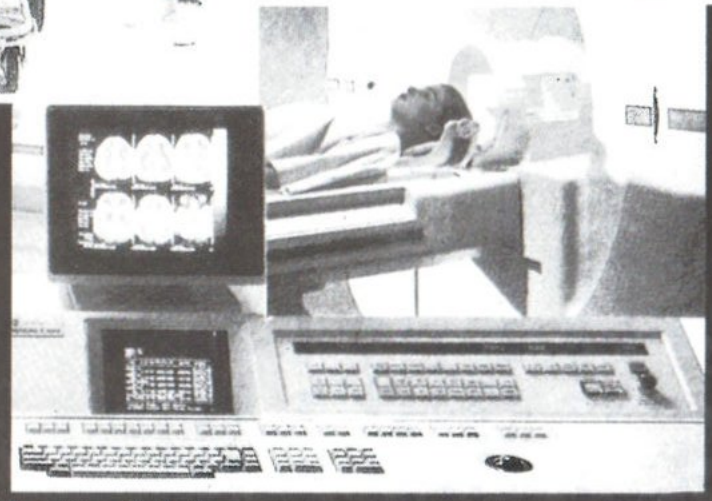

บริษัท รังสิภัณฑ์ จำกัด

RADIOLOGICAL EQUIPMENT CO.,LTD.

170-172/1 (ชั้น 2-3) ถนนบริพัตร ป้อมปราบ กรุงเทพฯ 10100

170-172/1 (Floor 2-3) BORIPHAT ROAD BANGKOK 10100 THAILAND

TEL: 2212386,2237954,2239791,2243402 TELEFAX: (02) 2251657

VERTEBRAL OSTEOMYELITIS AND EPIDURAL INFECTION BY RHODOTORULA RUBRA

Patchrin PEKANAN[1], Wiwatana THANOMKIAT[2],
Pimjai SIRIWONGPAIRAT[1], Janjira CHATCHAVALA[1].

ABSTRACT

We presented a case with mixed fungal infection of the thoracic spine, involving spinal bodies and posterior epidural space in the pregnant woman. Diagnosis was reached only by needle aspiration biopsy. Articles concerning Rhodoturula Rubra were reviewed.

INTRODUCTION

Rhodotorula is a yeast in the family Cryptococcaceae. Its synonyms are Saccharomyces ruber (Demme 1889), Rhodotorula mucilaginosa (Joergensen Harrison 1028), Torulopsis menu (Dodge 1935), Torulopsis sanguines (Ciferri et Redaelli, 1925), Rhodotorula sanniei (Lodder 1934) and 43 names more (Kreger-Van Rjj, 1984). (1). Fungal infections of the spine are uncommon. They frequently occur in immunosuppressed hosts with multiple medical problems. Rhodotorula is an infrequent cause of infection in humans (2).

CASE REPORT

A 28-year-old female patient had paraparesis for 3 months. There was also interscapular pain. The paraparetic symptom was progressively worse and she could not walk without support. She was 28-weeks-pregnant. The lower extremities showed spastic tone on both sides. The vital signs were all normal. Complete blood count, bone marrow aspiration, VDRL, antiHIV, serum histoplasma Ab, Cryptococcal Ag. Pseudomallei AB were all negative.

Plain film of the chest showed left pleural effusion (Fig. 1A). Cytology from the pleural fluid revealed marked lymphocytic infiltration with negative for bacterial culture and AFB stain.

Plain films of the thoracic spine in AP and lateral views showed a right paravertebral mass lesion at the mid thoracic level with slight narrowing intervertebral disc space (Fig. 1B). T1WI and T2WI coronal view MRI scan showed bilateral paravertebral soft tissue lesion at the mid thoracic level. The signal in the marrow of the vertebral body was bright on T2WI; two vertebral bodies were involved (Fig. 2 A). The soft tissue in the posterior central canal, elevating the spinal cord to the anterior aspect was well shown in the axial images (Fig. 2B). Needle aspiration biopsy specimen which was stained with GMS (Gromette's Methamamine Silver) revealed yeast from organisms and the culture of the fungus showed Rhodotorula rubra, Cladosporium Sp and Candida parapsilosis.

The patient refused surgery and was discharged with antifungal agents as a home medication.

DISCUSSION

Rhodotorula is a common airborne fungus found in skin, lungs, urine, and feces. The yeast has been isolated from cheese and mild products, air soil and water. It characteristically produces a coral red pigment (2). The genus Rhodotorula has eight species (3) of which R. rubra is the only species in

[1] Department of Radiology, Ramathibodi Hospital, Rama 6 Street, Bangkok 10400, Thailand.
[2] Department of Radiology, Prince of Songkla University Hospital, Songkla, Thailand

human infection. Infection with Rhodotorula species is rare; thus far, reports include fungemia (4), endocarditis (5), peritonitis (6), meningitis (7) and ventriculitis (8). A pseudoepidemic of Rhodotorula can occur in a hospital when equipment, such as brushes used to clean a bronchoscope, is contaminated (9). Fungemia has been the most common form of Rhodotorula infection. It has occurred typically in patients with cancer (10), bacterial endocarditis (11), or other debilitating diseases (12), who were receiving either chemotherapy for cancer or antibiotics through an indwelling intravenous catheter for other underlying illness. The most common sources of Rhodotorula infection in these cases were contaminated catheters or intravenous solutions (10,12). Once the source of contamination is removed, the symptoms typically disappear and blood cultures become negative for Rhodotorula.

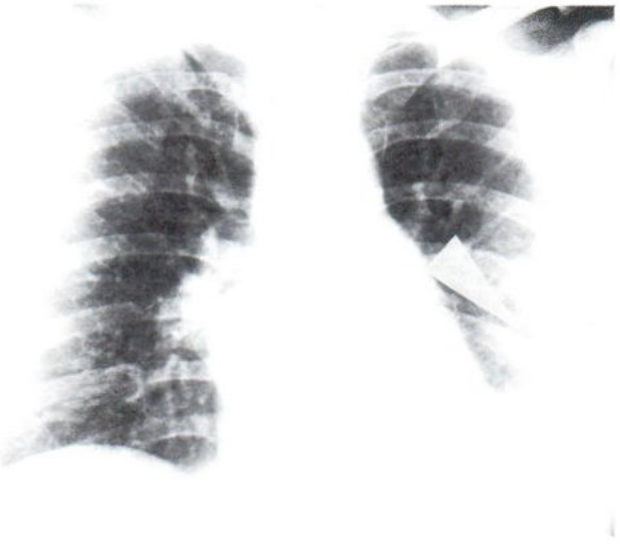

Fig. 1A PA chest film revealed left pleural effusion.

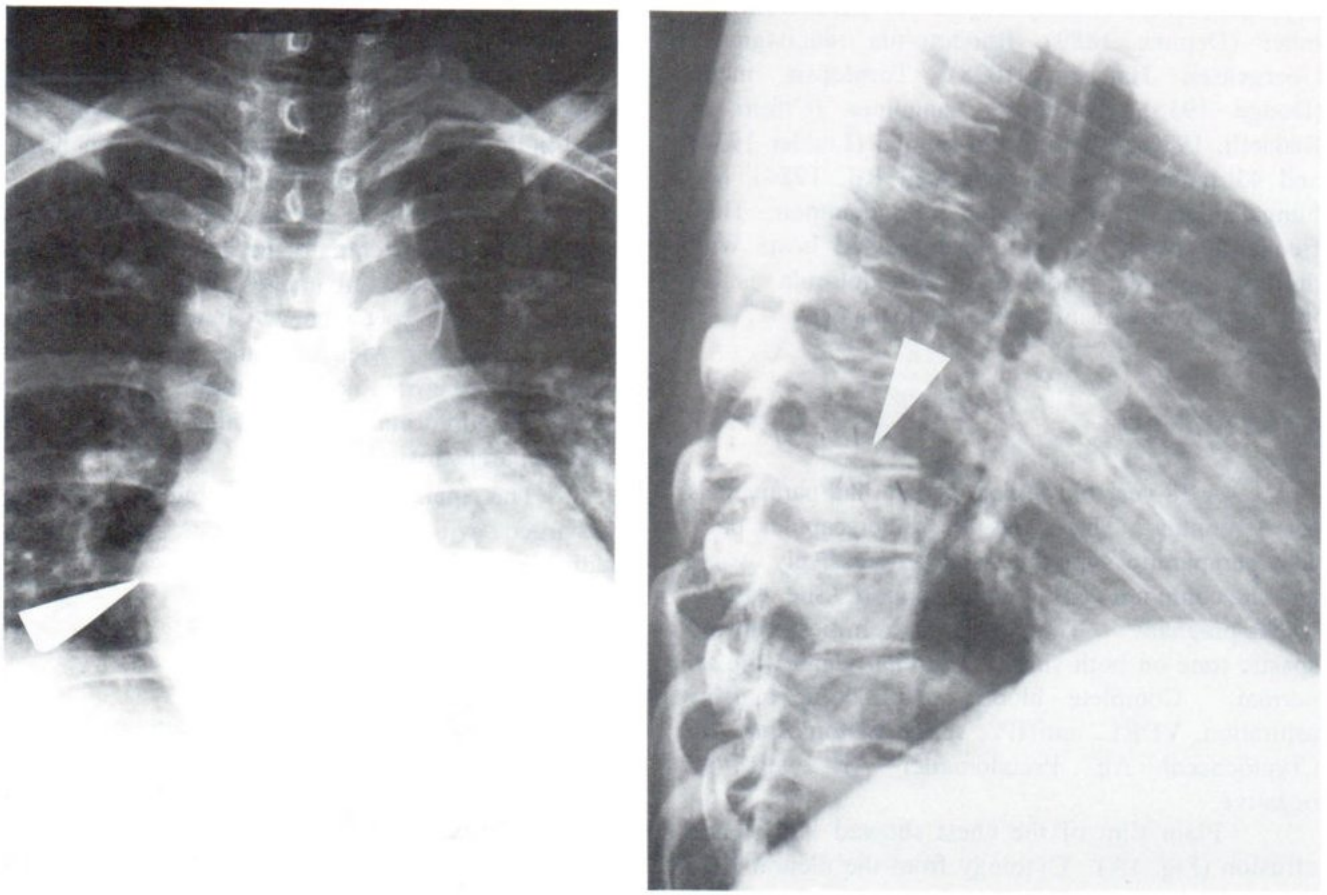

Fig. 1B AP view of the thoracic spine showed right paravertebral soft tissue mass at mid thoracic level. Lateral view of the thoracic spine showed slight narrowing of the involved intervertebral disc with normal end plates.

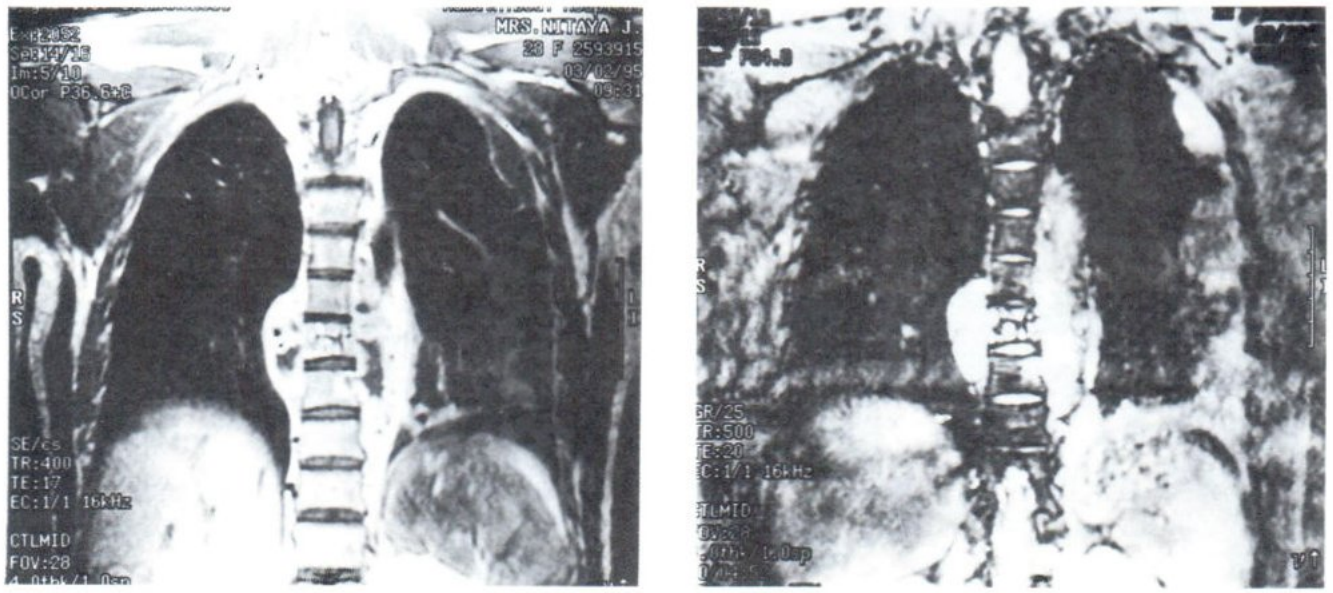

Fig. 2A Gd-DTPA enhanced T1WI coronal view of the thoracic spine showed bilateral paravertebral lesion with enhancement and some low signal areas in the enhanced portion. T2WI-coronal view of the same region showed brightness of the involved spine and the paravertebral soft tissue lesion.

Rhodotorula species do not ferment sugars and can be readily differentiated from the other red yeast, Sporobolomyces, by the lack of billistospore formation and from Cryptococcus species by the lack of inositol assimilation in addition to the presence of bright pigment. In tissue sections or spinal fluid, however, R rubra cells cannot be readily differentiated from those of C neoformans (7).

Infectious spondylitis and epidural abscesses have been caused by nearly all known microorganisms. Although certain radiographic features are characteristic of each type of infection, the diagnosis rests on the evaluation of a tissue specimen.Biopsies must be evaluated with fungal stains as well as cultures, because the latter may be negative or take several weeks or months before identification is possible. Closed biopsy was reported to be positive in only 50 per cent of cases, whereas open biopsy was positive in all cases in the series of Campbell (13). The treatment of fungal infection involves correcting host factors that may compromise wound healing or immune defense capabilities. Antifungal agents are the mainstay of treatment, but surgery frequently is necessary. The approach should be based on the pathologic features encountered, but in general, anterior debridement and stabilization is preferred (13). The prognosis for patients with fungal vertebral osteomyelitis depends on the organism as well as on the host. As with bacterial infections, it appears that patients with diabetes mellitus or neurologic deficits have a poorer prognosis (13).

ACKNOWLEDGMENTS

We thank Dr. Vorachai Sivikulchayanand (Dept. of Pathology) for the pathologic consultant and division of neurology for providing the case.

REFERENCES

1. Warren NG, Shadomy HJ. Yeasts of medical importance. In: Balows A, Hausler WJ Jr. Hermann KL, Isenberg HD, Shadomy HJ, eds. Manual of clinical microbiology. 5th ed. Washington. DC. American Society of Microbiology.1991:617-29.

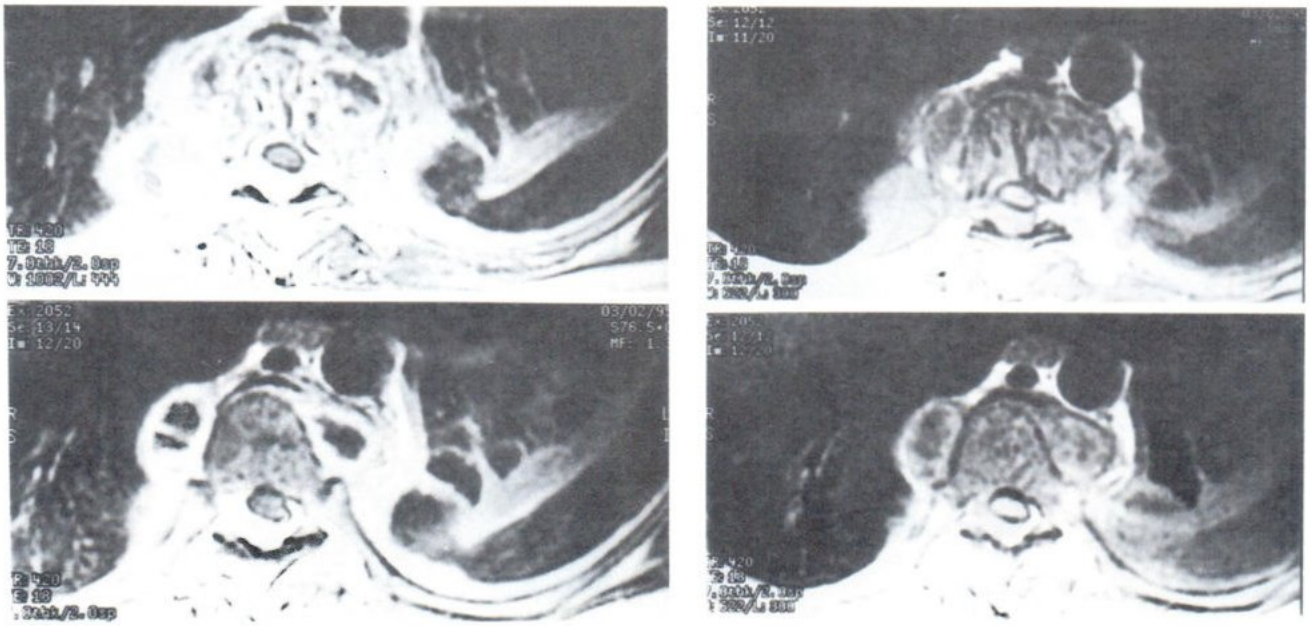

Fig. 2B Enhanced axial T1WI at the lesion revealed clearly the posterior epidural lesion, the anteriorly displaced cord and the bilateral paravertebral soft tissue lesion.

2. Kiehn TE, Gorey E, Brown AE, Edwards FF, Armstrong D. Sepsis due to Rhodotorula related to use of indwelling central venous catheters. Clinical Infectious Diseases 1992;14:841-6.
3. Fell JW, Tallman AS, Ahearn DG. Rhodotorula Harrison. In the Yeasts: A taxonomic study. 3rd Ed. Edited by NJW Kregervan Rjj, Amsterdam, Elsevier Science Publishers 1984:893-905.
4. Anaissie E, et al. New spectrum of fungal infection six patients with cancer. Rev. Infect Dis 1989;369-78.
5. Naveh YA, et al. Endocarditis caused by Rhodotorula successfully treated with 5-fluorocytosine. Br Heart J 1975;37:101-4.
6. Eisenberg Es, et al. Rhodotorula rubra peritonitis in patients undergoing continuous ambulatory peritoneal dialysis. Am J med 1983;75:349-52.
7. Pore RS, Chen J Meningitis caused by Rhodotorula Sabouraudia 1976;14:331-5.
8. Donald FE, Sharp JF, Rhodotorula rubra ventriculitis. J Infect 1968;16:187-91.
9. Koffman KK, Weber DJ, Rutalor WA. Pseudoepidemic of Rhodotorula rubra in patients undergoing fiberoptic bronchoscopy. Infect Control Hosp Epidemiop 1989;10:511-4.
10. Louria DB, Greengerg SM, Molander DW. Fungemia caused by certain nonpathogenic strains of the family Cryptococcaceae, N Engl J Med 1960;263:128-4.
11. Shelbourne PF, Carey RJ Rhodotorula fungemia complicating staphylococcal endocarditis JAMA 1962;180:38-42.
12. Leeber DA. Scher I. Rhodotorula fungemia presenting as endotoxic shock. Arch Intern Med 1969;123:78-81.
13. Campbell DR, Eismont FJ, Garvey T, et al. Diagnosis and treatment of fungal infections of the spine:report of eleven patients (unpublished data).

RHODOCOCCAL PNEUMONIA IN IMMUNOCOMPROMISED PATIENTS:

Wittane NA CHIANGMAI, Sanan SIMARAK

ABSTRACT:

Rhodococcus equi is a recognised pulmonary pathogen in foals,swine,and calves. Most human infection have been associated with immune system dysfunction. We reported four patients with chest involvement from this organism.

INTRODUCTION:

Rhodococcus equi (formerly Corynebacterium equi) is an aerobic, gram positive, weakly acid fast non-motile, non-spore forming, pleomorphic coccobacillus. Rhodococcus equi is a recognised pulmonary pathogen in foals,swine and calves and is an unusual cause of human pulmonary infection. Most human infections have been associated with immune system dysfunction especially in patients with acquired immunodeficiency syndrome.[1,2,3,4,5,6,7,8] We reported four patients,three with AIDS and the other with lupus nephritis whom pulmonary infections were caused by Rhodococcus equi.

CASE REPORTS:

Case 1:

A 22-year-old male with AIDS was seen for complaints of fever, non-productive cough for 1 month. Cervical adenopathy with crepitation and decreased breath sounds over the left upper chest area were detected on physical examination. Chest roentgenogram showed multiple thin-walled cystic lesion in LUL without pleural effusion. (Fig 1) Cultures of the sputum yielded Rhodococcus equi.

Case 2:

A 27-year-old male with AIDS was admitted with a l0-days history of fever, non-productive cough and chest pain. On physical examintion,decreased breath sounds and dullness on percussion at left lower lung area were detected. Chest roentgenogram showed pulmonary consolidation with subsequent cavitation in the lingular segment of the LUL. No pleural effusion was seen. (Fig.2) Cultures of the sputum and blood yielded Rhodococcus equi.

Case 3:

A 37-year-old male with AIDS presented with fever, nonproductive cough and weight loss for 3 months. On physical examination, decreased breath sounds and dullness on percussion at right upper lung area were detected. Chest roentgenogram revealed lung mass in RUL and subsequent CT scan one week later demonstrated irregular thick-walled cavity formation. Neither adenopathy nor pleural fluid were observed. (Fig.3a,3b) Culture of the aspirated pus yielded Rhodococcus equi.

Case 4:

A 25-year-old female with lupus nephritis and history of receiving prednisolone and cyclophosphamide presented with fever,dyspnea and productive cough for l month. On physical examination, only slightly decreased breath sound at the left upper lung area was detected. Chest roentgenogram demonstrated cavitary mass in LUL

Department of Radiology, Faculty of Medicine, Chiang Mai University, Chiang Mai, 50200 THAILAND

with no pleural fluid. (Fig.5) Rhodococcus equi was islolated from sputum culture.

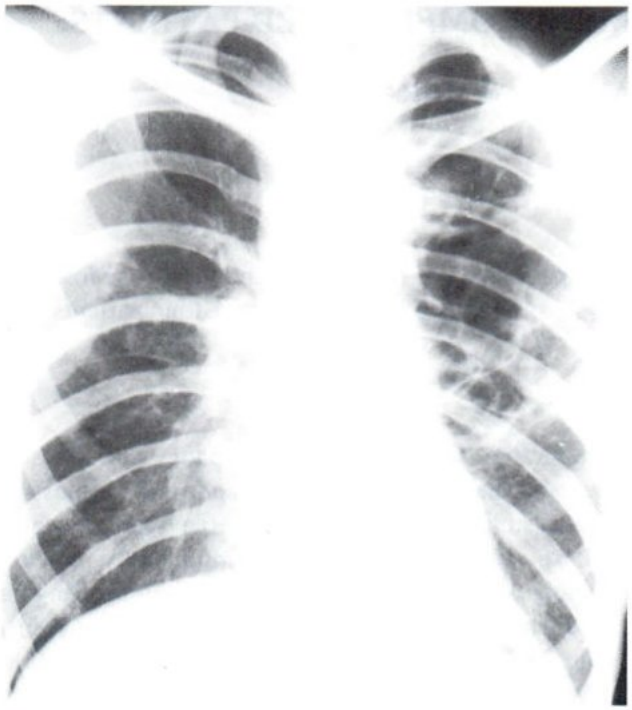

Fig.1 Multiple thin-walled cystic lesions LUL

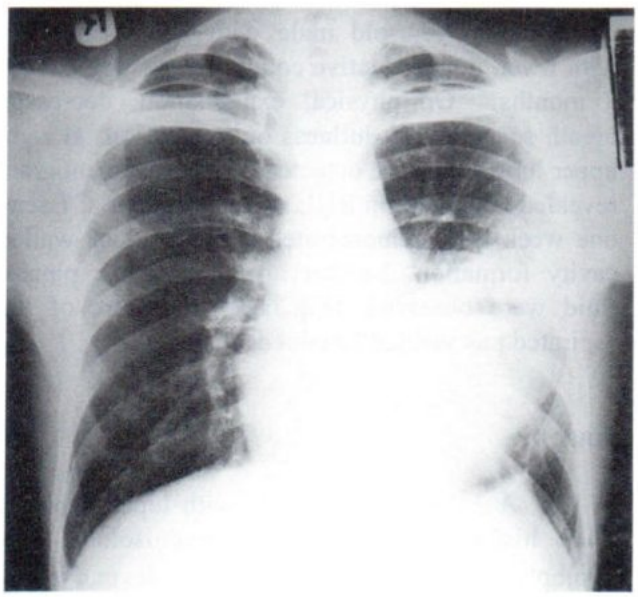

Fig.2 A big cavitary mass lingular segment of LUL

DISCUSSION:

Rhodococcus equi has been a rare cause of disease in humans. Most human infection have been associated with immune system dysfunction, particularly in HIV infection. To date at least 80 cases have been reported.[2] Pulmonary infections are the most common form of human disease caused by this organism. Most published cases of pneumonia have occured in immunocompromised hosts. The typical presentations are subacute onset of high fever, productive or non-productive cough and prominent fatique. Chest pain and weight loss are also common. Pulmonary infection is almost universal ,mass like consolidation progress to cavity formation and is infrequently associated with pleural effusion. Pulmonary infection is diagnosed by cultures of sputum, bronchial lavage fluid, pleural fluid or surgical biopsy specimens. Positive blood cultures are found in about half of the patients. The pathological findings include a necrotizing granulomatous reaction dominated by macrophages containing gram positive pleomorphic coccobacilli. Management requires a prolong course of at least 2 antibiotics. Clinical and radiographic progression often occurs and surgical resection has been performed in some cases. Our patients were immunocompromised hosts due to HIV infection and lupus nephritis. They had typical features of subacute onset of fever, cough and chest pain. Two patients developed pulmonary consolidation with subsequent cavity formation. One case presented with cavitary mass and the last one had multiple thin-walled cystic lesions. In immunocompromised patients who present with cavitary pneumonia,besides the possibility of tuberculous infection, other common causes include gram negative bacteria. The uncommon cause include MAI, nocardia, fungi and Rhodococcus equi. We suggested that Rhodococcus equi infection should always be considered in the differentail diagnosis in HIV infected patients who present with cavitary pneumonia of subacute onset.

ACKNOWLEDGEMENT:

The authors wish to thank Dr. Malai Muttarak for her encouragement and permission to report these cases.

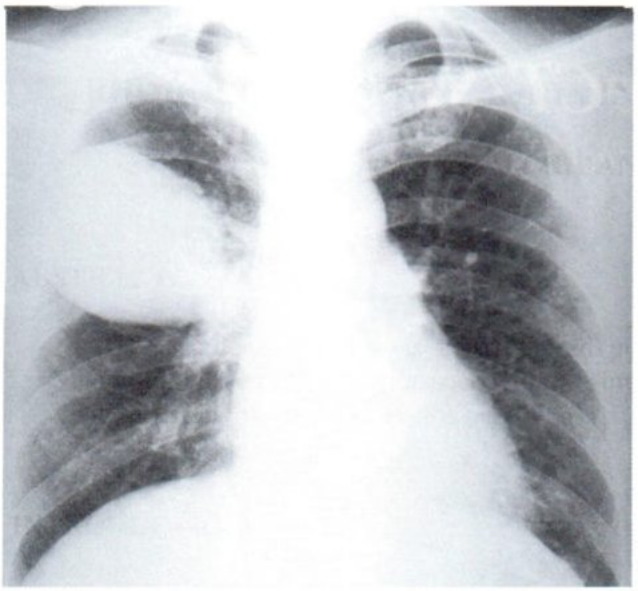

Fig 3a. Mass like consolidation RUL

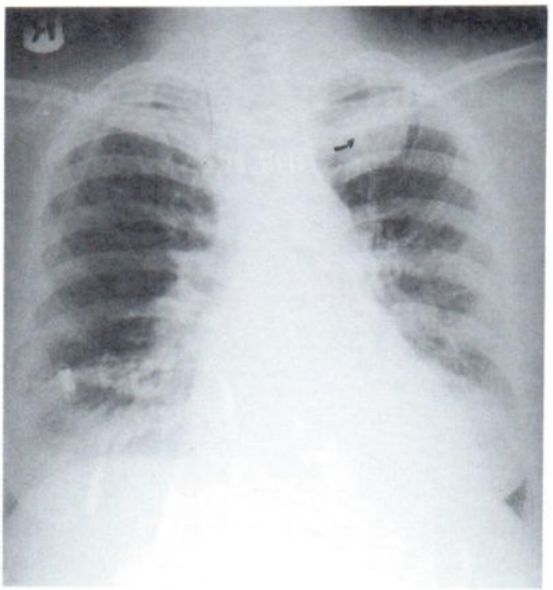

Fig.4 Cavitary mass lesion LUL

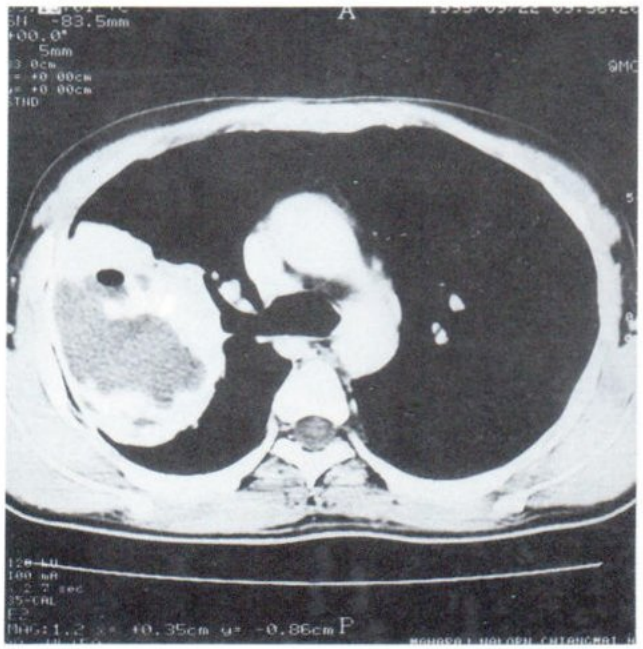

Fig.3b Large irregular thick-walled cavity RUL

REFERENCES:

1. Vestbo J, Lundgren JD, Gaub J, Roder B, Gutschik E,. Severe Rhodococcus equi pneumonia: case report and literature review. Eur J Clin Microbiol Infect Dis. 1991 Sep;10(9) :762-8.
2. Verville TD, Huycke MM, Greenfield RA, Fine DP, Kuhls TL, Slater LN. Rhodococcus equi Infections of Humans: 12 Cases and a Review of the Literature. Medicine,1994 May;73(3) :119-132.
3. Lasky JA, Pulkingham N, Powers MA, Durack DT. Rhodococcus equi causing human pulmonary infection: review of 29 cases. South Med J 1991 Oct;84(10)1211-20.
4. Doig C, Gill MY, Chorch DL. Rhodococcus equi-an easily missed opportunistic pathogen. Scan J Infect Dis. 1991;23(1):1-6.
5. Drancourt M, Bounet E, Gallais H, Peloux Y, Raoult D. Rhodococcus equi infection in patients with AIDS. J Infect. 1992 Mar;24(2) :123-31.
6. Autinori S, Meroni L, Esposito R, Rhodococcus equi pneumonia in a patient with AIDS: radiologic feature (letter) Am J Roentgenol.1993 Oct;161(4):901-2.
7. Mayor B, Jolidon RM, Wicky S, Giron J, Schnyder P. Radiologic findings in two AIDS patients with Rhodococcus equi pneumonia J Thorac Imaging. 1995 Spring;10(2)121-5.
8. Scott MA, Craham BS, Verrall R, Dixon R, Schaffner W, Than KT. Rhodococcus equi-an increasingly recognized opportunistic pathogen. Report 12 cases and review of 65 cases in the literature AM J Clin Pathol 1995 May; 103(5) :649-55.

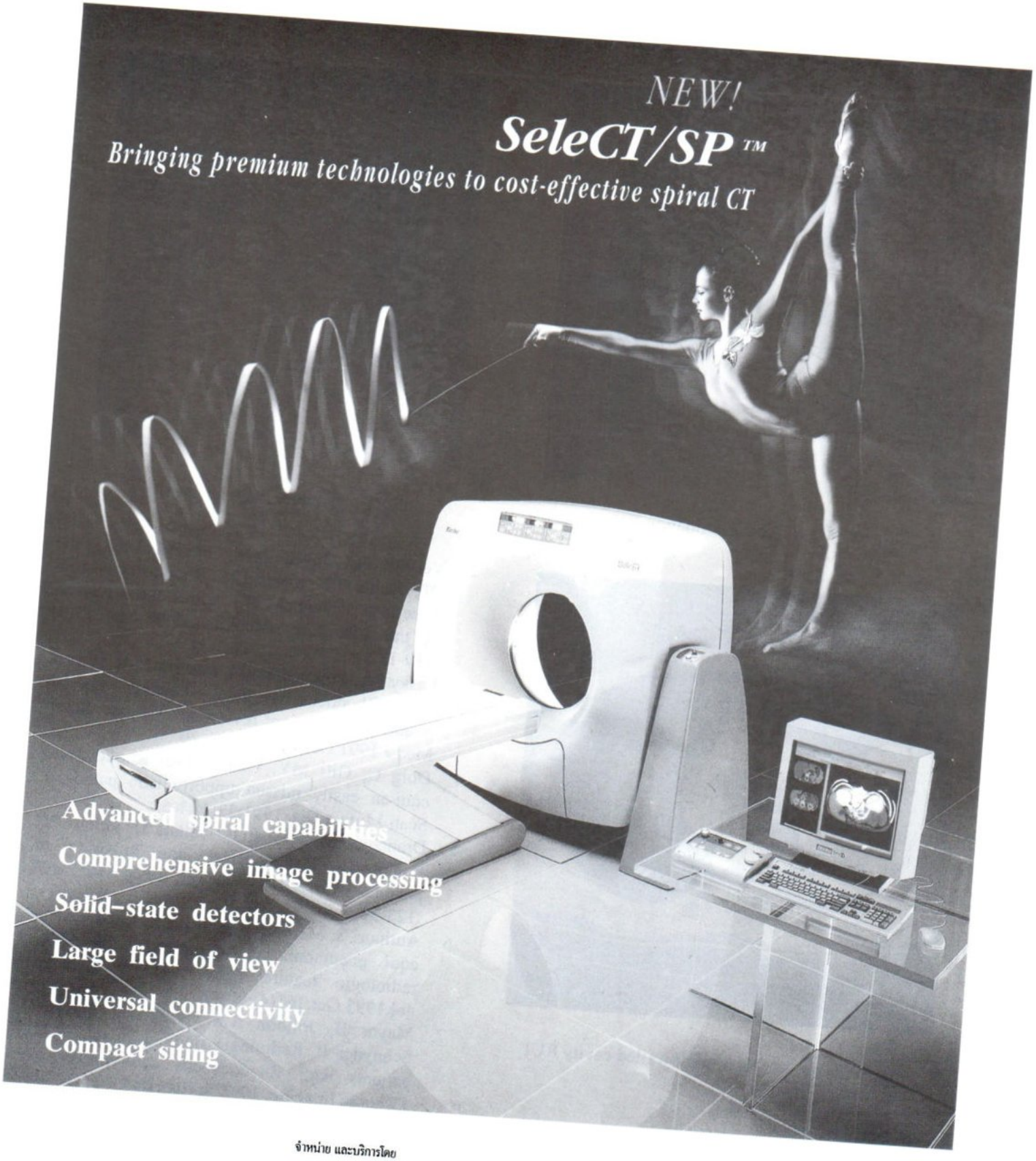

จำหน่าย และบริการโดย

supreme PRODUCTS CO.,LTD.

บริษัท สุพรีม โพรดักส์ จำกัด

163/81-82 ถ.พระปิ่นเกล้า แขวงบางยี่ขัน เขตบางพลัด กรุงเทพฯ 10700 แผนกขาย 434-0040,434-0050 แผนกบริการ 434-0060 โทรสาร 433-3971

DIFFUSE PULMONARY INFILTRATION BY PENICILLIUM MARNEFFEI INFECTION IN A PATIENT WITH HUMAN IMMUNODEFICIENCY VIRUS INFECTION

Patchrin PEKANAN[1], Sopon KUMPOLPUNTH[1],
Panpen UTTAMAKUL[1,2], Sompoj JITKASEMSUK[1,2].

ABSTRACT

A 31 years old male patient with HIV infection, had weight loss and cough. Diffuse reticulonodular lesions was seen on chest film in both lung fields, with lower lungs predominance. Multiple skin nodules were also present. Penicillium marneffei infection was proved by gram stain. Treatment of the mentioned pathogen resulted in complete disappearance of the pulmonary lesions. Review of the articles concerning this matter was presented.

INTRODUCTION

Penicillium marneffei, is a rare human fungal pathogen (1,2). Disseminated P. marneffei infection is endemic in Southeast Asian countries and China (1-4). The number of patients with this systemic mycosis is rising rapidly, especially in Thailand (5). This abrupt increase corresponds with the recent rapid increase in the number of cases of human immunodeficiency virus (HIV) infection (5). We report a case of systemic infection due to P. marneffei in an HIV-infected patient with skin and lung involvement.

CASE REPORT

A 31-year-old male patient had weight loss, and cough for 2 months. Chest film showed diffuse reticulonodular lesions in both lungs, more predominant at lower half of the lung fields. The heart size and pulmonary vasculature appeared normal. There was no pleural fluid. Multiple skin nodules was noted and the gram stain and culture of the skin lesion revealed Penicillium marneffei infection. Anti-HIV was positive. The treatment to the organism was given and the chest film 2 months later showed complete disappearance of the pulmonary lesions. (Fig. 1)

DISCUSSION

The clinical features of systemic P. marneffei infection are described (2-4, 6-8). Patients can range in age from infants to those over 60 years old. The patients are predominantly male, the male to female ratio being 4.5 to 9.0 to 1. Many patients are healthy before developing infection, but some have underlying diseases such as SLE or Hodgkin's disease. The incidence of infection caused by this fungus has recently been reported as increased in patients with HIV infection (3,6,8,9). Most patients have fever, anemia, hepatomegaly, splenomegaly, lymphadenopathy, subcutaneous abscesses and skin lesion.

The diagnosis of systemic P. marneffei infection is usually made by demonstrating the organism in smears of a skin lesion specimen and/or bone marrow and by culturing the organism from blood, bone marrow, and/or skin biopsy specimen (1,3).

Eight cases of bone and joint infection by this organism was reported by Louthrenoo W, et al (8). A case of cervical osteomyelitis and retropharyngeal abscess with upper airway obstruction was reported by Fu Ko K, et al (11).

In general, there are three distinctive tissue reactions to P. marneffei infection: granulomatous,

[1] Department of Radiology, Ramathibodi Hospital, Rama 6 Street, Bangkok 10400, Thailand.
[2] Department of Radiology, Songklanakarin University Hospital, Haadyai Songkla, Thailand.
[3] Department of Radiology, Mongkutwatana Hospital, Bangkok 10400, Thailand.

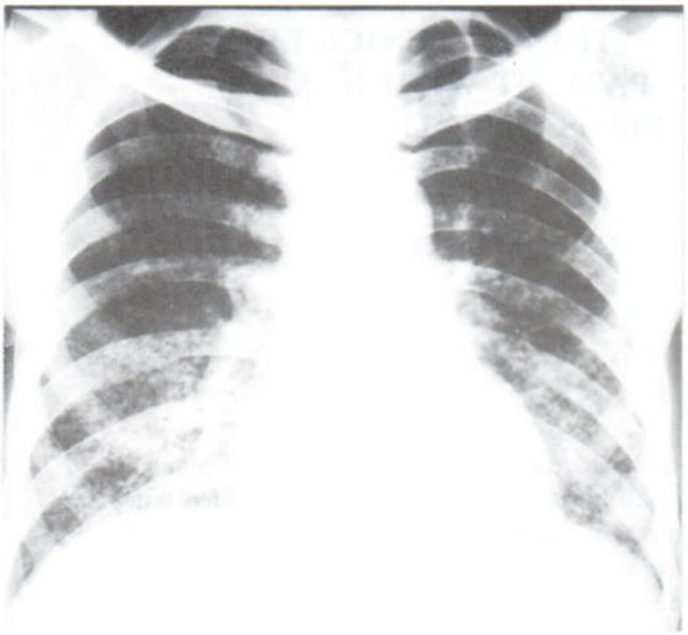

Fig. 1a PA chest film showed diffuse reticulonodular lesions in both lungs with more lower lung fields predominance

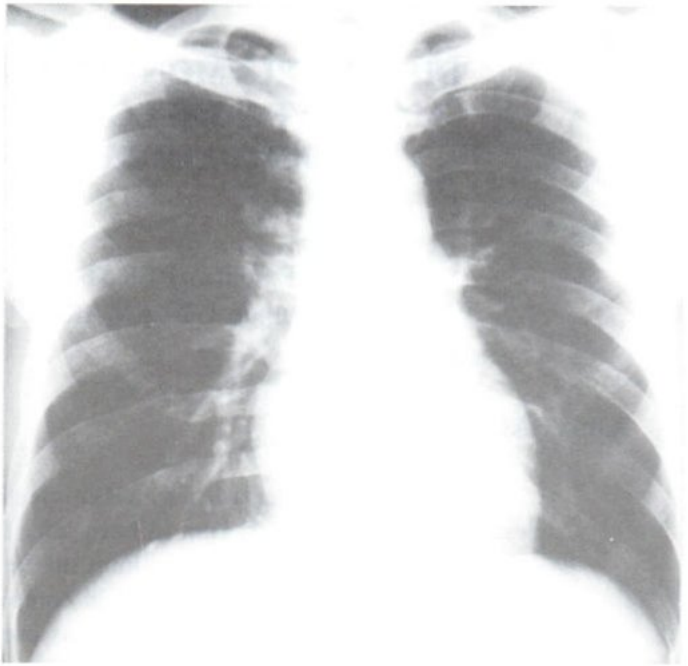

Fig. 1b Follow up chest film two months later showed complete disappearance of the lesions.

suppurative and anergic with necrosis (10). The granulomatous pattern consists of epitheloid granulomas with multinucleated giant cells, organisms are usually sparse and difficult to demonstrate. This form of reaction is seen in patients with normal immunity and is seen especially in organs of the mononuclear phagocytic system. The second form of reaction, suppuration with multiple abscesses, develops in a variety of organs but is common in the lungs, skin and subcutaneous tissue of patients with normal immunity. The suppuration is a reaction by neutrophils and fibrin to the numerous yeast-like cells.

The anergic and necrotizing is characterized by a diffuse infiltrate of histiocytes distended by proliferating fungi and focal necrosis. This pattern indicates a progressive and disseminated infection and is typically seen in patients with compromised immunity. Disseminated histoplasmosis closely mimics penicilliosis marneffei both in histological tissue reaction and in the morphology of the organism (10).

Most of the reported cases of natural infection had occurred in residents of Southeast Asia or visitors to the region. The natural reservoir is not known but the fungus appears to be freely present in the environment. The fungus may be inhaled and cause a primary pulmonary infection before dissemination, or it may be ingested and invade the intestine and liver as the first stage in dissemination (10).

Three patterns of pulmonary infiltration were reported by Supparatpinyo (5) by chest roentgenography. They were diffuse reticulonodular infiltrations as in our case, localized interstitial infiltrations and localized alveolar infiltrations. However, images were not shown in their report.

REFERENCES

1. Supparatpinyo K, Sirisanthana T. Disseminated Penicillium marneffei infection diagnosed on examination of a peripheral blood smear of a patient with human immunodeficiency virus infection. Clinical Infectious Diseases 1994; 18: 246-7.
2. Jayanetra P, Nitiyanant P, Ajello L. Penicilliosis marneffei in Thailand: report of five human cases. Am J Trop Med Hyg 1984; 33: 637-44.
3. Deng Z, Conner DH. Progressive disseminated penicilliosis caused by Penicillium marneffei: report of eight cases and differentiation of the causative organism from Histoplasma capsulatum Am J Clin Pathol 1985; 84: 232-7.

4. Deng Z, Ribas JL, Gibson DW, Conner DH. Infection caused by Penicillium marneffei in China and Southeast Asia: review of eighteen published cases and report of four more Chinese cases. Rev Infect Dis 1988; 10: 640-52.
5. Supparatpinyo K, Chiewchanvit S, Hirunsri P, Uthammachai C, Nelson KE, Sirisanthana T. Penicillium marneffei infection in patients infected with human immunodeficiency virus. Clin Infect Dis 1992; 14: 871-4.
6. Hilmarsdottir I, Meynard JL, Rogeaux O. Disseminated Penicillium marneffei infection associated with human immunodeficiency virus: a report of two cases and a review of 35 published cases. J AIDS 1993; 6: 466-74.
7. Disalvo AF, Fickling Am, Ajello L. Infection caused by Penicillium marneffei: description of first natural infection in man. Am J Clin Pathol 1973; 60: 259-63.
8. Louthrenoo W, Thamprasert K, Sirisanthana T. Osteoarticular Penicilliosis marneffei. A report of eight cases and review of the literature. British Journal of Rheumatology 1994; 33: 1145-4450.
9. Piehl MR, Kaplan RL, Haber MH. Disseminated penicilliosis in a patient with acquired immunodeficiency syndrome. Arch Pathol Lab Med 1988; 112: 1262-4.
10. Tsui WMS, Ma KF, Tsang DNC. Disseminated Penicillium marneffei infection in HIV-infected subject. Histopathology 1992; 20: 287-293.
11. Fu Ko K. Retropharyngeal abscess caused by Penicillium marneffei: An unusual cause of upper airway obstruction. Otolaryngol Head Neck Surg 1994; 110: 445-6.

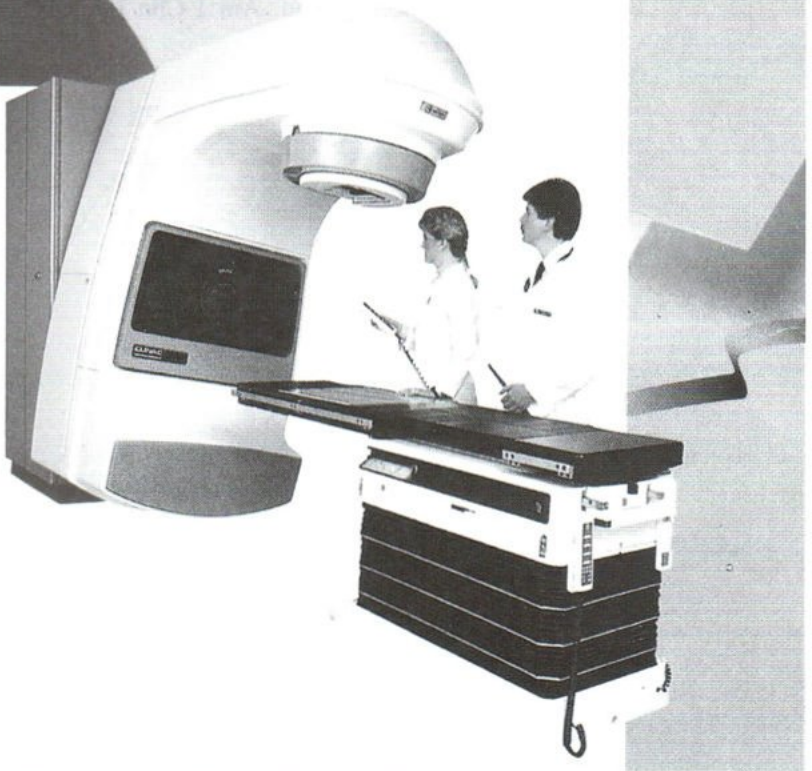

CLINAC 2100C

The standard in dual energy performance and operational efficiency.

The Clinac 2100C dual energy, standing-wave accelerator provides cost-effective, multi-modality treatments with a choice of x-ray energy combinations from 6 to 18 MV, literally two accelerators in one, and one of four electron combinations from 4 to 20 MeV.

The Clinac 2100C meets your unique clinical requirements with options like dual independent collimators, high dose-rate electrons, and electron arc therapy.

As with all the C-Series products, the Clinac 2100C can be linked to the RMS-2000 Radiotherapy Management System for efficient data entry and treatment verification.

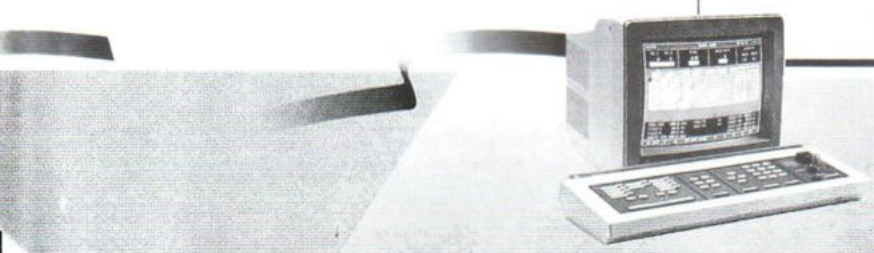

CTI TRADING CO.,LTD

415/9-10 MAHAPRUCKTARAM RD., BANGRAK, BANGKOK 10500
TEL: DIRECT LINE 234-6793, 234-5628, 233-3382
OPERATOR 233-1748, 233-1754, 233-1780
233-1787, 233-3383, 233-7724, 233-7803
FAX: 233-0794, 236-3190, 233-9660, TELEX: 22236 TRISIAM TH

DISSEMINATED COCCIDIOIDOMYCOSIS WITH RADIOGRAPHIC IMAGING OF THE INVOLVED BONES

Patchrin PEKANAN, Boonchuay SATAPATAYAVONGS, Pimjai SIRIVONGPAIRAT, Virat NGERNYAM

ABSTRACT

Bony lesions of a case of disseminated Coccidioidomycosis was presented. The lesions were observed to be small, ill defined border, and osteolytic. There was no periosteal reaction. The lesions usually located at either end or at the lateral or medial margin of the involved long-tubular bones. Roentgenographic arthritis or bursitis was evident at both ankle joints.

INTRODUCTION

Coccidioidomycosis results from inhalation of the fungus Coccidioides immitis in endemic areas of the Southwestern portion of the United States, in Mexico, and in some regions of South America. The fungus, which is an inhabitant of soil, is disseminated in dust. Following inhalation, the organisms lodge in the terminal bronchioles and alveoli of the lungs where an inflammatory reaction may ensue. In some individuals, disseminated disease may develop, with spread of infection to the liver, spleen, lymph nodes, skin, kidney, meninges, pericardium, and bones, as well as other sites. Men and women are affected equally, although the disseminated form is more common in men. Blacks, Mexican Indians and Fillipinos are especially susceptible. Pregnancy has a detrimental effect on the course of the disease. Patients younger than 5 years of age or older than 50 years of age account for a large proportion of cases with the disseminated form of the disease. Clinical manifestations vary in accordance with the distribution of the lesions, and in cases of wide dissemination, the mortality rate is high (1).

CASE REPORT

A Thai-male patient, age 27-years old, resided in the USA for a certain period. He was a known case of coccidioidomycosis for a year and was treated with Amphotericin B for 6 months. He was referred to his home-country for further treatment. He also had swelling of the wrist and ankle and decreased elasticity of the skin. Skin biopsy showed scleroderma. Bone biopsy at the medial malleolus, and the distal end of the 2nd metacarpal bone revealed coccidioidomycosis. During the hospital stay, multiple subcutaneous abscesses, meningitis and abrupt personality change were observed. Finally he was cardiac arrested. The autopsy revealed generalized coccidioidomycosis involving the pituitary gland, brain, lungs, liver, spleen and both kidneys.

Plain film of both elbows showed ill defined border osteolytic areas at supracondylar region of both distal humeri. Similar osteolytic lesions were seen at the left distal clavicle, both acromions, medial and lateral malleolus of both sides, distal metaphyses of metacarpal bones of both hands, proximal part of proximal phalanx of right 5th one (Fig. 1-4).

Other bones were not involved and the lungs appeared without infiltration.

Noteworthy mention was that this case was presented to us 27 years ago (in 1969).

Department of Radiology, Ramathibodi Hospital, Rama 6 street, Bangkok 10400, Thailand.

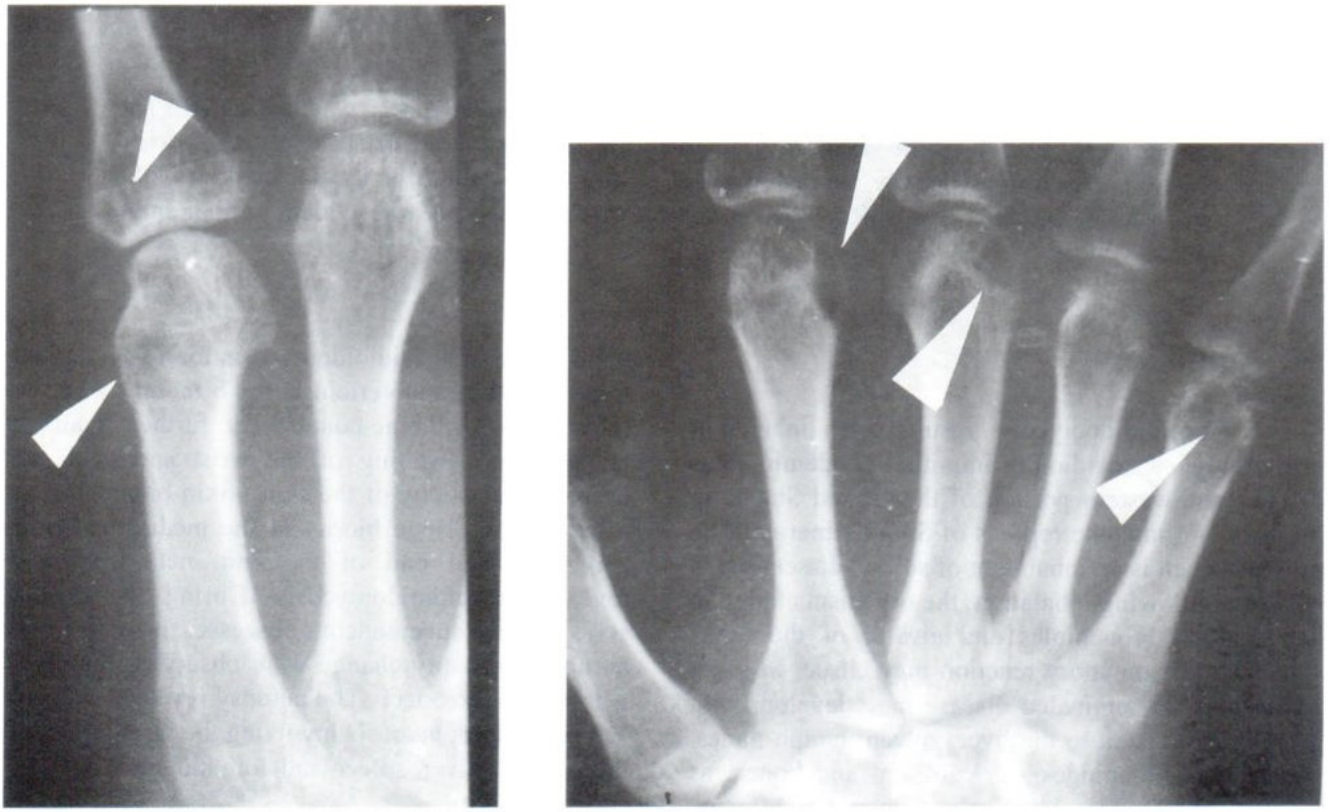

Fig. 1 AP view of both hands showed ill defined border-osteolytic foci at right 5th proximal phalanx, right 5th metacarpal bone, distal epiphyses of the left 2nd, 3rd and 5th metaca rpal bones.

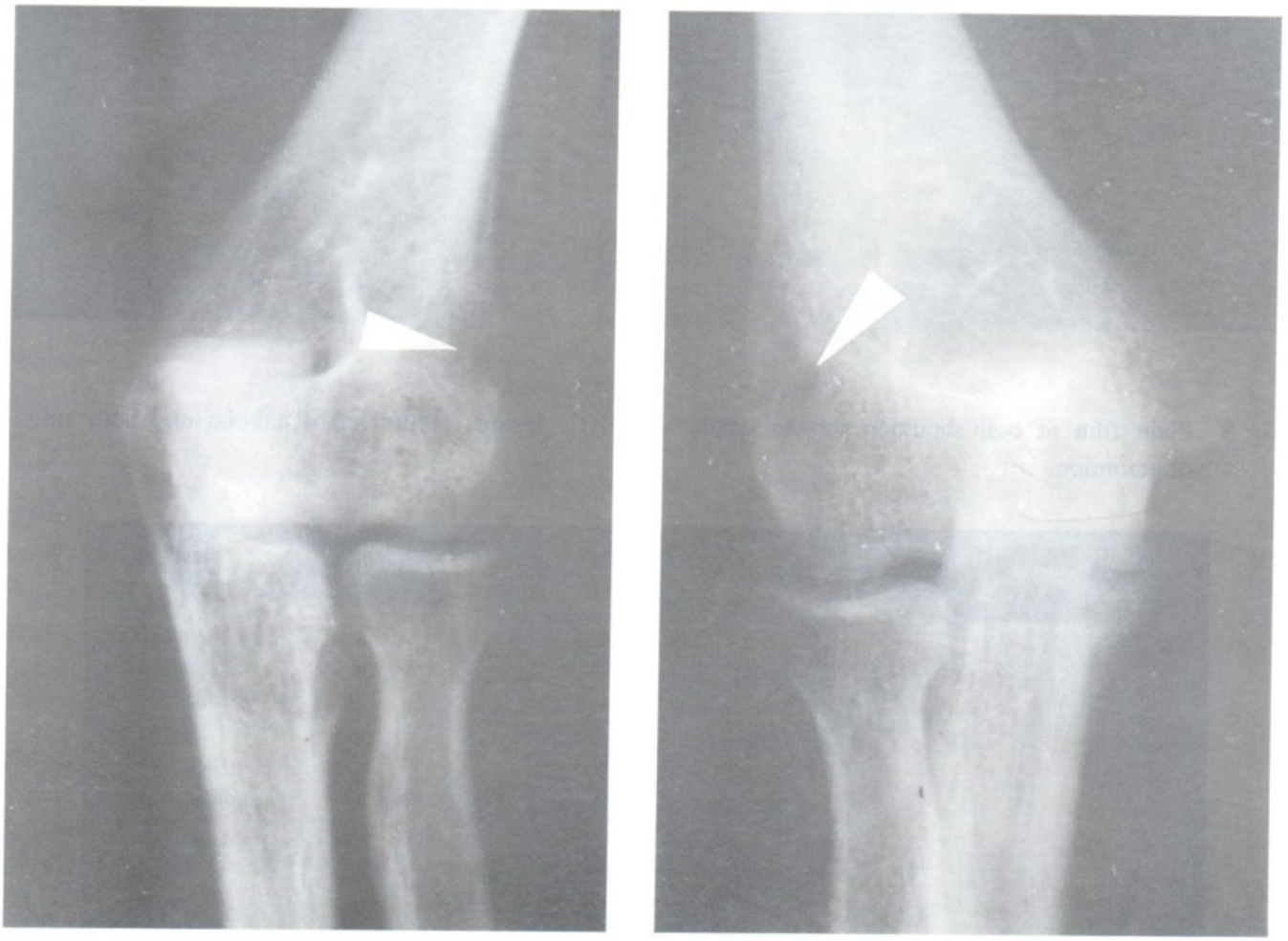

Fig. 2 Plain film of both elbows in AP view showed ill defined border small osteolytic foci at lateral supracondylar areas of both distal humeri

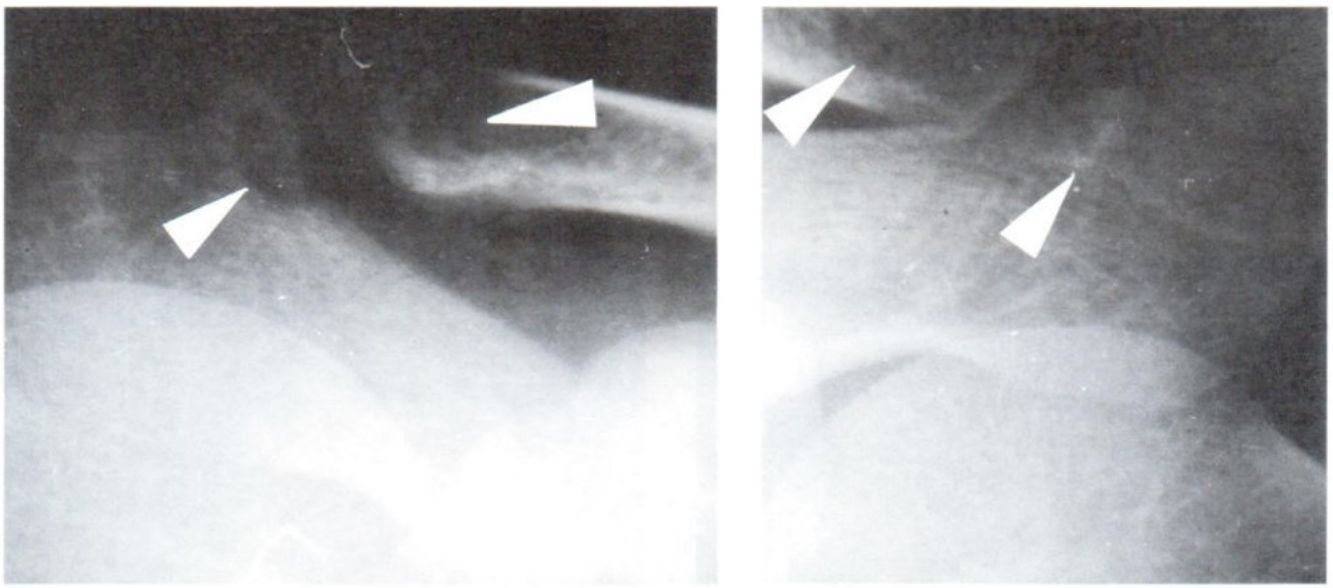

Fig. 3 Plain film of both shoulders showed similar osteolytic lesions at the left distal clavicle, both sides of acromion.

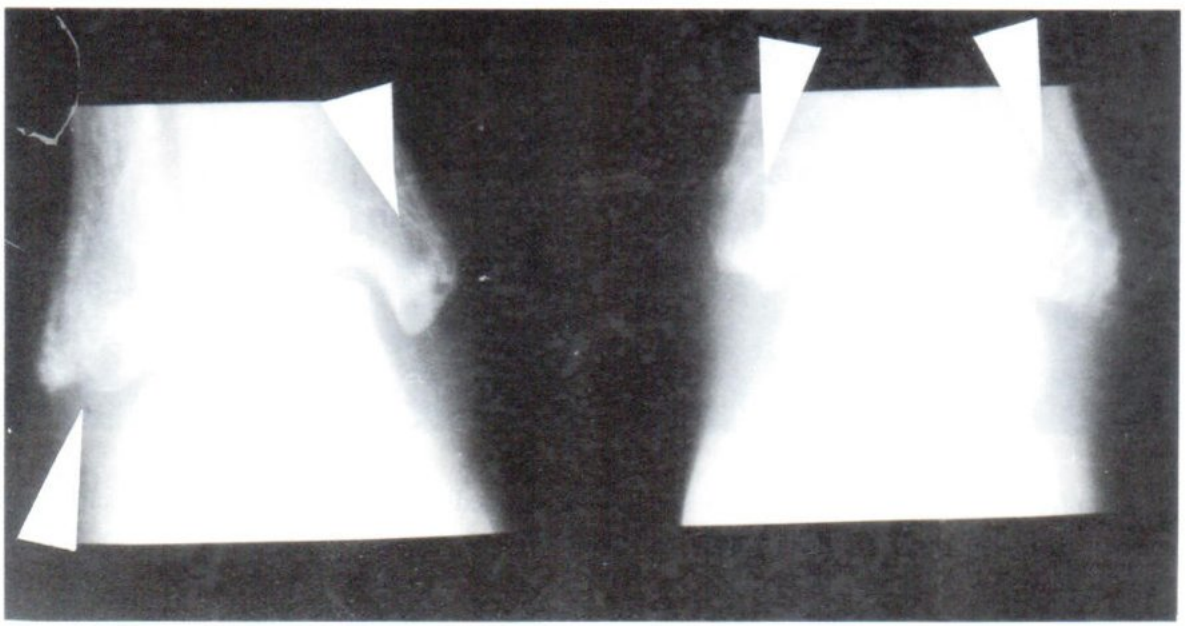

Fig. 4 AP view of both ankles revealed soft tissue swelling around both ankle joints. Small osteolytic areas are noted at the lateral and medial malleoli of both ankles, medial margin of the talus. The joint spaces appeared normal.

DISCUSSION

An acute, self-limited arthritis may develop in about 33 per cent of cases of coccidioidomycosis (1,2). Ten to 20 per cent of patients develop granulomatous lesions in the bones and the joints. In most cases, bone alterations relate to hematogenous spread, although cutaneous infection can lead to contamination of subjacent bones (and joints). Osseous involvement can be confined to a single bone (1,3,4) or multiple, symmetrically distributed bony foci (5). Involvement of the spine, the ribs, and the pelvis predominates, although any bone can be affected (1,5-8). Symptoms and signs can be prominent, even in the initial phases of the disease, and consist of pain, swelling and draining abscesses (1,9).

Radiographs frequently reveal multiple osseous lesions in the metaphyses of long tubular bones and in bony prominences (patella, tibial tuberosity, calcaneus, ulnar olecranon) (1). In the bones of the hands and the feet, diaphyseal alterations are also common. Well demarcated lytic foci of the spongiosa are typical. Periostitis can be seen, but bony sclerosis and sequestration are unusual. Lesions involving the ribs are typically marginal in location and can be associated with prominent extrapleural masses (5). In the spine, abnormalities of one or more vertebral bodies with paraspinal masses and contiguous rib changes are typical. There is relative sparing of the intervertebral discs, and vertebral collapse and fistulous tracts are uncommon and late manifestations. Rarely, significant vertebral sclerosis in coccidioidomycosis may simulate the changes that accompany neoplasm (metastatic disease from prostate carcinoma) (8,10).

Joint involvement is most common in the ankle and the knee, although other articulations of the appendicular and axial skeleton may be the site of an infective arthritis (11-13). In general, articular changes result from extension of an osteomyelitic focus, although, rarely direct hematogenous implantation of the organisms into a joint can occur. Monoarticular involvement is most typical. Synovial inflammation and cartilaginous and osseous erosion lead to radiographic findings (osteoporosis, effusion, joint space narrowing, bony destruction) simular to those in other granulomatous articular infections. In other cases, a sterile migratory polyarthritis without radiographic changes may be representative of a hypersensitivity syndrome (13).

Coccidioidal bursitis and tenosynovitis of the hand and wrist have been reported (14-16).

Biopsy of skeletal or articular foci in this disease reveals granulomatous lesions similar to those of tuberculosis (17); monocytes, giant and epithelial cells, necrosis, and caseation are identified (18). Accurate differentiation of coccidioidomycosis and tuberculosis requires isolation of the causative agent.

REFERENCES

1. Resnick & Niwayama. Diagnosis of bone and joint disorders. 2nd ed. Philadelphia: W.B. Saunders company, 1988:2771-8.
2. Dickson EC, Gifford MA. Coccidiodes infection (coccidiodomycosis). Primary type of infection. Arch Intern Med 1938;62:853.
3. Conaty JP, Biddle M, McKeever FM. Osseous coccidioidal granuloma. J Bone Joint Surg (Am) 1959;41:1109.
4. Thorpe CD, Cojut HJ. Coccidioidal osteomyelitis in a child's finger. A case report. J Bone Joint Surg (Am) 1985;67:330.
5. Dalinka MK, Dinnenberg S, Greendyke WH, Hopkins R. Roentgenographic features of osseous coccidioidomycosis and differential diagnosis. J Bone Joint Surg (Am) 1971;53:1157.
6. Wesselius LJ, Brooks RJ, Gall EF. Vertebral coccidioidomycosis presenting as Pott's disease. JAMA 1977;238:1397.
7. Santos GH, Cook WA. Vertebral coccidioidomycosis. Unusual polymorphic disease. NY State J Med 1972;72:2784.
8. Eller JL, Siebert PE. Sclerotic vertebral bodies: An unusual manifestation of disseminated coccidioidomycosis. Radiology 1969;93:1099.
9. Bried JM, Galgiani JN. Coccioides immitis infections in bones and joints. Clin Orthop Rel Res 1986;211:35.
10. McGahan JP, Graves DS, Palmer PES. Coccidioidal spondylitis. Usual and unusual radiographic manifestations. Radiology 1980; 136:5
11. Retting AC, Evanski PM, Waugh TR, Prietto Ca. Primary coccidioidal synovitis of the knee. A report of four cases and review of the literature. Clin Orthop Rel Res 1987;132:187.
12. Pankovich AM, Jevtic MM. Coccidioidal infection of the hip. A case report. J Bone Joint Surg (Am) 1973;55:1525.

13. Bayer AS, Guze LB. Fungal arthritis. II.Coccidioi dal synovitis. Clinical diagnostic, therapeutic, and prognostic considerations. Semin Arthritis Rheum 1979;8:200.
14. Iverson RE, Vistnes LM. Coccidioidomycosis tenosynovitis in the hand. J Bone Joint Surg (Am) 1973;55:413.
15. Danzing LA, Fierer J. Coccidioidomycosis of the extensor tenosynovium of the wirst. A case report. Clin orthop Rel Res 1977;129:245.
16. Winter WG, Larson RK, Honeggar MM, Hacobsen DT, Pappagianis D, Huntington RW. Coccioidal arthritis and its treatment-1975. J Bone Joint Surg (Am) 1976;57:1152.
17. Jaffe HL. Metabolic, degenerative and inflammatory diseases of bones and joints. Philadelphia, Lea & Febiger, 1972.
18. Pritchard DJ. Granulomatous infections of bones and joints. Orthop Clin North Am 1975;6:1029.

OSTEOBLASTOMA OF THE CERVICAL SPINE

Patchrin PEKANAN, Chitchanok TANTIWIWAT,
Pimjai SIRIWONGPAIRAT, Sirintara PONGPECH

ABSTRACT

An osteoblastoma lesion was shown at left lateral element of cervical level and left neural foramen. Plain x-ray and CT images showed an expansion of the involved bone, osteolytic blackground with calcified / ossified matrix. Rich blood supply to the tumor nidus was observed and the dense tumor stain was at the capillary phase. The staining was rather homogeneous.

INTRODUCTION

Osteoid osteoma and osteoblastoma have identical histologic features but differ in size, sites of origin and symptoms. By definition, osteoid osteomas are less than 2 cm in greatest dimension and osteoblastomas are larger (1).

Osteoblastoma occurs in the second and third decades of life (75% of patients are less than 25 years old), and males outnumber females 2:1. Osteoblastoma involves the spine more frequently, it may not be painful, or if pain is present, it is dull, achy, and not very responsive to salicylates; and it is not associated with a marked bony reaction. It is readily treated by conservative surgery; if not entirely excised, they can recur. The possiblility of malignant transformation is remote except when tumors are treated with radiation, which promotes this dreaded complication.

Plain radiographs, CT images and angiographic pictures of this tumor at the lateral elements of the cervical spine was presented.

CASE REPORT

A 22-year-old man presented with a complaint of pain at his left side of the neck for one year. The pain persisted at both day and night time. There was no radiating pain.

Plain radiographic films of the cervical spine in AP and lateral views showed a lesion at the left lateral element of C5. A round nidus had well defined border and calcified matrix area (Fig.1). The curve of the cervical spine was straightened. The disk spaces appeared normal. CT images revealed better information. The lesion was an expanding one, involving the pedicle, lamina, and the facet of left side of C5. The left C5-6 neural foramen was occupied by the lesion. The left C5 transversarium foramen was narrow due to the posterior wall involvement. The expanding component had a radiolucent background with calcified / ossified matrix. Epidural space of left central canal was mildly occupied. There was no density change of the adjacent back muscle (Fig. 2). Branches of the thyrocervical artery supplied the nidus with strongest staining at the capillary phase (Fig. 3).

Surgery was performed with partial removal of the mass at left lamina area and the section revealed an osteoblastoma (Fig. 4).

Department of Radiology, Ramathibodi Hospital, Rama 6 Street, Bangkok 10400, Thailand.

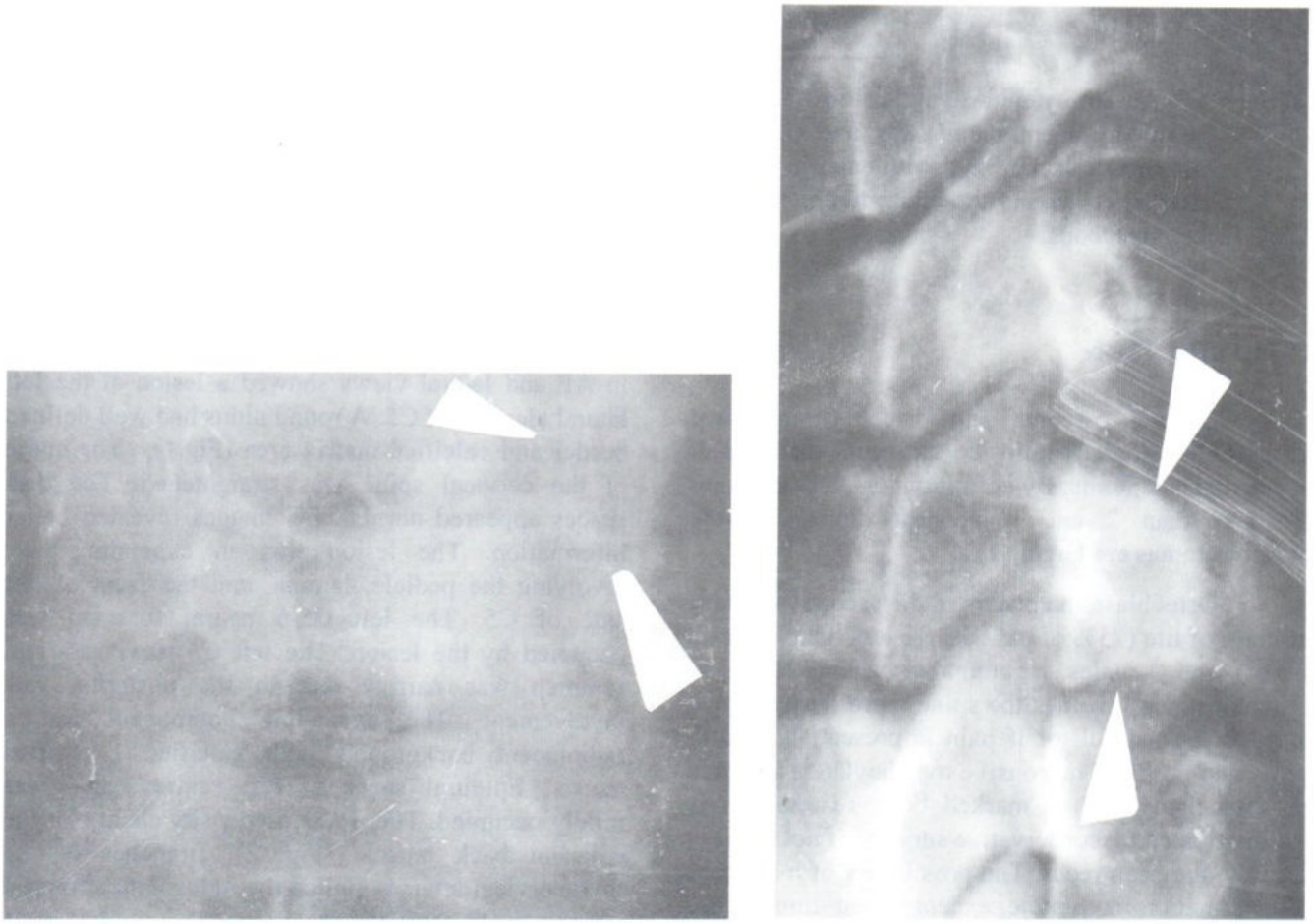

Fig.1 Plain films of the cervical spine of the lesion at left lateral arch of C5, calcification in the nidus was obvious.

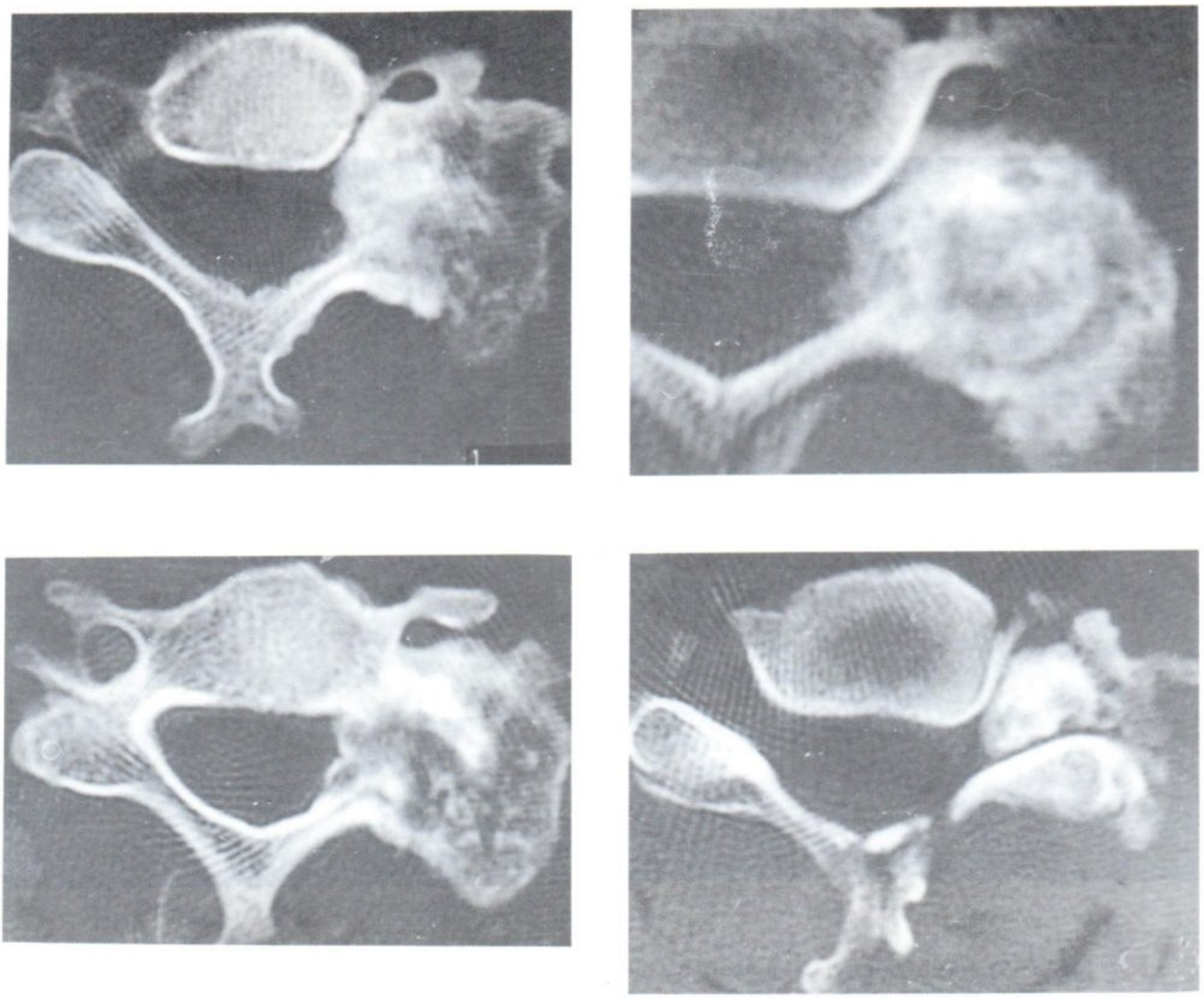

Fig. 2 Images from the CT scan gave clearer information, that the lesion had expanded the involved left lateral arch, osteolytic background, calcified matrix and involvement of the left lateral recess and the central canal.

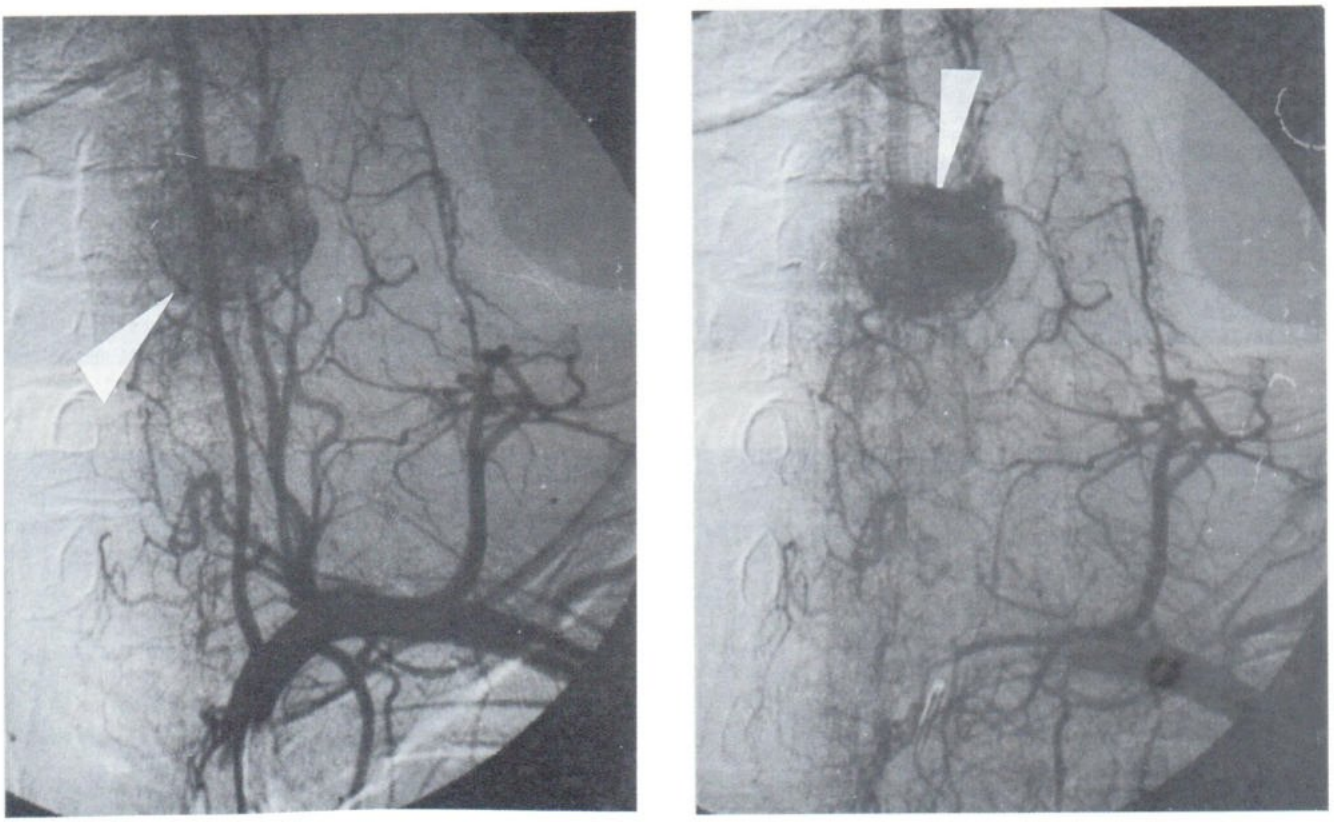

Fig. 3 At angiography, a densely vascular stained well defined border nidus was noted, the staining was most prominent at the capillary phase.Branches of the thyrocervical artery supplied the nidus.

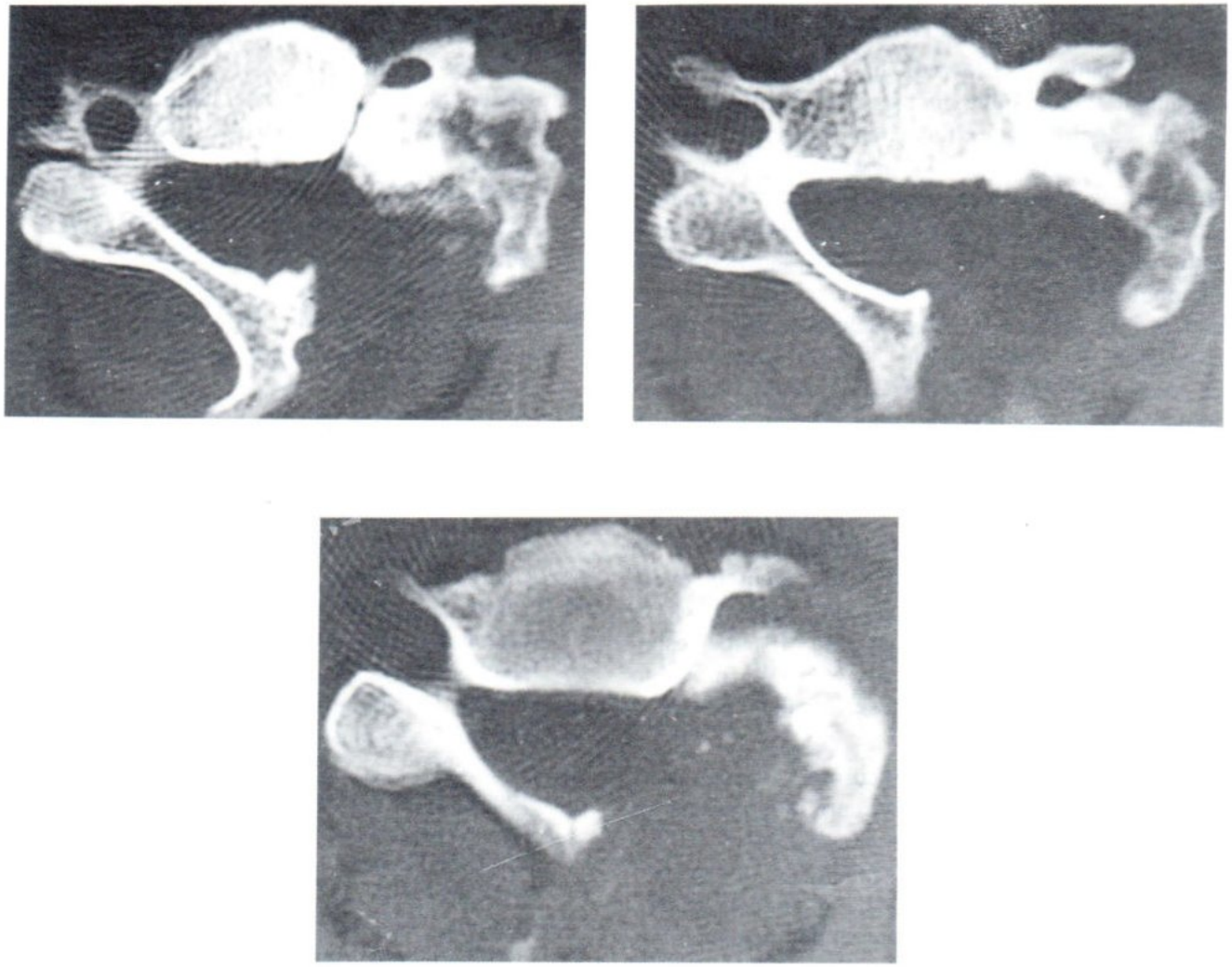

Fig. 4 Incomplete removal of the mass was obvious at the follow up CT scan.

Discussion

Benign osteoblastoma (conventional osteoblastoma) is a relatively uncommon primary neoplasm of bone that is composed of a well-vascularized connective tissue stroma in which there occurs active production of osteoid and primitive woven bone (2). Although osteoblastoma affect virtually any bone, it is most frequently observed in the flat bones or the vertebrae. The vertebrae were the site of origin in 30 per cent of patients (3).

Changes observed in radiographic and computed tomographic images are; (1) presence of radiolucent nidus larger than 2 cm (range of 2-12 cm) in size, (2) 83 per cent shows a well demarcation, (3) stippled or ringlike small flecks of matrix calcification can be present, (4) 25-64% shows radiolucent tumor matrix and 36-72% shows ossified tumor matrix, (5) 22-91% reveals reactive sclerosis and 9-56% without reactive sclerosis, (6) cortical expansion is observed in 75-94% and cortical destruction in 20-22%, (7) 25% of the lesion is progressively expansile and may rapidly increase in size, (8) the soft tissue component is sharply defined, (9) 58-77% have thin shell of periosteal new bone, (10) scoliosis is seen in 35%, (11) rapid calcification after radiotherapy. By nuclear medicine, there is an intense focal accumulation of bone agent in every lesion. Fifty per cent of lesions have tumor blush in capillary phase by angiography. At MR, the lesion has low to intermediate intensity on T1WI, mixed to high intensity on T2WI and surrounding edema is observed.

Ten per cent shows recurrent after excision, incomplete curettage can effect cure due to cartilage production and tapping of host lamellar bone.

Differential diagnosis are osteo / chondrosarcoma, cartilaginous tumors, giant cell tumor, aneurysmal bone cyst, osteomyelitis, hemangioma, lipoma, epidermoid, fibrous dysplasia, metastasis and Ewing sarcoma.

With regard to macroscopic pathology, an osteoblastoma may have a subperiosteal, cortical, or medullary location (5,6). Intracortical osteoblastomas are associated with a marked amount of surrounding sclerotic bone (7). Osteoblastomas located in the spongiosa lack abundant osteosclerosis (8). Vertebral osteoblastomas not infrequently have epidural extension and may even extend into the paraspinal tissue or involve adjacent vertebrae (9).

The aggressive or malignant osteoblastoma was identified by Mayer (10). The histology and the growth pattern of the tumor sometimes is similar to that of low grade osteosarcoma (11,12).

REFERENCES

1. Cotran, Kumar, Robbins. Pathologic basis of disease. 5th ed. Philadelphia: W.B. Saunders, 1994:1234.
2. Resnicks & Niwayama. Diagnosis of bone and joint disorders. 2nd ed. Philadelphia: W.B. Saunders, 1988:3635.
3. Shajowicz F. Tumors and tumorlike lesions of bones and joints. New York: Springer-Verlag, 1991.
4. Daehnert W. Radiology review manual. 2nd ed. Baltimore: Williams & Wilkins,1993:78-9.
5. Mirra JM. Bone tumors. Diagnosis and treatment. Philadelphia: JB Lippincott Co, 1980.
6. McLeod RA, Dahlin DC, Beabout JW. The spectrum of osteoblastoma. Am J Roentgenol 1976;126:321.
7. Schajowicz F, Lemos C. Osteoid osteoblastoma: Closely related entities of osteoblastic derivation. Acta Orthop Scand 1970;41:272.
8. Dahlin Dc. Bone tumors: General aspects and data on 6221 cases. 3rd ed. Springfield, III, Charles C Thomas, 1978.
9. Janin Y, Epstein JA, Carras R, Khan A. Osteoid osteomas and osteoblastomas of the spine. Neurosurgery 1981;8:31.
10. Mayer L. Malignant degeneration of so-called benign osteoblastoma. Bull Hop Joint Dis 1967;28:4.
11. Lichtenstein L, Sawyer WF. Benign osteoblastoma: Further observations and repost of twenty additional cases. J Bone Joint Surg (Am) 1964;46:755.
12. Mitchell ML, Ackerman LV. Metastatic and pseudomalignant osteoblastoma: A report of two unusual cases. Skel Radiol 1986;15:213.

SALMONELLA OVARIAN ABSCESS

Supranee NIRAPATHAPONGPORN [1,2], Patchrin PEKANAN [1,2], Prapee TANNAOWARAT[3], Mondej SUKPRANEE [4], Suphaneewan JAOVISITH[1]

ABSTRACT

An infected endometriotic cyst by Salmonella gr.A was presented. The patient was a 26-year-old woman with fever and chill for three weeks. Ultrasonography showed an adnexal mass, containing turbid fluid.

INTRODUCTION

Salmonella abscess of the ovary is a rare condition. Localized infections frequently occur during Salmonella bacteremia but may also occur with enteric fever or gastroenteritis (1,2). Ovaries are one of the rare sites for such local infections. In isolated ovarian Salmonella abscess bacteremia is usually the initiating factor. Salmonella species possess a tendency to localize to sites of preexisting disease. Almost all reported cases of isolated ovarian abscesses had ovarian abnormalities such as a dermoid cyst, an endometrioma, a cystadenoma, or a simple cyst as the predisposing factor (3-5).

CASE REPORT

A 26-year-old female patient admitted to the hospital for a work up of the cause of fever with chill for 3 weeks. Physicial examination revealed no abnormality. Her WBC was 9800; PMN 70%, L 16%, Mono 12%. The chest film, showed no pulmonary infiltration. The negative results were obtained from thick smear for Malaria, Widal test of Gr. A and B, heterophile, EBV titer, hemoculture and throat swab culture. The widal test for Gr. D was 1:20, and Typhoid H was 1:80.

Ultrasonography of the lower abdomen shows a fluid containing lesion, size 8.6 cm. in diameter at right adnexa. The fluid was turbid, evidenced by homogeneous high echo replacing the anechoic fluid. Operation was performed and the cyst was removed from right adnexa. Pathology and bacterology revealed infected endometriotic cyst by Salmonella Gr. A.

DISCUSSION

The common clinical features of salmonellosis have been grouped into four clinical syndromes: gastroenteritis, bacteremia with or without extra intestinal localization, typhoid-like patterns and the carrier state (either convalescent or asymptomatic) (6,7). Localization of infection following bacteremia is reported to occur in 8% of blood stream infections (6,8) and the tendency of these infections to occur in injured or damaged tissues or in sites of malignancy (9-11). Patients with Hodgkin's lymphoma, acquired immuno-deficiency syndrome and other diseases with T-cell defects are increased risk for severe infections with salmonella (12-14). Salmonellae can live intracellularly for long periods despite the presence of humoral antibodies and antibiotics. The main host

[1] Department of Radiology, Ramathibodi Hospital, Rama 6 Street, Bangkok 10900, Thailand.
[2] Department of Radiology, Samitivej Hospital
[3] Department of OB-GYN, Samitivej Hospital
[4] Department of Medicine, Samitivej Hospital

defense mechanism in salmonellosis appears to be mediated by cellular immunity. The bactericidal mechanisms of the reticuloendothelial system, which serve to eradicate S. typhimurium from the liver and spleen of normal mice, are severely impaired in animals with hemolysis (15-17). Recurrence of salmonella infections in immunocompetent patients was rare, but infectious developing in individuals with depressed cell-mediated immunity are usually prone to recurrences (13,14). Infection occurring in the presence of prosthesis such as vascular grafts and artificial joints, as well as in deep-seated areas such as joints, aneurysms, prostate and testes, also have a high rate of recurrence (18). Salmonellosis in focal infections is often detected only after a diagnostic biopsy, laparotomy or other surgery. However, a suspicion of an unusual organism causing the focal infection can arise from either inadequate or even no clinical improvement following the use of seemingly appropriate antibiotics (6).

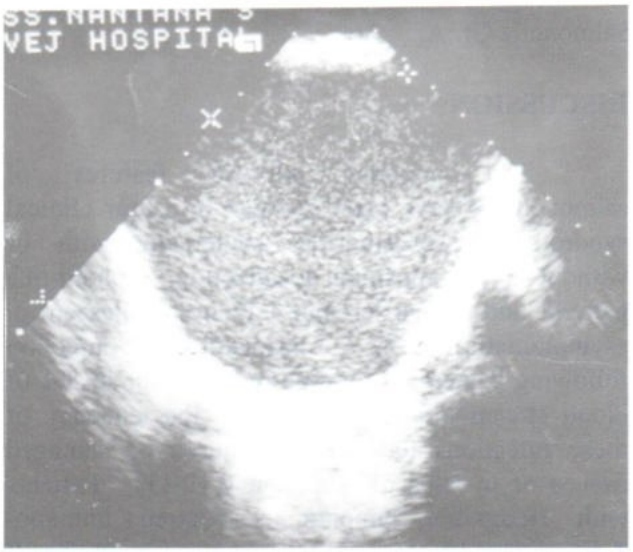

Fig.1 Ultrasonography of the pelvis showed a right adnexal lesion with well defined border, containing turbid fluid.

The most common type of purulent infection of the ovary is a tubo-ovarian abscess due to ovarian involvement secondary to acute salpingitis. This complication of acute salpingitis occurs in up to 34 percent of women admitted to the hospital with salpingitis (19,20). In contrast, primary ovarian abscesses unrelated to tubal disease are very rare (21). Ovarian abcesses are thought to arise by three mechanisms. Organisms in the abdominal cavity gain access to the ovary when its surface is damaged during ovulation, at the time of operation, or through contiguous spread of inflammation. Organism may enter the ovary via the bloodstream or via lymphatics (21). The first mechanism is the most common; the majority of ovarian abscesses have been reported to occur after a pelvic operation. A number of examples have been reported in women wearing intrauterine contraceptive devices. These devices cause colonization of the female genital tract by bacteria, which then gain access to the peritoneum by spreading through the fallopian tube. Ovarian abscesses have been associated with appendicitis or diverticulitis in a very small number of cases (20,21). Mixed aerobic and anerobic bacteria are usually cultured with E. coli, bacteroides fragilis, and streptococcus the most common organisms isolated (21).

Infections of the ovary, presumably secondary to hematogenous or lymphatic spread of organisms, have been described in cases of salmonella infection, tuberculosis, and mumps. The patients with ovarian involvement generally present with symptoms of an ovarian abscess from several weeks to months after their initial salmonella illness, although intervals of up to 35 years have been reported (22). In contrast to ovarian abscesses that are associated with diverticulitis, in which the underlying ovary is usually normal, almost all the patients with salmonella ovarian absceses have had infections in previously existing ovarian tumors, usually dermoid cysts or cystadenomas (23).

A wide variety of Salmonella species were isolated in the ovarian abscesses, including S. typhi, S. enteritidis, S. paratyphi, S. typhimurium, S. virchow (3-5) and S. newport (24).

REFERENCE

1. Chiva LM, Ergeneli M, Santisteban J. Salmonella abscess of the ovary. Am J Obstet Gynecol 1995;172:215-6.

2. Cohen JL, Bartlett JA, Corey GR. Extra-intestinal manifestation of salmonella infection. Medicine 1987;66:349-88.
3. Koshi G. Uncommon manifestations of salmonella infections. Ind J Med Res 1976;64:314-21.
4. Lalitha MK, Arupkumar R, Anandi V, John M, Walter A, Devadatta JO. Abscess thyroid due to Salmonella Choleraesuis-A rare presentation of salmonellosis. Indian J Pathol Microbiol 1988;31:324-6.
5. Rajamani K, John L. Salmonella parotid abscess. J Assoc Phy Ind 1984;32:546.
6. Lalitha MK, John R. Unusual manifestations of salmonellosis-a surgical problem. Quaterly Journal of Medicine 1994;87:301-9.
7. Saligmann E, Saphra I, Wassermann M. Salmonella infections in man. An analysis of 1000 cases bacteriologically identified by the New York salmonella center. Am J Hyg 1943;38:226-49.
8. Saphra I, Winter JW. Clinical manifestations of salmonellosis in man. An evaluation of 7779 human infections identified at the New York Salmonella Center. N Engl J Med 1957;256:1128-34.
9. MacCready Ra, Reardon JP, Saphra I. Salmonellosis in Massachusetts: a sixteen year experience. N Engl J Med 1987;256:1121-8.
10. Sinkovics JG, Smith JP. Salmonellosis complicating neoplastic diseases. Cancer 1969;24:631-6.
11. Wolfe MS, Armstrong D, Louria DB, Blevins A. Salmonellosis in patients with neoplastic disease. A review of 100 episodes at Memorial Centre over a thirteen year period. Arch Intern Med 1971;128:546-54.
12. Heine-man Hs, Jansen WN, Cooper WM, Braude AI. Hodgkin's disease and salmonella typhimurium infections. JAMA 1964;188:632-4.
13. Profeta S, Forrester C, Robert HK, Liu R, Johnson E, Palinkas R, Smith SM. Salmonella infections in patients with the acquired immunodeficiency syndrome. Arch Intern Med 1985;102:189-93.
14. Celum CL, Chaisson RE, Rutherford GW, Barnhart JL, Echenberg DF. Incidence of salmonellosis in patients with AIDs. J Infect Dis 1967;156:998-1002.
15. Gelzer J, Suter E. The effect of antibody on intracellular parasitism Salmonella typhimurium in mononuclear phagocytes in vitro. J Exp Med 1959;110:715-27.
16. Hopps HE, Smadel JF. Effect of antibiotics on intracellular Salmonella typhosa. J Immunol 1961;87:162-74.
17. Mitsukioshi S, Sato T, Tunaka T. Experimental salmonellosis intracellular growth of salmonella enteritidis ingested in mononuclear phagocytes of mice and cellular basis of immunity. J Bacteriol 1961;81:863-71.
18. Dhar JM, Al-Khoder AA, Al-Sulaiman M, Al-Hasani MK. Non-typhoid salmonella in renal transplant recipients: a report of twenty cases and review of the literature. Q J Med 1991;78:235-50.
19. Case records of the Massachusetts General Hospital. Weekly clinico pathological exercises. Case 13-1988. Pelvic mass in a 42-year-old woman with a history of salmonella sepsis. N-Engl J Med 1988;318:8635-42.
20. Landers DV, Sweet RL. Current trends in the diagnosis and treatment of tubo-ovarian abscess. Am J Obstet Gynecol 1985;151:1098-110.
21. Wetchler SJ, Dunn IJ. Ovarian abscess: report of a case and a review of the literature. Obstet Gynecol Surg 1985;40:476-85.
22. Tai FH, Chu BY. An ovarian dermoid cyst infected with Salmonella typhosa. Int J Gynecol Obstet 1971;9:36-8.
23. Evans-Hones JC, French GL. An ovarian cyst infected with Salmonella typhi:case report. Br J Obstet Gynecol 1983;90:680-2.
24. Thomas IL. Salmonella ovarian abscess. Aust NZ J Obstet Gynecol 1989;29:272.

ASDIR

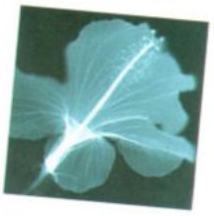

EDUCATION

Asian-Oceanian Seminars on Diagnostic and Interventional Radiology

MRI, CT, Ultrasound: Current Status & Future Direction

Programme Leader
L. Leong

Hong Kong
October 24-25, 1996

BRACCO
INTERNATIONAL

For further information please contact:
Tour East (Hong Kong) Ltd
Level 2, Ritz Plaza
122 Austin Road
TST, Kowloon, Hong Kong
Tel: ++852-236 63111
Fax: ++852-272 39715

HISTOPLASMOSIS OF THE ADRENAL GLANDS

Patchrin PEKANAN, Jiamjit TAPANEEYAKORN, Janjira CHATCHAVALA

ABSTRACT

A case of adrenal histoplasmosis was presented bilaterally in diabetic female patient. The disease caused an adrenal insufficiency. The involved adrenal glands had a bulgy oval shape configuration. The borders were well defined. Diffuse low echoic pattern of the mass was observed by ultrasonography. Non-enhanced CT scan of the masses revealed diffuse low density with a thick wall of hyperdensity. The inner and outer layers were both smooth. Some internal enhancement was noted after contrast medium was given. The diagnosis was made by a small-sized needle percutaneously under CT guidance.

INTRODUCTION

Approximately one in every 1000 cases of acute pulmonary histoplasmosis (caused by the soil fungus Histoplasma capsulatum) will lead to dissemination (1,2). The people most susceptible to this occurrence are the very young, the aged, and those who have an immune deficiency. The fungus has an affinity for the mononuclear phagocytes (histiocytes) that compose the reticuloendothelial system. There is a high incidence of liver, spleen, lymph node, bone marrow, and adrenal gland involvement by this fungus in disseminated disease (1,3,4). Mycobacterium tuberculosis has been considered the most common infection that causes adrenal insufficiency. With the decline of tuberculosis, H. capsulatum may now be the most common infection leading to adrenal insufficiency.

Adrenal histoplasmosis was diagnosed in our case by plain film, ultrasonography, CT scan and narrow Gauge needle aspiration biopsy.

CASE REPORT

A 53-year old female diabetic patient with chronic renal failure, developed hypotension, generalized hyperpigmentation and weight loss 30 kg in 2 months. A work up for the cause of adrenal insufficiency was thus performed. Plain KUB showed both adrenal masses. The masses were low echoic by ultrasonography. CT scan of the adrenal masses revealed low density masses with isodensity rim and faint internal enhancement. A biopsy needle was inserted to obtain the pathologic tissue under CT guidance. Histoplasmosis was noted at histology. (Fig.1-4).

DISCUSSION

The adrenal glands are the internal organs most commonly involved in disseminated histoplasmosis, and adrenal insufficiency is the most frequent cause of death when this disease is untreated (1,3,4). The reason for the frequent adrenal gland involvement is not known.

The most characteristic adrenal gland appearance in this disease by CT scan was bilateral symmetrical adrenal gland enlargement with low density areas of focal hemorrhage and necrosis. The glands tended to maintain their normal shape (1,5). Calcification of the adrenal glands was not observed in the acute phase of this disease and seems to be

Department of Radiology, Ramathibodi Hospital, Rama 6 Street, Bangkok 10900, Thailand.

associated more with the healing process. The differential diagnosis of bilateral adrenal enlargement must include other granulomatous infections such as disseminated tuberculosis (1,6,7), cryptococcosis and blastomycosis (9), lymphoma, bilateral adrenal metastases (6,11), bilateral hemorrhage (12), and rare bilateral primary adrenal tumors (13).

The principal cause of Addison's disease today is idiopathic atrophy: evidence suggests that an autoimmune mechanism may be involved (5,14-16). Less common causes of Addison's disease are tuberculosis, histoplasmosis, adrenal apoplexy (Waterhouse-Friderichsen syndrome), and metastatic carcinoma involving both adrenal glands.

The diagnosis of the adrenal histoplasmosis could be made by percutaneous needle aspiration biopsy, localized by CT scan, as is used in this case. The use of narrow gauge needles is relatively safe and high diagnostic yield could be obtained with modern cytologic preparation (17).

REFERENCE

1. Wilson DA, Muchmore HG, Tisdal RG, Fahmy A, Pitha JV. Histoplasmosis of the adrenal glands studied by CT. Radiology 1984;150:779-83.
2. Reddy P, Gorelick DF, Brasher CA, Larsh H. Progressive disseminated histoplasmosis as seen in adults. Am J Med 1970;48:629-36.
3. Crispell KR, Parson W, Hamlin J, Hollifield G. Addition's disease associated with histoplasmosis: report of four cases and review of the literature. Am J Med 1956;20:23-9.
4. Goodwin RA Jr, Shapiro JL, Thurman GH, Thurman SS, Des Prez RM. Disseminated histoplasmosis: clinical and pathological correlations. Medicine 1980;59:1-33.
5. Doppman JL, Gill JR, Jr, Nienhuis AW, Earll JM, Long JA Jr. CT findings in Addison's disease. J Comput Assist Tomogr 1982;6:757-61.
6. Wilms GE, Baert AL, Kint EJ, Pringot JH, Goddeeris PG. Computed tomographic findings in bilateral adrenal tuberculosis. Radiology 1983;146:729-30.
7. Morgan HE, Austin JH, Follett DA. Bilateral adrenal enlargement in Addison's disease caused by tuberculosis. Nephrotomographic demonstration. Radiology 1975;115:357-8.
8. Rawson AJ, Collins LH Jr, Grant JL. Histoplasmosis and torulosis as causes of adrenal insufficiency. Am J Med Sci 1948;215:363-71.
9. Halvorsen RA Jr, Heaston DK, Johnston WW, Ashton PR, Burton GM. Case report CT guided thin needle aspiration of adrenal blastomycosis. J Comput Assist Tomogr 1982;6:389-91.
10. Antoniou A, Spetseropoulos J, Vlahos L, Pontifex G, Papavasiliou C. The sonographic appearance of adrenal involvement in non-Hodgkin's lymphoma. J Ultrasound Med 1983;2:235-6.
11. Karstaedt MB, Sagel SS, Stanley RJ, Melson LG, Levitt RG. Computed tomography of the adrenal gland. Radiology 1978;129:723-30.
12. Karobkin M, White E, Kressel HY, Moss AA, Montage JP. Computed tomography in the diagnosis of adrenal disease. AJR 1979;-132:231-8.
13. Thomas JL, Bernardino ME, Samaan NA, Hickey RC. CT of pheochromocytoma. AJR 1980;135:477-82.
14. Bilizzard RM, Kyle M. Studies of the adrenal antigens and antibodies in Addison's disease. J Clin Invest 1963;42:1653-60.
15. Nerup J. Addison's disease-Serological studies. Acta Endocrinol 1974;76:142-58.
16. Volpe R. The role of autoimmunity in hypoendocrine and hyperendocrine function with special emphasis on autoimmune thyroid disease. Ann Intern Med 1977;87:86-99.
17. Heaston DK, Handel DB, Ashton PR, Korobkin M. Narrow gauge needle aspiration of solid adrenal masses. AJR 1982;138:1143-48.

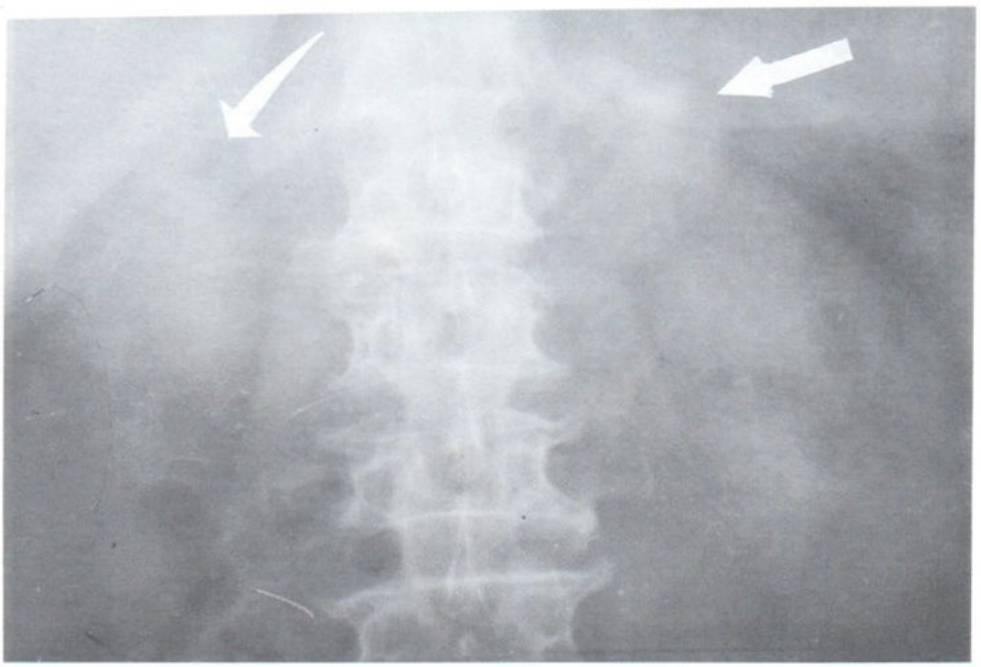

Fig.1 Plain KUB showed a well defined border bulgy oval shape mass at both suprarenal areas. The outlines of the kidneys were not obscured.

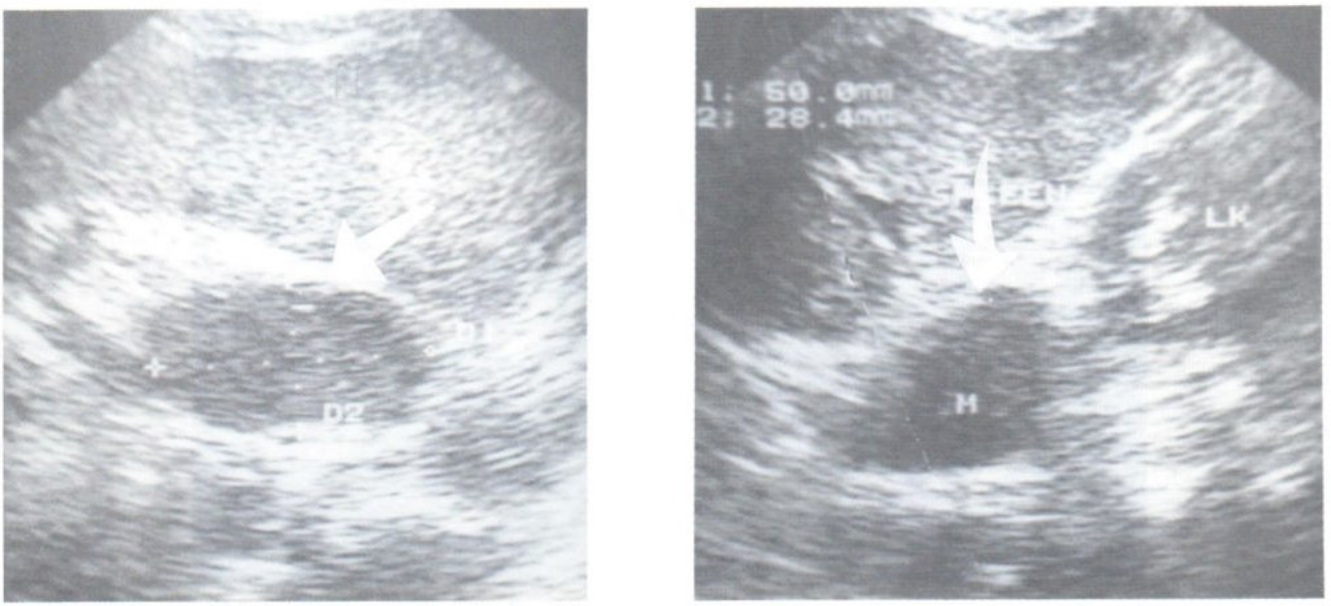

Fig. 2 Ultrasonography of the upper abdomen revealed an oval shape homogeneously low echoic mass, size 5.6 x 2.3 cm replacing right adrenal gland and 5 x 2.8 cm, replacing left adrenal gland. The masses had a well defined border.

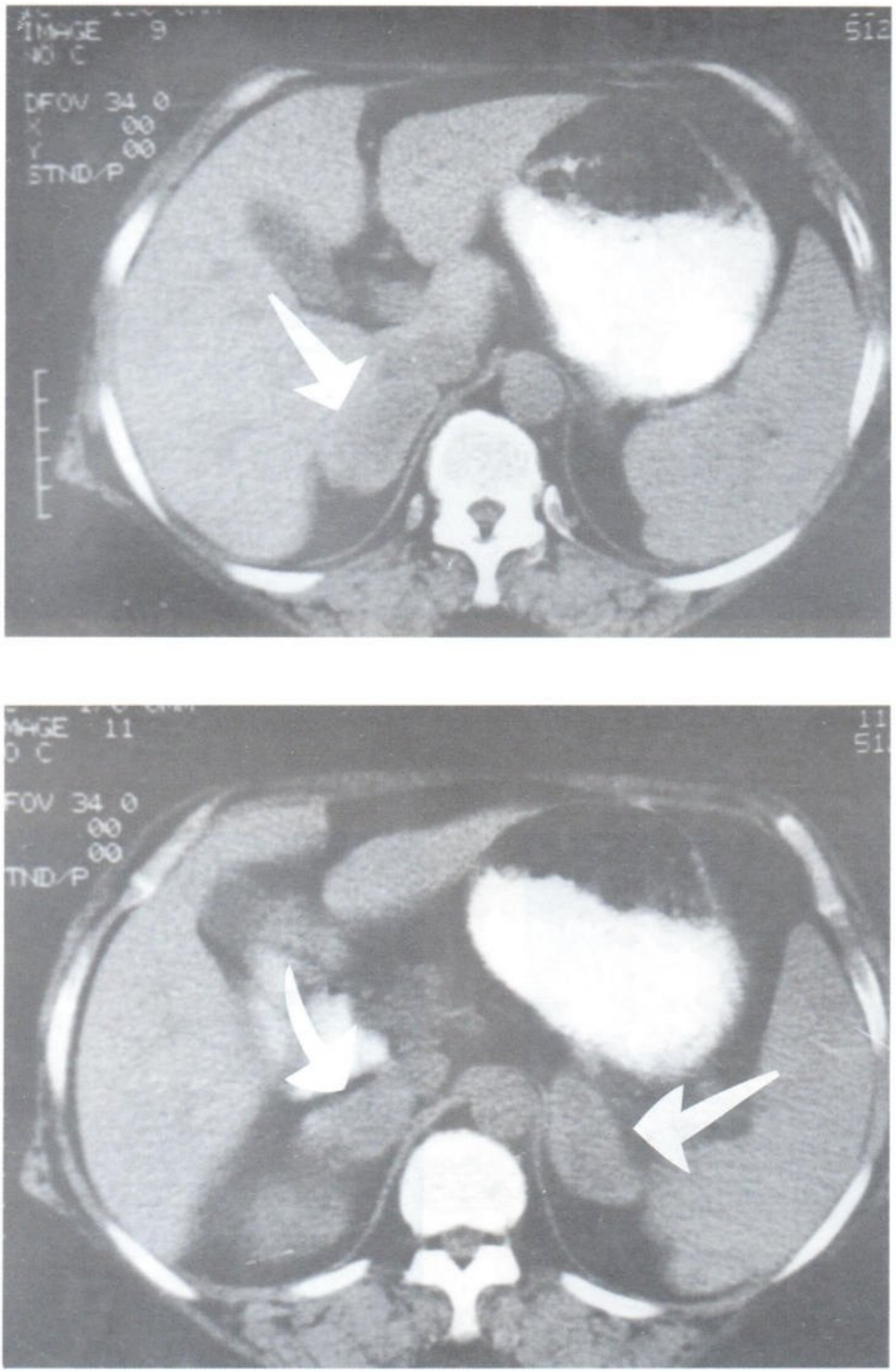

Fig. 3A. Non-enhanced axial CT scan of the adrenal glands showed the adrenal masses to have smooth isodensity border (isodensity to the liver) and low density center (similarly low density as the adjacent inferior vena cava).

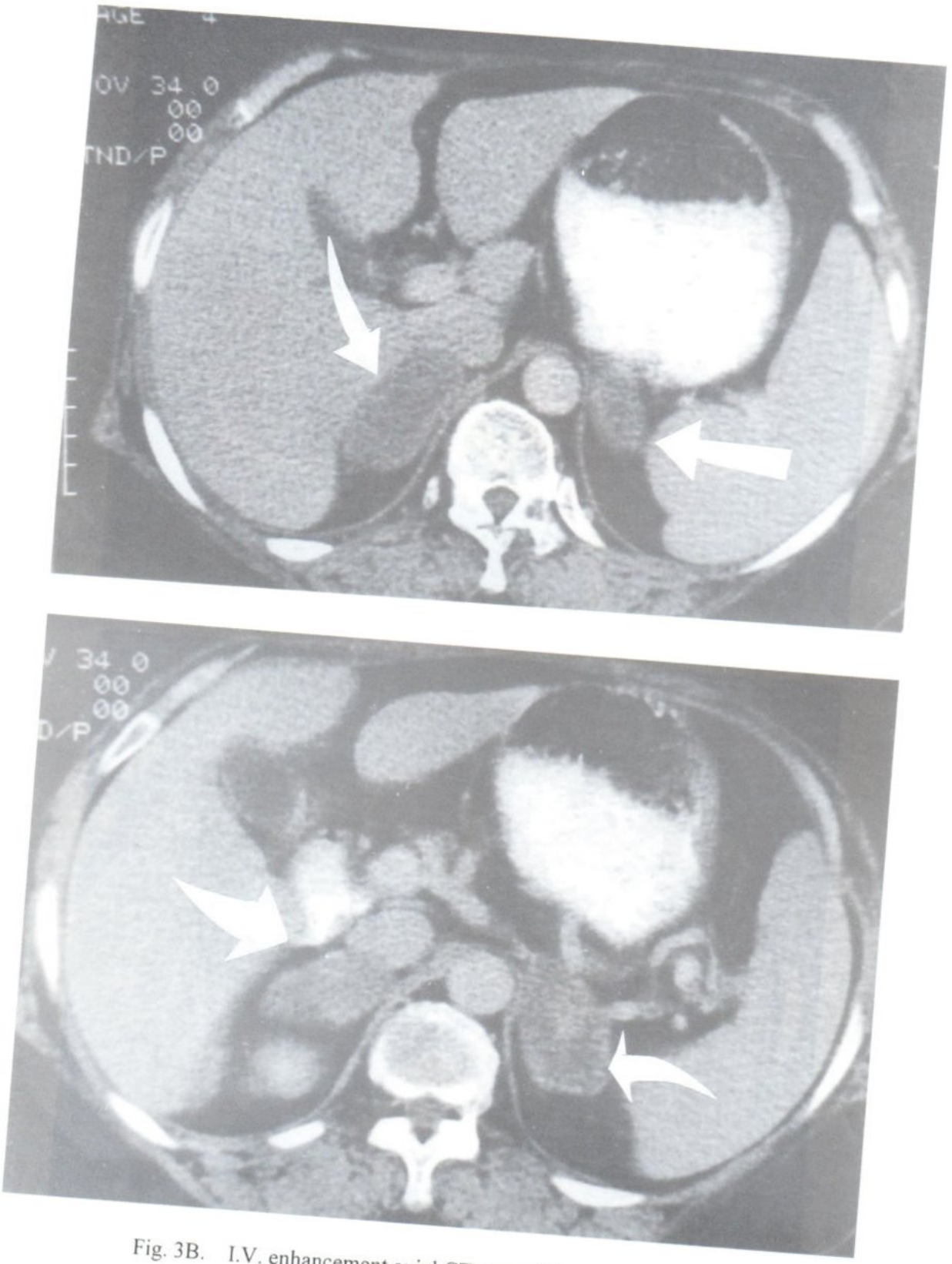

Fig. 3B. I.V. enhancement axial CT scan of the masses showed some faint internal enhancement of the masses.

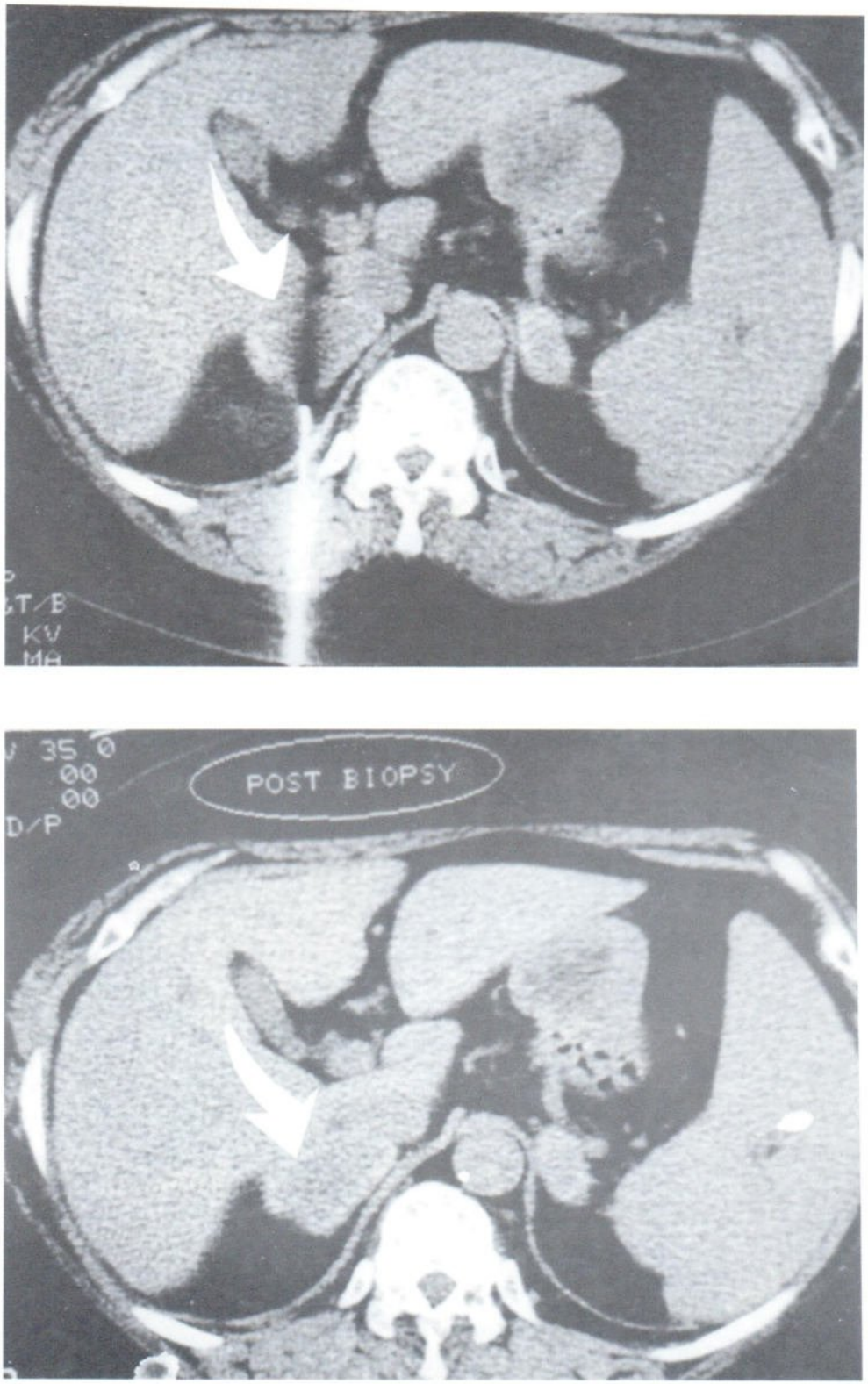

Fig. 4 The path of the aspiration biopsy needle under CT localization was shown with the patient in prone position. There was no significant changes of the appearance of the mass post biopsy.

BRONCHIOLITIS OBLITERANS IN A PATIENT WITH HYPEREOSINOPHILIC SYNDROME

Patchrin PEKANAN[1], Janjira CHATCHAVALA[1],
Somboon BUNKASEM[2], Mana ROJANAVUTINOND[3], Sopon KUMPOLPUNTH[1].

ABSTRACT

Plain chest film and CT scan of the thorax in a 30 year-old woman with bronchiolitis obliterans was presented. The patient was a known case of hypereosinophilic syndrome. The images showed ground glass appearance of both lungs. Reticular, reticulonodular and patchy lesion was observed, mainly at left lower lobe and left apex. Pleural effusion in small amount was seen in both sides of the pleural spaces. Mild volume loss was observed in left lung.

INTRODUCTION

Bronchiolitis obliterans was first described by Lange in 1901 (1). It is a descriptive term for a fibrosing inflammatory process that occludes the lumens of small airways (2,3). Histologically, bronchiolitis obliterans is defined by the presence of granulation tissue plugs within the lumen of small airways and alveolar ducts and the destruction of small airways with obliterative scarring (4).

We report the radiographic presentation of a case with bronchiolitis obliterans by plain film and CT scan.

CASE REPORT

A 30-year-old female patient had fever and blood stained sputum for 1 day. She was a known case of hypereosinophilic syndrome, diagnosed one year ago. She admitted to the hospital many times. Her previous problems were congestive heart failure, deep venous thrombosis of left arm, mitral and tricuspid valve regurgitation. She had a persistent abnormal chest film and CT scan of the chest (Fig.1,2), so that bronchoscope was performed. She had cardiac arrest during the scope and was improved after resuscitation. Lung biopsy was later performed by right thoracotomy. The lung was found to be multinodular and firm consistency. The 50 cc pleural fluid was seen with clear-yellow colour. Lower lobe biopsy was done and was compatible with bronchilitis obliterans with alveolar atelectasis. Restrictive cardiomegaly was found at cardiac catheterization.

DISCUSSION

Etiologically, bronchiolitis obliterans can be classified as (a) toxic fume bronchiolitis obliterans (2,5-7), the toxic fumes include sulfur dioxide, ammonia, chlorine, phosgene, oxides of nitrogen and ozone (b) postinfectious bronchiolitis obliterans which is usually seen in children or in young adults after Mycoplasma infection and in older adults after viral infection (c) bronchiolitis obliterans associated with connective tissue disease and organ transplantation (10-14) (d) localized lesion with bronchiolitis obliterans (6), histologically such lesions are referred to as "focal organizing pneumonia" (e) idiopathic bronchiolitis obliterans with organizing pneumonia (5).

[1] Department of Radiology, Ramathibodi Hospital, Rama 6 Street, Bangkok 10400, THAILAND.
[2] Department of Surgery, Ramathibodi Hospital.
[3] Department of Pathology, Ramathibodi Hospital.

Clinically, patients have cough, dyspnea, sputum, and fever. Both children and adults are affected, but more than 80% of patients are over 40 years old. There is a 2:1 male predominance (2,6). Good response to corticosteroid therapy, especially in the idiopathic group, is noted but recurrence after discontinuation of steroid therapy occurs in one-third.

There is a wide spectrum of radiographic patterns due to diverse causes of bronchiolitis obliterans and the varying degrees of organizing pneumonia which may be present (4). Intense exposure to the toxic-fume causes acute pulmonary edema and acute respiratory failure may develop after a 4-6 hour latency period. The chest radiograph at this stage reveals the changes seen in the adult respiratory distress syndrome (ARDS), which consist of difffuse alveolar or ground-glass opacifies uniformly distributed throughout both lungs. The heart size is normal and pleural effusions are absent. One to three weeks later, if survive, the development of irreversible airflow obstruction occurs. In mild cases the chest radiograph may be normal, whereas in severe cases hyperinflation can be identified. This stage may be characterized by multiple discrete nodular opacities of various sizes distributed uniformly throughout both lungs and may become confluent in severe cases.

The radiographic pattern in postinfectious bronchiolitis obliterans is highly variable. Most frequently the chest radiograph is either normal or demonstrates a diffuse nodular or reticulonodular pattern. The nodular pattern appears to correlate with histologic evidence of pure bronchiolitis obliterans, while the reticulonodular pattern reflects considerable interstitial fibrosis and scarring. If organizing pneumonia is extensive, patchy alveolar or ground-glass opacities may be identified. Difffuse hyperinflation is rare.

The chest radiograph in bronchiolitis obliterans associated with connective tissue disease or penicillamine treatment is normal or occasionally shows hyperinflated lungs. The histology is that of a pure bronchiolitis obliterans. Patchy areas of alveolar or ground-glass opacities are seen in organizing pneumonia in this group of patients. Course nodular or reticulonodular opacities with peribronchial thickening were seen in the long-term survivors of heart-lung transplantation.

Bronchiolitis obliterans may be associated with localized discrete radiographic opacities or nodules. They are frequently incidental radiographic findings in asymptomatic patients in whom lung biopsy specimens are obtained to exclude carcinoma. The appearance is usually that of an irregular, sublobar area of air-space consolidation or an irregular nodule.

In idiopathic bronchiolitis obliterans with organizing pneumonia, the chest radiograph shows bilateral, patchy ground-glass or air-space opacities. There is no zonal or lobar predominance. These sometimes begin as focal lesions and progressed bilaterally over time. Diffuse, small, linear and nodular opacities were uncommon. Cavities, effusions and hyperinflation were rare.

Diseases associated with eosinophilia include (1) infectious diseases, (2) allergic diseases, (3) myeloproliferative and neoplastic diseases, (4) other cutaneous diseases, (5) other pulmonary diseases, (6) connective tissue diseases, (7) immuno deficiency diseases, (8) gastrointestinal diseases, (9) occasional causes of esosinophilia e.g. post-irradiation (15).

Summary of radiographic findings of bronchiolitis obliterans are (1) normal, hyperinflation, difffuse nodular opacities in toxic-fume exposure, (2) normal, diffuse nodular or reticulonodular pattern, Swyer-James syndrome in postinfectious process, (3) normal, hyperinflation, patchy ground-glass opacities in connective tissue diseases, (4) nodule or focal irregular air-space consolidation in localized type, (5) patchy ground-glass opacities in idiopathic type (4).

Our patient had mildly hypoaerated lungs, reticulonodular pattern with ground glass appearance. Small component of patchy lesion was seen in every region. The patches could be the result of conglomuration of the reticular lesion.

REFERENCES

1. Lange W.Uber eine eigenthumliche: Erkrankung der kleinen Bronchien and Bronchiolen. Deutsche Arch Klin Med 1901;70:342-364.
2. Miki Y, Hatabu H, Takashashi M, Sadatoh N, Kuroda Y. Computed tomography of bronchiolitis obliterans. Journal of Computer Assisted Tomography 1988;12:512-514.
3. Katzenstein AA, Askin FB. Surgical Pathology of nonneoplastic lung diseases. Major problems in pathology. Philadelphia: WB Saunders, 1982, p 349.
4. McLoud TC, Epler GR, Colby TV, Gaensler EA, Carrington CB. Bronchiolitis obliterans. Radiology 1986;159:1-8.
5. Epler GR, Colby TV, McLoud TC, Carrington CB, Gaensler EA. Bronchiolitis obliterans organizing pneumonia. N Engl J Med 1985;312:152-158.
6. Gosink BB, Friedman PJ, Liebow AA. Bronchiolitis obliterans:roentgenologic-pathologic correlation. AJR 1973;117:816-832.

7. Lannuzzi MC, Farhi DC, Bostrom PD, Petty TL, Fisher JH. Fulminant respiratory failure and death in a patient with idiopathic bronchiolitis obliterans. Arch Intern Med 1985;145:733-734.
8. Laraya-Cuasay LR, DeForest A, Huff D, Lischner H, Huang NN. Chronic pulmonary complications of early influenza virus infection in children. Am Rev Respir Dis 1977;116:617-625.
9. Nikki P, Meretoja O. Valtonen V, et al. Severe bronchiolitis probably caused by varicella-zoster virus. Crit Care Med 1982;10:344-346.
19. Herzog CA, Miller RR, Hoidal JR. Bronchiolitis and rheumatoid arthritis. Am Rev Respir Dis 197;119:555-560.
11. Schwarz MI, Matthay RA,Sahn SA, et al. Interstitial lung disease in polymyositis and dermatomyositis : an analysis of six cases and review of the literature. Medicine 1976;55:89-104.
12. Epler GR, Snider GL, Gaensler EA, Cathcart ES, Fitgerald MX, Carrington CB. Bronchiolitis and bronchitis in connective tissue disease. JAMA 1979;242:528-532.
13. Ostrow D, Buskard N, Hill RS, Vickars L, Churg A. Bronchiolitis obliterans complicating bone marrow transplantation. Chest 1985;87: 828-830;
14. Burke CM, Theodore J, Dawkins KD, et al. Post transplant obliterative bronchiolitis and other late lung sequellae in human heart-lung transplantation. Chest 1984;86:824-829.
15. Wyngaarden, Smith, Bennett. Cecil textbook of medicine, 19th ed. Philadelphia: W.B. Saunders Company, 1992.

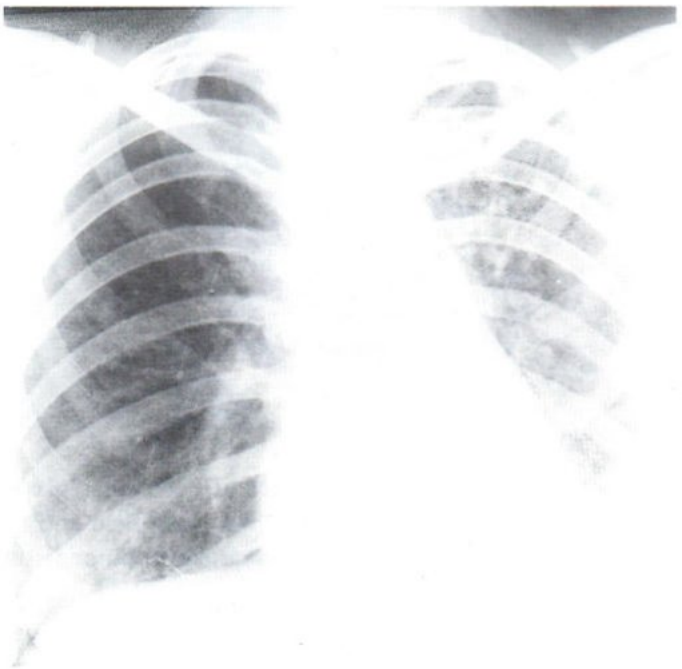

Fig.1 Plain chest film in PA view showed some volume loss in left lung. Mixed interstitial and alveolar process, mainly interstitial process involving the whole left lung, denser at lower zone. Less degree of involvement at right lung was noted.

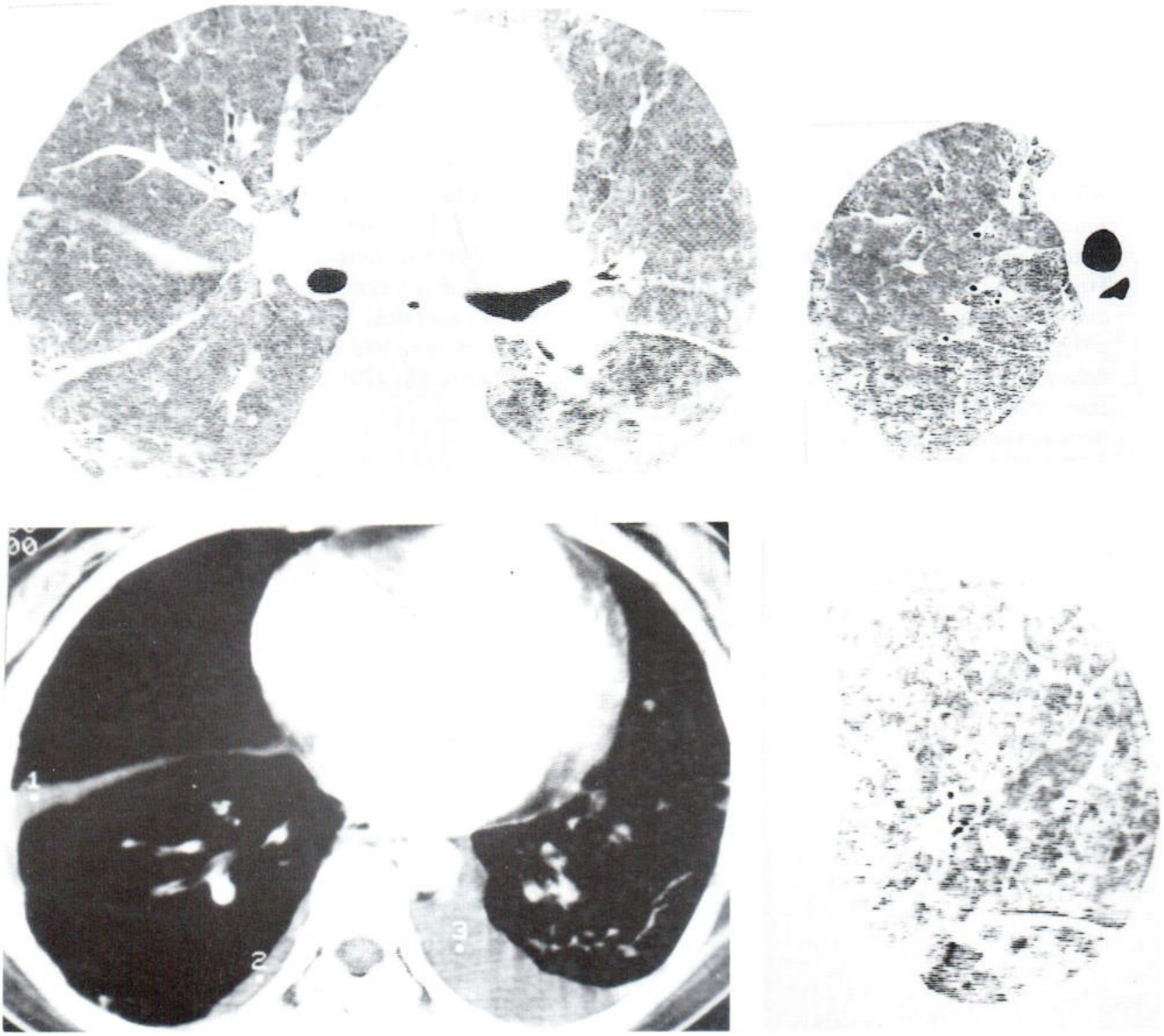

Fig. 2 I.V. contrast CT scan showed ground glass appearance of both lungs. Reticulonodular and patchy lesion was noted at left lower lung field; less dense at left upper lung field and right base. Left pleural fluid at dependent part was shown and right pleural fluid was noted at minor fissure.

SPHENOID MUCOCELES

Patchrin PEKANAN[1], Siripon HIRUNPAT[2],
Nakornchai PUENPATHOM[3], Kamolpong OSATHAVANICHVONG[4]

ABSTRACT

Four cases of sphenoid mucocele were presented. The lesions were confined to the expanded sinuses in two cases and with intracranial extension in other two cases. CT scan showed homogeneously low and high content lesions. MRI showed the lesions to be dark grey on T1WIs and fluid bright on T2WIs. The cases that lesions extended to intracranial cavity destroyed the bony skull bases widely but in smooth manner.

INTRODUCTION

Mucoceles are the most common expansile lesions of any paranasal sinuses. They are defined pathologically as being formed by a cuboidal epithelium that surrounds mucoid secretions (1). A mucocele develops from the obstruction of a sinus ostium or a compartment of a septated sinus. The wall of the lesion is the sinus mucosa and the sinus cavity is expanded as the bony walls are remodelled. Mucoceles occur primarily in the frontal sinuses (60-65%), but they also are found in the ethmoid sinuses (20-25%), maxillary sinuses (10%) and the sphenoid sinuses (1-2%) (1-5). The classical mucocele is a noninfected lesion that presents with signs and symptoms that result from the mass itself. Pain is rare and when noted indicates the presence of an infected mucocele or a pyocele. The sinus cavity expansion is the result of a dynamic process that consists of pressure necrosis that causes a slow erosion of the inner sinus bony wall while the outer periosteum responds by producing new bone. In this way, the sinus wall is remodelled and the sinus cavity slowly expands.

We presented four cases of sphenoid mucocele by images of plain film, CT scan and MRI study.

CASE REPORTS

CASE 1

A 50-year-old female patient had chronic sinusitis with several surgeries without improvement. She had no visual problem. Plain film of the paranasal sinuses showed an expansion of the sphenoid sinus with haziness. The lamina dura of the floor of the sella turcica was eroded without expansion of the fossa. Both ethmoid sinuses were cloudy (Fig.1). Contrast enhanced axial and coronal view CT scan of the paranasal sinuses revealed a homogeneous soft tissue lesion in the expanded sphenoid sinus. The density was measured 46-58 H.U. Extension of the lesion was noted to both posterior compartments of the ethmoid sinuses (Fig.1). The cavernous sinuses appeared normal. The pituitary gland was not involved. At surgery, there were polyps in the posterior ethmoid and sphenoid sinuses with thickened mucosa. No pus was obtained from the sphenoid sinus.

CASE 2

A 72-year-old female patient had bitemporal headache for 3 months. She developed double vision

[1] Department of Radiology, Ramathibodi Hospital, Rama 6 Street, Bangkok 10400, Thailand
[2] Department of Radiology, Prince of Songkla University Hospital, Hatyai, Songkla, Thailand 90112.
[3] Department of Surgery, Prince of Songkla University Hospital.
[4] Medical software development project, Mahidol University. BKK.

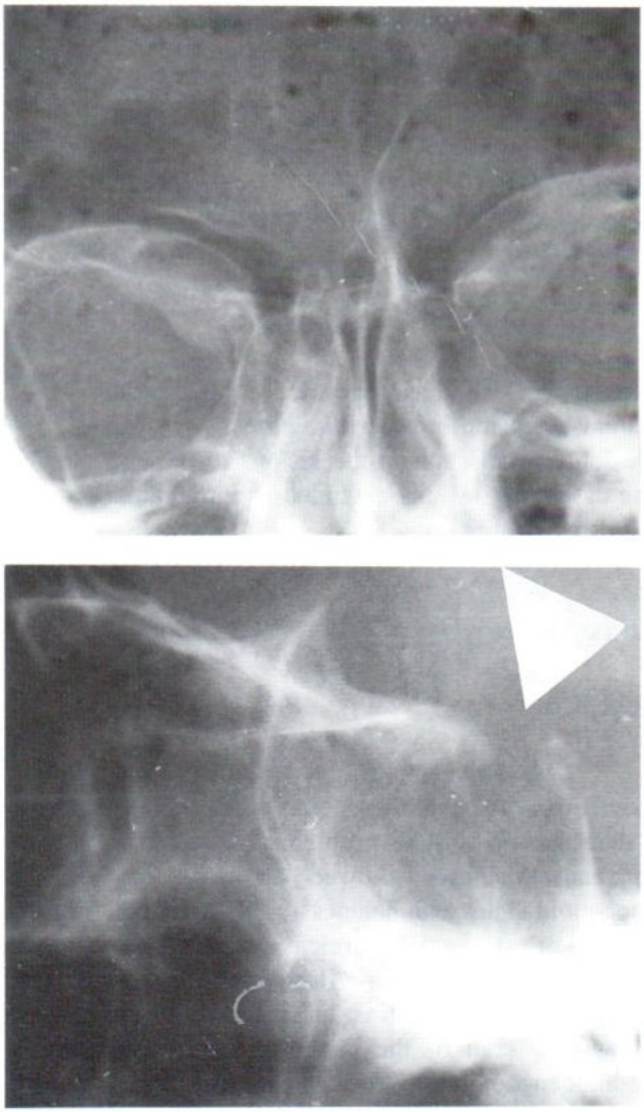

Fig. 1A. Case 1. PA and lateral film of the paranasal sinuses showed an expanded sphenoid sinus with ground glass appearance, erosion of the floor of the sella turcica and cloudiness of both ethmoid sinuses.

in the vertical orientation and hearing loss. Left eye proptosis was noted. The visual acuity of right eye was 15/200 and finger count at 2 feet for the left eye. Visual field defect was noted at the lateral half and superior medial 1/5 of right eye and it could not be evaluated for the left eye. The extraocular movement was normal for the right eye and was limited to 10-20% in all directions for the left eye. The corneal reflex was decreased in the left eye. MRI study was performed in axial, sagittal and coronal view. The T1WI and T2WI images were obtained at the paranasal sinuses. They showed an expansion of the sphenoid sinus with pressure erosion to the anterior clivus, floor of the pituitary fossa, left cavernous sinus and medial left orbital apex. Left optic nerve was compressed at the apex. The optic chiasma appeared normal (Fig. 2). The lesion had a homogeneous signal, grey on T1WI and fluid bright on T2WI. The contrast enhancement was not performed in this case. Sphenoid mucocele was found at surgery.

CASE 3

A 15-year-old female patient had a progressive blurred vision of left eye for two years. Visual acuity of left eye was hand-movement and normal for right eye. Positive left Marcus Gunn's sign was noted. Pale disc of right eye and optic atrophy of left eye was seen. Left exophthalmos was observed. Lateral view of the plain film of the skull showed an expansion of the sphenoid sinus, a totally destroyed pituitary fossa and soft tissue lesion in the nasopharynx. Non contrast enhancement of the base of the skull and the brain revealed a low density soft tissue lesion in the skull base with intracranial extension. The density of the lesion was 15 H.U. Contrast enhancement of the lesion in the axial and coronal view showed a non enhanced lesion in the expanded sphenoid sinus, extending to left nasopharyngeal airway, posterior left nasal cavity, left maxillary sinus, pre-medullary, pre-pontine region, medial left temporal fossa, sella and suprasellar area. Both sides of the cavernous sinuses were compressed and invaded at the left side (Fig. 3). The clivus, a part of left pterygoid bones, both petrous apices, medial and posterior walls of left maxillary sinus were disappeared. The lesions did not enter the left orbital cavity, though it had pressure effect on the posterior medial wall. The pituitary gland was not well identified. The chiasma was naturally compressed, judged from the location of the mass.

CASE 4

A 35-year-old male patient had poor vision for one week. Physical examination showed no

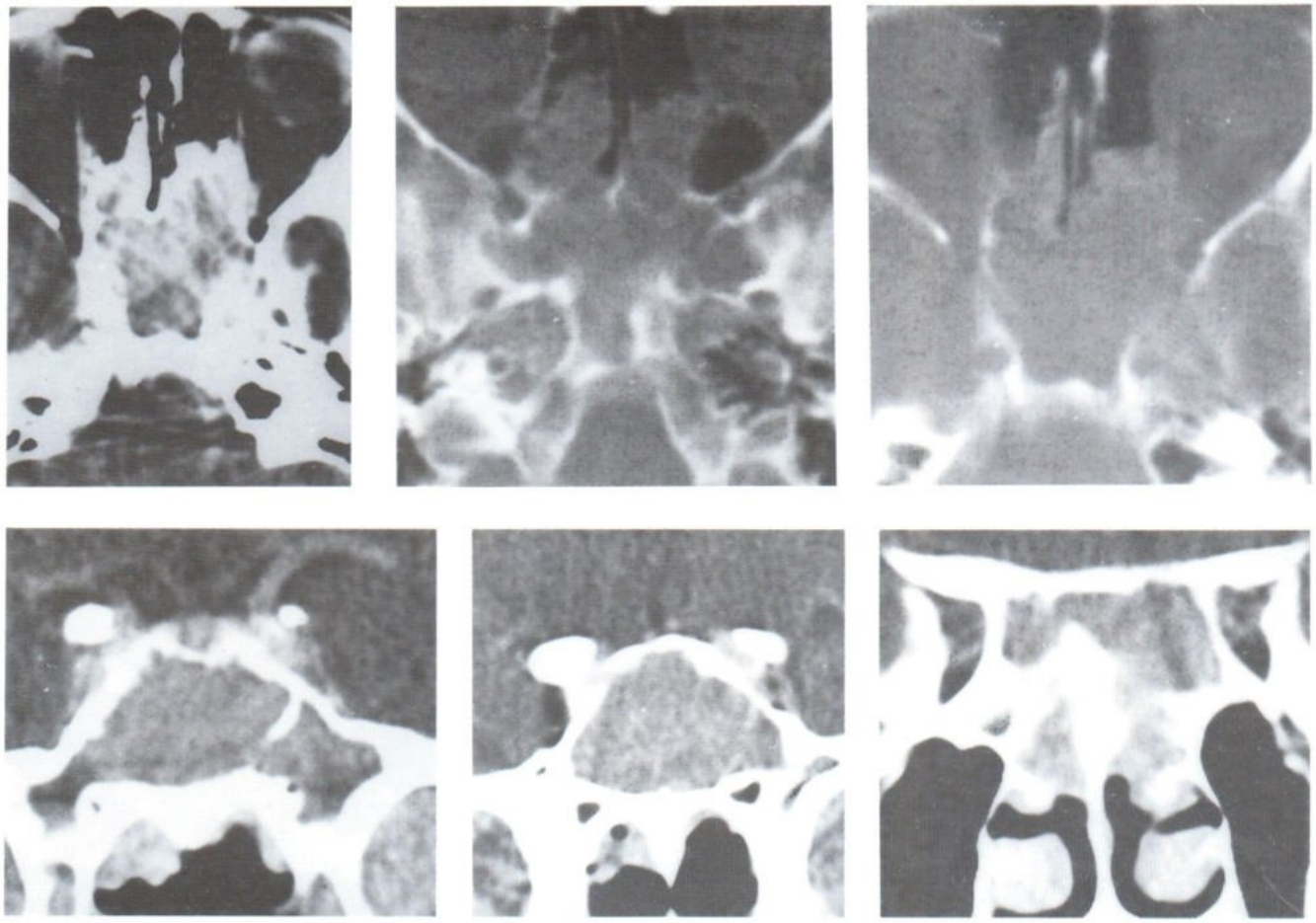

Fig. 1B. Case 1. Axial and coronal views enhanced CT scan of the paranasal sinuses showed soft tissue lesion of rather homogeneous density in the expanded sphenoid sinus and posterior compartment of both ethmoid sinuses. The intersphenoid sinuses septum disappeared. The cavernous sinuses and the pituitary gland were normal.

perception to light at right eye and finger count at 1.5 feet of left eye. Right pupil was 6 mm fixed and left pupil was 3 mm reacted to light. The pinprick sensation was decreased at right cranial nerve V. The Babinski's response was positive on both sides. Visual field defect at medial half of left eye was noted. The Marcus Gunn was positive at right side. Optic disc atrophy of both sides were seen. Non contrast enhancement CT scan of the brain and base of the skull in axial view showed a hyperdense soft tissue lesion in the sphenoid sinus. Post contrast enhancement axial and coronal CT scan of the base of the skull and brain revealed a homogeneous hyperdense soft tissue lesion in the expanded sphenoid sinus. The lesion extended to both sides of the cavernous sinuses (Fig. 4). Bony destruction was noted at clivus, superior part of left pterygoid plates, walls of the sphenoid sinuses and bony parts of the skull base.

DISCUSSION

Mucoceles involving the frontal and anterior ethmoid sinuses are relatively common, but those arising in the sphenoid and posterior ethmoid sinuses are rare. The terms " sphenoid sinus mucocele" and sphenoethmoidal mucocele" have been used interchangeably in describing these lesions (6,7). Mucoceles of the sphenoid and ethmoid sinuses gradually expand, resulting in resorption and eventual erosion of the bony walls of the sinus. The clinical and radiographic manifestations of sphenoidal mucoceles are usually related to sinus expansion and extension of the lesion beyond the

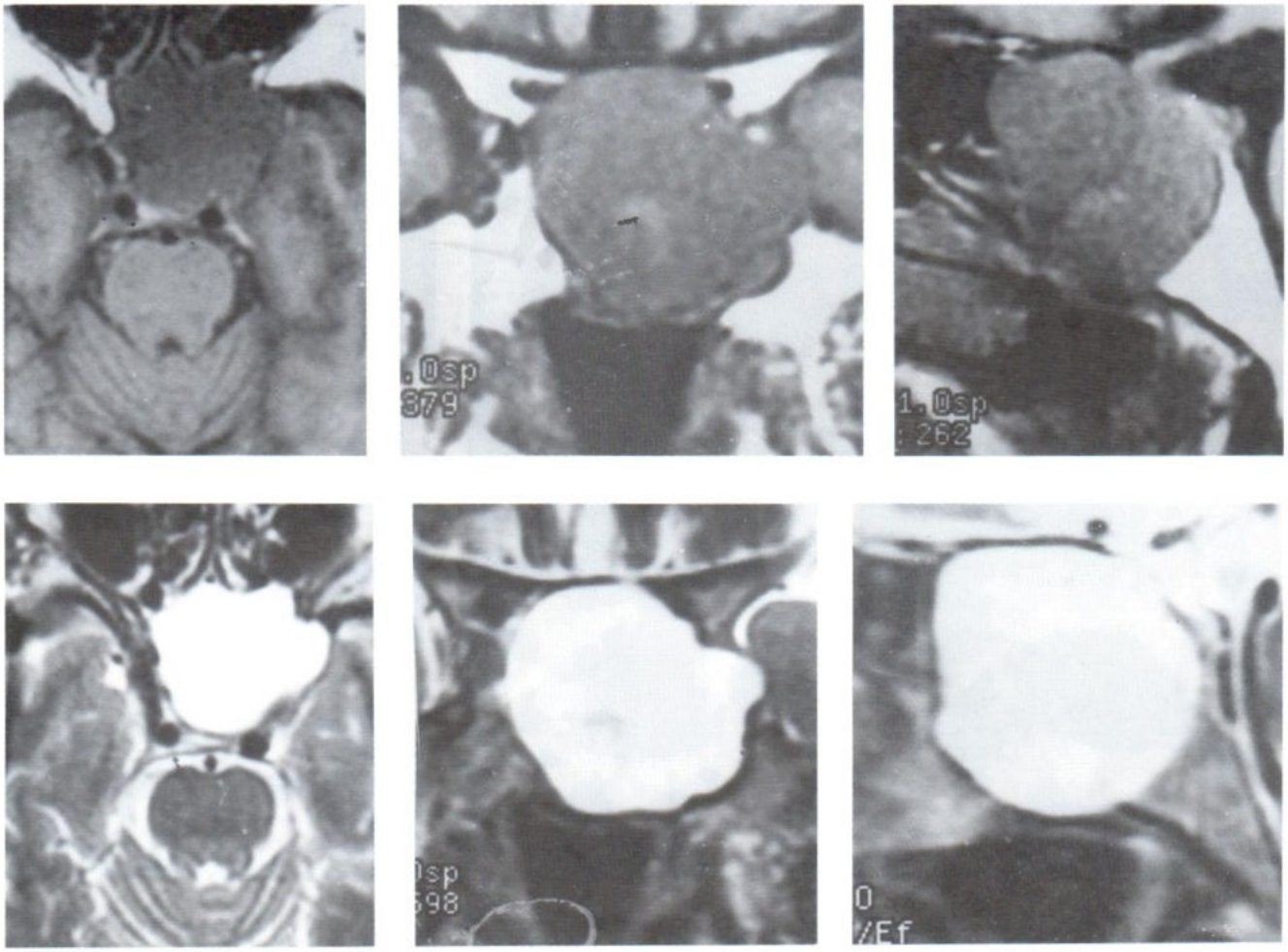

Fig. 2. Case2. T1WI and T2WI-axial, coronal and sagittal view MRI study of the sphenoid sinus showed an expansion of the sphenoid sinus with pressure erosion to the anterior clivus, floor of the pituitary fossa, left cavernous sinus and medial left orbital apex. Left optic nerve was compressed at the apex. The lesion has a homogeneous signal, grey on T1WI and fluid bright on T2WI.

confines of the sinus (8). Symptoms result from involvement of structures in the area. Sphenoid sinus enlargement will compress the upper six cranial nerves (9,10), the carotid arteries (11), and even the brain, together with erosion of the skull base.

The patients presented with headache due to stretch of the basal dura covering the planum sphenoidale and floor of the frontal fossa (12). The sphenoid sinus mucosa is supplied by the posterior ethmoidal branch of the ophthalmic division of the trigeminal nerve (13), so referred pain could be anywhere in the head. Anosmia and nasal symptoms were reported (11,13). Opthalmologic manifestations included bilateral visual failure (11), field defect (14), oculomotor nerve palsy (15), bilateral exophthalmos and conjunctival injection (16). Spontaneous pneumocephalus (17) and panhypopituitarism was also observed (10).

On plain films, most sphenoid mucoceles expand anterolaterally into the posterior ethmoids and the orbital apex. Less commonly, expansion may occur upward into the sella turcica and cavernous sinuses or downward into the nasopharynx and posterior nares. Intracranial extension in rare cases can even result in areas of brain necrosis (1,7,18). Rarely, they may extend into the sphenoid sinus recesses in the greater wings and the pterygoid processes (19).

On CT scans a mucocele usually appears as an expanded sinus cavity that is filled with a fairly

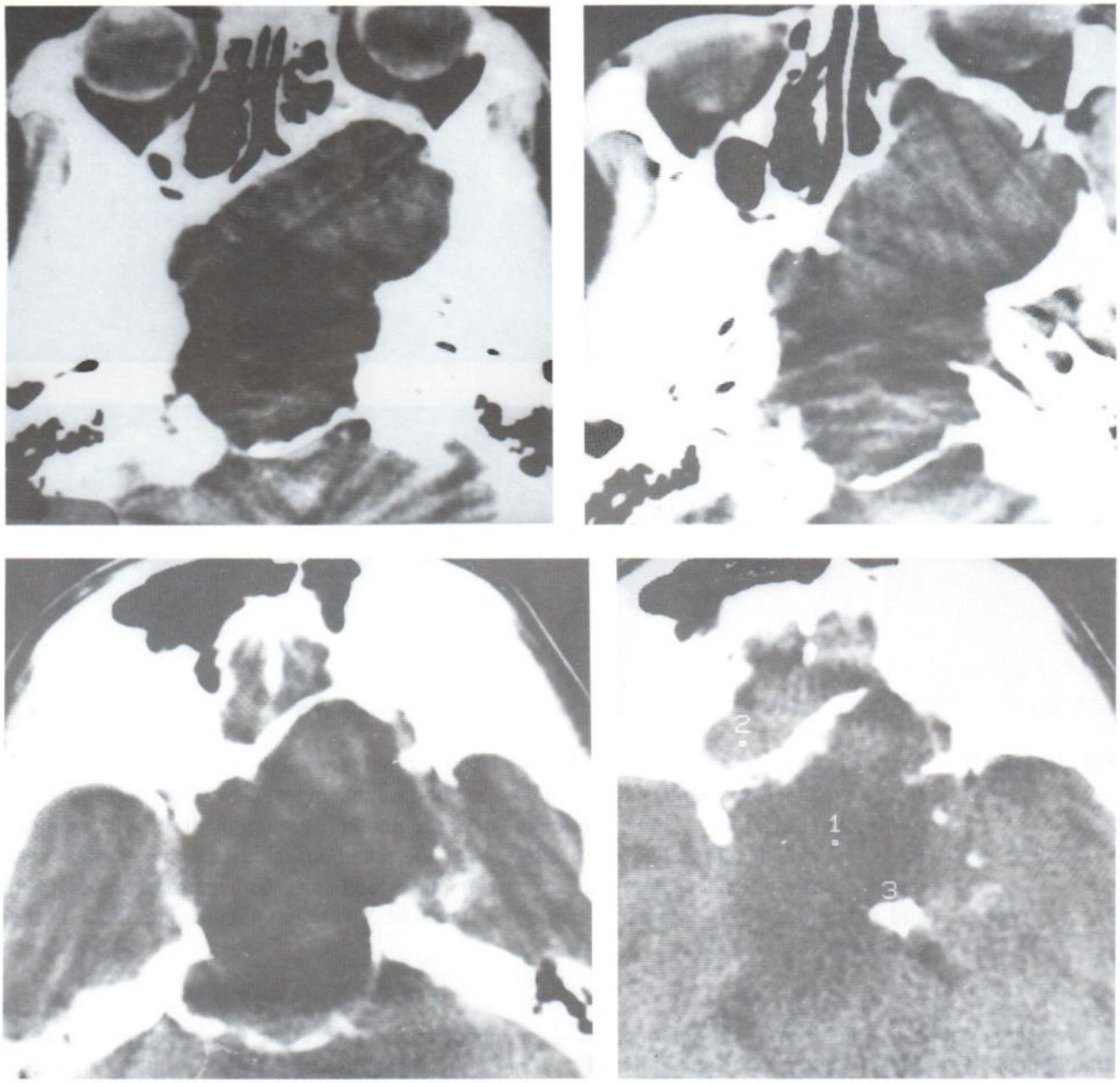

Fig.3A. Case 3. Non contrast enhancement CT scan of the base of the skull and the brain revealed a low density soft tissue lesion in the skull base with intracranial extension. The density of the lesion was 15 H.U.

homogeneous material of mucoid attenuation (10 to 18 HUs). In a few cases the mucocele secretions may be particularly viscid and proteinatious, and the attenuation may be in the 20 to 40 HU range. However, most mucoceles have an attenuation in the mucoid range less than that of muscle (1,20). The sinus walls are remodelled and may be either of almost normal thickness, thinned, or eroded. If a mucopyocele is present, the sinus mucosa surrounding the central mucous secretions is seen as a thin zone of enhancement just inside the bony sinus walls. This signifies the presence of an infected mucocele (1,21).

On MRI, the signal intensities are dominated initially by the high water content of the mucous secretions (about 95% water). Thus, there usually is

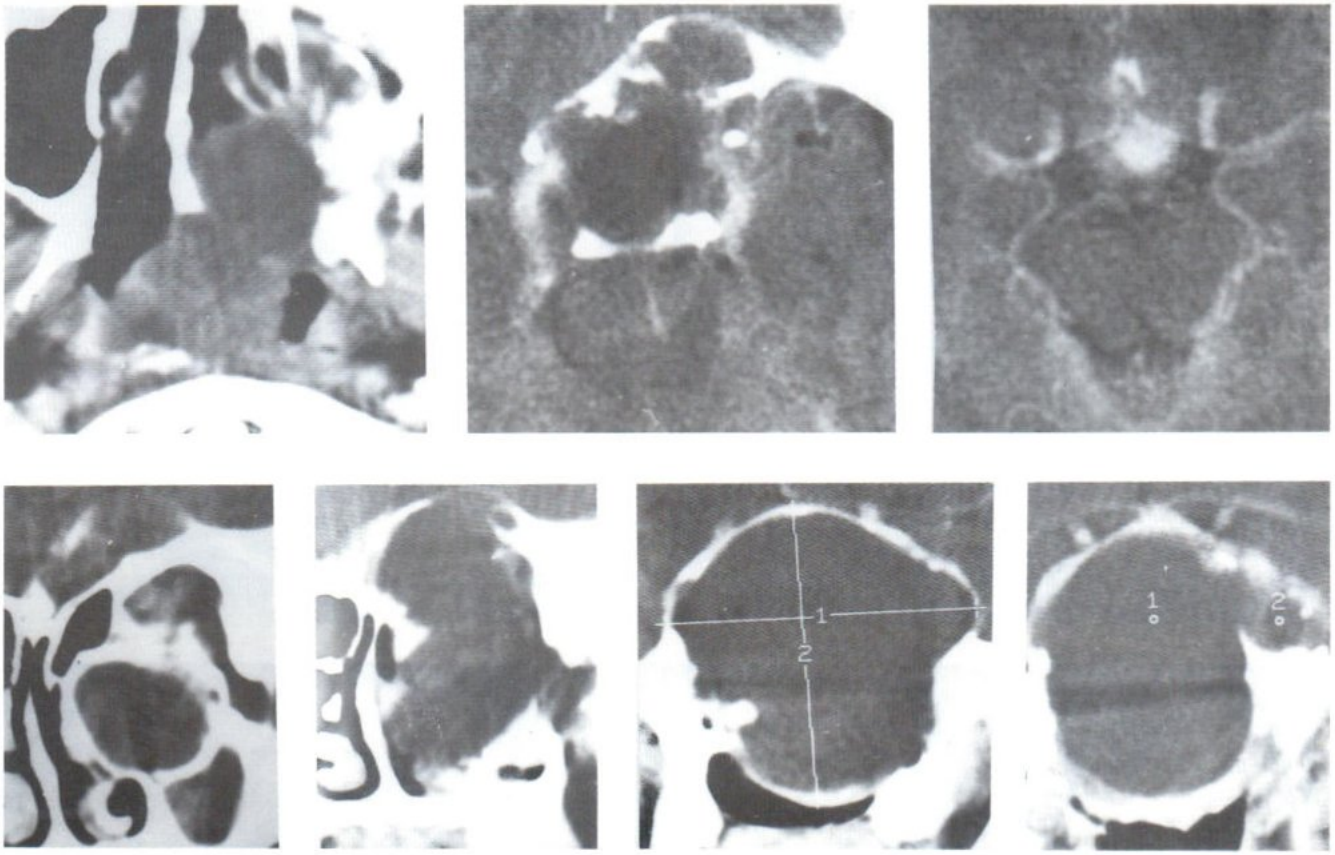

Fig.3B. Case 3 Contrast enhancement of the lesion in axial and coronal view showed a non enhanced lesion in the expanded sphenoid sinus extending to left nasopharyngeal airway, posterior leftnasal cavity, left maxillary sinus, pre-medullary, pre-pontine region, medial left temporal fossa, sella and suprasellar area. Both sides of the cavernous sinuses were compressed and invaded at the left side. The clivus, a part of pterygoid bones, both petrous apices, medial and posterior walls of left maxillary sinus diappeared. The lesion did not enter the left orbital cavity.

a low signal intensity on T1WIs, an intermediate signal intensity on PDWIs, and a high signal intensity on T2WIs. If the mucocele has been present for a long time (many months), the T1-and proton density-weighted signal intensities become higher. The primary causes appear to be a concentration of the proteinatious secretions, a slow resorption of water through the mucosa, and an increased viscosity of these secretions. When enough free water is resorbed from the mucocele and the protein concentration reaches about 25% to 35%, first the T2WI signal intensity and then the T1WI signal intensity become low (1,23). Thus, mucoceles can have the following progressive MRI appearances: low T1, high T2; intermediate T1, high T2: high T1, high T2; intermediate-to high T1, low T2; low T1, low T2. If a mucopyocele is present the infection appears to cause increased viscosity with a resulting shortening of the T1 signal.

Our first case, the lesion was confined in the expanded sphenoid sinus. The density of the lesion was high due to prolonged retention and was corresponded with the surgery which only thickened mucosa was found.

Our 2nd case, the lesion was also confined within the expanded sphenoid sinus. The signal character was of the classical rather clear fluid content.

Our 3rd and 4th cases, the lesions were quite extensive with intracranial involvement. There were wide skull base destruction. The concentration of the fluid in the 3rd case was less than the 4th case.

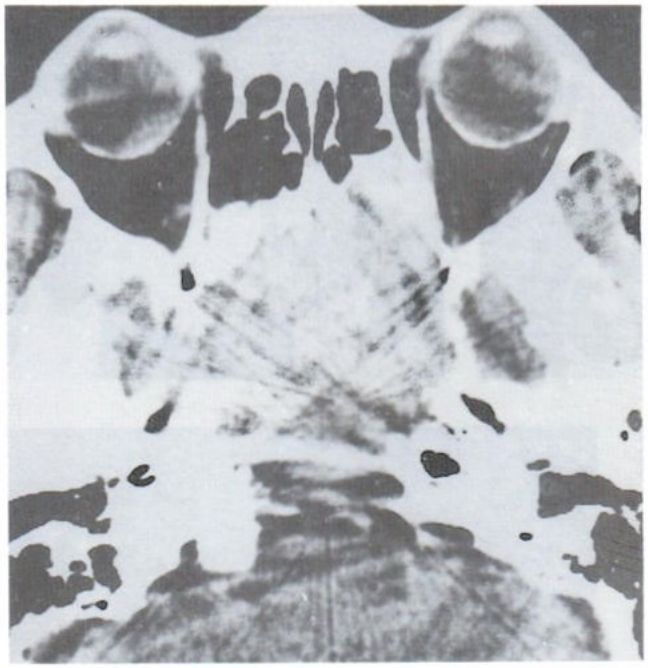

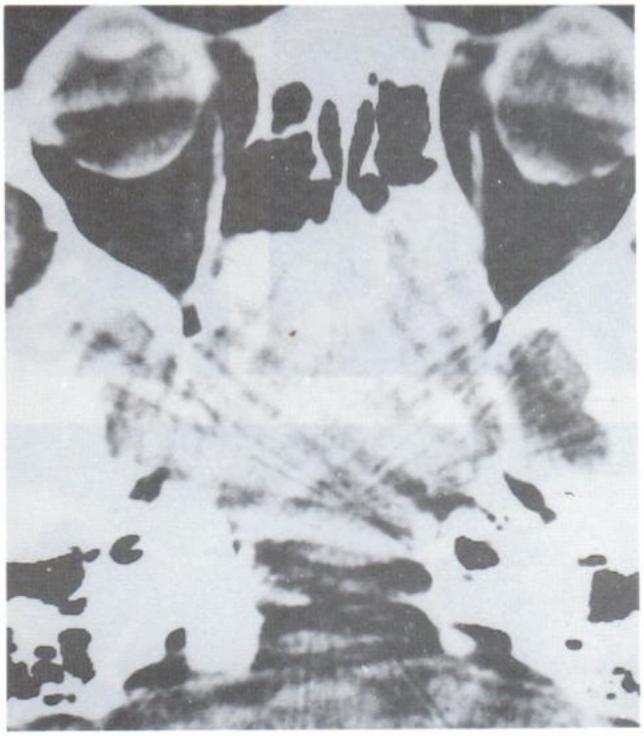

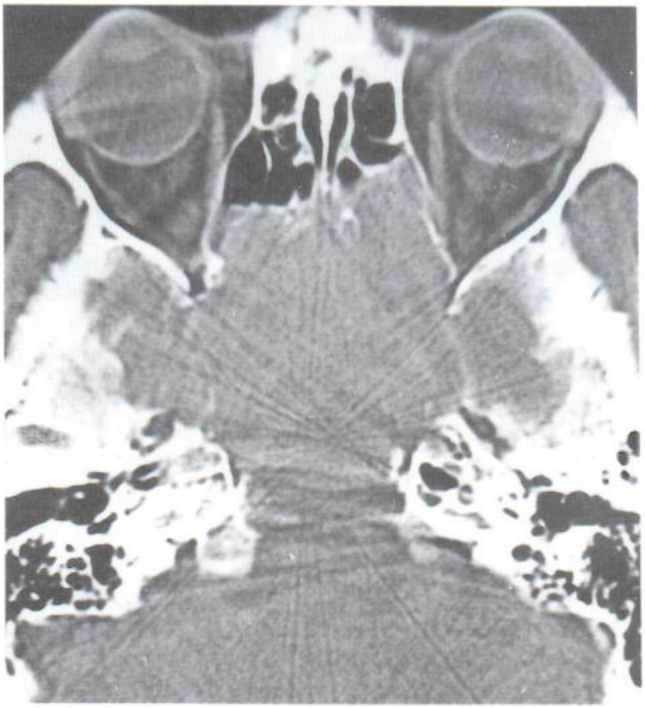

Fig. 4 Case 4. Non contrast enhanced CT scan of the brain and base of the skull in axial view showed a hyperdense soft tissue in the sphenoid sinus.

In conclusion, the lesion of the sphenoid mucocele demonstrated in our cases showed the following characters: 1) expansion of the sphenoid sinus 2) the content was hemogeneous, the density was low or high on CT images and dark grey on T1WI and fluid bright on T2WI 3) extension to the adjacent organs was of smooth manner, though bony destruction was present.

REFERENCES

1. Som PM, Bergeron RT. Head and neck imaging. 2nd ed. Mosby Year Book: St Louis, 1991:154.
2. De Juan EE, Green WR, Iliff NT. Allergic periorbital mucopyocele in children. Am J Ophthalmol 1983;96:299.
3. Finn DG, Hudson NR, Baylin G. Unilateral polyposis and mucoceles in children. Laryngoscope 1981;91:1444.
4. Sizmor J, Noyek AM. Cysts, benign tumors and malignant tumors of the paranasal sinuses. Otolaryngol Clin North Am 1973;6:487.
5. Rogers JH, Fredrickson JM, Noyek AM. Management of cysts, benign tumors and bony dysplasia of the maxillary sinus. Otolaryngol Clin North Am 1976;9:2330.
6. Nogent GR, Sprinkle P, Bloor BM. Sphenoid sinus mucoceles. J Neurosurg 1970;32:443-51.

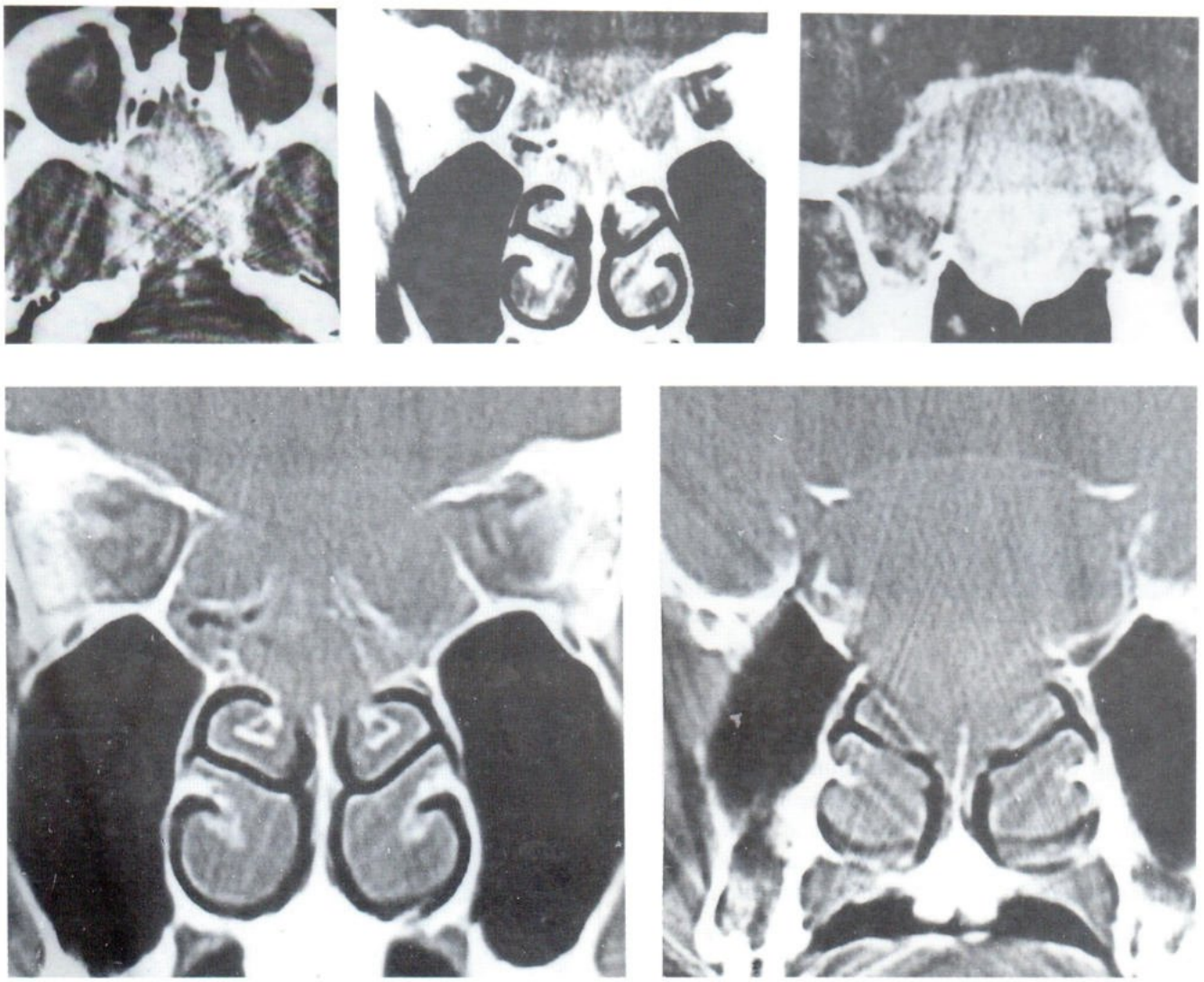

Fib. 4B. Case 4. Post contrast enhanced axial and coronal CT scan of the base of the skull and brain revealed a homogeneous hyperdense soft tissue lesion in the expanded sphenoid sinus. The lesion extended to both sides of the cavernous sinuses. Bony destruction was noted at clivus, superior part of leftpterygoid plates, walls of the sphenoid sinuses and bony parts of the skull base.

7. Close LG, O'Conner WE. Sphenoethmoidal mucoceles with intracranial extènsion. Otolaryngol Head Neck Surg 1983;91:350-7.
8. Gore RM, Weinberg PE, Kim KS, Ramsey RG. Sphenoid sinus mucoceles presenting as intracranial masses on computed tomography. Surg Neurol, 1980;13:375-9.
9. Johnson LN, Hepler RS, Yee RD, Bartzodorf U. Sphenoid sinus mucocoele (anterior clinoid variant) mimicking diabetic opthalmoplegia and retrobulbar neuritis. Am J Opthalmol 1977;9: 259-66.
10. El-Fiki ME, Abdel-Fattah HM, El-Deeb AK. Sphenoid sinus mucopyocele with marked intracranial extension: A more common phenomenon in the third world ? Surg Neurol 1993;39:115-9.
11. Bregear P. Ophthalmic manifestations of sphenoid mucoceles. Ann Ophthalmol 1977;9:259-66.
12. Nugent GR, Sprinkle P, Bloor BM. Sphenoid-sinus mucoceles. J Neurosurg 1970;32:443-51
13. Classen AJ. Empyema of the sphenoid sinus. A case report. S Afr J Surg 1983;21:55-60.

14. Alba AA, Maroon JC, Wilberger JE Jr, Kennerdell JS, Deeb ZL. Intrasellarmucocoele simulating pituitary adenoma. Case report. Neurosurgery 1986; 18:197-9.
15. Fody EP, Biner EF. Sphenoid mucocoele causing hyperprolactinemia:radiologic/pathologic correlation. South Med J 1986;79:1017-21.
16. Wilberger JR Jr, Alba A, Kennerdil J, Maroon JC. Mucocele of the pterygoid recess treated by laser surgery. Case report. J Neurosurg 1985;63: 970-2.
17. Breaget P. Ophthalmic manifestations of sphenoidal mucoceles. Ann Ophthalmol 1997;32:259-66.
18. Osborn AG, Johnson L, Roberts TS. Sphenoid mucoceles with intracranial extension. J Comput Assist Tomogr 1979;3:335.
19. Chut MC, Briant TDR, Gray T, et al. Computed tomography of sphenoid sinus mucocele. J Otolaryngol 1983;12:263.
20. Perugini S, Pasquini U, Menichelli F, et al. Mucoceles in the paranasal sinus involving the orbit: CT signs in 43 cases. Neuroradiology 1982;23:133.
21. Torjussen W. Rhinoscopical findings in nickel workers, with special emphasis on the influence of nickel exposure and smoking habits. Acta Otolaryngol (Stockh) 1979;88:279.
22. Som PM, Dillon WP, Fullerton GD, et al Chronically obstructed sinonasal secretions observations on T1 and T2 shortening. Radiology 1989;172: 515.

ASDIR

EDUCATION

Asian-Oceanian Seminars on Diagnostic and Interventional Radiology

1 9 9 7

Imaging and Interventional Radiology of the Hepatobiliary System
February 19-21
Khon Kaen, Thailand
Programme Leader:
B. Sitisara

Urogenital Imaging
April 25-27
Bombay, India
Programme Leader:
R. Sukthankar

Radiology of Cerebrovascular Disease, including interventional neuroradiology
October 23-24
Melbourne, Australia
Programme Leader:
B. Tress

Chest Radiology
November 1-2
Kuala Lumpur, Malaysia
Programme Leader:
Joginder Singh

BRACCO
INTERNATIONAL

For further information please contact:
Bracco International B.V.
47 Hill Street
S.C.C.C.I. Building
#06-05 Singapore 179365
Tel: ++65-337 1880
Fax: ++65- 337 7576

ANNULAR PANCREAS IN THE ADULT WITH STONES AND ADENOMYXOMA AT THE DISTAL COMMON BILE DUCT

Patchrin PEKANAN[1], Chirote SUCHATO[2], Payap CHOKSUWATANASKUL[1], Siricha GOEBEL[1].

ABSTRACT

A case of symptomatic annular pancreas complicated by CBD stones. CBD septum and adenomyxoma of the CBD was reported. UGI series showed circumferential narrowing of the second portion of the duodenal loop. Oral contrast CT scan showed pancreatic tissue around the contrast filled duodenal loop. Post PTC CT scan showed a well defined defect in the contrast filled dilated CBD which was due to stones.

INTRODUCTION

Annular pancreas was first described by Tiedemann in 1818 (1). It developed as a result of failure of the tip of the ventral pancreatic anlage to rotate completely to the right and posteriorly with the duodenum allergely produces a band of elongated pancreatic tissue about the viscus (2). A band of glandular tissue embraced the duodenum circumferentially. In the adult the annulus is consistently located about the second portion of the duodenum (3). Symptomatic annular pancreas in the adult is uncommon (2,4).

CASE REPORT

A 47-year-old woman developed jaundice two months post partum. She was a known thalassemia-Hb E patient. Liver function test indicated obstructive jaundice.

Upper GI series showed severe narrowing lumen of the 2nd portion of the duodenal loop by a circumferential lesion with partial obstruction (Fig.1). Percutaneous cholangiography revealed moderate degree of dilatation of the intrahepatic ducts and extrahepatic bile duct. Severe narrowing lumen of the distal CBD is seen with overhanging edge appearance of the upper border of the lesion (Fig.2). Oral enhanced and post PTC CT scan showed the pancreatic tissue to be around the 2nd portion of the duodenal loop (Fig.3a) and a round filling defect in the contrast filled CBD (Fig.3b).

At surgery and pathology, annular pancreas was seen. Adenomyxoma was noted involving the ampulla of Vater and distal CBD. Choledocholithiasis and CBD septum were also found.

PTC = Percutaneous Transhepatic Cholangiography

DISCUSSION

Annular pancreas is seen in patients from the neonate to the eighth decade of life. In adults, it is most common between the third and fifth decades of life, and is seen twice as frequently in men as in women (6). The symptoms of annular pancreas are frequently those of secondary pathologic states, most commonly peptic ulceration and pancreatitis (7). Annular pancreas in infants is often associated with many other congenital malformations. In adults, the annular pancreas is usually an isolated findings (8).

Changes in the duodenal loop by upper GI series had been reported (6,9,11) including the following: a) eccentric smooth annular defect of the

[1] Department of Radiology, Ramathibodi Hospital, Rama 6 Street, Bangkok 10400, Thailand.
[2] Department of Radiology, Bangkok General Hospital, Bangkok.

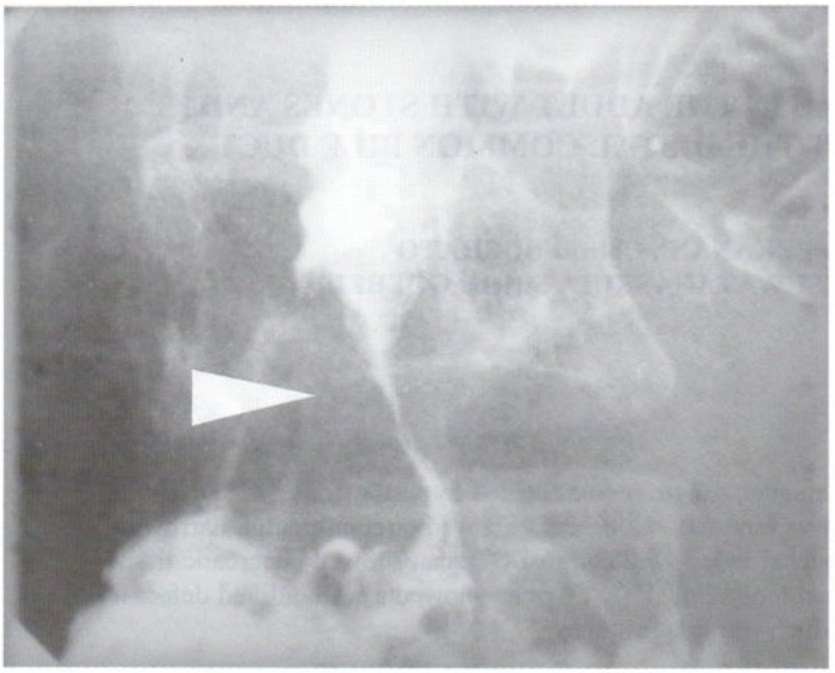

Fig.1 UGI series showed a circumferential narrowing lumen-lesion at the second portion of the duodenal loop; overhanging edge was seen at both ends of the lesion. Only partial obstruction was seen.

outer margin of the second portion of the duodenum retracting it medially, b) symmetric dilatation of the proximal duodenum with bulging of the recesses on either side of the annular band, c)mucosal effacement without destruction, d) reversed peristalsis in the proximal dilated duodenum, e) absence of spastic phenomena, f) accentuation of the findings in the right anterior oblique position, and g) lack of change on repeated examinations. the "double bubble" sign associated with pediatric cases is of no value in adults(7).

Contrast material in the duct of annular pancreas on ERCP was reported by Glazer (12) and Yogi (13). Pancreatic tissue encircled the second portion of the duodenal loop was shown on CT scan (14,15) and on MRI (15).

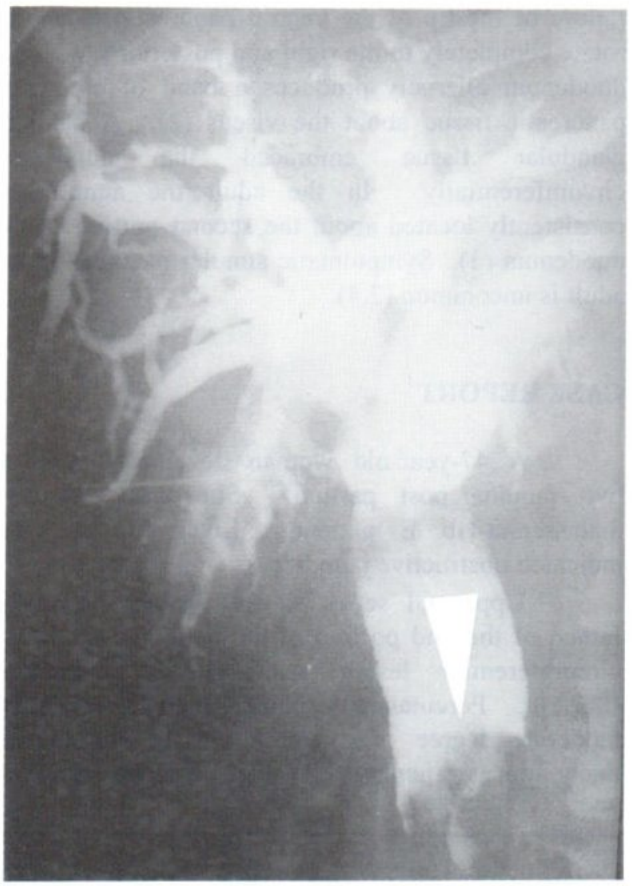

Fig.2 Percutaneous transhepatic cholangiography (PTC) revealed dilatation of both intra-and extrahepatic bile duct. A filling defect was noted at the distal part of the CBD, causing nearly complete obstruction of the lumen. An overhanging edge was seen at the superior end of the lesion, caused by stones. The lesion distal to the stones was difficult to evaluate.

ERCP = Endoseopic Retrograde Cholangio-pancreatography

Similar findings by upper GI series and oral contrast CT scan were also shown by us. PTC findings in this case were the combined results of annular pancreas, CBD stones, adenomyxoma and septum in the CBD. Stones in this case, is probably secondary to prolonged CBD obstruction and hemolysis in the thalassemic patient.

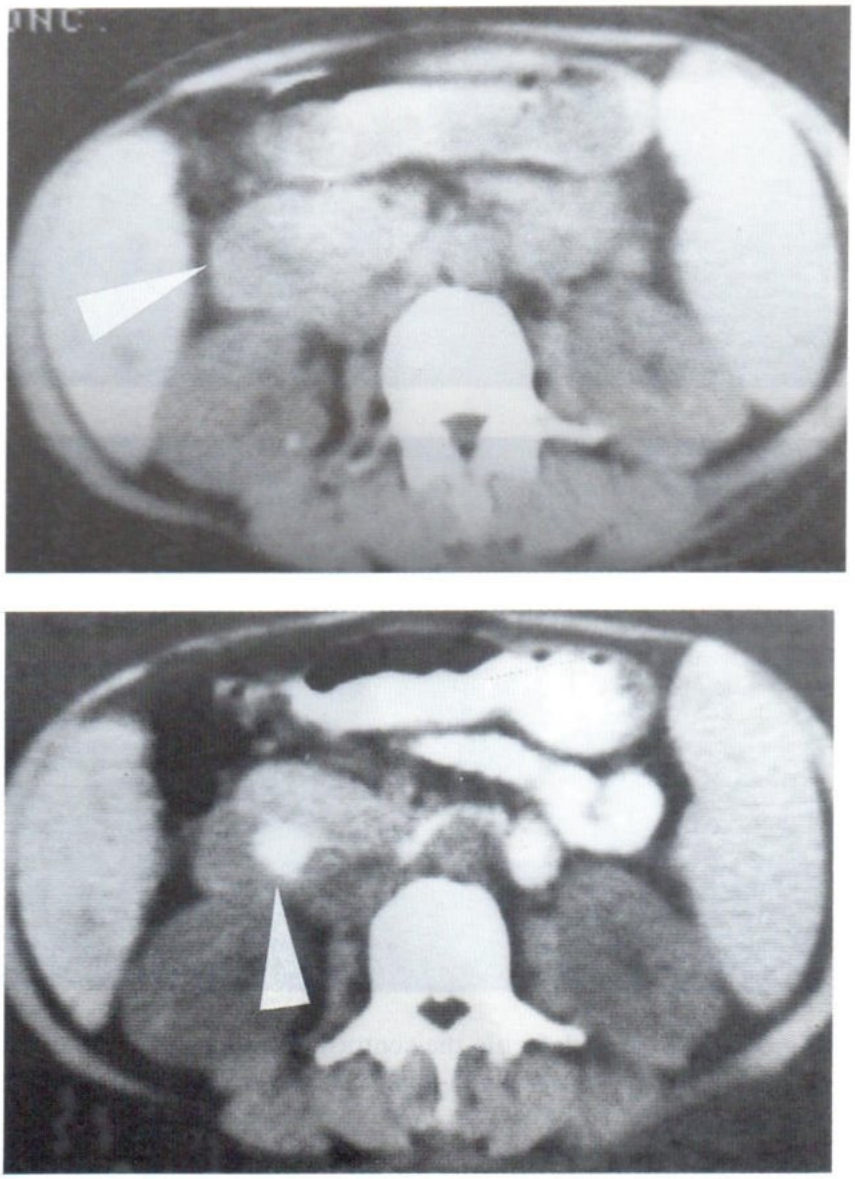

Fig. 3a. Plain CT scan showed bulging contour of the pancreatic head with a faint low density area in the center represent CBD. Oral contrast filled CBD was seen in the center of the bulged pancreatic head.

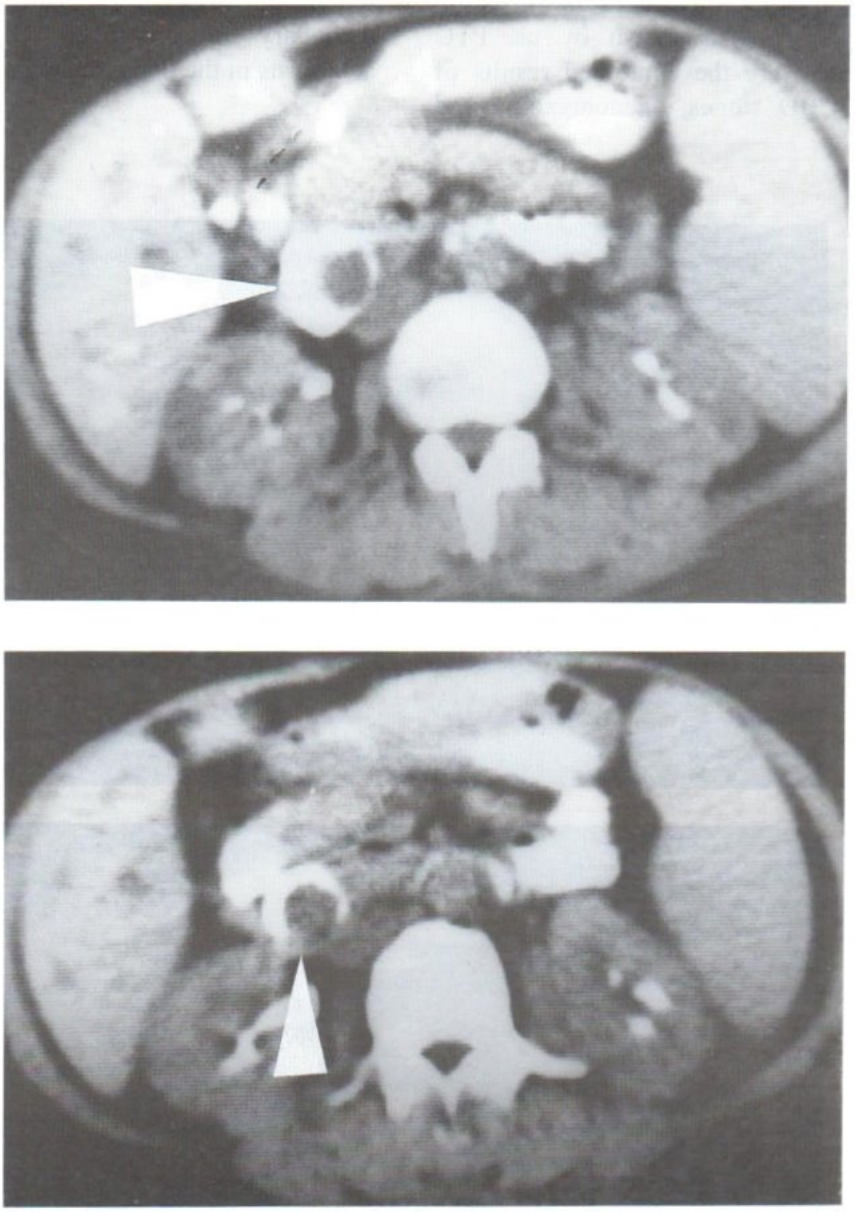

Fig. 3b. Soft tissue defect in the contrast-filled lumen of the dilated CBD represented non-opaque stones, visualized on post PTC CT scan.

REFERENCES

1. Tiedemann F. Annular Pancreas. Deutsch, Arch f.d. Physiol 1818;4:403.
2. Lecco TM. Concerning Cord's case of annular pancreas. Anat Anz 1911;39:535.
3. Thomford NR, Knight PR, Pace WG, Madura JA. Annular pancreas in the adult: selection of operation. Ann Surg 1972;176:159-62.
4. Drey NW. Symptomatic annular pancreas in the adult, Am Intern Med 1957;46:750.
5. Silvis RS. Annular pancreas. Am Surg 1952;135:278-83.
6. Beachley MC, Lankau CA Jr. Symptomatic adult annular pancreas. Digestive Diseases 1973;18:513-6.
7. Grossman MS. Annular pancreas in adults. Tex Med J 1964;60:580.
8. Huebner GD, Reed PA. Annular pancreas. Am J Surg 1962;104:869.
9. Dodd GD, Nafis WA. Annular pancreas in adult, Am J Roentgenol Radium Ther Nucl Med 1956;75:333.
10. Mast WH. Telle Ld, Turek RO. Annular pancreas. Am J Surg 1957;94:180.
11. Poppel MH, Beranbaum SL. Annular pancreas: roentgen manifestations. Am J Dig Dis 1956;1:476.
12. Glazer GM, Margulis AR. Annular pancreas: Etiology and diagnosis using endoscopic retrograde cholangiopancreatography. Radiology 1979;133:303-6.
13. Yogi Y, Shibue T, Hashimoto S. Annular pancreas detected in the adult diagnosed by endoscopic retrograde cholangiopancreatography: report of four cases. Gastroenterol Jpn 1987;22:92-9.
14. Nuguyen K, Pace R, Groll A. CT appearance of annular pancreas: a case report. J Can Assoc Radiol 1989;40:322-3.
15. Reinhart RD, Brown JJ, Foglia RP, Alipertic G. MR imaging of annular pancreas. Abdom Imaging 1994;19:301-3.

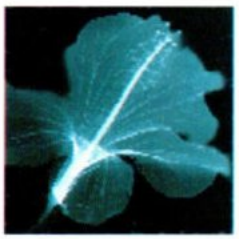

Bracco AAR 1997 Award

Bracco International continues its support of AAR by offering a Bracco Award which will be presented on the occasion of the 9th AAR Congress in Singapore. The purpose of this award is to stimulate high quality research in the area of diagnostic and interventional radiology among the young radiologists in the ASEAN countries. This prize will be awarded for original and pioneering works and the winners will be selected by the host country's Scientific Committe.

Total Value of Award: SF 30,000

The prize SF 30,000 will be divided equally among the participating AAR six member countries. There can, however, be only one winner from each participating country. To be eligible for the Bracco Award, the candidates must meet the following criteria:

1. *Principal author below 40 years of age at the deadline of submission*
2. *Papers must originate from one of the AAR member countries*
3. *Candidate must indicate an intention to participate in the Bracco Award when submitting the abstract*
4. *Submitted scientific papers should pass through and be endorsed by the Radiological Society of the country*

Both oral and poster presentations can be considered for the Bracco Award.

Deadline for submitting abstract: November 1, 1996

BRACCO IMAGING

ACUTE LEUKEMIA PRESENTING AS ACUTE PANCREATITIS

Janjira JATCHAVALA, Patchrin PEKANAN

ABSTRACT

A pediatric patient presented with acute pancreatitis, was found to have acute leukemia. Leukemic nodules was shown in the liver and kidneys by CT scan. The pancreas was diffusely enlarged and had low density which suggested acute inflammatory process and leukemic deposition was likely the cause of pancreatitis. Acute leukemia should be in a differential diagnosis of the pediatric patients who present with acute pancreatitis.

INTRODUCTION

Acute pancreatitis is an inflammation of the pancreas which may go on to suppuration, necrosis or hemorrhage (1,2). The final diagnosis of pancreatitis is usually based on the presence of a typical clinical syndrome consisting of upper abdominal pain, elevation of serum or urine amylase levels (25-30% over upper limit of normal), an amylase creatinine clearance ratio of 4% or greater, exclusion of other causes of abdominal pain and a response to therapy specific for pancreatitis (3). Acute leukemia is the result of a malignant event, or events, occurring in an early hematopoietic precursor. Instead of proliferating and differentiating normally, the affected cell gives rise to progeogeny that fail to differentiate and instead continue to proliferate in an uncontrolled fashion. As a result, immature myeloid cells (in acute myelogenous leukemia) or lymphoid cells (in acute lymphocytic leukemia); often called "blasts" rapidly accumulate and progressively replace the bone marrow, leading to diminished production of normal red cells, white cells, and platelets. This loss of normal marrow function in turn give rise to the commom clinical complications of leukemia: anemia, infection and bleeding. With time, the leukemic blasts pour out into the bloodstream and eventually occupy the lymph nodes. spleen, and other vital organs (4). Acute pancreatitis is occasionally a manifestation of leukemic or lymphomatous involvement of the pancreas (5,6).

CASE REPORT

A 5-year-old boy, had abdominal and back pain for one week. She was found to have hepatomegaly, tender epigastric region and swelling of both eyelids. A mass was noted at his left submandibular region for a month. The serum amylase one week after the onset of the epigastric pain was 533 unit, urine amylase 15,240 unit, alkaline phosphatase 423 unit. Bone marrow aspiration revealed acute lymphocytic leukemia. She was given Vincristine and endoxan and lost follow up.

CT scan at the admission time showed leukemic nodules in the liver, and kidneys (Fig. 1). The pancreas was diffusely enlarged and had low density (Fig. 2).

DISCUSSION

The etiology of most leukemic gastrointestinal complications is believed to be threefold:(1) primary invasion by leukemic cells to the bowel and related structures, causing bowel obstruction; diffuse mucosal ulceration and hemorrhage; infarction and rupture of the liver and spleen; portal hypertension with ascites and varices; obstruction of

Department of Radiology, Ramathibodi Hospital, Rama 6 Street Bangkok 10400, Thailand.

biliary and pancreatic duct systems; protein losing enteropathy; and pneumatosis intestinalis (2) altered immune state causing increased susceptibility to common infections appendicitis; wound infections, perianal inflammation, abscess formation, peritonitis, septicemia; opportunistic infections-esophageal and gastric candidiasis, pseudomembranous enterocolitis, typhlitis, toxic megacolon (3) direct and indirect toxicity of antileukemic therapy-profound nausea and vomiting, severe adynamic ileus; vincristine-induced megacolon; peptic ulcer disease, tissue necrosis in bowel wall, pancreatitis and hemorrhagic colitis (7).

Massive invasion by leukemic cells may cause bowel, biliary and pancreatic duct obstruction which produces acute pancreatitis (7). Malpica (6) reported a case of plasma cell leukemia in an old age patient who had clinical acute pancreatitis. Diffusely enlarged pancreas was found at surgery and diffuse infiltrate of typical and atypical plasma cells was found at autopsy.

Patients whose immune systems have been compromised either through disease processes or for therapeutic reasons are highly susceptible to infection by viruses. Viral infection could create acute pancreatitis, e.g. mumps, hepatitis A, hepatitis B, coxackie B, Epstein-Barr, adenovirus (7,8). It was suggested that a primary adenovirus infection to the gastrointestinal tract ascends to and involves the pancreatic parenchyma via the pancreatic ducts (9). The viral antigen could be found in acinar cells, pancreatic duct cells and duodenal mucosal epithelium in the case of adenoviral pancreatitis.

The acute pancreatitis in this leukemic patient was probably caused by leukemic infiltration of the pancreas. The lack of fluid in the anterior pararenal space in the presence of acute pancreatitis was quite unusual and was not mentioned in the literature.

REFERENCE

1. Silverstein W, Isikoff MB, Hill MC, Barkin J. Diagnostic imaging of acute pancreatitis:-prospective study using CT and sonography. AJR 1981;137:497-502.
2. Brandborg LL. Acute pancreatitis. In: Sleisinger MH, Fordtran JS, eds. Gastrointestinal disease. Philadelphia: Saunders, 1973:1158-84.
3. Fleischer AC, Parker P, Kirchner SH, James Jr AE. Sonographic findings of pancreatitis in children. Radiology 1983;146:151-5.
4. Appelbaum FR. The acute leukemia. In Wyngaarden, Smitt, Bennett, ed. Cecil textbook of medicine. 19th ed. Philadelphia; W.B. Saunders Company, 1992:944-5.
5. Francis IR, Glazer GM. Burkitt's lymphoma of the pancreas presenting as acute pancreatitis. J. of Computer Assisted Tomography 1982;6:395-7.
6. Malpica A, Phillips CC, Estrada RE, Banez EI. Plasma cell leukemia presenting as a pancreatic mass. Arch Pathol Lab Med 1993;117:844-5.
7. Steinburg WM. Pancreatitis. In Wyngaarden, Smitt, Bennett, ed. Cecil textbook of medicine. 19th ed. Philadelphia: W.B. Saunders Company, 1992:722.
8. Niemann TH, Trigg ME, Winick N, Penick GD. Disseminated adenoviral infection presenting as acute panceatitis. Human Pathology 1993;24:-1145-8.
9. Chandler FW, McClure HM. Adenoviral pancreatitis in rheses monkeys: current knowledge. Vet Pathol 1982;19:171-80.

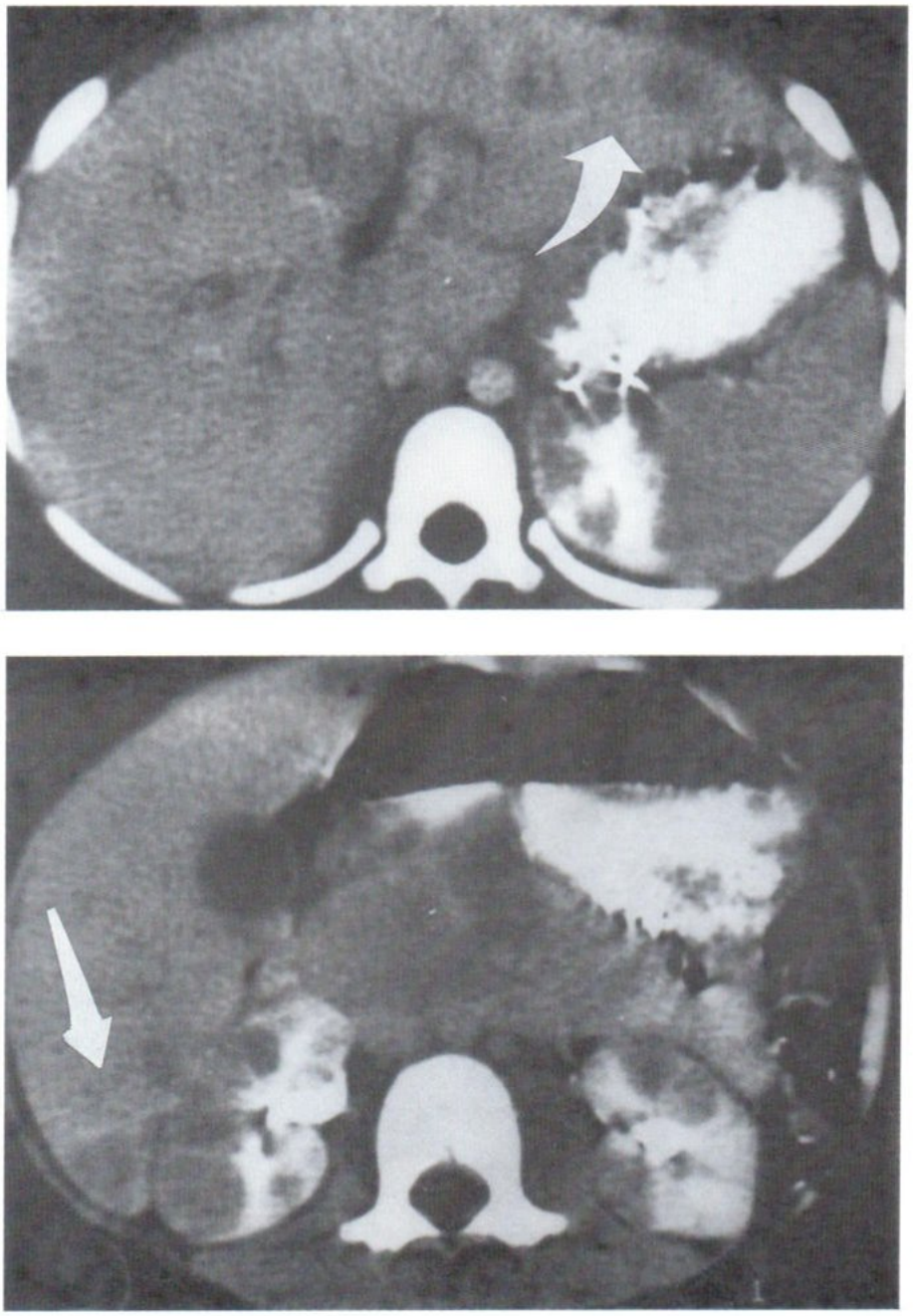

Fig. 1A. I.V. contrast enhanced axial CT scan of the liver showed multiple low density leukemic nodules.

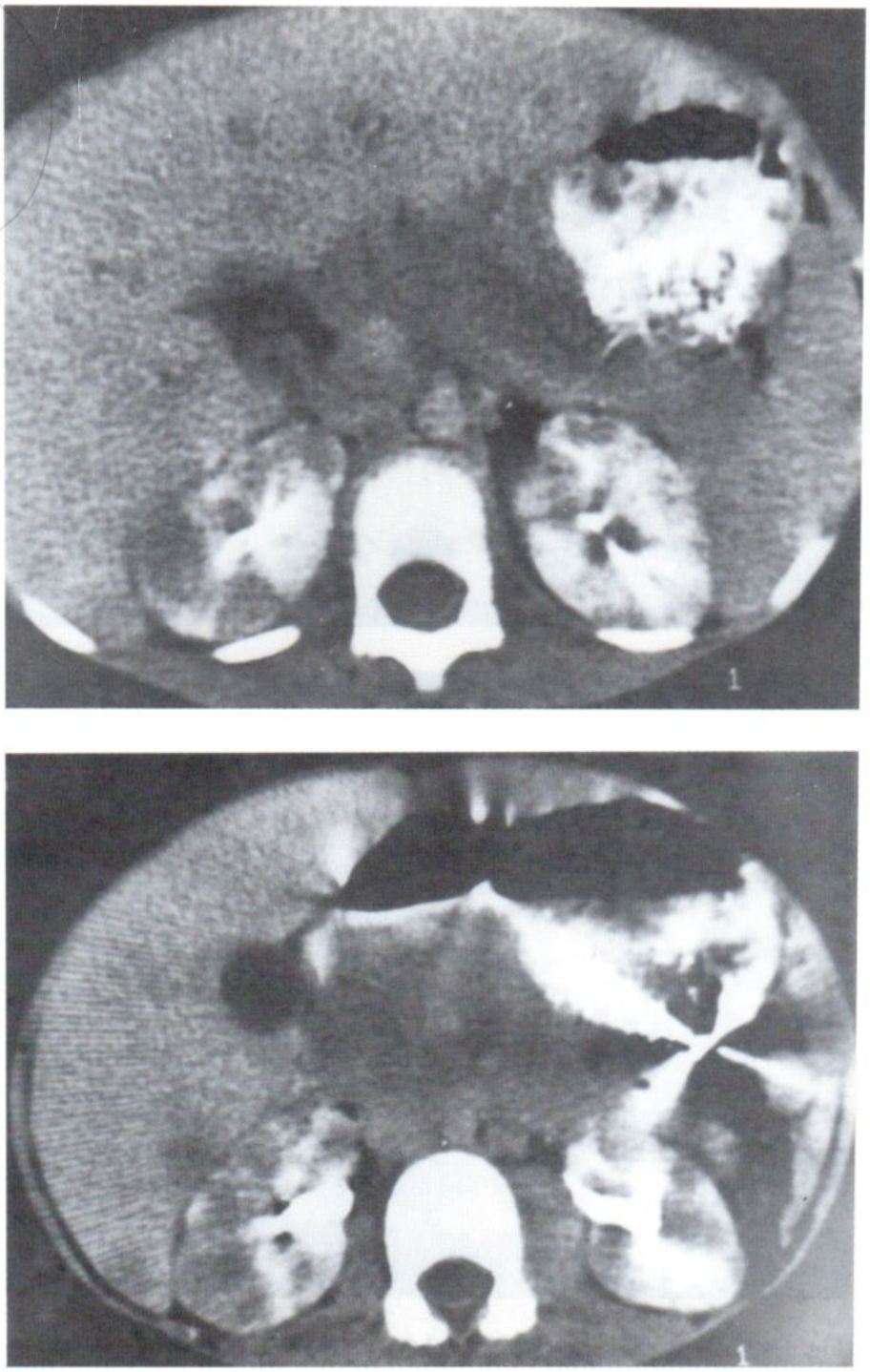

Fig. 1B The same study showed multiple low density leukemic nodules in both kidneys.

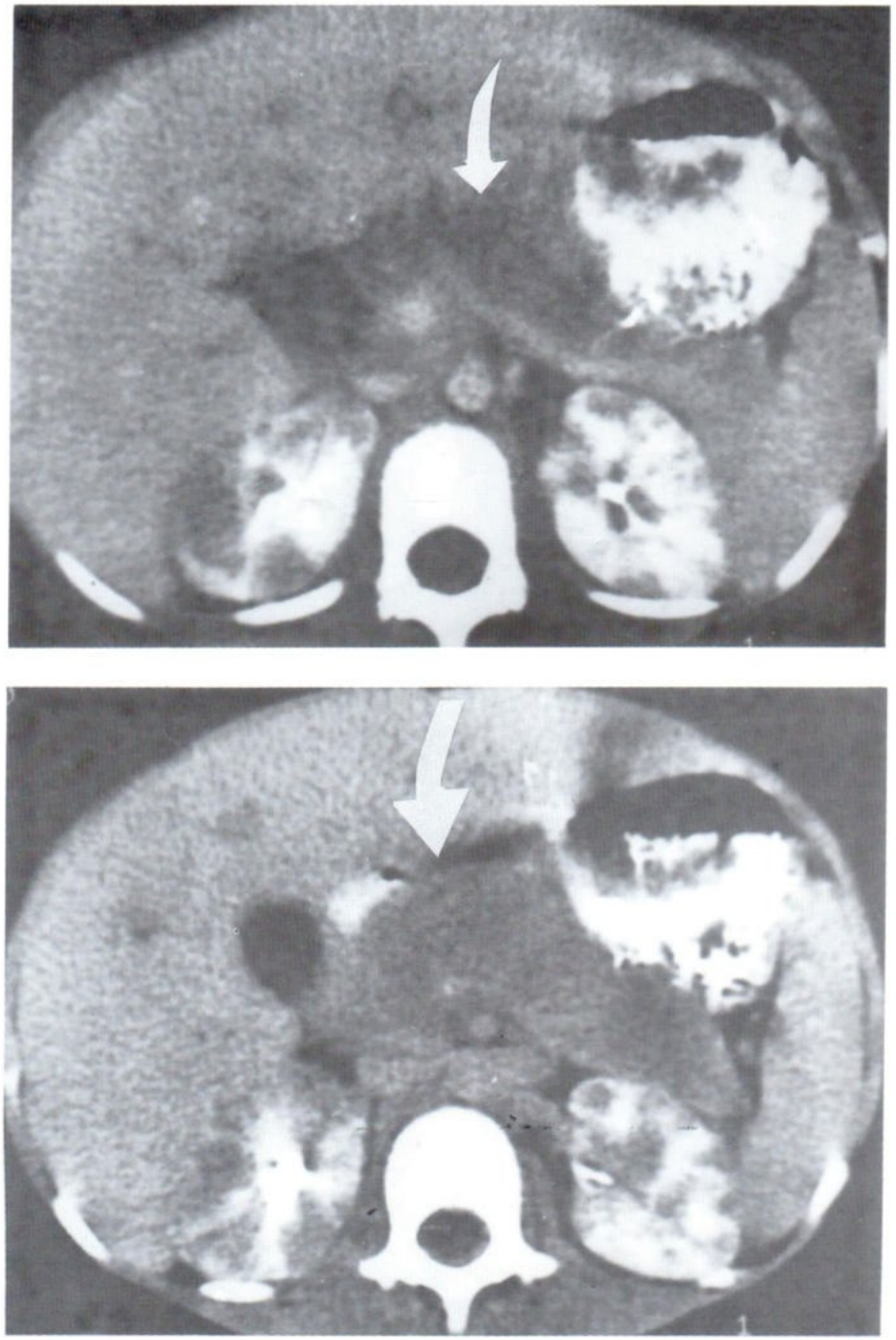

Fig. 2 Diffuse thickened parenchyma of the pancreas with diffuse low density which suggest acute pancreatitis due to leukemic deposition. Lack of fluid in the peripancreatic space is quite unusual for the process of acute pancreatitis.

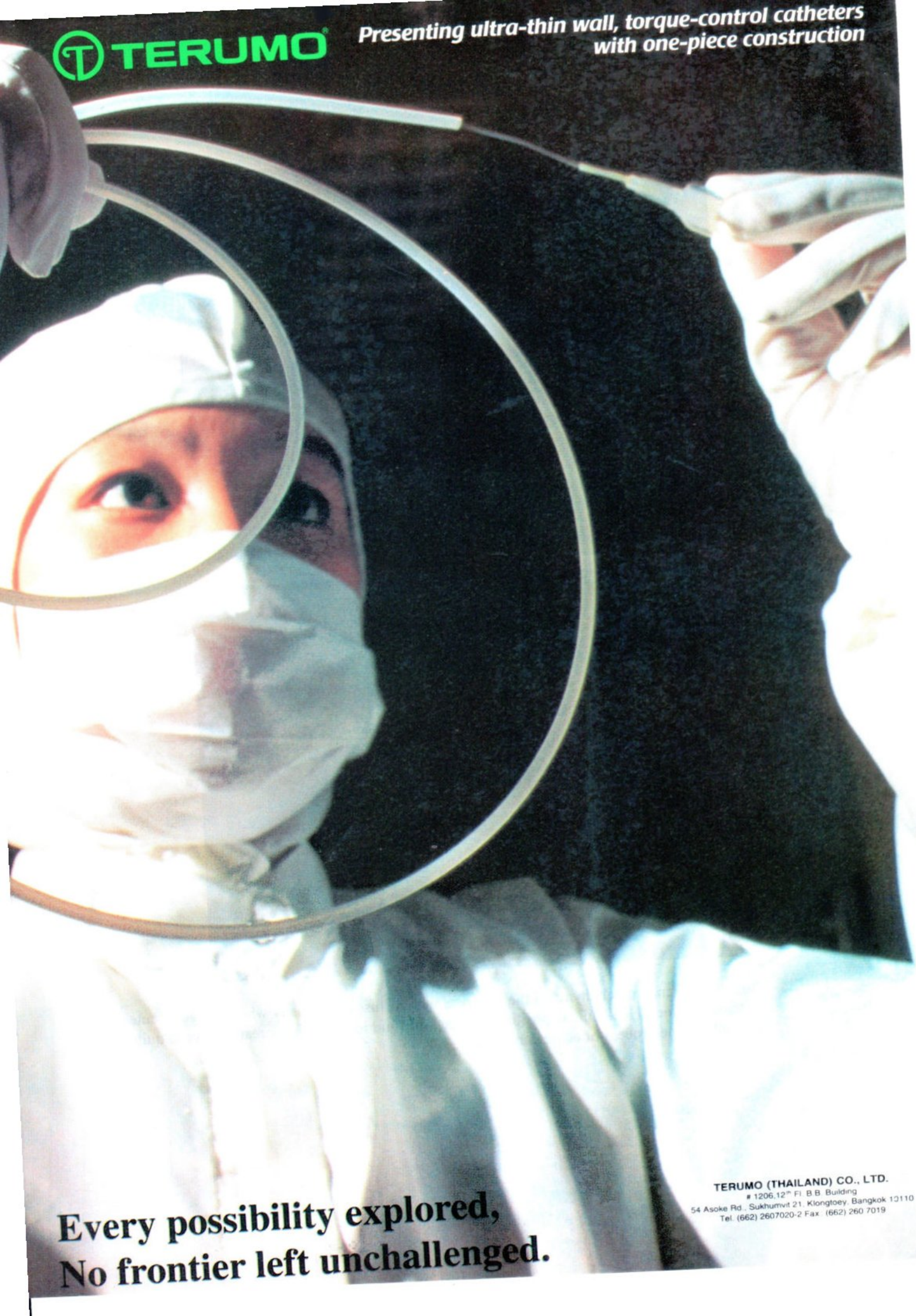
TERUMO
Presenting ultra-thin wall, torque-control catheters with one-piece construction
Every possibility explored,
No frontier left unchallenged.
TERUMO (THAILAND) CO., LTD.
1206,12th Fl. B.B. Building
54 Asoke Rd., Sukhumvit 21, Klongtoey, Bangkok 10110
Tel. (662) 2607020-2 Fax. (662) 260 7019

MRI AND CT IMAGING OF SYMPTOMATIC CALCIFICATION OF THE LIGAMENTUM FLAVUM

Patchrin PEKANAN[1,2], Sopon KUMPOLPUNTH[1],
Sashilekha BALACHANDRA[1,2], Janjira CHATCHAVALA[1,2]

ABSTRACT

A 43-years old man with motor and sensation abnormality, involving left knee and the pedal extensor, was shown to have calcified or ossified ligamentum flavum on both sides of the thoracic levels. Epidural type of cord compression was shown. Images were of MRI and CT studies.

INTRODUCTION

Calcification or ossification of the ligamentum flavum causes spinal cord compression. It occurs mostly in the Japanese population, predominantly in men, and mostly affects the lower thoracic region. Calcification (or ossification) of the ligamentum flavum may be a prominent feature of degenerative spinal disease and it is rare in the cervical region (1).

We present a case of calcified ligamentum flavum in a symptomatic patient by MRI and CT studies.

CASE REPORT

A 43-year-old Thai male patient was requested for MRI study of the thoracolumbar spine. The patient had pain and numbness of left knee and leg for 10 days. There was a hyperreflexia of left knee, decreased pin-prick sensation and weakness of the pedal extensor.

MRI of the thoraco-lumbar spine was performed and showed no intrinsic cord lesion. Calcified ligamentum flavum is noted in multiple levels by MRI and CT studies as shown in the figures 1 and 2. Pressure effect was noted on the adjacent cord.

DISCUSSION

The ligamentum flavum (LF) or yellow ligaments are composed mainly of elastic connective tissue fibers in a longitudinal array. They are the most purely elastic tissue in the human body (2-5). The ligaments extend from the anterior/inferior aspect of the lamina above a disk space to posterior superior surface of the lamina below the disk space. Each half of the LF extends laterally from midline to the intervertebral foramen forming the posterior boundary and roof of the foramen. The ligaments then turn dorsally outside the foramina and fuse with the capsule of the articular facets. The thickness of the LF gradually increases from the cervical to the lumbar regions. The LF is approximately 1.5 mm in thickness at the C2-C3 level, 2.0 mm at the T11-T12 level and 4-6 mm in the lower lumbar region. Thickening of the LF was due to an increase in the amount of fibrous tissue within the ligaments, which is believed to be from a degenerative change or aging (6). Associated mucoid swelling and hyalinization of the interelastic fibrous connective tissue may contribute to a relatively radiolucent appearance of the involved noncalcified LF. LF thickening is also believed to be caused by a buckling

[1] Department of Radiology, Ramathibodi Hospital, Rama 6 Street, Bangkok 10400, Thailand.
[2] Urupong Medical Center, Thoeddamri Street, Bangkok 10300, Thailand.

of the ligaments secondary to degenerative facet-joint changes and spondylosis.

Myelopathy due to ossification or calcification of the ligamentum flavum was reported by Miyasaka K (7). Eighteen patients were described with 15 ossified LF and 3 calcified LF. Ossification was found most often in the lower third of the thoracic spine, particularly at the T9-T10 and T10-T11 levels. Certain histopathologic features were found in almost all the ossification cases. The ligamentum flavum was replaced by mature bone. Lamellar bone structure which reached to the edges of two laminae extended in places over the proliferated cartilage and fibrous tissue adjacent to the intervertebral joint. Bone tissue was definitely differentiated from cartilage in some parts but mingled with it in others. Islands of fibrous tissue of undetermined origin were seen in and around bone tissue, but there were no inflammatory cells. Calcification was seen less prominently. The ossification of the LF was considered to be endochondral in nature.

Calcification of the LF was found predominantly in the cervical spine at the C5-7 levels. On CT, this calcification presented in a unique fashion, as an oval calcified mass ventral to the lamina. The dense mass was seen in the interlaminar part of the ligament but not in the capsular part, and the unossified part of the ligament was thickened. On histologic examination, the ligamentum flavum was thickened and degenerated. Calcified granules were deposited within the degenerative ligamentous fibers. The superior layer was pushed toward the canal by the calcification and the degenerated fibers of the ligament. No mature bone was formed within the ligament.

It is assumed that ossification begins at the edges of the laminae near the capsular insertion of the ligament and extends medially, upward, and downward as it involves the ligament. General ossification diathesis in individuals and chronic mechanical stress on the site of ligamentous insertion might cause this ossification.

The calcification of the LF tends to occur within the degenerated and thickened ligament in the cervical spine. The calcified mass has no continuity with the lamina and the superficial and deep layers of the ligament are relatively preserved. The nodular shape of such lesions seems to be specific to the LF (8).

REFERENCES

1. Quencer RM. MRI of the spine. pp 191. New York: Raven Press, 1991.
2. Stollman A, Pinto R, Benjamin V, Kricheff I. Radiologic imaging of symptomatic ligamentum flavum thickening with and without ossification. AJNR 1987; 8: 991-994.
3. Ramsey RH. The anatomy of the ligamentum flavum. Clin Orthop 1996; 44: 129-140.
4. Braus H. Anatomie des Menschen, Vol 1, Auflage 3 Berlin: Springer-Verlag, 1954.
5. Herzog W, Morphologie and Pathologie des Ligamentum Flavum. Frankfurter Z Pathol 1950; 61: 250-267.
6. Dockerty MD, Love JG. Thickening and fibrosis (so called hypertrophy) of the ligamentum flavum. Mayo Clin Proc 1940; 15: 161.
7. Miyasaka K, et al. Myelopathy due to ossification or calcification of the ligamentum flavum: Radiologic and Histologic evaluations. AJNR 1983; 4: 629-632.
8. Kawano N, Yoshida S, Ohwada T, Yada K, Sasaki K, Matsuno T. Cervical radiculomyelopathy caused by deposition of calcium pyrophosphate dihydrate crystals in the ligamenta flava. Case report. J Neurosurg 1980; 52: 279-283.

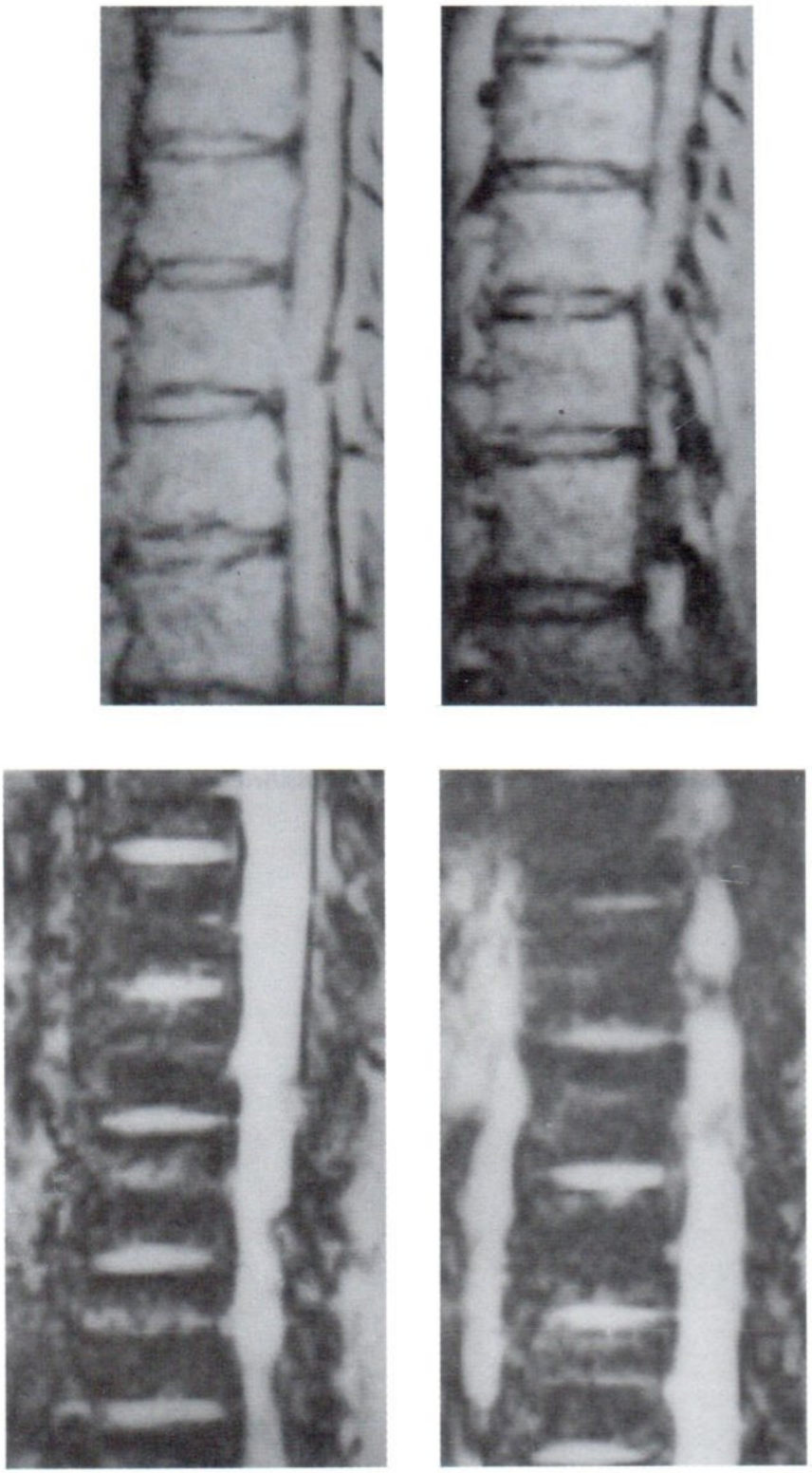

Fig. 1 T1WI, T2WI-sagittal view MRI study of the thoracic spine showed low signal ligamentum flavum on both T1WI and T2WI at multiple levels.

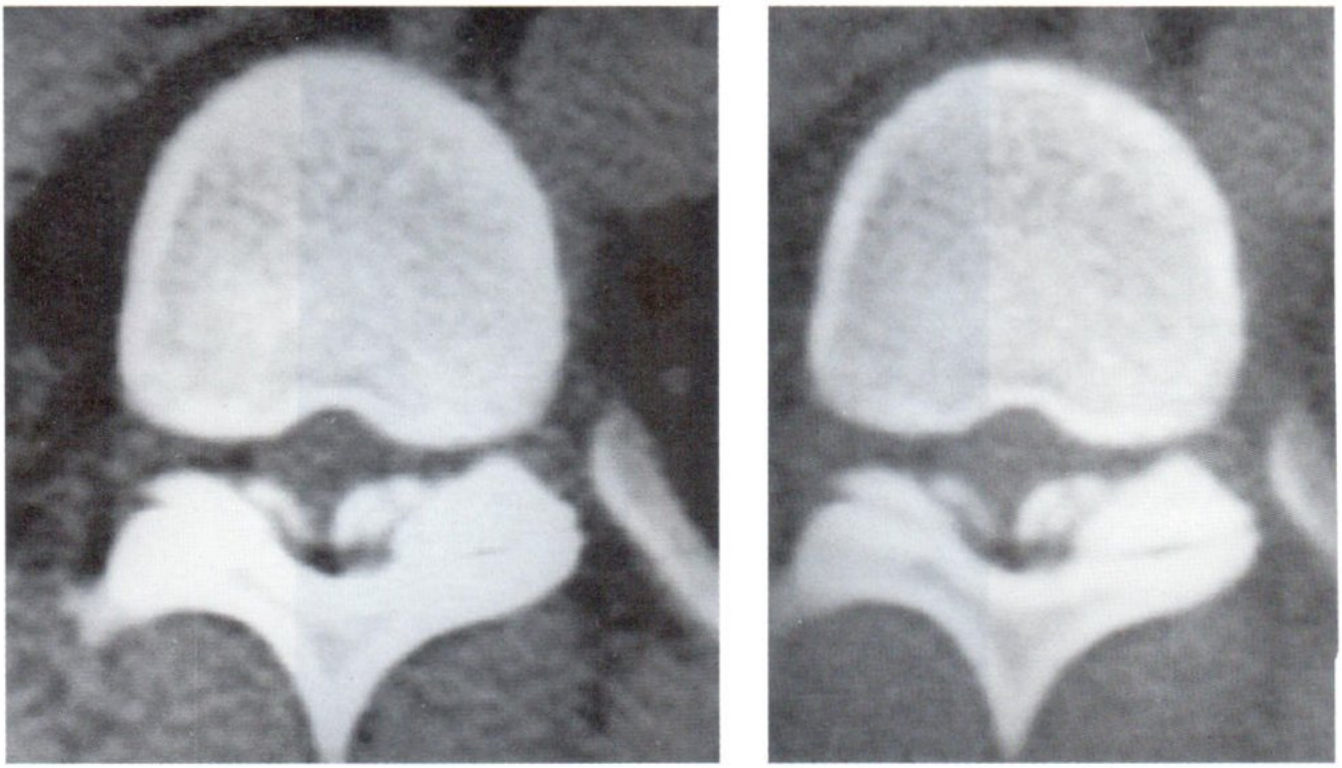

Fig. 2 Axial CT scan of the involved level showed calcified or ossified the thickened ligamentum flavum on both sides with cord compression.

CT AND MRI OF THE BRAIN IN WILSON DISEASE (WILSON'S DISEASE)

Patchrin PEKANAN[1], Rojana SRIPRADITPONG[1], Komolpong OSATHAVANICHVONG[2]

ABSTRACT

Two cases of Wilson disease were presented. One case was 14 years old girl, had low density at pons, midbrain, thalamus, putamen and brain atrophy. New low density lesions and expanded areas of the previous low density areas were noted by CT scan after 4 months follow up. Another case of 31 years old male, his pons and thalamus contained bright signal on T2WI-MRI study. Brain atrophy, mild ventriculomegaly, were seen. Low signal at red nucleus, substantia nigra, globus pallidus and dentate nuclei was shown on T2WI-MRI study.

INTRODUCTION

Wilson disease (hepatolenticular degeneration) is a hereditary disorder characterized by the accumulation of copper in the body, especially in the liver, brain, kidneys and corneas. The excess copper leads to tissue injury and ultimately, if effective treatment is not instituted, to death (1).

The neurologic signs at onset may take a variety of forms. Patients may start with dystonic facies, dystonic postures. Tremor, loss of coordination of fine movements, dysarthria, rigidity, drooling and titubation could be seen. Seizures are infrequent and sensory abnormalities are absent.

Psychological symptoms of Wilson disease are prominent and consist of early development of intellectual deterioration, personality changes, and unstable behavior.

Pathologic changes primarily involve the basal ganglia with neuron loss, spongiform degeneration and demyelination in the putamina and the caudate nuclei. Later, similar changes are seen in the pallidum, dentate nuclei and substantia nigra. Thalamic and cerebellar involvement is less frequent. Scarring and cavitation of the globus pallidus represent late changes (2).

CASE REPORTS

Two patients presented with bradykinesia and dysarthria. One patient was 14 years old girl. Her first CT scan of the brain was on March 3, 1988. It showed multiple low density areas, involving pons, midbrain, both thalami, and putamen. Her second CT scan was on July 22, 1988. There were new low density lesions, at the left cerebellum, and the lesions at pons, thalamus and putamen have enlarged. There was no enhancement within the lesions. The ventricles were midly dilated without midline shift. The ventricles did not change in size after 4 months follow-up (Fig.1).

The second patient was male, age 31 years old. T1WI-axial view MRI scan showed mild brain atrophy with mild ventriculomegaly. T2WI-axial MRI scan showed bright signal, involving pons and both thalami (Fig.2). Dark signal was observed at red nucleus, substantia nigra, globus pallidus, and dentate nucleus (Fig.2)

[1] Department of Radiology, Ramathibodi Hospital, Rama 6 Street, Bangkok 10400, Thailand.
[2] Medical software development project, Mahidol University. BKK.

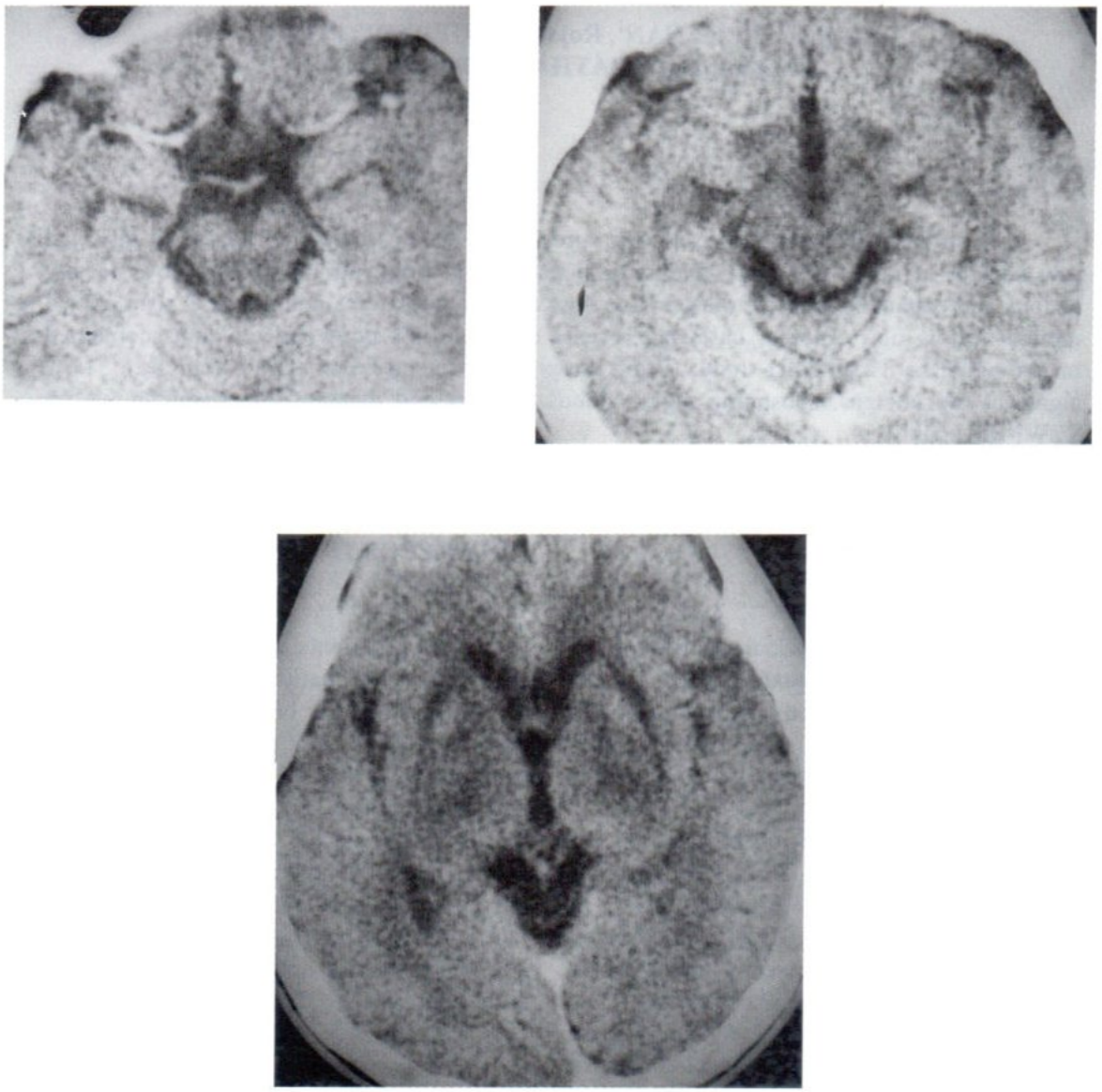

Fig.1A. Case 1. The 1st CT scan on March 3, 1988, showed low density areas at both sides of posterior aspect of pons, midbrain, both thalami and putamens, external capsules without significant contrast enhancement

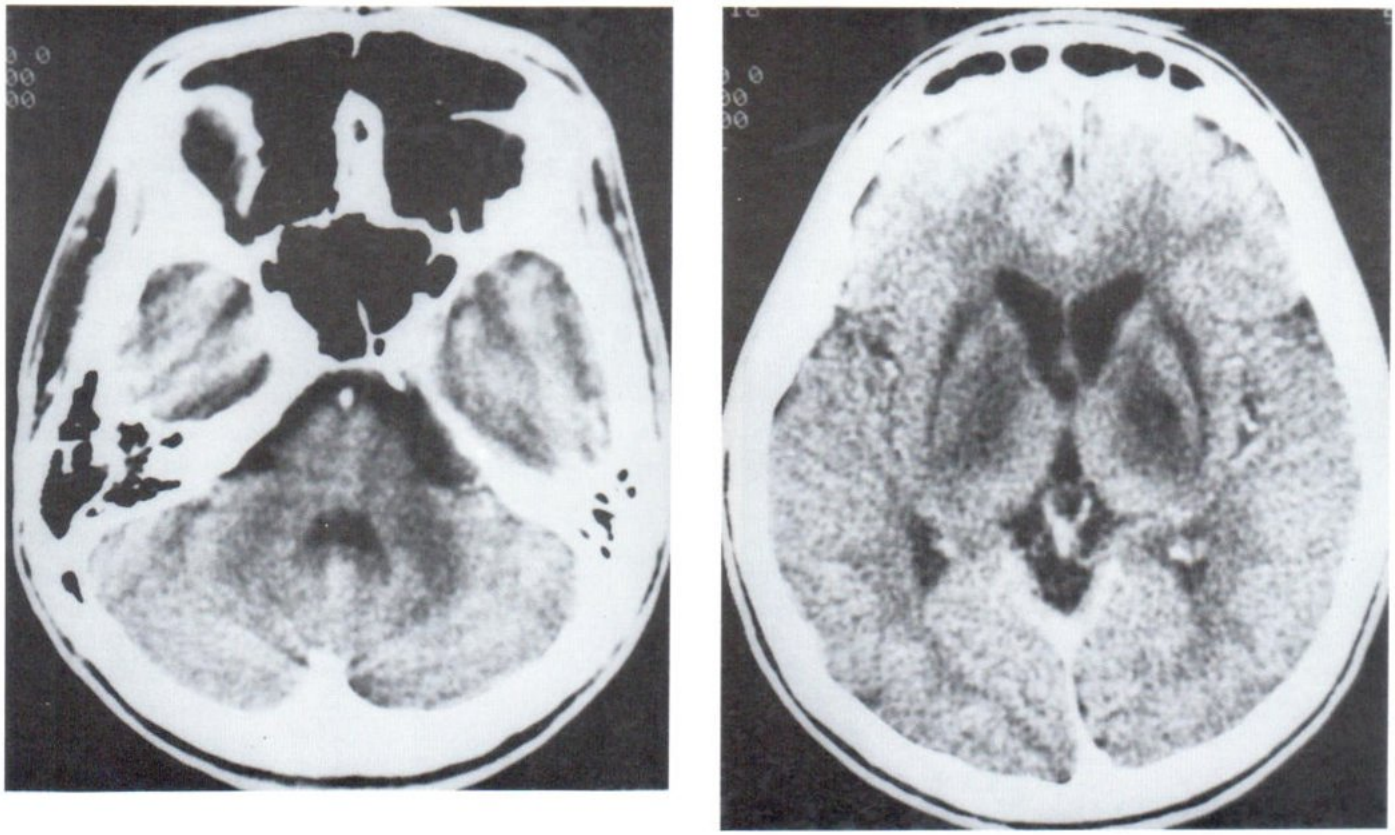

Fig.1B. Case 1. The 2nd CT scan on July 22, 1988 showed a new low density lesion in the left cerebellum. Larger lesions at pons, thalamus, putamen, internal capsules was noted without increasing size of the ventricles.

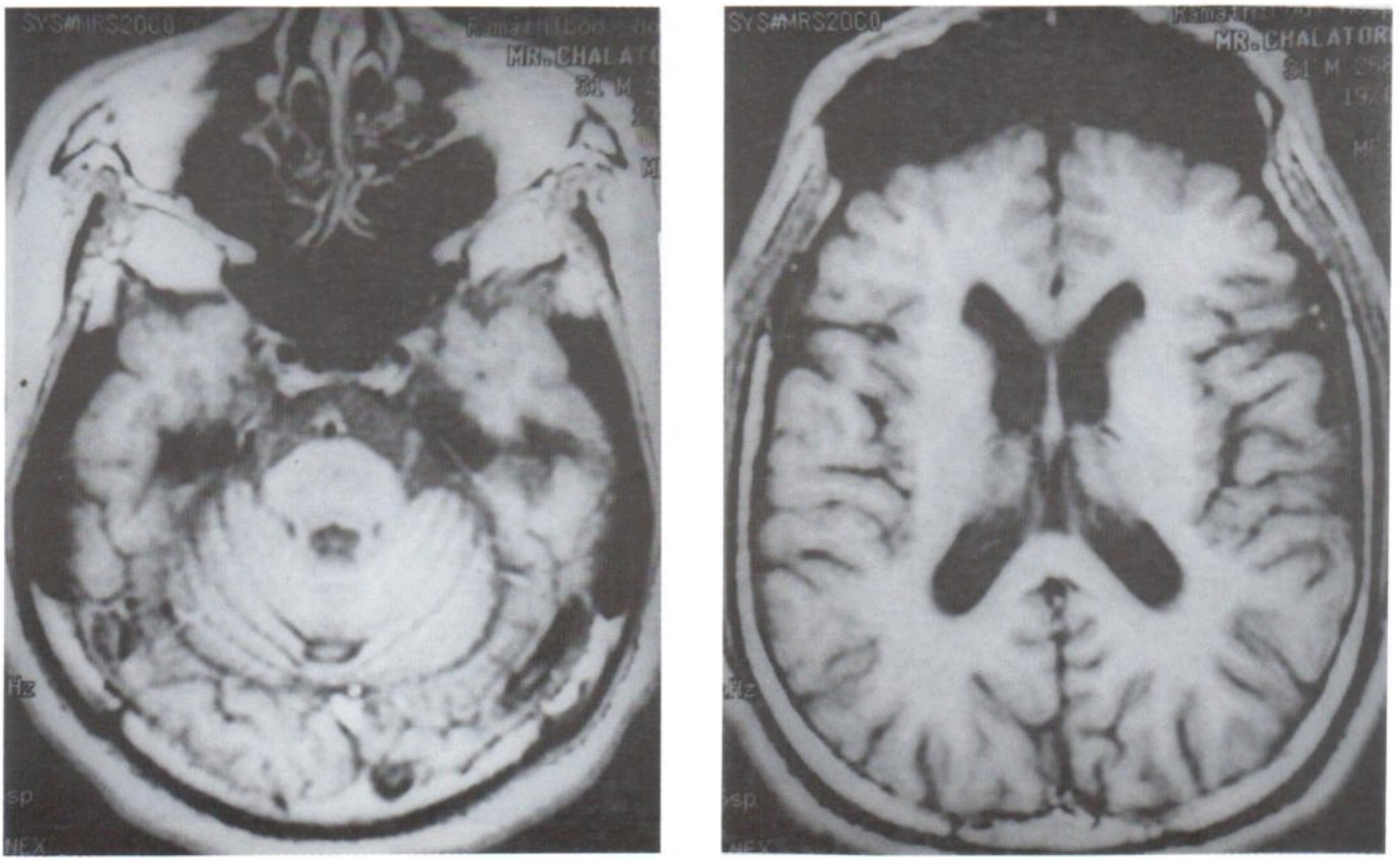

Fig.2A. Case 2. T1WI-Axial view MRI study of the brain showed generalized brain atrophy.

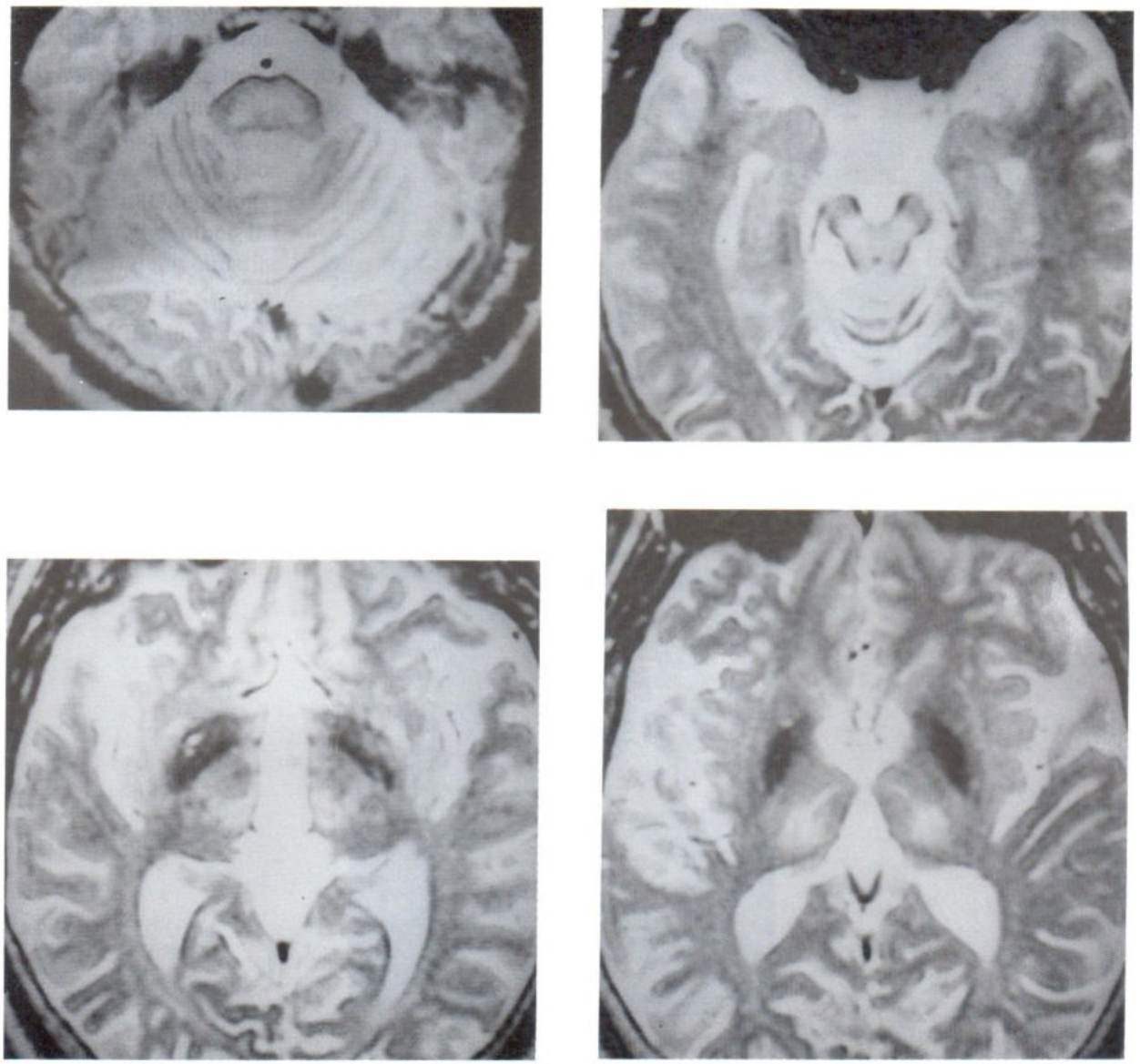

Fig.2B. Case 2. T2WI axial MRI of the brain showed bright signal at pons, thalami and midbrain.

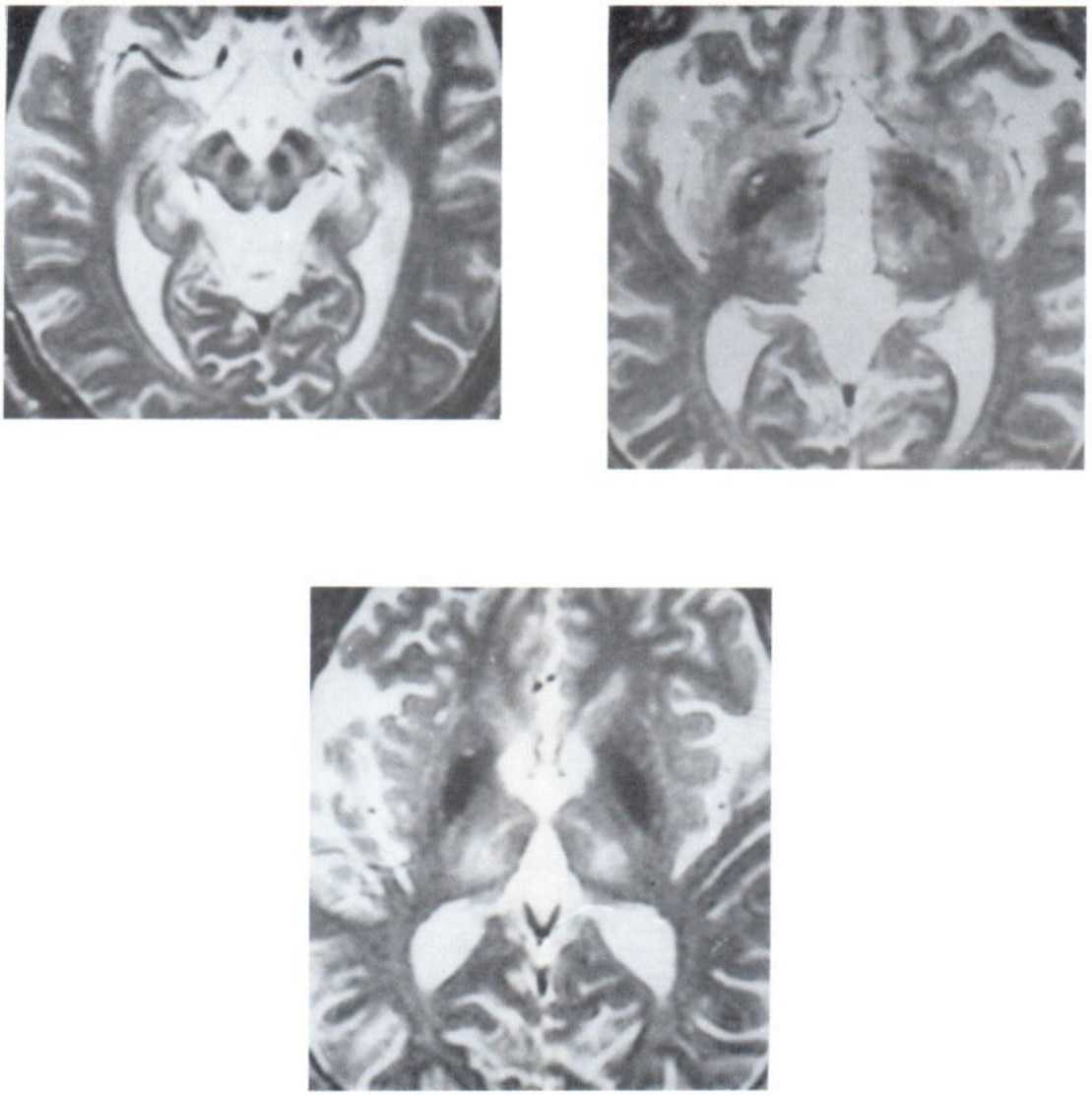

Fig.2C. Case 2. T2WI-axial MRI of the brain showed dark signal at red nucleus, substantia nigra, globus pallidus and dentate nucleus.

DISCUSSION

In Wilson disease, the most dramatic finding in the brain is cavitation in the lenticular nucleus and the tip of the frontal lobe (3), but pathologic changes are widespread throughout the brain (including brain stem) and gray matter is predominantly involved. These changes range from focal degeneration to cavitation and a diffuse loss of myelinated fibers (4-6). In the brain stem, there is an increased number of astrocytes and occasional Alzheimer glia in both the gray and white matter; focal degeneration has been reported in various locations, including the base of the pons (7). On the other hand, several articles have described focal demyelinating lesions of the pons base in Wilson disease as central pontine myelinolysis (8-11).

Wilson disease in an inborn error of copper metabolism. The precise biochemical defect is unknown, but likely involves inadequate synthesis of ceruloplasmin, a serum alpha-2-globulin for copper transport (12,13). Defective copper transportation and utilization results in abnormal deposition of the metal in the liver, brain and other organs. Here the copper is sequestered into lysosomes where it may disrupt membrane lipids and cause cellular degeneration (14).

In the brain, copper deposition takes place mainly in the basal ganglia, which appear brick-red at autopsy. The putamen, globus pallidus, and caudate are most involved, in that order. Neuronal loss occurs, but the pathologic picture is dominated by a marked gliosis, mainly composed of astrocytes (14,15). It is this gliosis rather than paramagnetic effects of copper that account for the imaging changes noted on MRI.

Copper deposition and lesser degenerative changes also occur in the brain stem, cerebellum, substantia nigra, and convolutional white matter.

Wilson disease is slightly more common in males than females. The age of onset is usually 10 to 40 years old. Computed tomography abnormalities are seen in about two-thirds of patients with Wilson disease (16-18). These include atrophy (focal or diffuse) and areas of hypodensity in the basal ganglia, brain stem, and white matter. CT has not proven particularly useful in correlating clinical symptoms, in assessing prognosis, or evaluating response to therapy (16-19).

About 80 percent of patients will have abnormal MRI scans, making MR more sensitive than CT (20,21). Symmetric areas of increased signal on T2WI were seen in the lenticular, thalamic, caudate, and dentate nuclei. A smaller number of patients showed brain stem and asymmetric white matter lesions. Clinical correlation was generally good. Dystonia correlated with putamen, caudate, and nigra lesions; bradykinesia with putamen lesions (21). The lesions detected as bright signal on T2WI on MR likely represent gliosis and edema rather than paramagnetic effects of copper, which would serve to decrease signal intensity.

Sener (22) reported bright claustrum on T2WI-MRI in his four cases of symptomatic Wilson disease.

The hyposignal seen on T2WI at red nucleus, substantia nigra, globus pallidus and dentate nuclei in our patient could reflect copper deposition in the basal ganglia, since copper is paramagnetic (23). The hypointensity of these mentioned structures are also found in normal aging (24). A possible explanation of such a signal is represented an iron deposition which accumulates commonly in areas which already have excessive copper accumulation. Phagocytes containing iron pigment are commonly observed in Wilson disease, in the pallidum and the substantia nigra (25). Furthermore siderophages are seen in relation to the cavitation observed in the putamen in late stages of Wilson disease or in relation to recent hemorrhages (25).

ACKNOWLEDGMENTS

We thank Prof.. Athasit Vejjajiva (the rector of mahidol university) and Dr. Jaroenpin Jenjittranan (Ramkamhang Hospital) for providing us the cases.

REFERENCES

1. Wyngaarden, Smith, Bennett. Cecil Textbook of medicine. Philadelphia: W.B. Saunders Company, 1992:1132-1133.

2. Brugieres P, Combes C, Ricolfi F, Degos JD, Poirier J, Gaston A. Atypical MR presentation of Wilson disease: A possible consequence of paramagnetic effect of copper? Neuroradiology 1992;34:222-224.

3. Robbins SL, Cotran RS, Pathologic basis of disease. 2nd ed. Philadelphia: Saunders, 1979:1592.
4. Finlayson MH, Superville B. Distribution of cerebral lesions in acquired hepatocerebral degeneration. Brain 1981;79-95.
5. Duchen LW, Jacobs JM. Familial hepatolenticular degeneration (Wilson's disease). in: Adams JH, Corsellis AN, Duchen LW, eds. Greenfield's neuropathology. 4th ed. London: Edward Arnold, 1984;595-599.
6. Imiya M, Ichikawa K, Matsushima H, Kageyama Y, Fujioka A. MR of the base of the pons in Wilson disease. AJNR 1992;13:1009-1012.
7. Schulman S. Wilson's disease. In: Minckler J, ed. Pathology of the nervous system. New York: Mc Graw Hill, 1968:1089-1103.
8. Goebel HH, Herman-Ben Zur P. Central pontine myelinolysis. In: Vinken PJ, Brryyun GW, ed. Handbook of clinical neurology. Amsterdam:North-Holland Publishing Co, 1976;28:285-316.
9. Nishiyama S, Watanabe K, Abe H. A case of Wilson's disease with central pontine myelinolysis. Shinkei Kenkyu no Shinpo 1966;10:159-160.
10. Matsuoka T, Miyoshi K, Hayashi S, Kageyama N. Central pontine myelinolysis: a report of three cases. Acta Neuropathol (Ben) 1965;5:117-132.
11. Gocht A, Colmant HJ. Central pontine and extrapontine myelinolysis: a report of 58 cases. Clin Neuropathol 1987;6:262-270.
12. Wilson SAK: Progressive lenticular degeneration: a familial nervous disease associated with cirrhosis of the liver. Brain 1912;34:295.
13. Menkes JH: Disorders of metal metabolism. P. 426. In Rowland LP (ed): Merritt's Textbook of Neurology, 7th Ed. Lea & Febiger, Philadelphia, 1984.
14. Elster AD. Cranial magnetic resonance imaging. New York: Churchill Livingstone, 1988:226-227.
15. Schulman S: Wilson's disease. p. 1113. In Minckler J (ed): Pathology of the Nervous system. McGraw-Hill, New York, 1968.
16. Kvicala V, Vymazal J, Nevsimalova S: Computed tomography of Wilson's disease . AJNR 1983;4:429.
17. Kendall BE, Pollock SS, Bass NM, Valentine AR: Wilson's disease. Clinical correlation with cranial computed tomography. Neuroradiology 1981;22:1.
18. Williams JB, Walsche JM: Wilson's disease:analysis of the cranial computerized tomographic appearances found in 60 patients and the changes in response to treatment with chelating agents. Brain 1981;104:735.
19. Aisen AM, Martel W, Gabrielsen TO et al: Wilson disease of the brain: MR imaging. Radiology 1985;157-137.
20. Lawler GA, Pennock JM, Steiner RE et al: Nuclear magnetic resonance (NMR) imaging in Wilson disease. J Comput Assist Tomogr 1983;7:1.
21. Starosta-Rubenstein S, Young AB, Kluin K et al: Quantitative clinical assessment of 25 Wilson's patients: correlation with structural changes on MRI. Neurology 1985;35:175.
22. Sener RN. The claustrum on MRI: normal anatomy, and the bright claustrum as a new sign in Wilson's disease. Pediatr Radiol 1993;23:594-596.
23. Runge VM, Clanton JA, Smith FW, et al. Nuclear magnetic resonance of iron and copper disease states. AJR 1983;141:943-948.
24. Drayer BP, Olanow W, Burger P, et al. Parkinson syndrome: diagnosis using high field MR imaging of brain. Radiology 1986;159:493-498.
25. Greenfield's neuropathology. Arnold, London 1976, pp 172-177.

IMAGING OF OCULOMOTOR NERVE PALSY : LESIONS AT MEDIOVENTRAL PART OF THE THALAMUS AND MIDBRAIN

Patchrin PEKANAN[1], Siriporn HIRUNPAT[2], Pitoon WICHIWANIWED[3], Kamolpong OSATHAVANICHVONG[4]

ABSTRACT

Two patients presented with third nerve palsy. One patient had an ischemic focus at anteromedial part of the thalamus and another patient had a subacute hematoma at anteromedial part of the thalamus, upper pons and midbrain. The images were demonstrated by MRI study. Discussion concerning the path of the oculomotor nerves and the pathologic processes were performed.

INTRODUCTION

The third cranial nerve palsy was second in frequency in 4000 cases of patients with ocular motility palsies (1,2). Patients may present with an isolated or nonisolated, pupil-sparing or nonpupil-sparing cranial nerve III palsy. Isolated major dysfunction of a single third nerve palsy is demonstrated by MRI study to be caused by brain stem lesions (ischemia, mass, cryptic vascular malformation, hemorrhagic shearing injury, and hemorrhagic infarct), subarachnoid space lesion (aneurysm, lymphoma, ophthalmoplegic migraine, viral meningitis, coccidioidomycosis. trauma, syphilis, Miller-Fisher syndrome) and cavernous sinus/superior orbital fissure lesions (lymphoma, carcinoma, Tolosa-Hunt syndrome, cavernous carotid aneurysm, pituitary apoplexy, and craniopharyngioma) (1).

Two cases presented by us, the third cranial nerve palsy was found in the patients who had medioventral thalamic and midbrain lesions.

CASE REPORT

CASE 1

A 50-year-old male patient had double vision for one week prior to searching for the medical advice. The visual symptom was preceded by severe vertigo. His blood pressure was 210/120 mgHg. Left lateral rectus palsy, impaired upward gaze of left side and downward gaze on the right side. Clinical impression was left cranial nerve III and VI palsy. MRI study (Fig.1) showed a subacute ischemic focus at ventromedial part of right thalamus and smaller ischemic foci at left dorsomedial part of thalamus and dorsolateral part of right thalamus. The patient had also hypercholesterolemia. He was treated medically and the eye symptoms improved after two weeks.

CASE 2

A 17-year-old man had diplopia for twenty days prior to admission. He developed ptosis for

[1] Department of Radiology, Ramathibodi Hospital, Rama 6 Street, Bangkok 10400, Thailand.
[2] Department of Radiology, Prince of Songkla University Hospital, Songkla.
[3] Department of Radiology, Klang Hospital, BKK.
[4] Department Software Development Project, Mahidol University.

one day. Numbness of left face and left hemiparesis was also present. Right pupil was 8 mm diameter non-reacted to light, there was no reaction to consentual light reflex. Impaired upward gaze of both sides. Palsy of right medial rectus muscle, superior rectus muscle, inferior oblique muscle was observed. The tongue was deviated to the left. MRI study (Fig.2) showed small intracerebral hematomas at ventromedial aspect of right upper pons and midbrain-right thalamus, and superficial white matter of posterior right parietal lobe. Evidence of previous small hematomas are noted at posterior aspect of left pons, right deep parietal white matter, left deep parietal white matter, high right deep parietal white matter. Bleeding from the parasitic tract was suspected. The serum antibody and CSF antibody was negative of Gnathostomiasis; and the antibody-serum was positive for Angiostrongyliasis but was negative in CSF.

DISCUSSION

The oculomotor nucleus extends through the entire dorsal portion of the midbrain. Nerve fibers that supply the levator palpebrae superioris divide into right and left bundles from one central caudal nucleus. The other nuclei are represented bilaterally, with the superior rectus being the only subnucleus with contralateral representation. This subnucleus is located in the more caudal portion of the nuclear complex. These fibers cross intraparenchymally, and all fibers run ventrally and slightly rostrally to exit through the interpeduncular fossa. The oculomotor nerve then courses anteriorly within the subarachnoid space until it pierces the dura covering the roof of the cavernous sinus. In the anterior cavernous sinus the oculomotor nerve divides into superior and inferior divisions. The superior division innervates the levator palpebrae superioris and the superior rectus muscles, whereas the inferior division innervates the inferior and medial rectus muscles, the inferior oblique muscle, and the iris sphincter (3,4). Traditionally, divisional oculomotor pareses are localized to the anterior cavernous sinus or posterior orbit. Aneurysms of the internal carotid artery, diabetes mellitus, enlargement of the third ventricle, and presumed viral syndromes have all been reported to cause superior division paresis (5-9). Inferior division third nerve palsies have been ascribed to viral disorders, trauma, or local orbital disease (10-12).

The oculomotor fascicles sweep ventrally and laterally from the oculomotor complex, pass through and medial to the red nucleus, and converge to exit the brain stem medial to the cerebral peduncles (13,14). The clinical localization of lesions along the dorsal-ventral course of the oculomotor fascicles relies on associated neurologic findings. Damage to the ventral fascicles and the nearby cerebral peduncle causes ipsilateral third-nerve palsy and contralateral hemiparesis (Weber's syndrome)(15). Involvement of fascicles within the red nucleus leads to oculomotor palsy with contralateral involuntary movements (Benedikt's syndrome). Extension of such a lesion to the brachium conjunctivum produces additional contralateral ataxia (Claude's syndrome)(15). When sufficiently small, fascicular lesions can mimic complete or partial extra-axial third nerve palsies (16-21). Most of these have been located in the ventral midbrain, sparing the red nucleus and cerebral peduncles. Small lesion of the proximal oculomotor fascicles have been reported only rarely. Extension of such a lesion would involve the oculomotor subnuclei, the medial longitudinal fasciculus, and the mesencephalic reticular formation, causing ipsilateral oculomotor paresis and combinations of bilateral ptosis, bilateral superior rectus palsy, internuclear ophthalmoplegia, and lethargy (13).

Bithalamic hyperintensity on T2WI has been described in a relatively small number of pathologic states. Causes include birth asphyxia, bithalamic glioma, bilateral germ cell tumors, carbon monoxide poisoning, Wernicke encephalopathy, and vascular events such as "top of the basilar" syndrome and deep cerebral vein thrombosis (22). T2 hyperintensity in the mesodiencephalic region, occipital lobes and posterior fossa is well described in cases of basilar artery occlusion and strongly suggests this diagnosis (23). Changes characteristic of infarction by MR are not present for approximately 12 hours, potentially delaying diagnosis and intervention. T2 hyperintensity develops in the thalami and basal ganglia in patients with deep cerebral vein thrombosis, corresponding to the venous vascular territories, and infarctions that are usually hemorrhagic develop (24). MR alone is not sufficient for evaluation of the venous system. It cannot consistently distinguish between flow and

occlusion, given the phenomenon of flow-related enhancement and the different signal characteristics of blood products within a thrombus (25). Two-dimensional phase-contrast MR angiography is the optimal technique for evaluating occlusion of cerebral veins (26).

REFERENCES

1. Blake PY, Mark AS, Kattah J, Kolsky M. MR of oculomotor nerve palsy, AJNR 1995;16:1665-72.
2. Carpenter MB. Core Text of Neuroanatomy. 4th ed, Baltimore, Md: Williams & Wilkins:-1991:133-56.
3. Ksiazek SM, Repka MX, Maguire A, Harbour RC, et al. Divisional oculomotor nerve paresis caused by intrinsic brain stem disease. Ann Neurol 1989;26:714-8.
4. Warwick R. Representation of the extra-ocular muscles in the oculomotor nuclei of the monkey. J Comp Neurol 1953;98:449-504.
5. Derakhashan I. Superior branch palsy of the oculomotor nerve with spontaneous recovery. Ann Neurol 1978;4:478-9.
6. Feder R, Camp A. Superior branch palsy of oculomotor nerve and pupillary constriction caused by intracranial carotid artery aneurysm. Ann Neurol 1979;5:493-5.
7. Masucci EF, Kurtzke JF. Diabetic superior branch palsy of the oculomotor nerve. Ann Neurol 1980;7:493.
8. Osher RH, Corbett JJ, Schatz NJ, et al. Neuro-ophthalmologic complications of enlargement of the third ventricle. Br J Ophthalmol 1978;62:536-42.
9. Trobe JD, Glaser JS, Post JD. Meningiomas and aneurysms of the cavernous sinus. Arch Ophthalmol 1978;96:457-67.
10. Cross AG. The ocular sequelae of head injury. An R Coll Surg Engl 1948;2:233-40.
11. Susac JO, Hoyt WF. Inferior branch palsy of the oculomotor nerve. Ann Neurol 1977;2:336-9.
12. Walsh FB, Hoyt WF. Clinical neuro-ophthalmology, vol 1. 3rd ed. Baltimore:-Willians & Wilkins 1969:256.
13. Liu GT, Carrazana EJ, Charness ME. Unilateral oculomotor palsy and bilateral ptosis from paramedian midbrain infarction. Arch Neurol 1991;48:983-6.
14. Castro O, Johnson LN, Mamourian AC. Isolated inferior oblique paresis from brain-stem infarction: perspective oculomotor fascicular organization in the ventral midbrain tegmentum. Arch Neurol 1990;47:235-7.
15. Miller NR. Walsh and Hoyt's Clinical Neuroophthalmology. 4th ed. Baltimore, Md: Williams & Wilkins;1985:657-63.
16. Nadeau SE, Trobe JD. Pupil sparing in oculomotor palsy: a brief review. Ann Neurol. 1983;13:146-8.
17. Keane JR. Isolated brain-stem third nerve palsy. Arch Neurol 1988;45:813-4.
18. Ksiazek SM, Repka MX, Maguire A, et al. Division oculomotor nerve paresis caused by intrinsic brain stem disease. Ann Neurol 1989;26:714-8.
19. Collard M, Saint-Val C, Mohr, Kiesmann M. Paralysis isolee du nerf moteur oculaire commun par infarctus de ses fibres fasciculaires. Rev Neurol 1990;146:128-32.
20. Hriso E, Miller A, Masdeu JC. Monocular elevation weakness and ptosis: an oculomotor fascicular syndrome? Neurology 1990;40(suppl 1):309-10.
21. Hopf HC, Gutmann L. Diabetic 3rd nerve palsy: evidence for a mesencephalic lesion. Neurology 1990;40:1041-5.
22. Bell DA, Davis WL, Osborn AG, Harnsberger HR. Bithalamic hyperintensity on T2-Weighted MR: vascular causes and evaluation with MR angiography. AJNR 1994;15:893-9.
23. Biller J, Yuh WTC, Mitchell GW, Bruno A, Adams HP Early diagnosis of basilar artery occlusion using MRI. Stroke 1988;19:297-306.
24. Erbguth F, Brenner P, Schulerer G, Druschky K-F, Neundorfer B. Diagnosis and treatment of deep cerebral vein thrombosis. Neurosurg Rev 1991;14:145-8.
25. Ashforth RA, Melanson D, Ethier R. MR of deep cerebral venous thrombosis. Can J Neurol Sci 1989;16:417-21.
26. Rippe DJ, Boyko OB, Spritzer CE, et al. Demonstration of dural sinus occlusion by the use of MR angiography. AJNR 1990;11:199-201.

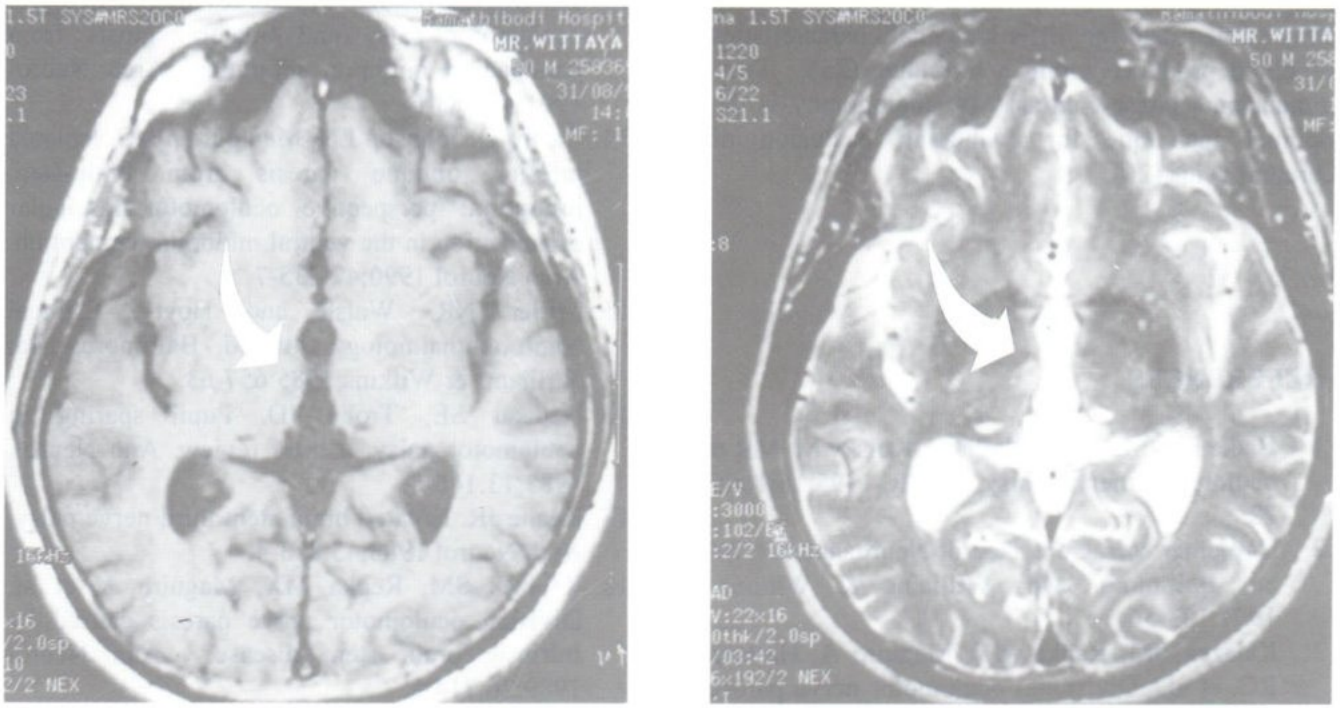

Fig. 1A. Axial T1WI, showed a faint small low signal lesion at ventromedial aspect of right thalamus, one smaller low signal area at dorsoloteral aspect of right thalamus and another at dorsomedial aspect of left thalamus. These lesions appeared bright on T2WI, however, the largest lesion at the ventromedial aspect showed less bright signal because the lesion is probably newer than the more posteriorly lesions.

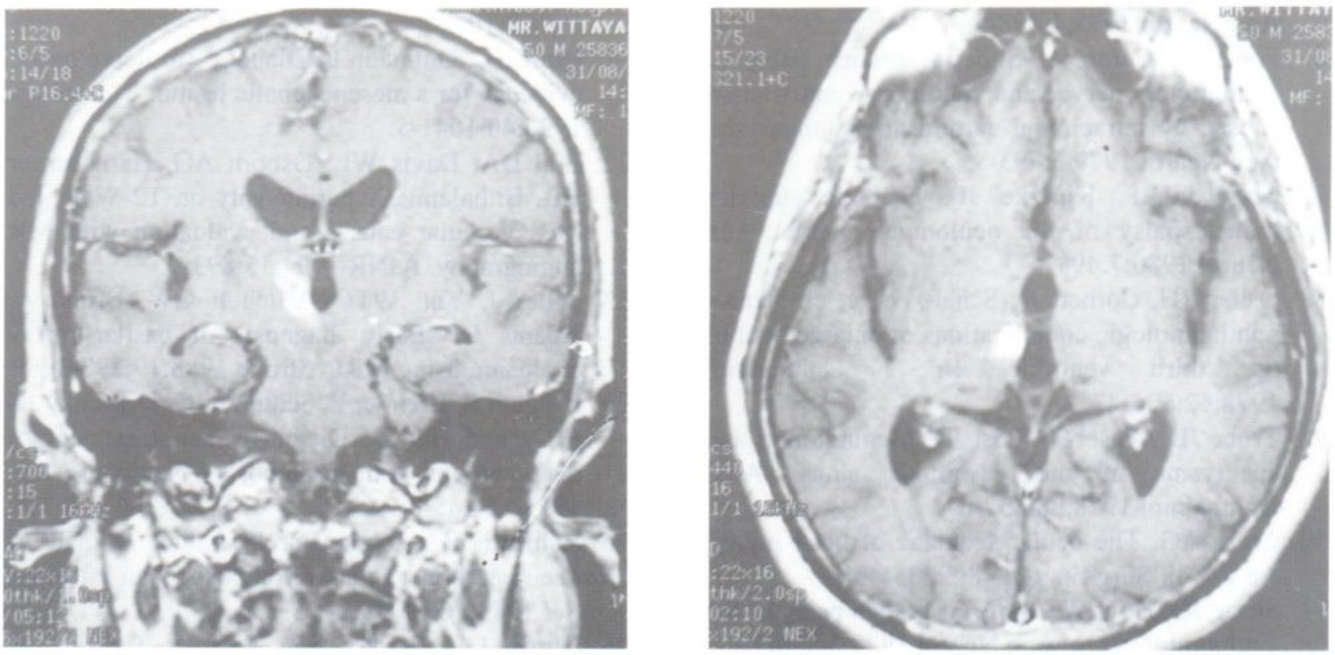

Fig. 1B. Coronal and axial view of the lesions post Gadolinium enhancement showed dense nodular and ring enhancement of the larger lesion at the ventromedial aspect of right thalamus due to subacute process with loss of blood brain barrier. The smaller more posteriorly located lesions were not enhanced and were probably old lesions.

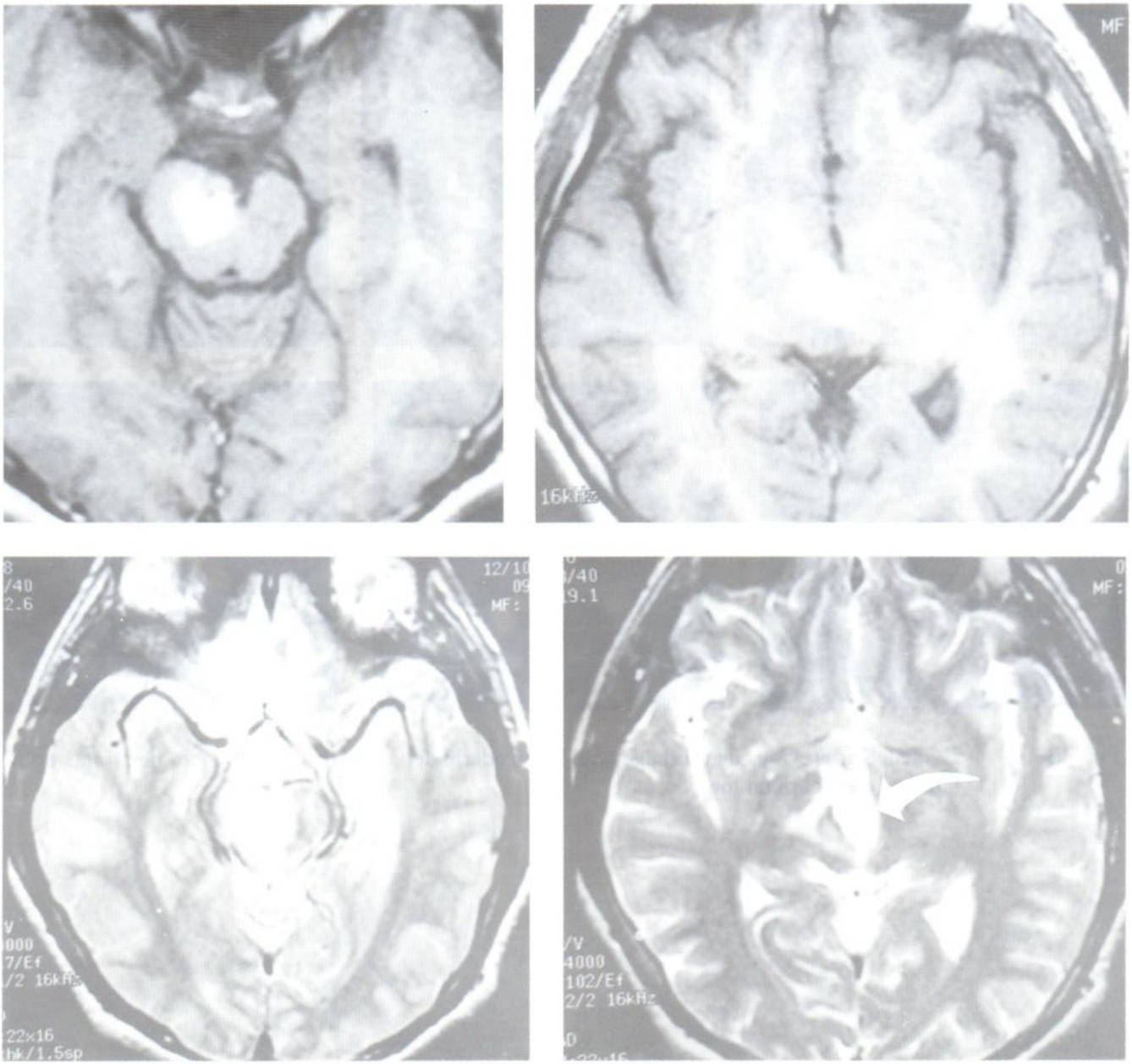

Fig. 2A. Axial T1WI and T2WI showed small subacute hematoma at right parietal lobe, right ventroparamedian area of upper pons, midbrain and thalamus.

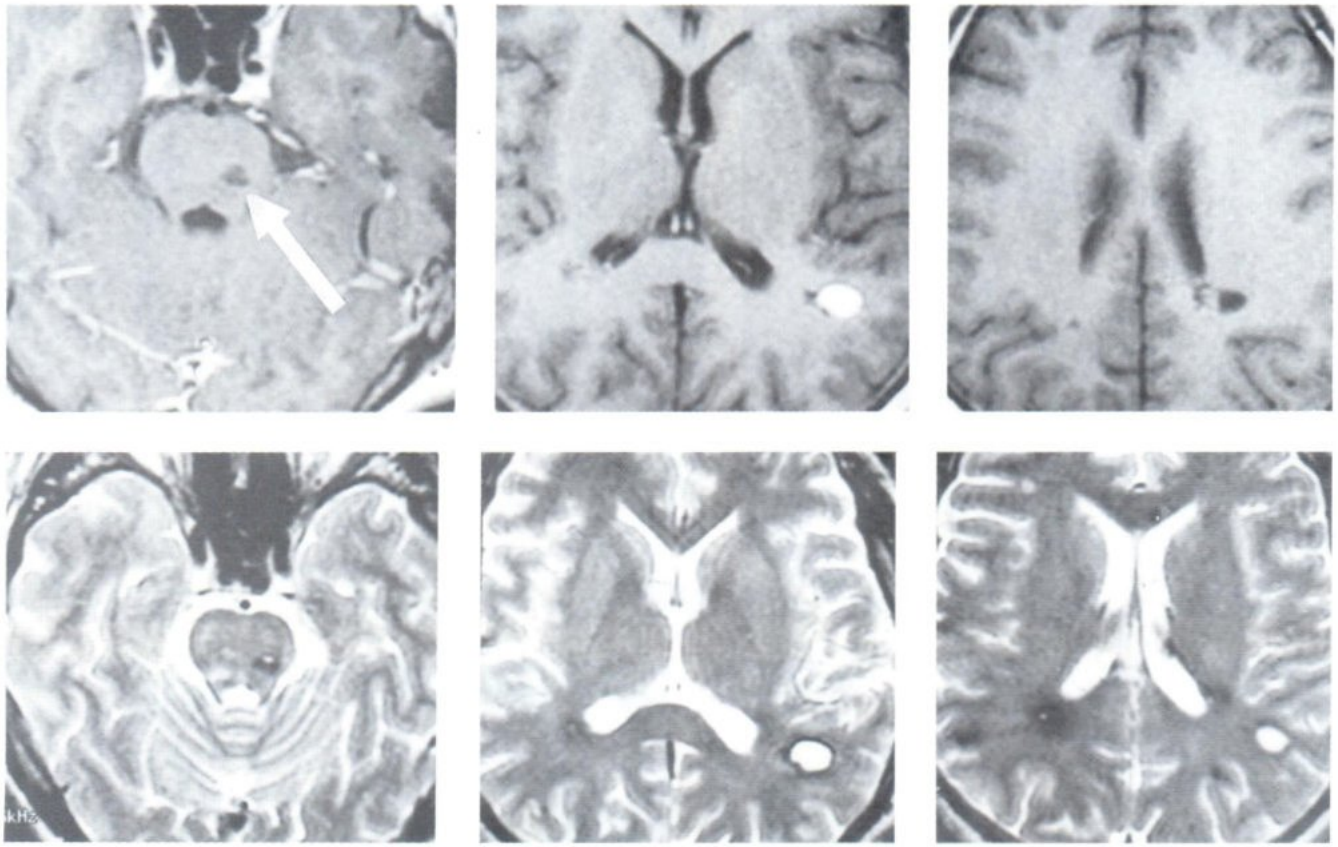

Fig. 2B. Evidence of previous hemorrhage with hemosiderin deposit was noted at left pons and both sides of deep parietal lobe.

SONOGRAPHY OF THE PARTIAL MOLAR PREGNANCY

Supranee NIRAPATHAPONGPORN[1,2], Patchrin PEKANAN[1,2], Ratanaporn LEELAVIVAT[3], Yaowalak RAPEEPATANA[3]

ABSTRACT

A case of partial mole was presented in a 30-year-old female patient by an ultrasonographic examination. The study was performed intervally from 9 to 19 weeks-gestation. It showed thickening of the placenta with detectable small cysts at 19 weeks-gestation. Ovarian corpus lutein cysts was noted at 9 weeks-gestation. The growth of the fetus was retarded. Oligohydramnios was present.

INTRODUCTION

Gestational trophoblastic disease describes a spectrum of proliferative diseases of the trophoblast, from the benign hydatidiform mole to the more malignant and frequently metastatic choriocarcinoma (1). There are presently two different classification schema for gestational trophoblastic disease. The older, histopathologic scheme divides trophoblastic disease into hydatidiform mole (complete, partial, with coexistent fetus), invasive mole (chorioadenoma destruens) and choriocarcinoma (2). The clinical classification divides this disease into benign trophoblastic disease, malignant (non metastatic disease) and malignant (metastatic disease).

The role of sonography in gestational trophoblastic disease is greatest in establishing the diagnosis of hydatidiform mole (2). A characteristic sonographic appearance of hydropic villi occurs with most molar pregnancies. Sonography is considered an important adjunctive test to serial beta-hCG assays in malignant trophoblastic disease since the size of the tumor and the presence of distant metastases can be ascertained (3).

CASE REPORT

A 30-year-old female primigravida patient was 9 weeks pregnant at the time that left sided abdominal pain developed. Ultrasonography at 9 weeks pregnancy showed normal fetus with CRL 20 mm. and left ovarian cyst, size 3 cm. (Fig.1).

The second ultrasonographic examination was performed at 11 weeks-gestation, the growth of the fetus is normal with CRL 40 mm. The size of left ovarian cyst remained the same (Fig.2).

The patient developed hyperemesis gravidarum at 15 weeks gestation. The 3rd ultrasonography was performed at 17 weeks-gestation. It showed enlarged placenta, occupying two-thirds of the uterus, the fetal size was 14 weeks and the oligohydramnios was seen. The left ovarian cysts has increased size to 10 x 12 cm. (Fig.3) and multiloculated appearance was noted.

The patient had dyspnea and severe hypertension, two weeks later cardiomegaly with left ventricular enlargement was observed at plain radiograph of the chest (Fig.4). Portable

[1] Department of Radiology, Ramathibodi Hospital, Rama 6 Street, Bangkok 10400, Thailand.
[2] Department of Radiology, Samitivej Hospital, Bangkok.
[3] Department of OB-GYN, Samitivej Hospital.

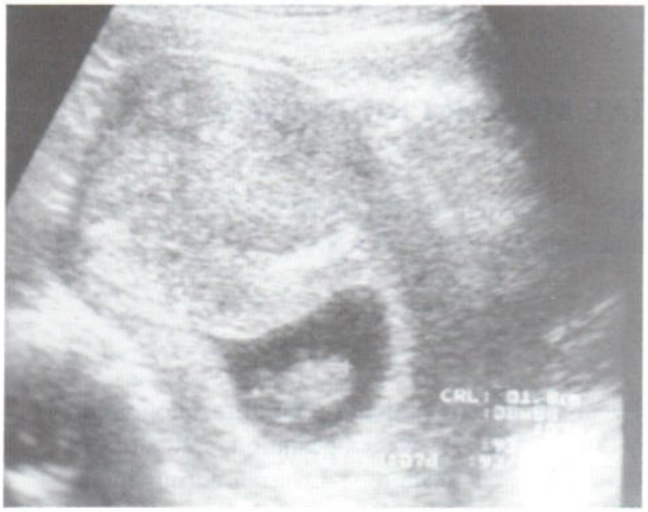

Fig. 1A. Sonography at 9 weeks-pregnancy, the CRL of the fetus corresponded with the gestational age.

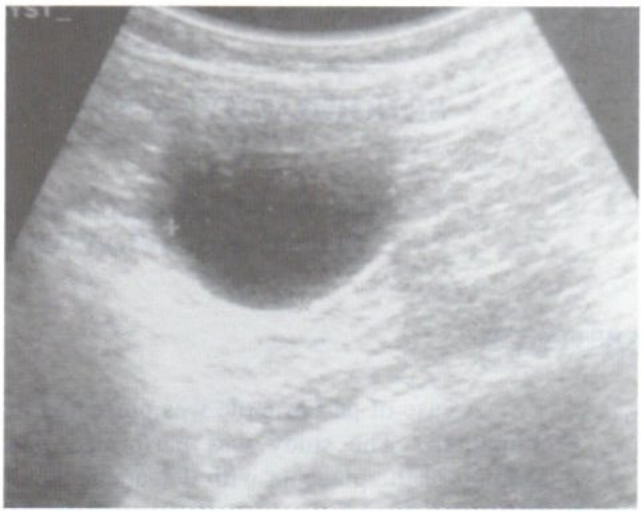

Fig. 1B. Sonography at 9 weeks-pregnancy showed at left ovarian cyst size 3 cm. and the cyst appeared uniloculated.

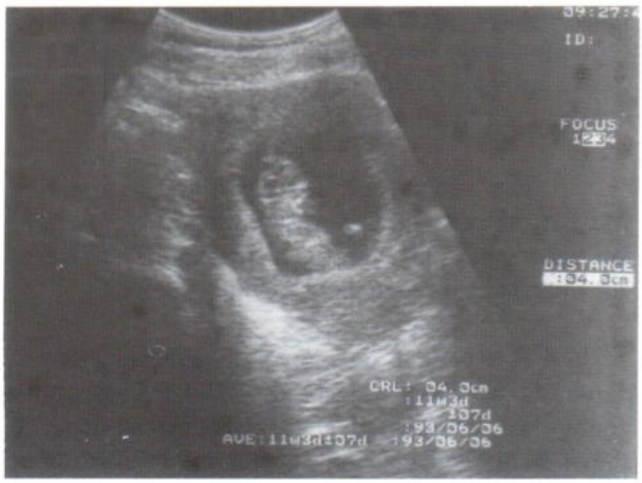

Fig. 2 Sonography at 11 weeks gestation, the fetus has grown up at a normal rate.

ultrasonographic examination at 19 weeks-gestation showed the viable 14 weeks size fetus. The placenta was markedly enlarged with presence of small cysts and the molar pregnancy was suggested (Fig.5). Doppler echocardiography showed a high output failure. The serum T3 was 278 mg% (80-200), T4 was 14.55 mg% (4.5-12.5) which was increased. The serum TSH was 0.03 mg% which was decreased. The hCG level was high (103,130 mIU/ml).

The curettage was performed and pathologic section of the placenta and the fetus was compatible with partial molar pregnancy and there was no obvious gross anomaly of the fetus. The vesicle placenta weighted 800 grams. The chromosome analysis was not performed.

DISCUSSION

Hydatidiform mole is characterized by marked edema and enlargement of the chorionic villi, which is the characteristic that allows sonography identification. This is accompanied by disappearance of the villous blood vessels and proliferation of trophoblast that line the villi (2). Although moles with an abundantly proliferative trophoblast have a greater likelihood of being malignant, it is not possible to accurately predict on the basis of histologic appearance the malignant potential of a given mole. Approximately 20 percent of complete moles are followed by malignant sequelae of invasive mole or choriocarcinoma. The histopathologic classification of hydatidiform mole has not proven to be an accurate prognostic indication to select the 20 percent of patients with a molar pregnancy who will subsequently develop malignant disease (2,5).

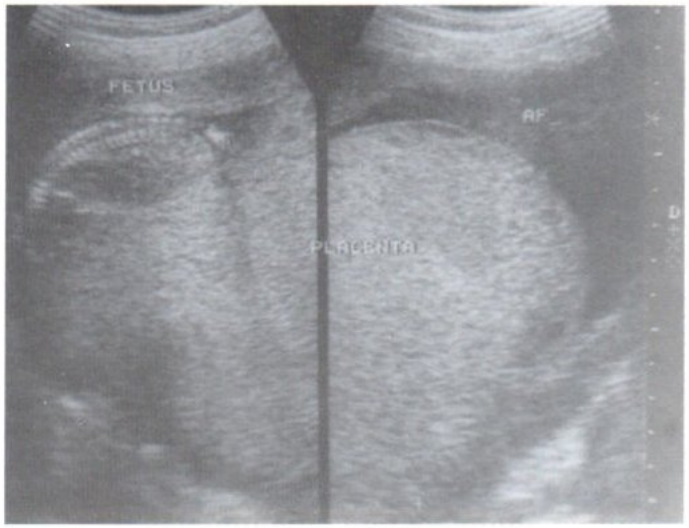

Fig. 3A At 17-weeks-gestation, ultrasonography revealed marked thickening of the placenta and the fetal size corresponded to only 14 weeks size.

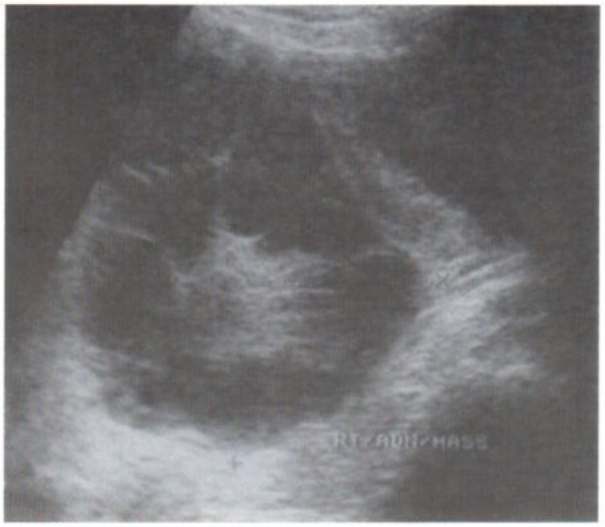

Fig. 3B At 17 weeks gestation, the left ovary has increased in size, containing multiple lutein cysts.

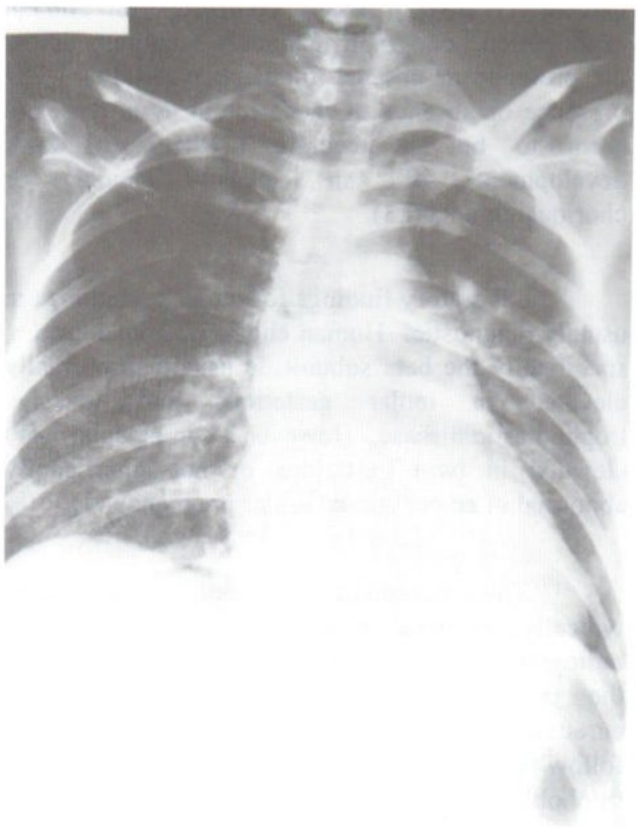

Fig. 4 Portable chest film at ICU, showed mild cardiomegaly and pulmonary congestion.

Hydatidiform mole results from the fertilization of an "empty egg"; that is, an ovum with no active chromosomal material (2,6). The chromosomes of the sperm, finding no chromosomal complement from the ovum, reduplicate themselves, resulting in a 46xx mole. There are no fetal parts or chorionic membrane associated with this situation, which is called a "complete mole" or "classic mole". Complete moles have varying degrees of trophoblastic proliferation and may be either benign or malignant. Malignant gestational trophoblastic disease may follow a mole or be associated with a spontaneous abortion, ectopic pregnancy, or full term pregnancy.

Some hydatidiform moles may contain a small complement of fetal structures such as a placenta with membranes. This is classified as a "partial mole". Such cases usually involve some edema of the villi but relatively little trophoblastic proliferation. Although malignancy has been reported, "partial moles" are almost always benign (2,7). The fetus in such cases usually has significant congenital anomalies and a triploid karyotype (8). Two chromosomes are of paternal origin and the third is of maternal origin (9). About two-thirds of triploid fetuses are xxy and one-third are xxx (10).

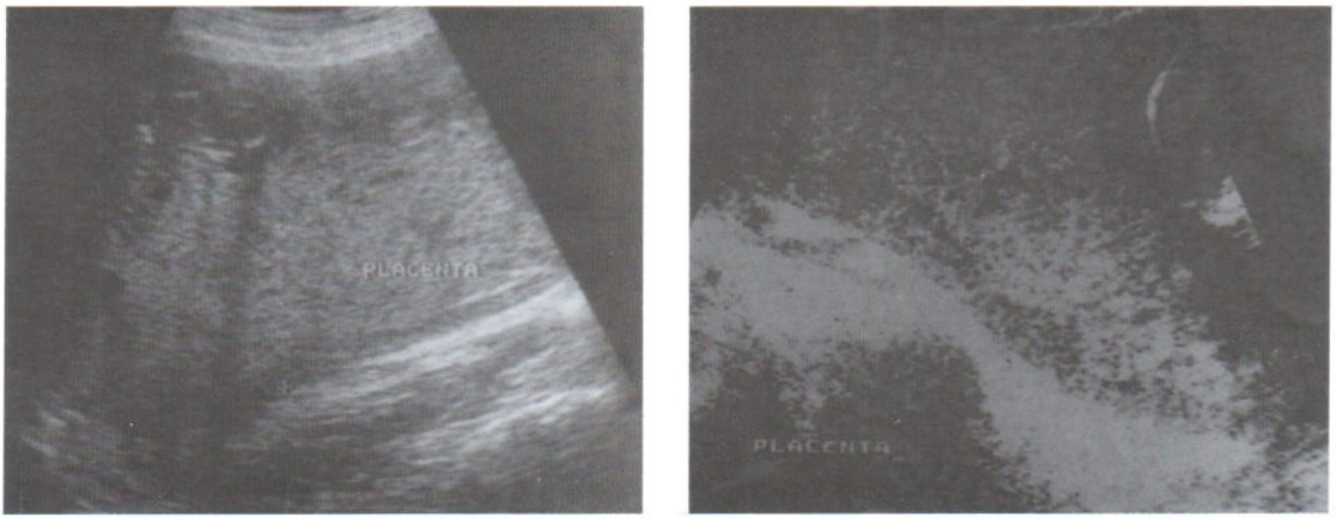

Fig. 5 Portable ultrasonography at 19 weeks-gestation showed multiple small cysts in the thickened placenta.

Morphologically similar, but much less common than the partial mole, a fetus can coexist with a complete mole. This disorder is thought to result from molar degeneration of one conceptus of an identical twin pregnancy, with the other conceptus developing into a fetus and placenta (11). In these patients, a fetus and normal placenta can usually be identified as opposed to a partial mole where a normal placenta is not present.

Hydropic degeneration of the placenta may have a similar sonographic appearance to a complete or partial mole but, histologically, is not associated with trophoblastic proliferation. The villi in hydropic degeneration of the placenta are swollen and edematous thus resembling abnormal trophoblastic tissue. Hydropic degeneration may be seen in 20 to 40 percent of placentae from abortuses (4).

Clinically, a molar pregnancy is first considered in the differential diagnosis of a patient who presents with severe preeclampsia prior to 24 weeks' gestation, a uterus that is too large for dates, and first trimester bleeding. Occasionally, the patient may notice grape-like vesicles passed per vaginum which are diagnostic of this condition (2). The bleeding may be so intense as to result in shock. The uterus is frequently too large for dates in patients with this condition. However, if significant expulsion of molar tissue has occurred prior to sonographic examination, the uterus may be normal size or even too small for dates.

Theca lutein cysts are frequently encountered in patients with a molar pregnancy. The actual incidence of these cysts with molar pregnancy described in reported series ranges from 18 to 37 percent (12,13). When compared to clinical examination, sonography can more accurately assess the presence or absence of these cysts (14). The presence or absence of theca lutein cysts does not seem to be an accurate predictor of later development of an invasive mole or choriocarcinoma (13).

Laboratory findings for molar gestations are usually diagnostic. Human chorionic gonadotropin, specifically the beta subunit, is usually abnormally elevated in molar gestations and invasive trophoblastic disease. However it can be spuriously elevated in twin gestations or not significantly abnormal in an occasional molar pregnancy (1).

The treatment of molar pregnancies typically involves suction curettage. A chest radiograph should be obtained in order to exclude the possibility of metastatic disease. After curettage, serial beta-hCGs are obtained in order to follow the activity and presence of remaining trophoblastic tissue. The serum level of this glycoprotein hormone should return to normal 10 to 12 weeks after evacuation (15). Although theca lutein cysts, if present prior to curettage, should regress with successful treatment of molar

pregnancy, the presence or absence of these cysts should not be taken as reliable indications of the presence or activity of residual disease (16). Sonography does have an important role in these patients in which the beta-hCG rises, since it can detect the presence or absence of intrauterine pregnancies, which may occur after curettage. Fetal heart tones may be absent in patients with molar gestations due to intrauterine fetal demise. Approximately 2 percent of molar gestations will have a coexistent fetus (17).

The sonographic appearance of a hydatidiform mole is quite distinctive (2). In most cases, a sonographic pattern arising from molar tissue consists of echogenic intrauterine tissue that is interspersed with numerous punctuate sonolucencies. Irregular sonolucent areas may occur secondary to internal hemorrhage or an area of unobliterated uterine lumen.

The sonographic appearance of a hydatidiform mole varies according to the gestational duration and the size of the hydropic villi (18). For instance, hydatidiform moles that occur from 8 to 12 weeks typically appear as homogeneously echogenic intraluminal tissue, since the villi at this stage have a maximun diameter of 2 mm. As the hydatidiform mole matures to 18 to 20 weeks, the vesicles have a maximum diameter of 10 mm, which is readily delineated on sonography (19).

As opposed to the complete mole, partial molar pregnancy, hydatidiform mole coexistent with fetus and hydropic degeneration of the placenta are associated with the presence of a fetus or fetal parts. Although it may be difficult to differentiate between a partial molar pregnancy and a complete mole with a coexistent fetus on the basis of sonography, these two entities can be differentiated from a complete mole when an identifiable fetus is present (11,19,20).

Hydropic degeneration of the placenta associated with incomplete or missed abortions is the most common condition that can simulate the appearance of a molar pregnancy. This is due to the sonographic similarity of a hydropic placenta with marked swelling of the villi to molar tissue. A fetus may or may not be present with hydropic degeneration of the placenta. Serum beta-hCG levels are generally lower in hydropic degeneration than in partial or complete moles probably due to the reduced number of functioning trophoblasts (4).

Occasionally uterine leiomyoma, some ovarian tumors and patients with retained products of conception with hemorrhage can simulate the sonographic appearance of molar pregnancies (4,21,22).

REFERENCES

1. Callen PW, Ultrasonography in evaluation of gestational trophoblastic disease. In:Callen P, ed. Ultrasonography in obstetrics and gynecology. Philadelphia: Saunders; 1983:259-70.
2. Fleischer A, James A, Krause D. Sonographic patterns in trophoblastic disease. Radiology 1978;126:15.
3. Requard C, Mettler F. Use of ultrasound in the evaluation of trophoblastic disease and its response to therapy. Radiology 1980;135:419.
4. Reid M, McGohan JO. Sonographic evaluation of hydatidiform mole and its look-alike. Am J Roentgenol 1983;140:307.
5. Jones Jr H. Gestational trophoblastic diseases, in Jones III H, Jones S (eds), Novak's textbook of Gynecology, 10th ed, Baltimore, Williams and Wilkins; 1981 : 659-89.
6. Kajii T, Ohama K. Androgenetic origin of hydatidiform mole. Nature 1977;168:633.
7. Szulman A, Surti J, Berman M. Patient with partial mole requiring chemotherapy. Lancet 1978;1:1099.
8. Szulman A, Surti N. The syndromes of hydatidiform mole. I. Cytogenic and morphologic correlations. Am J Obstet Gynecol 1978;131:665
9. Szulman A, Surti N. The syndromes of hydatidiform mole. II. Morphologic evaluation of the complete and partial mole. Am J Obstet Gynecol 1978;132:20.
10. Sauerbrei E, Salem S, Fayle B. Coexistent hydatidiform mole and the fetus in the second trimester. An ultrasound study. Radiology 1980;135:415.

11. Munyer T, Callen P, Filly R, et al. Further observations on the sonographic spectrum of gestational trophoblastic disease. J Clin Ultrasound 1981;9:349.
12. Kobayashi M. Use of diagnostic ultrasound in trophoblastic neoplasms and ovarian tumors. Cancer 1978;38:441.
13. Santos-Rasmos A, Forney J, Schwartz B. Sonographic findings and clinical correlations in molar pregnancies. Obstet Gynecol 1980;56:-186.
14. Pritchard J, Hellman L (eds): Williams' Obstetrics. New York: Appleton Century Crofts ;1971 : 578.
15. Goldstein D, Berkowitz R, Cohen S. The current management of molar pregnancies. Curr Prob Obstets Gyn 1979;3:1.
16. MacVicar J, Donald I. Sonar in the diagnosis of early pregnancy and its complications. J Obstet Gynaecol Br Commonw 1968;70:387
17. Jones W, Lauerson N. Hydatidiform mole with coexistent fetus. Am J Obstet Gynecol 1975;122:267.
18. Reuter K, Michlewitz H, Kahn P. Early appearance of hydatidiform mole by ultrasound: a case report. Am J Roentgenol 1980;134:588.
19. Wittmann B, Fulton L, Cooperberg P, et al. Molar pregnancy: Early diagnosis by ultrasound. J Clin Ultrasound 1981;9:153.
20. Naumoff P, Szulman A, Weinstein B, et al. Ultrasonography of partial hydatidiform mole. Radiology 1981;140:467.
21. Rinehart JS, Hernandez E, Rosenshein NB, et al. Degenerating leiomyomata: An ultrasonic mimic of hydatidiform mole. J Repord Med 1981;26:142.
22. Nelson LH, Fry FJ, Homesely HD, et al. Malignant ovarian tumors simulating hydatidiform mole on ultrasound. J Clin Ultrasound 1982;10:244.

MR AND ULTRASONOGRAPHIC IMAGING OF AN IMPERFORATE HYMEN WITH HEMATOMETRA AND HEMATOCOLPOS

Patchrin PEKANAN M.D.[1,2], Supranee NIRAPATHAPONGPORN M.D.[1,2], Sankiat VAYAKORNVICHIT M.D.[3]

ABSTRACT

Ultrasonographic and MR images of the imperforate hymen with hematocolpos and hematometra was shown in an 11-year-old girl. Turbid fluid was seen by ultrasonographic examination in the dilated uterine cavity and vaginal canal. Bright fluid on T1WI and T2WI in both cavities, indicated subacute blood. MRI also demonstrated the thickness of the imperforate hymen.

INTRODUCTION

An imperforate hymen is the most frequent female genital anomaly. Retained secretions and menstrual blood may distend the vagina and uterus to produce hematocolpos and hematometra resulting in an abdominal mass. An underlying hematometra should be included in the differential diagnosis of a pelvic mass with primary amenorrhea (1). Both ultrasonography and MRI study confirm the clinically suspected this pathology.

CASE REPORT

An eleven-year-old girl had lower abdominal pain for two weeks. A firm mass, size about 20 weeks pregnancy, was palpated at the lower part of the abdomen. She denied a transvaginal examination. She still had no menstruation. The secondary sex characteristics such as breast enlargement, and axillary hair was observed. Transvesical ultrasonography of the pelvic cavity revealed distended uterus and vagina with turbid fluid (Fig.1). The uterus and vagina had mildly thickened wall. MRI was performed to confirm the diagnosis of hematocolpos and hematometra. Axial and sagittal T1W images of the pelvic cavity showed distended uterine and vaginal cavity with hypersignal content, the content was as bright as the subcutaneous fat. The content was brighter on sagittal and coronal views T2W images (Fig.2). The grey signal membrane, 1 cm. thick was noted at sagittal T2W image.

An imperforate hymen was found and was excised. A considerable amount of bloody fluid was drained (Fig.3).

DISCUSSION

Normally the hymen originates from the urogenital sinus at the origin of the embryonic vagina. An imperforate hymen occurs if a normal lumen fails to develop (1-4). A simple imperforate hymen is usually not associated with other congenital abnormalities (5-7).

Obstructed uterovaginal anomalies most frequently become manifest at puberty, when the onset of menses results in the accumulation of

[1] Department of Radiology, Ramathibodi Hospital, Rama 6 Street, Bangkok 10900 Thailand.
[2] Department of Radiology, Samithivej Hospital.
[3] Department of OB-GYN, Samithivej Hospital.

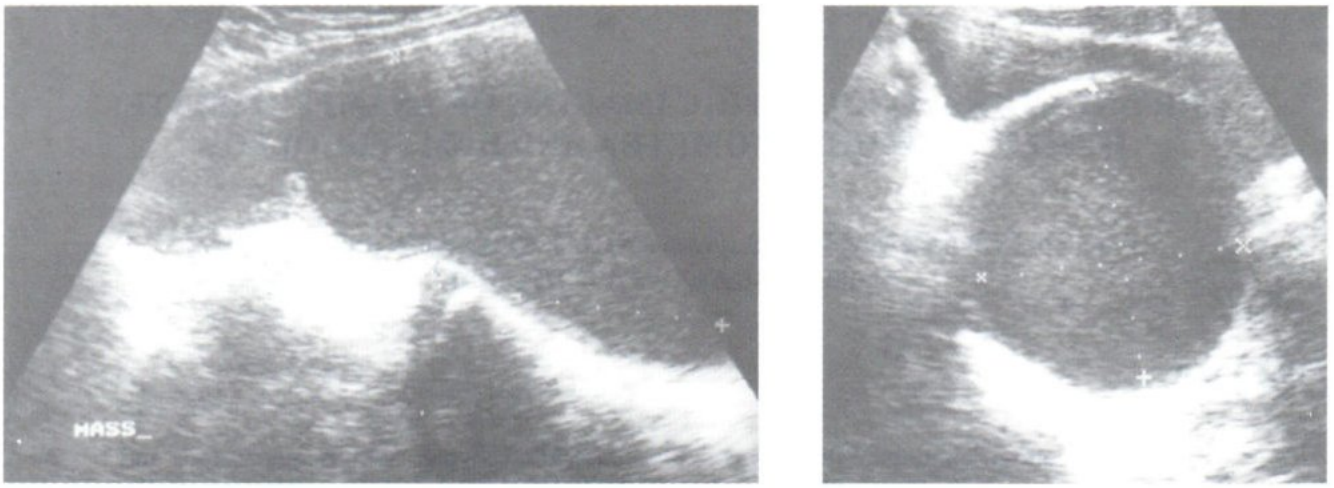

Fig.1 Longitudinal and cross section transvesical ultrasonography of the pelvis showed distended uterine and vaginal cavity with high proteinaceous fluid content.

menstrual blood and secondary distention of the vagina and/or uterus. Uterovaginal anomalies are best classified into three groups (8,9). The first group is agenesis of the uterus and vagina or Mayer-Rokitansky-Kuester-hauser syndrome, and is due to a dysplasia of the Muellerian ducts with absence of the normal uterus and most or all of the vagina. An active uterine anlage with functioning endometrial tissue may be present, resulting in a unilateral hematometra. The second group consists of disorders of vertical fusion, or faults in the junction between the down-growing muellerian ducts and up-growing derivative of the urogenital sinus, and includes transverse vaginal septum and congenital absence of the cervix and much of the vagina with a normal uterus. Imperforate hymen, while not a muellerian anomaly, is another cause of a low vaginal obstruction that must be distinguished from a transverse vaginal septum. The third group, disorders of lateral fusion, result from failure of lateral fusion of the two muellerian ducts or failure of absorption of the uterine septum. When vaginal obstruction occurs, it is usually unilateral.

A large amount of blood can also accumulate in the follopian tubes resulting in hematosalpinx and secondary infection may lead to closure of the tubes.

Before menstruation, the accumulation of secretions in the vagina and uterus is referred to as hydrometrocolpos. Following menstruation, hematometrocolpos results from the presence of retained menstrual blood (10). If seen before puberty, the accumulation of secretions is anechoic. Following menstration, the presence of old blood results in echogenic material within the fluid, as in our case. There may also be layering of the echogenic material, resulting in a fluid-fluid levels.

The ability of diagnose the presence of blood reliable in virtually any body part or tissue and to characterize the relative age of blood is unique to MR imaging. In this regard the magnetic susceptibility effect of the diamagnetic deoxyhemoglobin present within red blood cells in acute hemorrhage has a pronounced effect on T2 proton relaxation and is manifested as prominent hypointensity particularly on long TR/long TE imaging sequences at high-field strengths. Shortening of T1 in subacute and chronic hematomas has been attributed to the paramagnetic effects of methemoglobin, resulting from the oxidation of hemoglobin (11,12). The menstrual products within the hematocolpos should be a combination of acute, subacute and chronic blood produced at different monthly periods. Sagittal images also showed the thickness of the imperforate hymen.

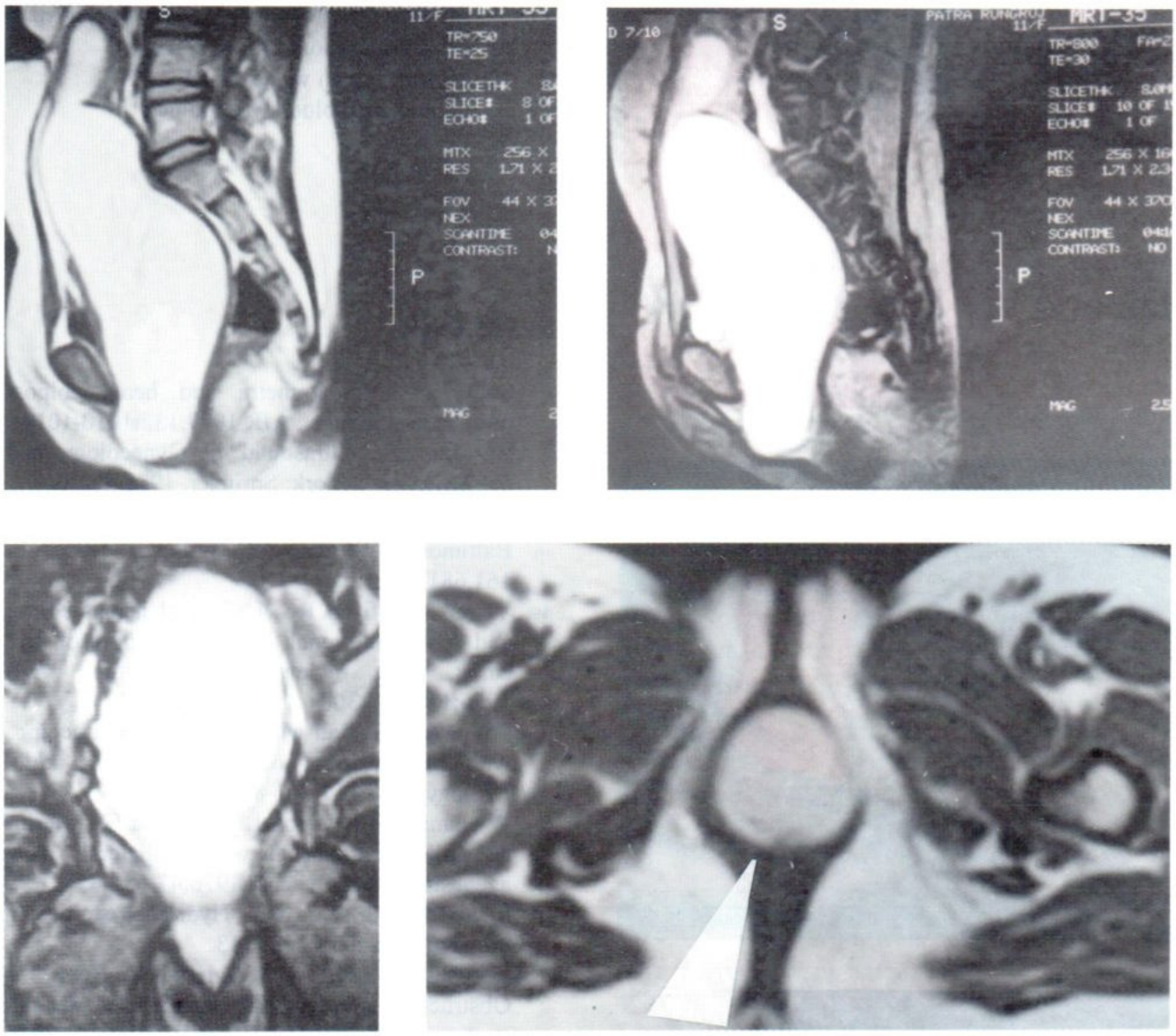

Fig.2 MR images of the distended uterine and vaginal cavity with subacute blood in sagittal and axial T1W and in coronal T2W. The fluid is bright on T2WI and brighter on T2WI and is homogeneous in signal. The arrow shows the imperforate hymen.

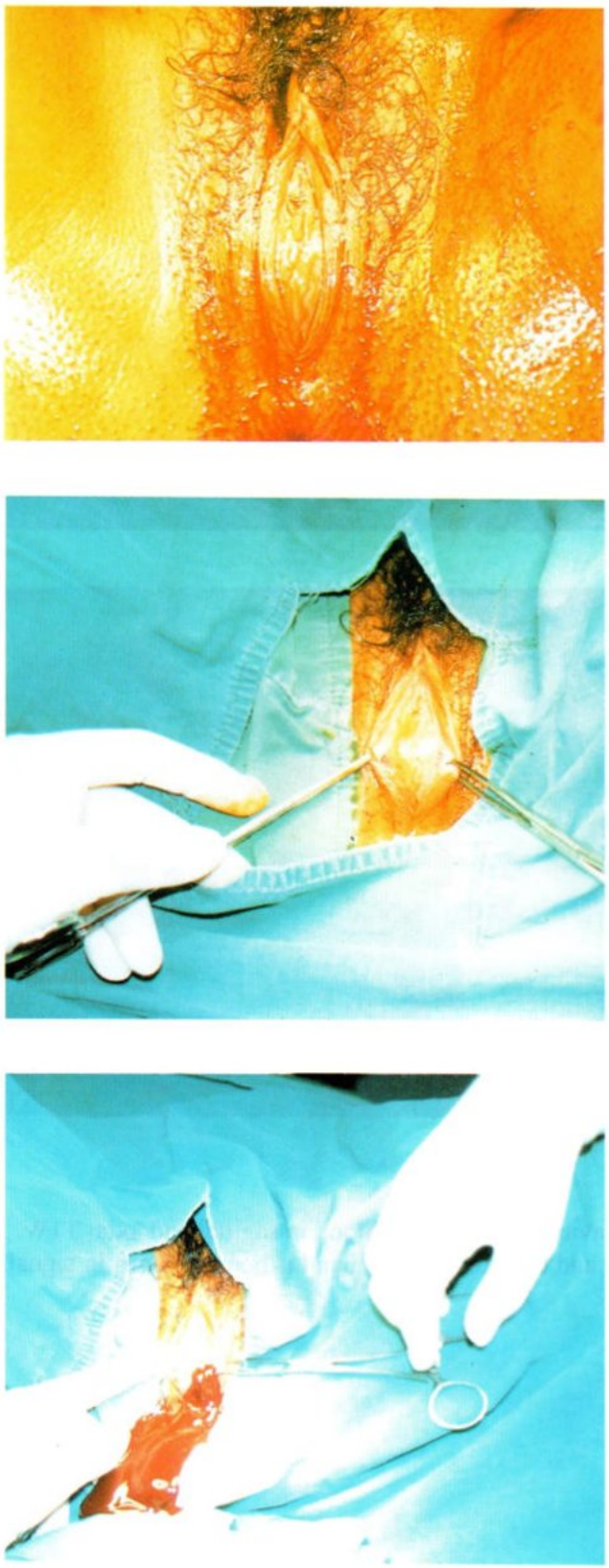

Fig.3 (A) imperforate hymen was seen at physical examination prior to surgery
(B) the hymen was excised
(C) retained blood was drained

REFERENCE

1. Sailer JF. Hematometra and hematocolpos-:ultrasound findings. AJR 1979;132:1010-1011.
2. Hassani SN. Ultrasound in Gynecology and obstetrics. New York: Springer, 1978:40-70.
3. Novak. Textbook of gynecology. 9th ed. Baltimore: Williams & Wilkins, 1975:156-161,681-683.
4. Yoder IC, Pfister RC. Unilateral hematocolpos and ipsilateral renal agenesis: Report of two cases and review of literature. AJR 1976;127:303-308.
5. Soloway MS, Rad MK, Kest L. Hematocolpos with urinary tract obstruction in an adult. Urology 1977;117:811-812.
6. Wiersma AF, Peterson LF, Justema EJ. Uterine anomalies associated with unilateral renal agenesis. Obstet Gynecol 1976;47:654-657.
7. Reed MH, Griscom NT. Hydrometrocolpos in infancy. AJR 1973;118:1-13.
8. Nussbaum Blask AR, Sanders RC, Rock JA. Obstructed uterovaginal anomalies: demonstration with sonography. Radiology 1991;-179:84-88.
9. Rock JA. Anomalous development of the vagina. Semin Reprod Endocrinol 1986;4:13-31.
10. Rumack CM, Wilson SR, Charboneau JW. Diagnostic ultrasound. Baltimore: Mosby year book, 1991:392-393.
11. Vainright JR, Fulp CJ, Schiebler ML. MR imaging of vaginal agenesis with hematocolpos. Journal of Computer Assisted Tomography 1988;12:891-893.
12. Rubin JI, Gomori JM, Grossman RI, Gefter WB, Kressel HY. High field MR imaging of extracranial hematomas. AJR 1987;148:813-7.

MRI OF THE ANTERIOR SPINAL ARTERY SYNDROME

Patchrin PEKANAN[1], Kamolpong OSATHAVANICHVONG[2], Suthikorn TANPAIROJ[3]

ABSTRACT

MRI of the anterior spinal artery syndrome was demonstrated at the lower thoracic level and the conus medullaris, in a 63-year-old female diabetic patient. The size and the signal of the cord was not change on T1WI and there was central bright signal at the cord on T2WI. Aortic dissection was noted at the abdominal aorta in the axial images.

CASE REPORT

A 63-year-old female diabetic patient, had sudden onset of back pain and paraplegia, 12 hours prior to the MRI study. The motor power of the lower extremities was of grade 0, the reflex of the lower extremities was absent. There was a decreased pinprick sensation from L1 downward. The touch, proprioceptive and vibration sense was intact. The sphincter tone was loose. The bulbocavernosus test was absent. Clinical diagnosis was anterior two-third spinal syndrome.

MRI study was performed and showed normal size of the lower thoracic cord and the conus medullaris (Fig.1). The signal of the cord on T1WI was normal and the signal was increased in the cord on T2WI and was a central type of hypersignal (Fig. 2,3). The abdominal aortic dissection was shown clearly at the axial view of both T1WI and T2WI (Fig. 3,4). The contrast medium was not given due to short onset-examination interval.

INTRODUCTION

The diagnosis of anterior spinal artery syndrome is made from the characteristic clinical presentation (1,2). Onset is often abrupt with the maximum deficit occurring either immediately or after progression over a few hours. Neurologic deficits include initial flaccid paralysis and depression or absence of muscle stretch reflexes. As time progresses the reflexes become hyperactive and involved muscle groups atrophy. A sensory level is present, below which pain and temperature sensations are not perceived. Sensation of proprioception and vibration, mediated through the dorsal columns in the posterior aspect of the spinal cord is preserved. Bowel and bladder paralysis are common features of the clinical picture. Occlusion of the spinal artery is rare.

We present a case of anterior spinal artery syndrome, studied by MRI.

DISCUSSION

The spinal cord has a unique pattern of blood supply with one anterior and two posterior arteries. In the lower cervical cord and upper thoracic segments of the thoracic cord, the anterior spinal artery is supplied by two or four anterior radicular arteries arising from the vertebral, deep cervical, superior intercostal, and ascending cervical arteries (1,3-5). Radicular arteries are less prominent in the midthoracic cord. The thoracolumbar region is supplied by the great anterior radicular artery of

[1] Department of Radiology, Ramathibodi Hospital, Rama 6 Street, Bangkok 10400, Thailand.
[2] Medical software development project, Mahidol University, Pin-Klao-Nakornchaisri Street, Bangkok.
[3] Pumipol Hospital, Bangkok.

Adamkiewicz. The cauda equina is supplied by lower lumbar, iliolumbar and lateral sacral arteries.

The anterior spinal artery supplies approximately 70% of the blood to the cord, including all of the gray matter except for the posterior horns, and the corticospinal tracts. It does this in a centrifugal fashion via numerous central arteries that traverse the anterior median fissure and alternately penetrate the cord to the right or left. Within the inferior of the cord there are no anastomoses, and the central penetrating vessels are essentially end arteries. The paired posterior spinal arteries supply approximately 30% of the cord, including the posterior horns, posterior columns, and a peripheral rim of white matter. They do this in a centripetal fashion via numerous peripheral perforating arteries that are richly connected by anastomotic channels (6-8). The periphery of the gray matter is at the border zone of these centrifugal and centripetal circulations.

The intrinsic arterial supply to the cord is directly proportional to the cross-sectional area of the gray matter, which is most abundant in the thoracolumbar segment. The central gray matter has a much higher metabolic rate than white matter and consequently receives five times more blood flow (6-8).

Because of the limited but critical sources of blood supply to the spinal cord, any pathologic processes that interfere with this crucial blood supply may result in ischemia and or infarction in the spinal cord (9). Most spinal cord infarctions occur at the

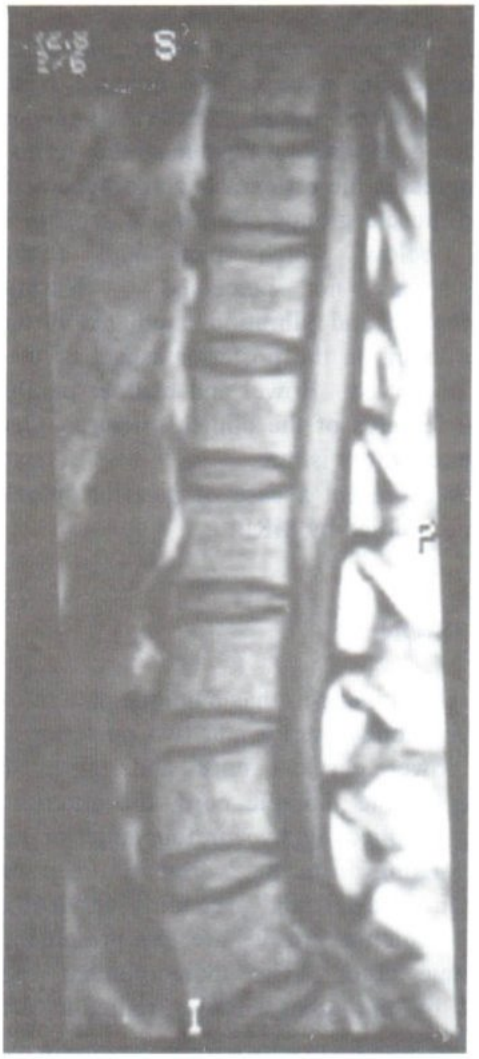

Fig.1 Sagittal view, T1WI MRI study at the thoracolumbar junction showed a normal sized cord with unchanged signal pattern

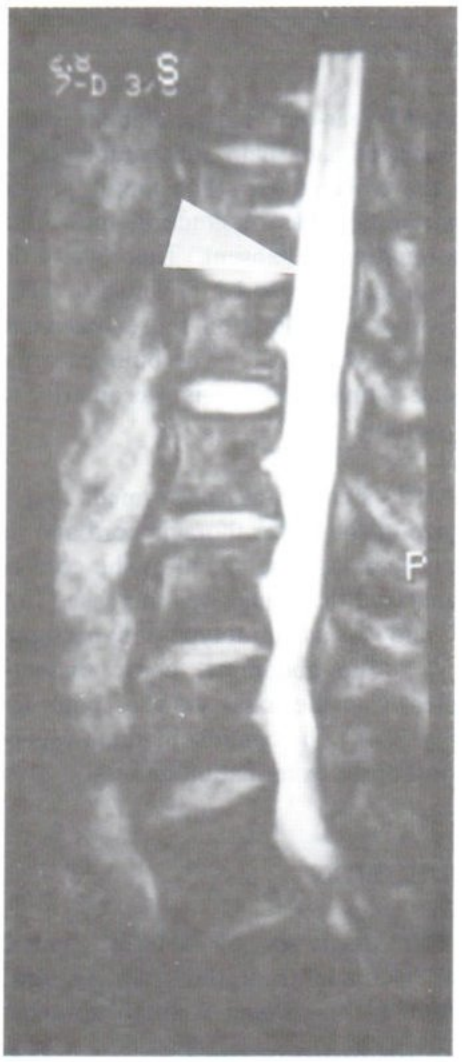

Fig.2 Sagittal view, T2WI MRI study at the thoracolumbar junction showed an increased signal diffusely in the central part of the cord

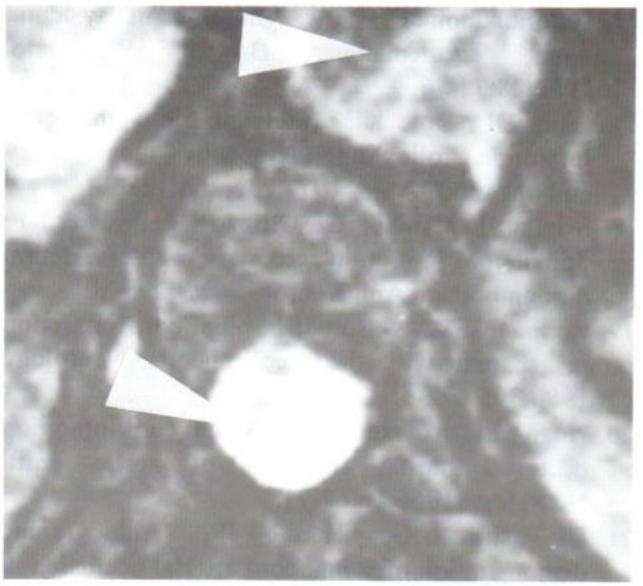

Fig.3 Axial view, T2WI, showed again a hypersignal central type at the cord and an abdominal aortic dissection

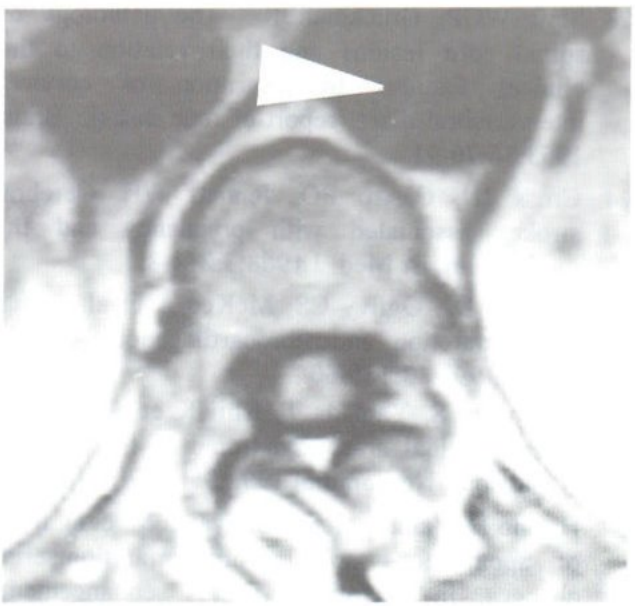

Fig. 4. Axial view MRI showed an abdominal aortic dissection.

upper thoracic region or thoracolumbar junction. Infarctions in the latter site may result from occlusion of the artery of Adamkiewicz, which is frequently the only blood supply to the thoracolumbar junction (10). In the upper thoracic regions, medullary feeder arteries are sparse, the anterior spinal artery is narrow, sulcus arteries are fewer and smaller, the spinal canal is narrow, and the spinal cord is in a watershed area between major feeding arteries (11). The vertical extent of spinal cord infarction may have from one to 15 segments, depending on the vascular anatomy of the cord and extent of occlusion. Single segmental infarction is frequently caused by ischemia in the watershed area, as occurs in hypotension (12). Single segmental infarction may also be seen in diseases that affect the small end arteries, such as emboli or focal vasculopathies.

Spontaneous anterior spinal cord infarction primarily affects individuals with severe atherosclerotic disease or aortic dissection (13), infection (14), vasculitis (15,16), embolic events (17,18), sickle cell anemia (19), surgery (20), radiation (21), trauma (22), bulging disc (23), associated with pregnancy (24).

Patient age in reported cases ranges from 15 to 75 years (2). Treatment of spinal cord infarction is mainly supportive. Early diagnosis and differentiation of venous versus arterial vaso-occlusive disease may be beneficial since venous, nonhemorrhagic infarction due to thrombosis progresses more slowly and is more protracted than the arterial counterpart, indicating that intervention with thrombolytic agents early in the course of thrombotic veno-occlusive disease may improve the outcome (9,3). It is now possible to detect spinal cord infarction early in the course of the disease, but differentiating arterial from venous sources awaits further study.

Magnetic resonance imaging is a sensitive modality in evaluating the spinal cord for infarction. T1-weighted MR scans in acute cord infarction may demonstrate an enlarged cord. Central or anterior intramedullary high signal is typically present on T2WI. Enhancement following contrast may be initially absent but occurs a few days to a few weeks following symptom onset (25-28). Follow-up scans may show focal cord atrophy with myelomalacia and residual high signal intensity on T2WI (27).

REFERENCES

1. Elksnis SM, Hogg JP, Cunningham ME. MR imaging of spontaneous spinal cord infarction. Journal of Computer Assisted Tomography 1991;15:228-32.

2. Steegmann AY. Syndrome of the anterior spinal artery. Neurology 1952;2:15-35.
3. Satran R. Spinal cord infarction. Stroke 1988;19:529-32.
4. Brown E, Virapongse C, Gregorios JB. Clinical images. MR imaging of cervical spinal cord infarction. J Comput Assist Tomogr 1989;13:920-2.
5. Henson RA, Parsons M. Ischemic lesions of the spinal cord: an illustrated review. Q J Med 1967;36:205-22.
6. Friedman DP, Flanders AE. Enhancement of gray matter in anterior spinal infarction. AJNR 1992;983-85.
7. Lazorthes G, Gouaze A, Zadeh JO, et al. Arterial vascularization of the spinal cord. J Neurosurg 1971;35:253-69.
8. Herrent RY, Alexander L. Sulcal and intrinsic blood vessels of human spinal cord. Arch Neurol Psychiatry 1939;41:678-87.
9. Yuh WTC, Marsh E, Wang AK, et al. MR imaging of spinal cord and vertebral body infarction. AJNR 1992;13:145-54.
10. Piscol K. Blood supply of the spinal cord. Berlin: Springer-Verlag, 1972.
11. Sandson TA, Friedman JH. Spinal cord infarction: report of 8 cases and review of the literature. Medicine (Baltimore) 1989;68:282-92.
12. Lasjaunias P, Berenstein A. Surgical neuroangiography. 3 Functional vascular anatomy of brain, spinal cord and spine. Berlin: Springer-Verlag 1990:40-55.
13. Modic MT, Masaryk T, Paushter D. Magnetic resonance imaging of the spine. Radiol Clin North Am 1986;24:229-45.
14. Haupt HM, Kurlinski JP, Barnett NK, Epstein M. Infarction of the spinal cord as a complication of pneumococcal meningitis. J Neurosurg 1981;48:945-8.
15. Gibb WRG, Urry PA, Lees AJ. Giant cell arteritis with spinal cord infarction and basilar artery thrombosis. J Neurol Neurosurg Psychiatry 1985;48:945-8.
16. Markusse HM, Haan J, Tan WD, Breedveld FC. Anterior spinal artery syndrome in systemic lupus erythematous. Br J Rheumatol 1989;28:344-6.
17. Gang DL, Dole KB, Adelman LS. Spinal cord infarction following therapeutic renal artery embolization JAMA 1977;237:2841-2.
18. Srigley JR, Lambert CD, Bilbao JM, Pritzker KP. Spinal cord infarction secondary to intervertebral disc embolism. Ann Neurol 1981;9:296-301.
19. Rothman SM, Nelson JS. Spinal cord infarction in a patient with sickle cell anemia. Neurology 1980;30:1072-6.
20. Hogan EL, Romanul FCA. Spinal cord infarction occurred during insertion of aortic graft. Neurology 1966;16:67-71.
21. Di Chiro G, Herdt JR. Angiographic demonstration of spinal cord arterial occlusion in post radiation myelomalacia. Radiology 1973;106:317-9.
22. Shukla RD, Lynch VP. Spinal cord ischemia following repair of ruptured thoracic aorta: a successful outcome. Irish J Med Sci 1985;154:35-7.
23. Mair WGP, Druckman R. The pathology of spinal cord lesions and their relation to the clinical features in protrution of cervical intervertebral discs (report of four cases). Brain 1953;76:70-91.
24. Cross JN, Castro PO, Jennett WB. Cerebral strokes associated with pregnancy and the puerperium. Br Med J 1968;3:214-8.
25. Mikulis DJ, Ogilvy CS, McKee A et al. Spinal cord infarction and fibrocartilagenous emboli. AJNR 1992;13:155-60.
26. Takahashi S, Yamada T, Ishii K et al: MRI of anterior spinal artery syndrome of the cervical spinal cord. Neuroradiol 1992;35:25-9.
27. Hirono H, Yamadori A, Komiyama M, et al. MRI of spontaneous spinal cord infarction:serial changes in gadolinium-DTPA enhancement. Neuroradiol 1992;34:95-7.
28. Osborn AG, Diagnostic neuroradiology. St. Louis:Mosby, 1994;834-35.

WYBURN-MASON SYNDROME ASSOCIATED WITH MOYAMOYA DISEASE

Siriporn HIRUNPAT[1], Patchrin PEKANAN[2], Nakornchai POENPATHOM[3]

ABSTRACT

A report case of subcutaneous hemangiomas of the head and face, intraorbital hemangiomas, intracranial AVM and occlusion of distal left internal carotid artery was shown in a 17-year-old man. The association of the Wyburn-Mason Syndrome and Moyamoya disease in this patient was rare and was not seen in the literature. The imaging modalities were CT scan and angiography of the head.

INTRODUCTION

Wyburn-Mason syndrome is one of the rare group of disorders collectively known as phakomatoses. It consists of arteriovenous malformations affecting the visual pathways, the mid-brain and subcutaneous facial structures (1). Moyamoya disease is a kind of occlusive arteriopathy which is congenital or acquired (2). Cases of association between Wyburn-Mason syndrome and Moyamoya disease is considered rare. We report such a case by CT and angiographic imaging.

CASE REPORT

A 17-year-old woman developed right hemiparesis for 10 days. She was a known case of left orbital cavernous hemangioma and hemangioma at left temporal part of the soft tissue of the head, diagnosed 3 years ago. Thirty days prior to the admission she was infected by herpes zoster at her right part of the face. Afterwards, there was swelling of left eyelid, left exophthalmos and right hemiparesis. Blindness of left side was noted. Motor power of right extremities was grade III. Sensation of right side was impaired. The response of the Babinki's was abnormal.

Non contrast enhancement and contrast enhancement axial and coronal CT scan of the brain and orbits showed large calcified known hemangiomas at the subcutaneous part of the left side of the head and face and in the left orbital cavity. In the brain, a large nidus of arteriovenous malformation is noted at left splenium of corpus callosum and left deep parietal lobe. Left common carotid injection showed nearly complete occlusion of the distal internal carotid artery. Mild degree of collateral vessels or moyamoya vessels are noted at both left common and right internal carotid arterial injection. Due to this occlusion of left internal carotid artery, the demonstration of the intracranial AVM is not possible. (Fig. 1,2).

DISCUSSION

Phakomatoses is a group of disorders described by Van Der Hoeve in 1923. It includes angiomatosis retinae (Von Recklinghausen's disease), tuberous sclerosis (Bourneville's disease), encephalotrigeminal angiomatosis (Sturge-Weber disease), ataxia telangiectasis (Louis-Bar syndrome), and Wyburn-Mason syndrome (1).

[1] Department of Radiology, Prince of Songkla University Hospital, Hatyai, Songkla, Thailand 90112.
[2] Department of Radiology, Ramathibodi Hospital, Bangkok.
[3] Department of Surgery, Prince of Songkla University Hospital.

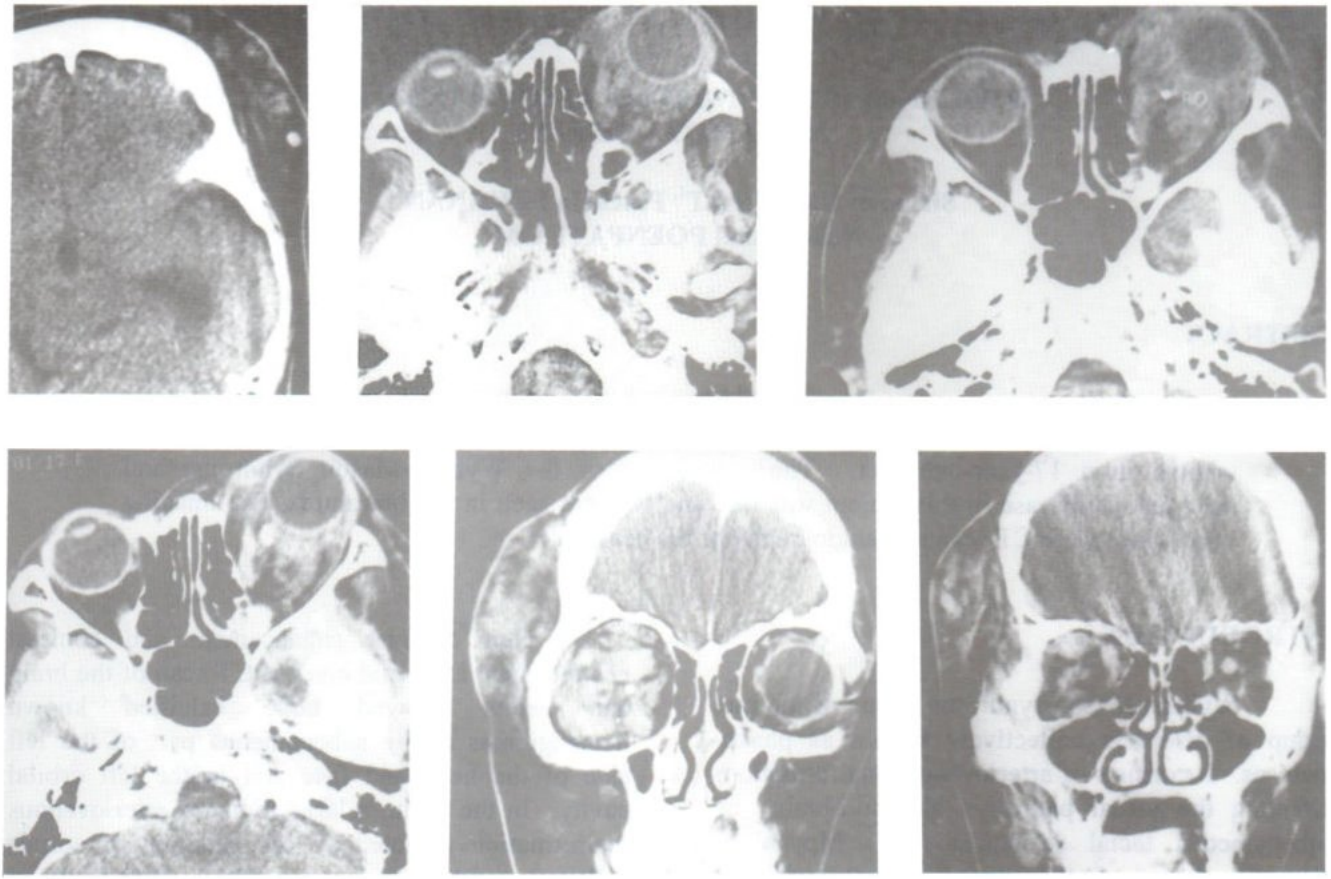

Fig. 1A. Axial nonenhanced CT scan of the orbits and enhanced coronal CT scan of the orbits showed the lesion of known hemangioma in the left orbital cavity, subcutaneous plane of left side of the head. Small calcification was noted in the lesions of both sites was shown.

Bonnet et al, first reported the association of retinal vascular malformations with ipsilateral cerebral arteriovenous malformations and facial naevi (3). The disorder stems from a vascular dysgenesis in the early embryonic period and extensions of the lesions vary widely. The first English report was by Wyburn-Mason who reviewed a large series in 1943 (4). The diagnosis was done only by other examinations than imaging.

The vascular abnormalities in the other phakomatoses are distinct from the arteriovenous malformations arising in Wyburn-Mason syndrome. In neurofibromatosis anomalies of the ophthalmic vessels and cavernous sinus are associated with sphenoid dysplasia. The vascular abnormality in Sturge-Weber syndrome is leptomeningeal angiodysplasia, with atrophy and calcification of the underlying cerebrum, Von Hippel-Lindau disease is an autosomal dominant angiodysplasia which consists of retinal capillary angioblastomas with multiple haemangioblastomas of the brain and spinal cord. Tumors affecting other viscera, especially the kidneys, are also a feature (1).

Manifestations of Wyburn-Mason syndrome can be cerebral or ocular or both. Headaches, seizures, or subarachnoid hemorrhage are the usual indicators of involvement of the central nervous system. The arterial blood supply is more often from the internal carotid system than from the vertebro-basilar or external carotid system. Venous drainage is primarily via the cavernous sinus or vein of Galen (1,5).

Damage to structures adjacent to the arteriovenous malformation can be due to compression from expansion of the vascular

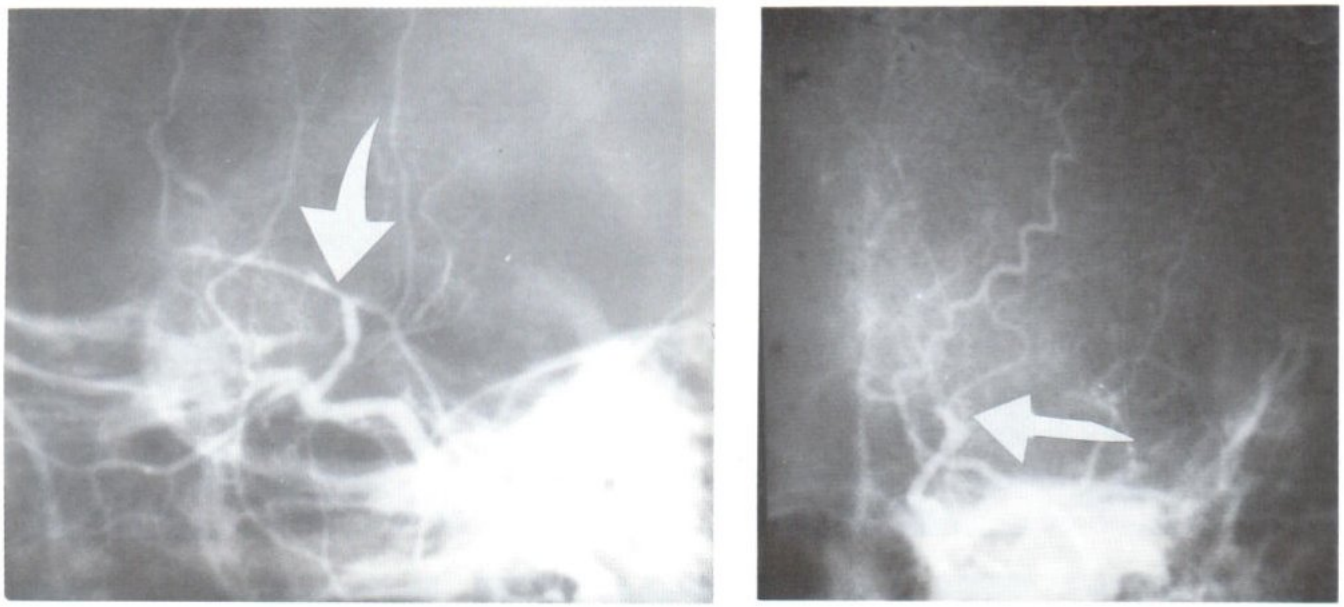

Fig. 2A. At left common carotid injection, nearly complete occlusion of distal left internal carotid artery was noted with moyamoya vessels.

malformation, hemorrhage into the adjacent structure, or due to ischemia from impaired perfusion (6).

Ocular manifestations are usually an important clue to the diagnosis of this syndrome. The retinal lesions, generally unilateral, range from ophthalmoscopically barely visible communications to large masses of tortuous and dilated vessels covering a substantial portion of the retina. The larger complexes usually cause cystic retinal degeneration between the dilated vessels and result in impaired vision (1,7). However, retinal involvement is not essential for the diagnosis of the Wyburn-Mason syndrome.

In the original series by Wyburn-Mason six patients had normal fundi. Other orbital manifestations which can occur include optic atrophy, enlargement of the optic foramen, and occasionally exophthalmos which may or may not be pulsatile (1,8).

Dermatologic lesions occur in a minority of cases and the clinical manifestation of these lesions varies from faint discolouration to extensive naevus involvement of the skin the trigeminal distribution, ipsilateral to the retinal or cerebral lesions. The deeper structures of the face such as the frontal and maxillary sinuses and the mandible can be involved (5).

Although arteriovenous malformations have little neoplastic potential they are dynamic structures and change with time. Substantial remodelling of an arteriovenous malformation has been observed in the retina and is evident on pathologic evaluation of intracranial lesions. Atrophy of some vessels occurs concurrently with dilation and expansion of others within the same lesion. These changes are most likely to be directed by haemodynamic factors caused by spontaneous thrombosis in parts of the complex. Progression of neurological signs can occur secondary to these changes (1,9).

Cases of association between these congenital disease and Moyamoya disease have been reported (10,11). Many other congenital diseases, such as von Recklinghausen's disease, tuberous sclerosis, Fanconi's anemia, and sickle cell anemia, are sometimes linked with a kind of occlusive arteriopathy termed Moyamoya syndrome (2,12-15). This seems to be the first report, demonstration of Wyburn Mason syndrome with associated Moyamoya disease.

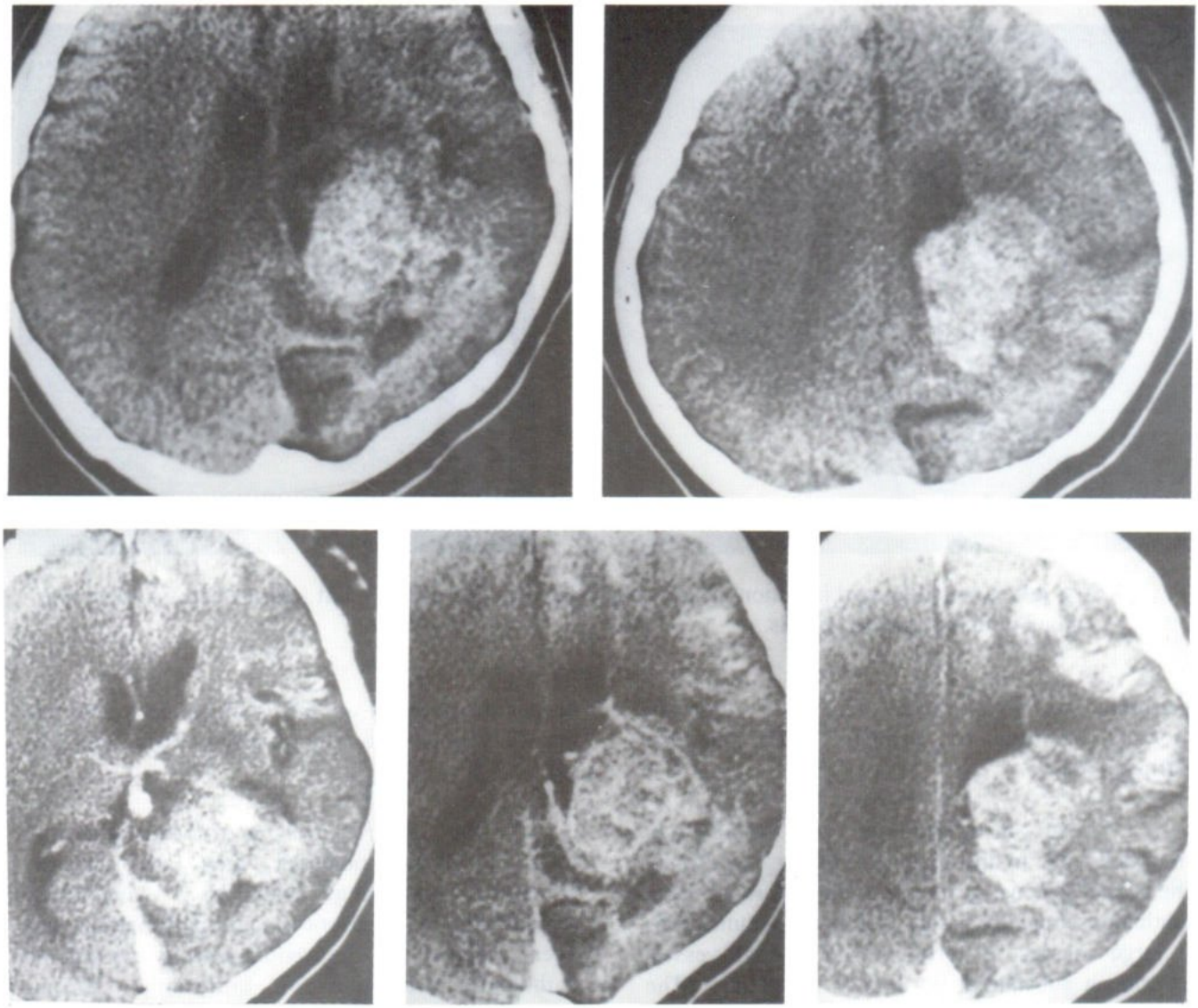

Fig. 1B. Axial CT scan of the brain with and without contrast enhancement revealed a large dense AVM nidus in the region of left splenium of corpus callosum, and around left posterior horn of left side. Gyriform enhancement of subacute left hemispheric ischemia was noted.

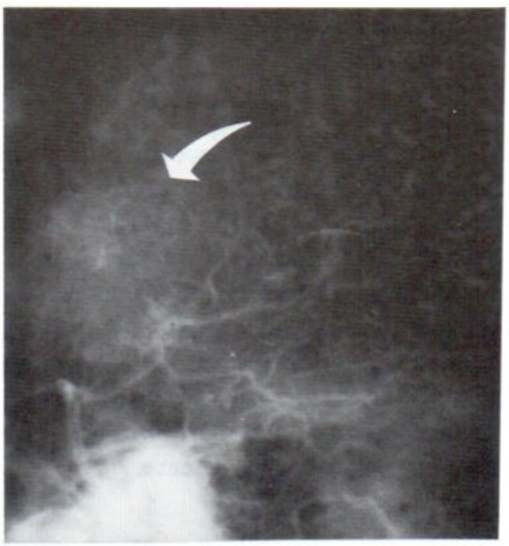

Fig.2B. At left vertebral injection, partial obstruction of left posterior cerebral and left cerebellar artery was noted. Moyamoya vessels are also noted from this injection.

REFERENCES

1. Patel U, Gupta SC. Wyburn-Mason syndrome: A case report and review of the literature. Neuroradiology 1990;31:544-6.
2. Aihara N. Nagai H, Mase M, Kanai H, Wakabayashi S, Mabe H. Atypical Moyamoya disease associated with brain tumor. Surg Neurol 1992;37:46-50.
3. Lalonde G, Duqutte P, Laflamme P, Vezina J. Bonnet-Dechaume-Blanc syndrome. Can J Ophthalmol 1979;14:47-50.
4. Wyburn-Mason R. Arteriovenous aneurysm of midbrain and retina, facial naevi and mental changes. Brain 1943;66:163-209.
5. Theron J, Newton T, Hoyt W. Unilateral retino-cephalic vascular malformations. Neuroradiology 1974;7:185-97.
6. Danis R, Appen RE. Optic atrophy and the Wyburn-Mason syndrome. J Clin Neuro Ophthalmol 1984;91-5.
7. Brown D, Hilal S, Tenner M. Wyburn-Mason syndrome: report of two cases without retinal involvement. Arch Neurol 1973;28:67-8.
8. Sutton JB. The lateral recesses of the fourth ventricle: their relation to certain cysts and tumours of the cerebellum, and to occipital meningocele. Brain 1887;9:352-61.
9. Leon RG, Schatzki SC, Wolopow ER. Neurofibromatosis with extensive intracranial arterial occlusive disease. AJNR 1982;3:572-6.
10. Kitamura K, Kurokawa T. Annual report of the research committee on spontaneous occlusion of the circle of Willis (Moyamoya disease). Japan Ministry of Health and Welfare 1982;73-9.
11. Watanabe Y, Todani T, Fujii T, Toki A, Umemura S, Koike Y. Wilms' tumor associated with moyamoya disease: a case report. Z Kinderchir 1985;40:114-6.
12. Brook BS, Gammal TE, Adams RJ, Harlage PL, Smith WB. MR imaging of moyamoya disease in neurofibromatosis. AJNR 1987;8:178-9.
13. Horae AM, Keogh AJ. Cerebrovascular moyamoya disease. Br Med J 1974;1:430-2.
14. Leone RG, Schatzki SC, Wolopow ER. Neurofibromatosis with extensive intracranial arterial occlusive disease. AJNR 1982;3:572-6.
15. Makoyo PZ, Rapoport AM, Fleming RJ. Moyamoya disease in black adults. Arch Neurol 1977;34:130.

The INTEGRIS H systems

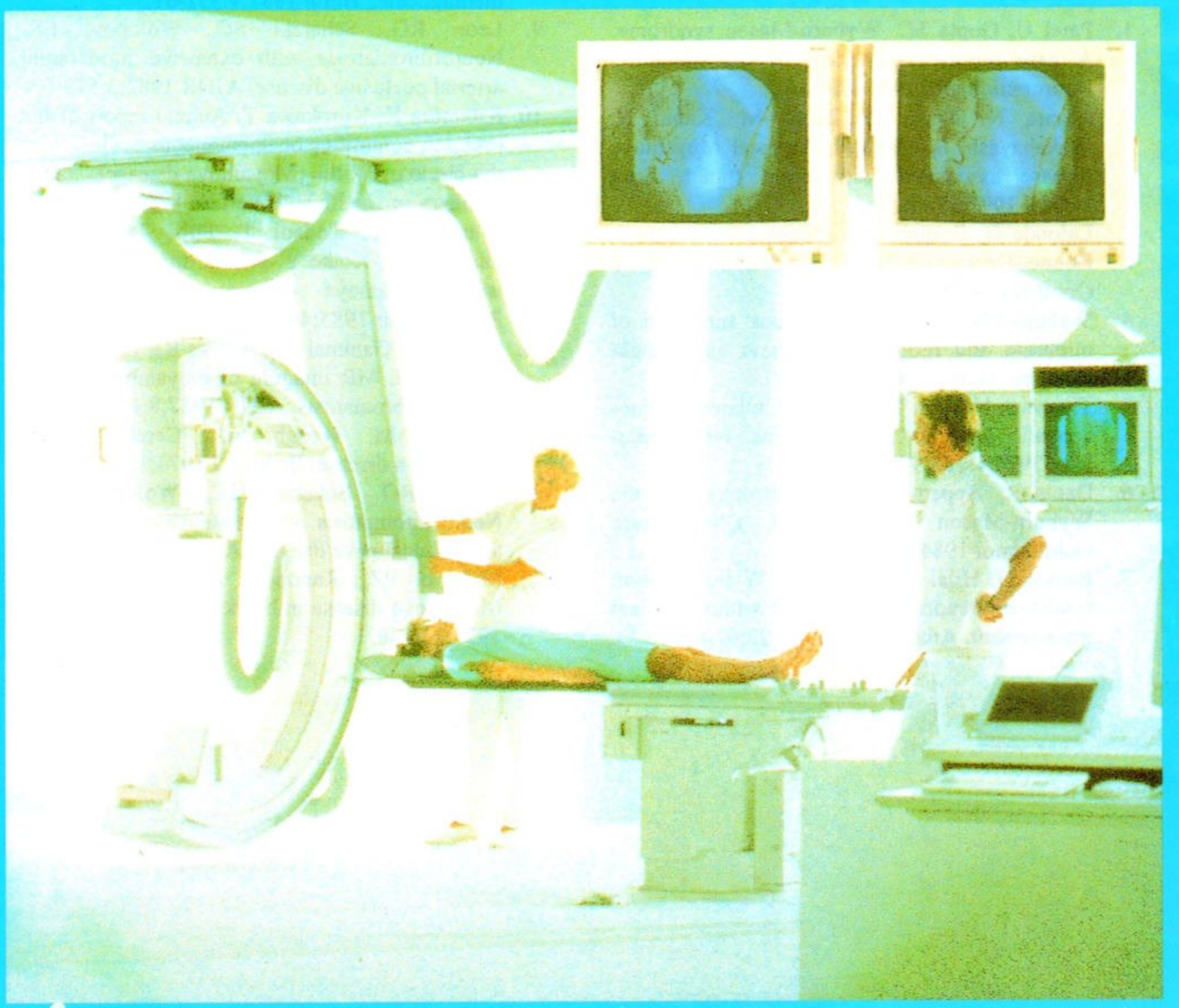

Let's make things better.

ร่วมสรรค์สิ่งที่ดีกว่า

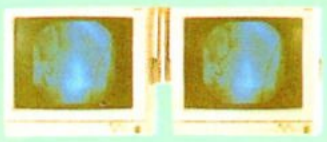

FOR MORE INFORMATION
PLEASE CONTACT
PHILIPS MEDICAL SYSTEMS
TEL .7454090 [3332]
FAX 3980792

PHILIPS

CONCURRENT CHEMO-RADIOTHERAPY FOR LIVER METASTASIS FROM BREAST CANCER: TWO CASES REPORT

P.PATTARANUTAPORN, MD.
Y.CHANSILPA, MD.

ABSTRACT

Two cases of multiple liver metastases from breast cancer, failed to the previous chemotherapy, were treated with concurrent chemo-radiotherapy. Thirty Grays of external irradiation was given to the whole liver in 3 weeks and 300 mg/m²BSA of carboplatin on day 1 and 750 mg/m²BSA of 5FU from day 1 to day 4 were also combinely given. After then, chemotherapy of the same regimen were repeated every four weeks. The tumor showed good response within 1-2 months after treatment. The metastatic areas in the liver were replaced with regenerating nodules in one case at one and a half year later. The patients could tolaterate the treatment very well without any complications, both clinicals and liver function test. Concurrent chemo-radiotherapy might be an alternative treatment for metatstatic breast cancer to the liver.

Key Words : Breast Cancer, Liver metastasis, Concurrent chemo-radiotherapy.

INTRODUCTION

Forty-one per cent of the cancer patient will develope liver metastases during the course of their illness because of the high blood flow through its capillary bed. Especially in breast cancer patient, the evidence of liver metastases is as high as 64 per cent.(1-2) Multiple liver metastatic sites were found in 70-75 per cent. The average survival for the patients with clinically evidences are about 5 months.(3-5) Radiation therapy for liver metastases has been limited by the low radiation tolerance of the hepatocyte with a threshold dose of 25-30 Gys, dose related venous occlusion and parenchymal fibrosis.(6,7)

The application of chemotherapy for metastatic breast cancer has improved overall survival modestly. Nonetheless, in the good response group, it has effectively ameliorated many tumor related symptom, but also has increased treatment-related toxicity , often at the expense of life.(8)

Several investigators have attempted to use chemotherapy as a radiosensitizer in various organs and showed a promising result, not only in the squamous cell carcinoma but also adenocarcinoma and transitional cell carcinoma. Thus the concurrent chemo-radiation was used to provide benifit without a corresponding increased toxicity. Chemotherapy such as carboplatin and 5 FU have shown the good radiosensitizing activity and have also been investigated as a single agent for treatment of breast cancer with 25-30 per cent response.(9-10)

From the rational of concurrent chemo-radiation therapy , and from effectiveness of

Division of Radiation Oncology, Department of Radiology.
Faculty of Medicine, Siriraj Hospital.
Mahidol University.

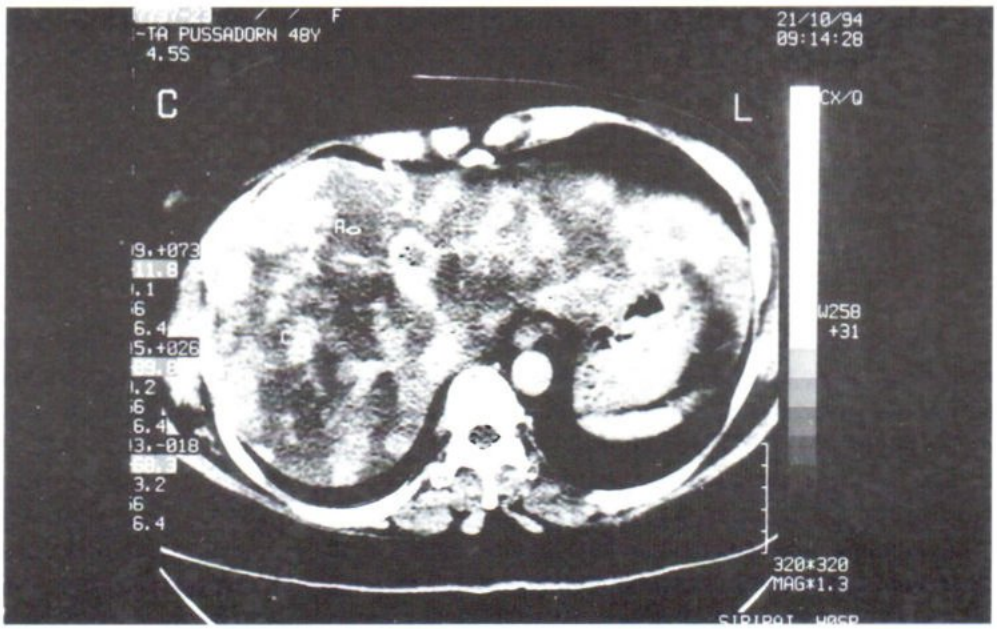

Fig.1 The CT scan showed multiple liver metastatsis in both lobes.

platinum compound and 5FU, we used carboplatin and 5FU as the chemotherapeutic agents in conjunction with 30 Gys of radiation to the whole liver. Two breast cancer patients with multiple liver metastases were treated.

Case No. 1

A known case of stage 4 breast cancer patient having a large 10x6 cm2 primary tumor mass with skin invasion was treated with 6 courses of chemotherapy (CMF) followed by modified radical mastectomy 4 years ago. The pathological report was invasive ductal carcinoma, moderate differentiation with negative estrogen and progesterone receptors. Postoperative radiation with the dose of 46 Gy was given to the chest wall. Three years later, she suffered from moderate to severe pain at right costal margin. Physical examination showed no abnormality detectable except enlarged liver about 4 cm. below right costal margin with moderate tenderness. CT scan showed massive metastasis in both lobes of liver as shown in figure 1.

The whole liver were irradiated daily with 2 Gy per fraction to a total dose of 30 Gy. The 300 mg/m² of carboplatin was given on day 1 and 700 mg/m² of 5FU per day were infused from day 1-4. After completion of radiation treatment, the chemotherapy was given intravenously every 28 days for 12 courses.Liver function test at the beginning and during chemotherapy were shown in the table 1 and CT scan were repeated at 1, 6 and 12 months after radiation respectively for evaluation of the response
and toxicity.

Table 1. Liver function test at the beginning and during treatment.

	before treatment	3rd month	1 year
SGOT	133	52	43
SGPT	67	51	44
AP	267	213	312

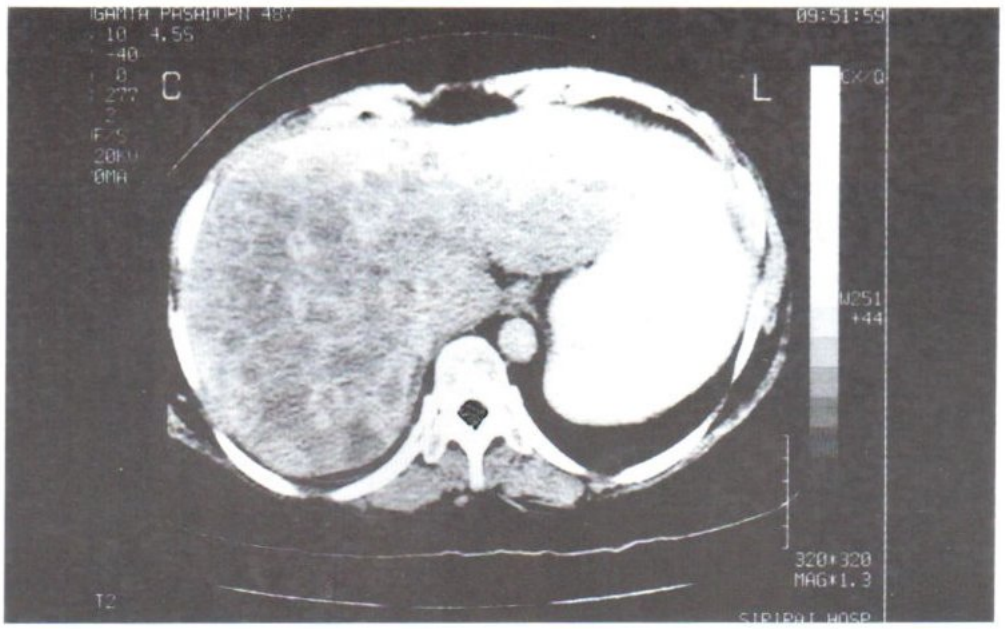

Fig.2 One months after completion of radiation, CT scan showed significant changes of the tumor.

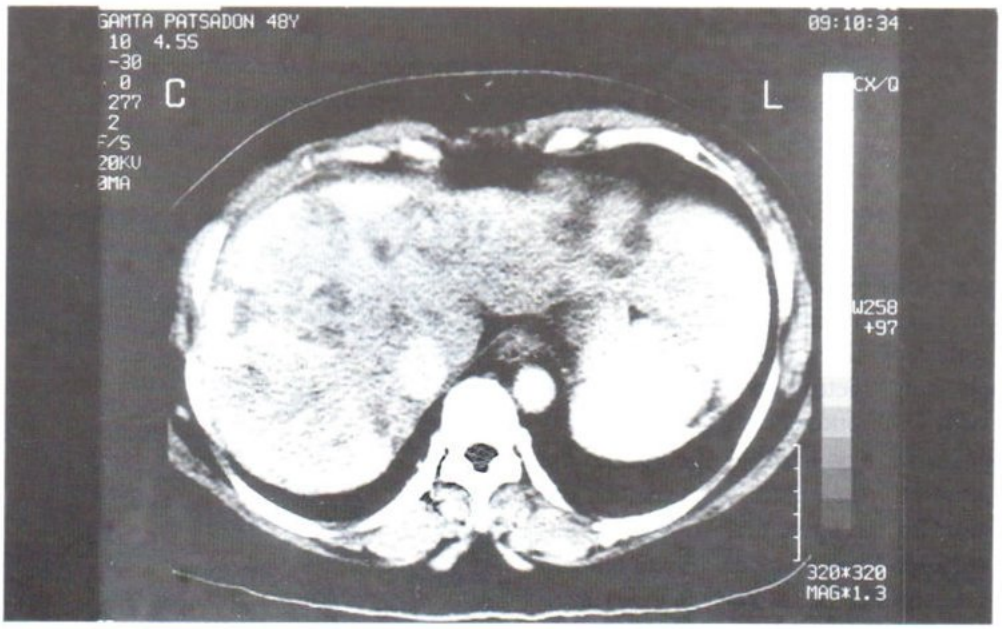

Fig.3 At 6 months after radiation treatment.

One months after completion of radiation, the liver showed more homogeneous than before irradiation and chemotherapy. The patient looked healthy. There was no sign of hepatic dysfunction. Chemotherapy was kept on.

At the 6th month of chemotherapy, CT scan showed significant changes of the liver. The size was decreased and the inhomogenicity was much improved.

At one year after treatment, the patients was very healthy. The liver function still showed a high level of alkaline phosphatase, but SGOT and SGPT were normal. CT scan revealed homogeneous liver with regenerating nodule, no definite space occupying lesion was seen. The last course of chemotherapy ,the twelfth course, were given.

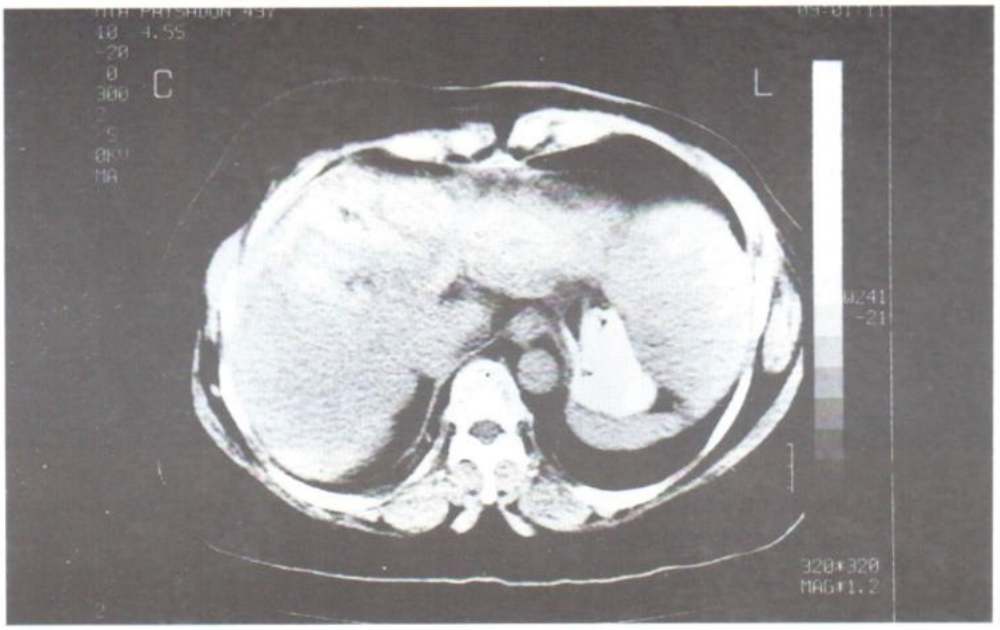

Fig.4 At one year after chemo-radiotherapy treatment, the lesions are totally replaced by regenerating nodules in almost the entire liver.

Case No. 2

A 48 years old female with stage 2 breast cancer treated by modified radical mastectomy and adjuvant chemotherapy 2 years ago, developed bone, brain and lung metastases. Multi-agents chemotherapy with CAF and Taxol were given and the tumor responses were on and off. She has got the brain bath radiation for brain metastases, and palliative radiation for the spine metastatsis. On her later visit, she suffered from dyspnea, bone pain and abdominal pain due to livermetastasis. The CT scan of the upper abdomen were shown to have multiple hypodensed areas in the liver as in Fig.5 and liver function test were shown in table 2.

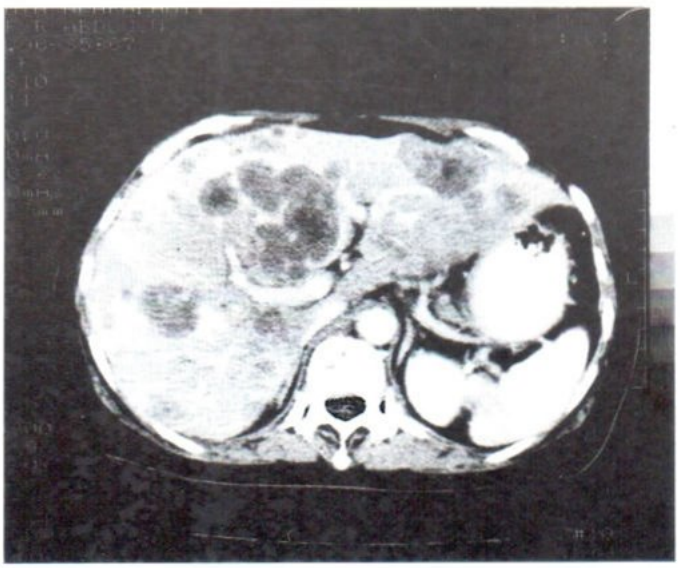

Fig. 5 CT scan showed multiple liver metastases occupied in both lobe of liver.

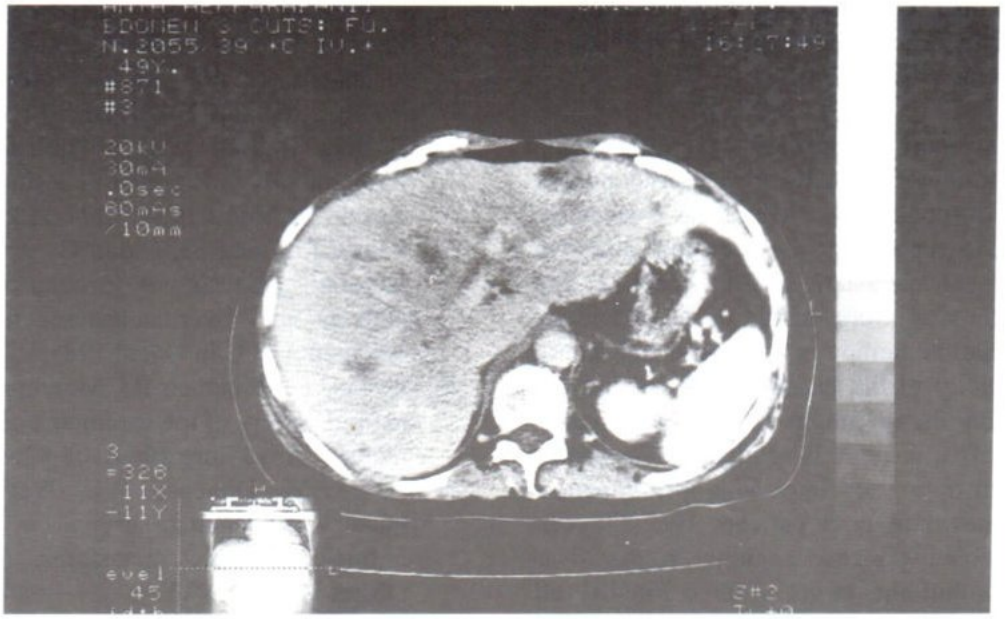

Fig 6. At the end of radiation treatment, the liver showed significant improvement of the lesion and the reduction in size of the liver.

She refused chemotherapy due to scarring of the previous toxicities, but she requested for the palliative treatment to relieve the discomfort from liver and lung symptoms. Concurrent chemo-radiation therapy was then offerred, base on the rationale of improving or enhancing each other with minimized toxicities. The treatment procedures were the same as in the patient No.1, with additional radiation lung bath to the right lung. After completion of radiation treatment, the discomfort at the right costal margin was relieved. CT scan of the upper abdomen revealed reduction in size of the liver with the improvement of metastatic lesions.

Table 2. Liver function test at the beginning and during treatment.

	before treatment	3 month after
SGOT	365	97
SGPT	247	38
AP	595	408

DISCUSSION

Extensive experience in the treatment of liver metastases has shown that the external radiation is effective in palliating symptom with 50-90 per cent relieving of the symptoms and 25 percent demonstrating of improving performance status. However, most of the disease will progress within a few months, resulting in a median survival of 3-6 months.11-13

Various schemes of radiation dose, techniques and combinationsof chemotherapy or radiosensitizer were studied . All are under the clinical investigations with comparable results. 14-18.

Recently, high-dose radiation therapy to the liver performed by using overlapping portals defined by a three-dimensional treatmentplanning system (conformal radiation therapy) is a new method for treatment of hepatic tumors. Meanwhile, the combination of the intraarterial hepatic chemo-therapy were also initiated.19-20

Anyhow, the cases of multiple sites of liver metastasis and failure to chemotherapy are still the

major problems. Concurrent chemo-radiation therapy were reported in several diseases that can reduce the radiation doses or provide the better result with the same radiation doses.

In this report, the disease were progressing after chemothe-rapy.Especially the second patient who failed to respond after CMF and 3 courses of Taxol that were reported to be the most effective chemotherapy for metastatic breast cancer.21 The liver metastatic sites were unable to be treated by conformal radiation therapy in both patients because of the multiplicity of the lesions. The concurrent chemo-radiation therapy might be the most suitable method. The effectiveness in palliating symptoms and the demonstration of improving performance status were shown in both patients. The CT scan showed reversible hypodense regions in the liver parenchyma within the target volume. Finally, all metastatic sites were replaced by the regenerating nodules. The liver fuction test did not show the hepatitis features. On the contrary, it showed an improvement of the liver functions in comparison with the ones prior to the treatment.

This report suggested that concurrent chemo-radiation therapy might be the alternative treatment procedure that can palliate the metastatic symptoms and prolong the survival in patients who response well to this scheme of treatment. The synergistic effect could provide a good response with minimizing the toxicity from each therapeutic modalities.

CONCLUSION

1. Concurrent chemo-radiation therapy is an alternative treatment for liver metastasis from breast cancer.

2. Radiation dose of 30 Gy may be the optimal dose for whole liver irradiation with no acute and late complications.

3. Carboplatin and 5FU might be a good radiosensitizer and also a candidate for palliative chemotherapeutic agent for metastatic breast cancer.

REFERENCES

1. Pickren JW, Tsukada M, Lane WW. Liver metas-tases : Analysis of autopsy data. In : Weiss L, Gilbert HA (Eds). Liver Metas-tasis. Boston, GK Hall Medical Publishers, 1982, p 2.
2. Cameron GR. The liver as a site and source of cancer. Br Med J 1954;1:347-350.
3. Lahr CJ, Soong SJ, Cloud G, et al. A multi-factorial analysis of prognostic factors in patients with liver metastases from colorectal carcinoma. J Clin Oncol 1983;1:720-726.
4. Pestana C, Reitemeir RJ, Moertal CG, et al. The natural history of the carcinoma of the colon and rectum. Am J Surg 1964;108:826.
5. Jaffe BM, Donegan WL, Watson F, et al. Factors influencing survival in patients with untreated hepatic metastases. Surg Gynecol Obstet 1968;27:1-11.
6. Ingold JA, Reed GB, Kaplan HS, et al. Radiation hepatitis. Am J Radiol 1965;93:200-208.
7. Kim TH, Panaher AM, Friedman H, et al. Acute treatment radiation hepatitis following whole abdominal irradiation. Clin Radiol 1976;27:449-454
8. Henderson IC, Garber JE, Breitmeyer, et al. Comprehensive management of disseminated breast cancer. Cancer. 1990;66:1439-1448
9. Margolin KA, Doroshow JH, Akman SA, et al. : Effective initial therapy of advanced breast cancer with fluorouracil and high-dose continuous infusion calcium leucovorin. J Clin Oncol. 1992;10:1278-1283.
10. Martin M, Rubio DR, Casado A, et al. : Carboplatin : An active drug in metastatic breast cancer. J Clin Oncol. 1992;10:433-447.
11. Borgelt BB, Geibar R, Brady LW, et al. The palliation of hepatitis metastasis : Results of the radiation therapy oncology group pilot study. Int J Radiat Oncol Biol Phys 1981;7:587-591.
12. Prasad B, Lee M, Hendrickson FR. Irradiation of hepatic metastasis.Int J Radiat Oncol Biol Phys 1977;2:129-132.
13. Sherman OM, Weichselbaum R, Order SE, et al. Palliation of hepatic metastasis. Cancer 1978;-41:2013-2107.

14. Webber BM, Soderberg CH, Leone LA, et al. A combined treatment approach to management of hepatic metastasis. Cancer 1978;42:1087-1095.
15. Barone RM, Byfield JE, Goldfarb PB, et al. Intra-arterial chemotherapy using an implantable infusion pump and liver irradiation for the treatment of hepatic metastasis. Cancer 1987;-50:850-862.
16. Raju PI, Maruyama Y, Desimone P, et al. Treatment of liver metastasis with a combination of chemotherpy and hyperfractionated external radiation therapy. Am J Clin Oncol 1987;-10:41-43.
17. Leibel SA, Pajak TF, Mossullo V, et al. Comparison of misonidazole sensitized radiation therapy to radiation therapy alone or the palliation of hepatic metastasis. Int J Radiat Oncol Biol Phys 1988;13:1057-1064.
18. Wiley AL, Wirtanen GW, Stephenson JA, et al. Combined hepatic artery 5-fluorouracil and irradiation of liver metastasis. Cancer 1989;-64:1783-1789.
19. Yamasaki SA, Marn CS, Francis IR, Robertson JM, Lawrence TS. High-dose localized radiation therapy for treatment of hepatic malignant tumors - CT findings and their relation to radiation hepatitis. Am J Roentgenol 1995;-165:79-84.
20. Robertson JM, Lawrence TS, Walker S, et al. The treatment of colorectal liver metastasis with conformal radiation therapy and regional chemotherapy. Int J Radiat Oncol Biol Phys 1995,32:445-450.
21. Per Dombernowsky, Julie Gehl, Marianne Boesgaard, et al. Treatment of metastatic breast cancer with paclitaxal and doxorubicin. Sem in Oncol 1995;22 :13-17.

บริษัท คงศักดิ์เอ็กซเรย์การแพทย์อุตสาหกรรม จำกัด
KONGSAK X-RAY MEDICAL INDUSTRY COMPANY LIMITED
212/1 PHAHONYOTHIN SOI 55 BANGKHEN BANGKOK 10220
TEL. 5213214, 5511794 CABLE: KELEX FAX: 5523744

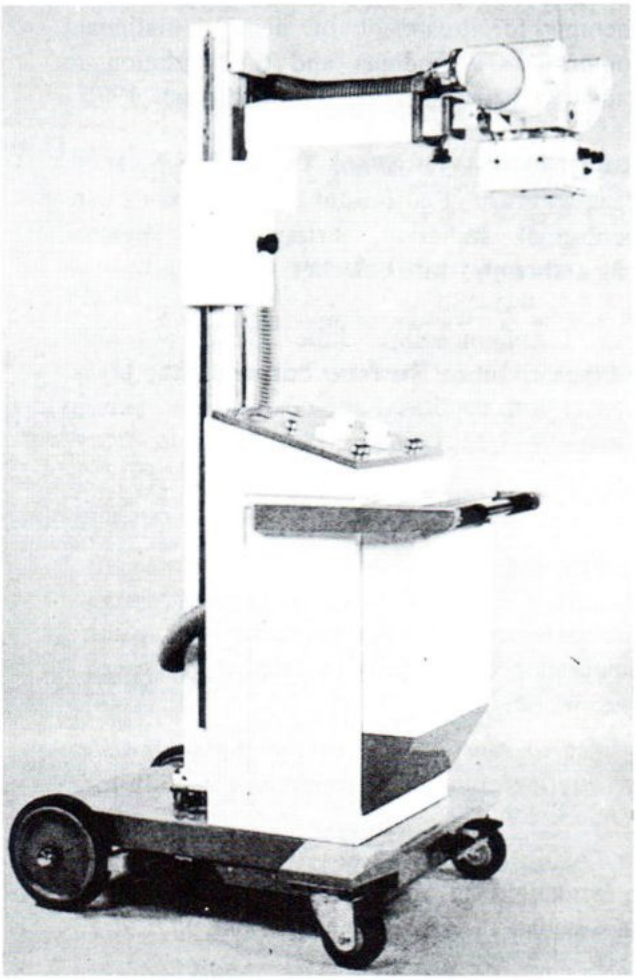

KELEX
50 mA 100 KV MOBILE TYPE DIAGNOSTIC X-RAY UNIT MODEL MD 50-99

- # เหมาะสำหรับคลินิคเอกชนและโรงพยาบาลทั่วไป
- # มีช่างผู้ชำนาญให้การบริการ ตลอดอายุการใช้งาน
- # พร้อมทั้งจำหน่ายอุปกรณ์เอ็กซเรย์

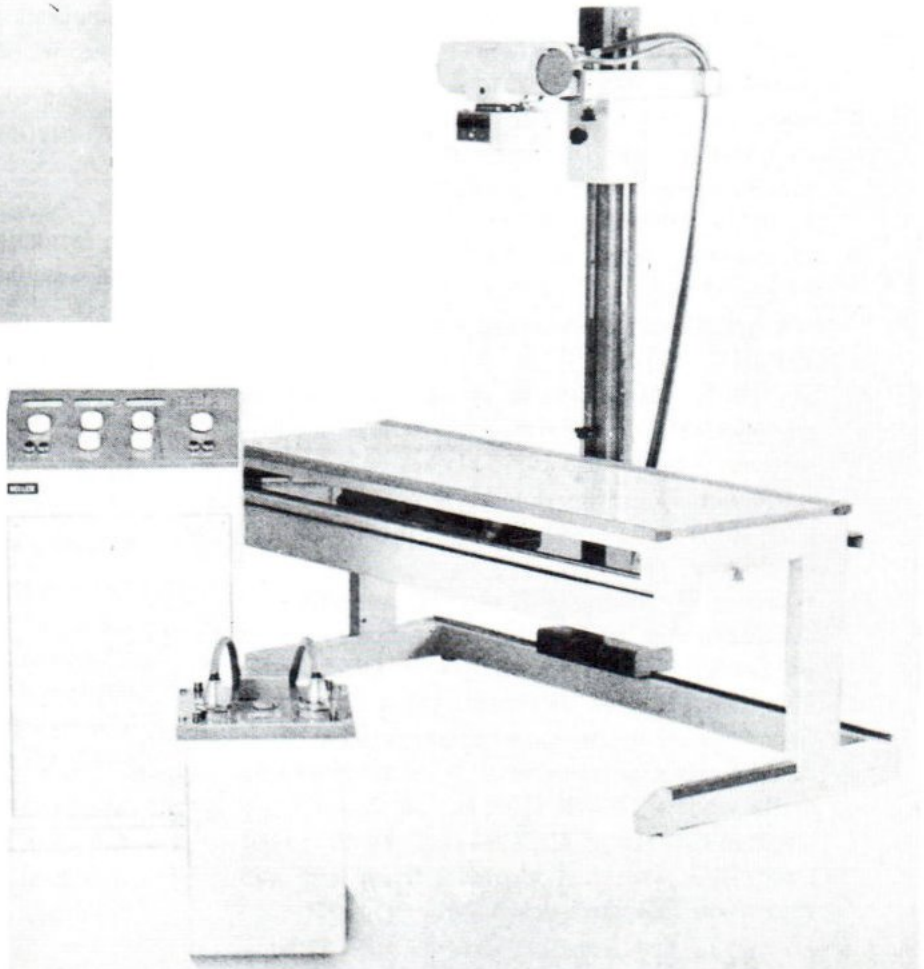

KELEX
MD 100-99 X-RAY SYSTEM
FULL WAVE 100 MA 100 KV

POST-MYELOGRAPHY HEADACHE AND ITS MANAGEMENT

Wiroj PENGPOL*
Bussaba PAKDIRAT**

ABSTRACT

A case of postdural puncture headache due to lumbar myelography is reported. Conservative treatment by hydration, analgesics and bed rest are not successful. Epidural blood patch is performed as the curative treatment which brings an immediate relief.

INTRODUCTION

Headache as a result of dural puncture (PDPH), is not a frequent complication of myelography. It is more often found in spinal anesthesia. Potential development of this condition remains the main objection to its use. Myelography can also be the cause of this symptom. Whenever a headache occurs in a patient undergoing myelographic study, it is important to recognize as a serious symptoms. A prompt diagnosis and treatment must be made.

CASE REPORT

A 43-yr-old female presented with a sciatica pain all over her left leg for 3 weeks. The lumbar myelography was done to find out the cause and degree of its severity. The lumbar puncture was performed through an L2-3 interspace with the patient in lateral decubitus position by 20 G spinal needle, Quinke type. Having established free flow of cerebrospinal fluid (CSF) through the needle, 10 ml. of Iopamiro, a water soluble non-ionic contrast medium, was injected. After the myelography, the patient stayed in bed with the head 45 degree up for 6 hours. The pulse rate and the blood pressure were closely monitored. She was recommended to drink plenty of water and 2 tablets of paracetamol were taken for pain relief.

Next morning, a headache with dizziness occurred after she helped herself to a sitting position. It was relieved by lying flat. The headache was so severe that she could not get out of bed to attend the physical therapy clinic. She was suggested to stay in bed for further 24 hours and 10 mg. intramuscular Diazepam was given but she did not get better. The anaesthesiologist was then consulted. Epidural blood patch was selected as the treatment for this patient.

A 17 G epidural needle was introduced with " loss of resistance technique " into the epidural space at the same intervertebral level as that used for the previous dural puncture (L2-3) Using full aseptic and antiseptic precaution, 10 ml. of blood was withdrawn from the patient's antecubital vein and injected into the epidural space. The headache disappeared immediately in a dramatic response and she could sit with a smile. The patient could attend the physical therapy clinic on the following day.

* Department of Anaesthesia, Ratchaburi Hospital, Ratchaburi 70000, THAILAND
** Department of Radiology, Ratchaburi Hospital, Ratchaburi 70000, THAILAND

DISCUSSION

Post-myelography headache occurs as a result of dural puncture which is similar to the mechanism of postdural puncture headache (PDPH), the complication of spinal anesthesia. It is thought to be caused by leakage of spinal fluid through the needle hole in the dura, as suggested by Bier in 1899 (1). Due to the pressure gradient between the intradural and extradural space , about 40-50 cm water in the sitting position, spinal fluid is lost into the epidural space as long as the dural hole exists. The amount of fluid lost is dependent on the size of the hole and the rate of the CSF production. In experiments with patients in the erect position, withdrawal of 20 ml. spinal fluid resulted in headache, which was promptly relieved by reinjection(2). The consequences of CSF loss are, a drop in spinal subarachnoid fluid pressure, and a decreased subarachnoid fluid volume. In the vertical position, the brain tends to descend as it is deprived of its fluid cushion, this leads to traction on the pain-sensitive supporting structures of the brain and traction on venous sinuses and cerebral vessels. Moreover, a compensatory mechanism to restore the intracranial volume results in dilatation of intracranial blood vessels(3).

According to Brownridge(4), pain is referred above the tentorium via the trimeginal nerve (V) to the frontal region, and below the tentorium via the glossopharyngeal and vagal nerves (IX,X) to the occiput and via the upper cervical nerves (C1,2,3) to the neck and shoulders. A headache is considered a typical PDPH if it fulfills the criteria laid down by Driessen et al(5), i.e. : (a) the headache occurs typically after the patient becomes ambulatory, is aggravated in the erect or sitting position, and is relieved by the patient's lying flat; (b) the localization is mostly occipital or frontal; and (c) the headache is accompanied by dizziness, vomiting, rigidity of the neck, and visual or auditory disturbance.

The incidence of PDPH has been reported to vary from less than 1 % to more than 30 % after accidental dural punctures or diagnostic dural puncture using large needles (3-11). The following factors are thought to influence the incidence of PDPH(8) : (a) age - higher incidence in younger patients; (b) gender - higher incidence in females; (c) needle size - the larger the diameter of the needle, the higher the incidence and the more prolonged and severe the PDPH; (d) multiple dural punctures - higher incidence associated with increased number of the perforations of the dura mater; (e) needle level, direction, and relationship to dural fibers - higher incidence if the needle is inserted perpendicularly to the longitudinal dural fiber, thus cutting instead of separating them ; (f) duration of postoperative recumbency - conflicting results indicate questionable relevance of this factor on the incidence of PDPH; and (g) previous history of PDPH - higher incidence in this group.

However, the incidence of PDPH as a complication of post - myelography is relatively low in our hospital. This may be due to the lack of post myelography visit. If headache occurs, the anaesthesiologist should be consulted for proper management. Since PDPH is mild or moderate in 85 % of patients, it is self-limiting and in most cases disappears within 1 week, the initial management is usually conservative(3). Bed rest is advised as the headache is postural, but it is not a recommended use as a preventive measure against PDPH. Normal fluid intake is necessary to guarantee a good state of hydration. Analgesics and sedatives have no beneficial effect but help to alleviate the symptoms. The curative treatment of PDPH is closure of the hole in the dura by injection of homologous blood into the epidural space : the epidural blood patch. This treatment is so effective and free of serious complications that there is little reason for delay in the following conditions: when headache is severe which does not diminish or disappear within a few days of conservative treatment, or affects the time of patient to be discharged from hospital. The headache disappears rapidly, often immediately , and in 90 % of the patients the relief is permanent. Reported minor complications are backache and paresthesias during injection.

In conclusion, headache as a complication of myelographic study should not be neglected, proper and immediate treatment should be sought for.

REFERENCES

1. Bier A. Versuche uber Cocainisirung des Ruckenmarkes. Dtsch Z chir 1899; 51: 361.
2. Kunkle EC,Ray BS, Wolf HG. Experimental studies on headaches, analysis of the headache associated with changes in intracranial pressure. Neurol Psychiatr 1943; 49: 323-358.
3. Brownridge P. The management of headache following accidental dural puncture in obstetric patient. Anaesth Intensive Care 1983; 11: 4-15.
4. Driessen A, Mauer W, Fricke M, Kossmann B, Schleinzer W. Prospective studies of the post-spinal headache. Reg Anaesth 1980; 3: 382-41.
5. Flaatten H, Rodt SA, Vannes J,Rosland J, Wisborg T, Koller ME. Postdural puncture headache using 26- or 29-gauge needles in young patients. Reg Anaesth 1988; 11: 5.
6. Gielen M. Postdural puncture headache: A review.Reg Anaesth 1989; 14:101-6.
7. Gielen M. How to prevent postdural puncture headache. International Monitor on Regional Anesthesia 1994; 6: 2-7.
8. Lybecker H, Moller JT, May O, Nielsen HK. Incidence and prediction of postdural puncture headache. Anesth Analg 1990; 70: 398-94.
9. Flaatten H, Rodt SA, Rosland J, Vannes J. Postoperative headache in young patients after spinal anesthesia. Anesthesia 1987 ,42 :202-5.
10. Morewood GH. A rational approach to the cause, prevention and treatment of postdural puncture headache. Can Med Assoç J 1993; 149:
11. Vandem LD, Dripps RD. Long-term follow up of patients who received 10,098 spinal anesthetics : Syndrome of decreased intracranial pressure (headache and ocular and auditory difficulties). JAMA 1956; 161: 586-91.

บริษัท กรมศิลป์วรรณ จำกัด
SONGSITTIVAN CO.,LTD.
TEL. 585-3233, 587-5292 FAX : 5872084

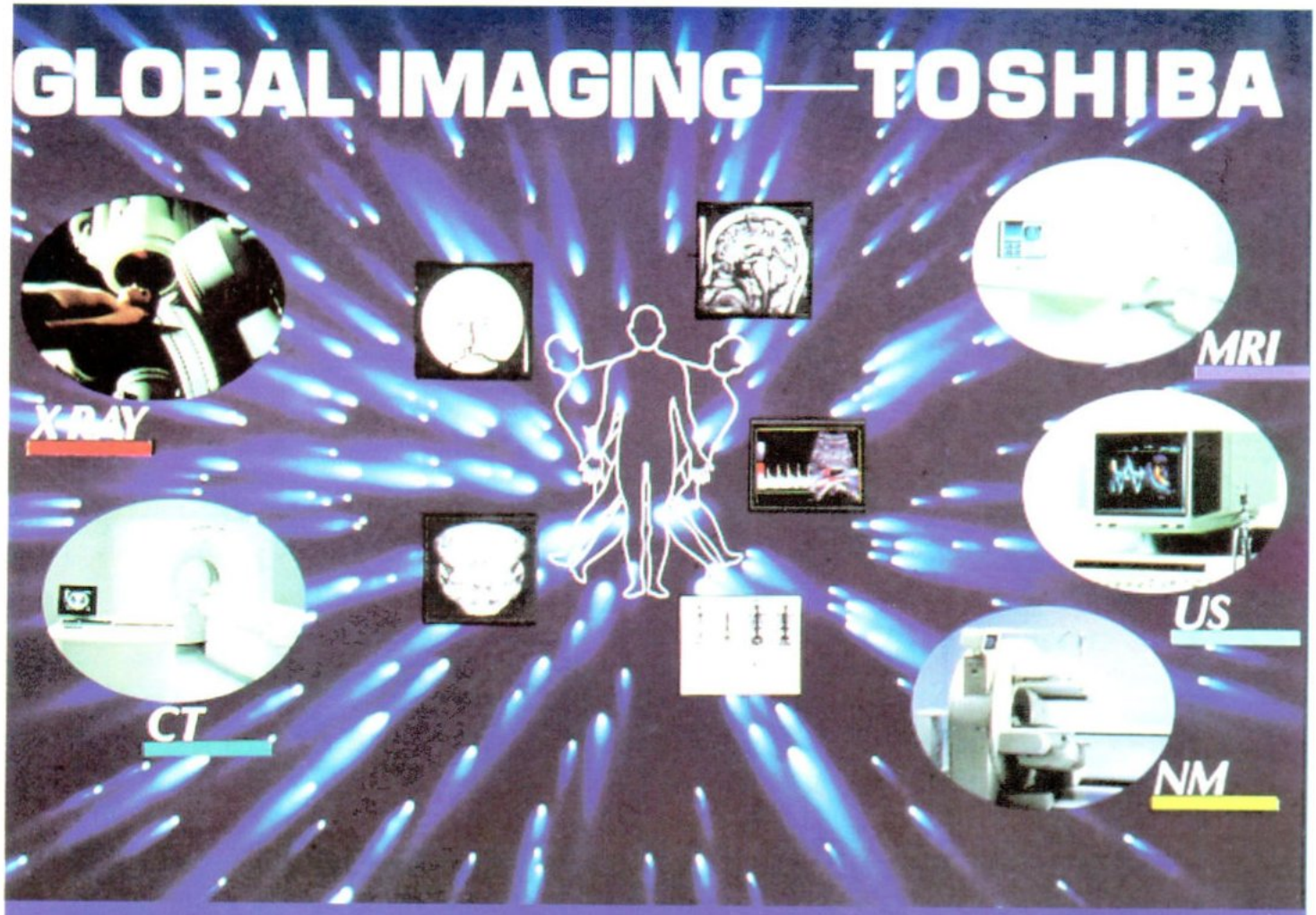

Total Commitment to Improvement of Health and Quality of Life

In Touch with Tomorrow

TOSHIBA

MEDICAL SYSTEMS

CMC BIOTECH

CMC BIOTECH CO., LTD
1433 Soi 3/3 Muban Town-in-Town,
ladphrao 94 Road, Bangkapi Bangkok 10310
Tel. 530-4995-6, 559-3261-2 Fax : (662) 539-6903
Company Phonelink (151, 152) 125165